ACKNOWLEDGEMENT

This material is based upon work supported by the Department of Energy under Award Number DE-FE0029474.

Integrated CCS for Kansas (ICKan)

Award Number: DE-FE0029474
DUNS NUMBER**:** 076248616
Final Technical Report

Submitted to:

The Department of Energy
National Energy Technology Laboratory

Recipient:

University of Kansas Center for Research &
Kansas Geological Survey
1930 Constant Avenue
Lawrence, KS 66047

Submitted by:

Joint Principal Investigators:

Yevhen 'Eugene' Holubnyak
785-864-2070
eugene@kgs.ku.edu

& Martin Dubois
785-218-3012
mdubois@ihr-llc.com

Date of Report: 12/31/18

Project Period: March 15, 2017 to September 15, 2018
Signature of submitting official:

Yevhen 'Eugene' Holubnyak

Executive summary

The goal of the Phase I activity under CarbonSAFE was to evaluate and develop a plan and strategy to address the challenges and opportunities for commercial-scale Carbon Capture and Storage (CCS) in Kansas, ICKan (Integrated CCS for Kansas). The objectives of this project included identifying and addressing the major technical and nontechnical challenges of implementing CO_2 capture and transport and establishing secure geologic storage for CO_2 in Kansas capable of storing 50Mt. In order to achieve these objectives, it was necessary to establish CCS Coordination Team that consisted of professionals from multiple technical and nontechnical disciplines such as geoscience, policy and law, public relations, engineering and others. The Team conducted an integrated and multi-disciplinary assessment of CCS in Kansas. The assessment included: (1) high-level technical, sub-basinal evaluations of CO_2 storage; (2) high-level technical examination of three of Kansas' largest CO_2 point sources and considered other alternatives; (3) high-level evaluation of transportation systems required, 4) evaluation of energy, environmental, regulatory, business law, and public policy; (5) public outreach and acceptance; and (6) identification of economic, commercial, and financial challenges for deployment of commercial-scale CCS in Kansas.

Two geologic complexes identified in the initial proposal as potential sites for storing >50 million tonnes (Mt) are the Pleasant Prairie field geologic site, considered the primary storage site in the proposal, and the Davis Ranch and John Creek fields, in the Forest City Basin storage complex (FCB), in combination, considered a secondary site (Figure 1). A total of five geologic sites were characterized, modeled in Petrel™ and had dynamic simulations performed using Computer Modeling Group GEM™ simulator. Preliminary capacity evaluation for the FCB site indicated it is probably not capable of storing >50Mt CO_2 (Bidgoli and Dubois, 2017a). In the process of evaluating the Pleasant Prairie site, four separate geologic structures were identified as each having potential for storing 50Mt. The four structures, aligned on the same regional geologic structure, are similar in size, have >100 ft of closure, have similar geologic histories, and storage reservoirs, Mississippian Osage, Ordovician Viola, and Cambrian-Ordovician Arbuckle at depths from 5200-6400 ft. The four potential sites—Rupp, Patterson, Lakin and Pleasant Prairie—are situated in what we have named the North Hugoton Storage Complex (NHSC). The Patterson site is one of several geologic sites that has been demonstrated by initial simulation analysis to be capable of injecting and storing 50Mt of CO_2 in a 25- to 30-year timeframe and has been selected as the primary site of in approved CarbonSAFE Phase II project named the *Integrated Midcontinent Stacked Carbon Storage Hub*.

A primary driver for CCS implementation in Kansas is the cost of CO_2 capture and compression. The main focus for CO_2 sources in the ICKan project were initially coal-fired power plants and a refinery (Figure E-1 for locations) because of CarbonSAFE FOA stipulations. However, under current market conditions in the midcontinent region, the aggregation of CO_2 captured from multiple ethanol plants provides the most economical, and frankly, the only viable option for a CCS project of the scale envisioned by CarbonSAFE without substantially more subsidy than currently available. Preliminary technical and economic evaluations of two coal-fired power plants and a refinery in this study suggest that CO_2 capture from these sources is cost prohibitive, even when 45Q tax incentives are applied. Estimated the cost ranges for capture and compression to 150 bar (2200 psi) are $45–$67/tonne for Westar's Jeffrey Energy Center (2.5 Mt/yr), $46–$72/tonne, for Sunflower Energy's Holcomb Station (1.7 Mt/yr) and $60–$94/tonne for the CHS Refinery (0.67 Mt/yr). This compares with capture and compression costs of $19/tonne from ethanol plants in Kansas and Nebraska. All cost estimates include

both capital and operating expenses over a 2-year construction period followed by 20 years of operation, and a 10% cost of capital (or Return on Investment-ROI).

Compressing CO_2 to a supercritical state and transporting it via pipelines is the most cost-effective manner in which to transport large volumes. Because there is currently no infrastructure capable of transporting CO_2 from sources to injection sites in Kansas, the economics of a wholly integrated system, including capture, initial compression and delivery to the injection site via pipeline, must be considered. For ease in modeling complex pipeline systems ICKan modified National Energy Technology Laboratory's (NETL) CO_2 Transport Cost Model (Grant et al., 2013; Grant and Morgan, 2014) so it would handle multiple pipeline segments rather than just one. Multiple scenarios were evaluated in the ICKan project, six of which are discussed in detail in this report. Pipeline transportation costs ranged from as little as $4/tonne to $28/tonne, using the same economic criteria as for capture, 2-year construction period, 20-year operating life, and 10% ROI. Pipeline cost is primarily a function of distance, the shortest being 25 miles (Holcomb Station power plant to Patterson injection site) and the longest covers 1546 miles (gather CO_2 from 34 ethanol plants and deliver to Permian Basin, dropping off CO_2 to the Patterson site along the way). None of the scenarios are economically feasible for saline storage without an EOR component. Having EOR CO_2 as part of the system increases pipe diameter, is accompanied by economic gains from scale and, potentially, additional subsidy for CO_2 destined for saline storage. In the most economically favorable case, 15 ethanol plants in Nebraska and Kansas could deliver 4.3 Mt/year CO_2 to southwest Kansas to the Patterson site for a delivered cost of $2/tonne, including 45Q tax credits, if all CO_2 were to be used in saline storage. If 2 to 2.5 Mt were dedicated to saline aquifer storage and the other1.8 to 2.3 Mt sold for EOR in nearby fields, the CO_2 delivered cost ($2/tonne) and estimated injection site costs (~$3.00/tonne) could be offset by profits from the sale of CO_2 for EOR. Five fields within or nearby the NHSC could readily take 1.8 to 2.3 Mt/yr for EOR. They include the Patterson Morrow waterflood and the Chester and Morrow waterfloods in four fields studied for EOR by Dubois et al. (2015c) as part of a DOE-funded study (DE-FE0002056).

CCS cannot work economically without financial support (subsidies), because no economic value is derived by the physical process of injecting CO_2 into geologic sites for permanent storage. Fortunately, 45Q tax credits were extended and expanded in February 2018, making CCS economically viable, at least CO_2 from ethanol plants. In brief, 45Q provides tax credits of up to $35/tonne for CO_2 stored during EOR and $50/tonne if stored in a saline aquifer reservoir, and can be captured for a 12-year period. Ethanol plants that have the ability to ship to California already see economic benefits under California's Low Carbon Fuel Standard (LCFS) program. Their LCFS benefits could increase dramatically if ethanol plants are able to decrease their carbon intensity (CI) by sequestering their CO_2 byproduct permanently in a saline storage site like the Patterson site. When current and potentially larger benefits from LCFS are considered, the economic viability for saline aquifer storage of ethanol-derived CO_2 could extend to a larger array of project possibilities that could include capture from power plants as part of larger regional systems.

Legal, regulatory, public (LRPP) policy and outreach are critically important for the planning and execution of a 50Mt CCS project. The ICKan project's LRPP team reviewed current State and Federal regulations and policies, and those of other states, examined gaps and needed regulatory and policy modifications, and developed possible solutions that would facilitate capture, transportation and long-term injection and storage. Key obstacles include pore space ownership rights and pooling, pipeline right of ways (ROW), and long-term post closure liability. The LRPP team developed a model statutory scheme that would establish a CCS public utility, resolving key obstacles and other issues. It would establish regulations allowing eminent domain to be utilized for ROW and pooling of pore space. The

team also developed a strategy for complex legal and contractual arrangements to address ownerships, liabilities, and financial arrangements. Extensive public outreach served to engage and enlighten State governmental offices including the Governor, state regulatory agencies, legislators, and industry (oil and gas, midstream-pipeline, power generation, ethanol, refineries) through two very-well attended CCUS in Kansas Forums. The one-day workshops were co-hosted by the Kansas Geological Survey (ICKan) and the State CO_2 EOR Deployment Workgroup, a 14-state organization.

CarbonSAFE Phase II: The KGS-led ICKan project joined Battelle, the lead institution, and the Energy and Environmental Research Center (EERC) in pooling their Phase I projects in Nebraska with the Kansas ICKan project for a single project covering Nebraska and Kansas. The project, Integrated Midcontinent Stacked Carbon Storage Hub, was successful in its bid under DE-FOA-0001450, and the project (DOE—$9.6 million, Total—$13.3 million) kicked off in October 2018. The project will evaluate the feasibility of capturing CO_2 from ethanol plants for storage in saline aquifer reservoirs in Nebraska (Sleepy Hollow field) and Kansas (Patterson site). Capture from coal-fired power plants from Nebraska and Kansas also will be evaluated.

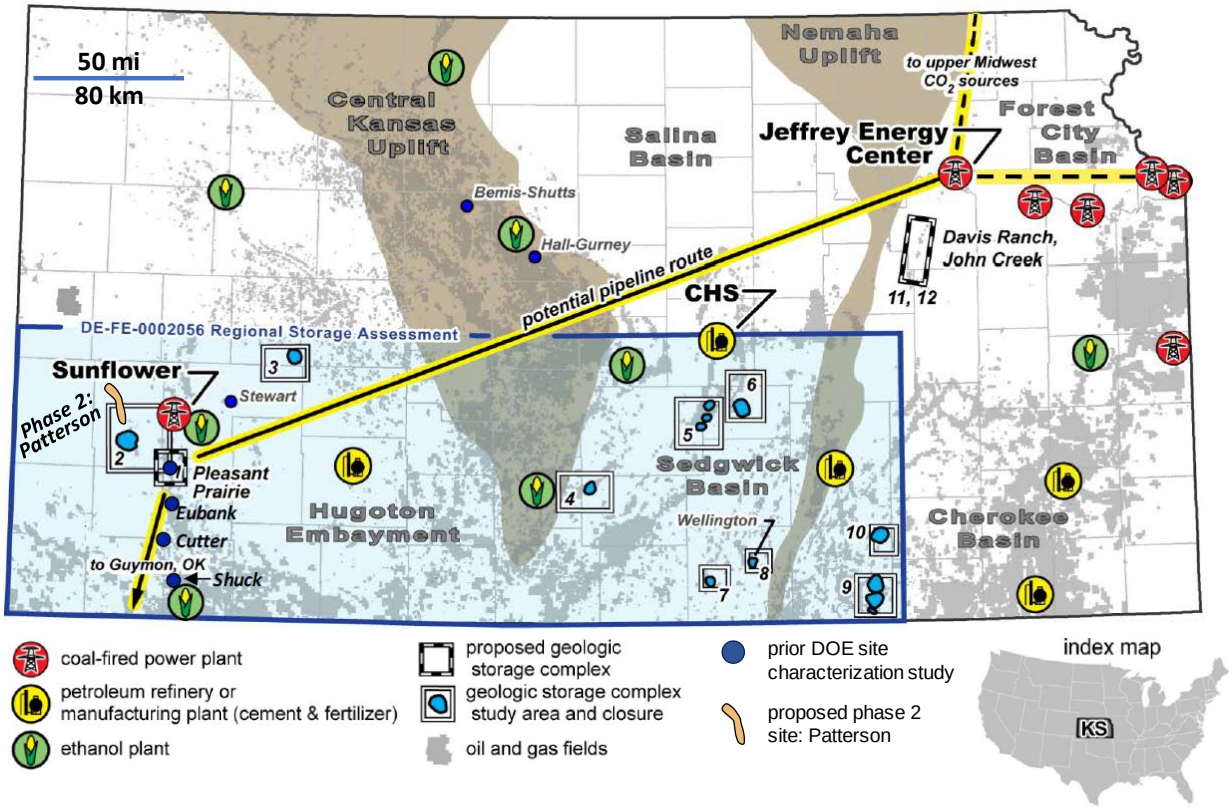

Figure E.1. Kansas map showing location of the Patterson site, a variety of CO_2 sources, possible CO_2 pipeline routes, other possible CO_2 injections sites (numbered 1–12) identified in Watney et al. (2015) located inside the DE-FE0002056 study areas (blue), and oil fields (gray). The primary sources in this study are labeled. The figure is modified from ICKan proposal SF 424 R&R, 2016 (Watney et al., 2016).

List of acronyms and abbreviations

API gravity	American Petroleum Institute gravity (petroleum density measurement)
AVAZ	Azimuthal anisotropy analysis
AVO	Amplitude versus offset
BHP	Bottom hole pressure
BOE	Barrel of oil equivalent (unit of energy)
BOPD	Barrels of oil per day
C	Carbon
CCS	Carbon capture and storage
CCUS	Carbon capture utilization and storage
CMG	Computer Modeling Group
CO_2	Carbon dioxide
CO_2-EOR	Carbon dioxide enhanced oil recovery
DOE	Department of Energy
DST	Drill stem tests
EOR	Enhanced oil recovery
EPA	U.S. Environmental Protection Agency
FMI	Formation micro-imager
ft	Foot, feet
FZI	Flow zone index
GEM	Composition and unconventional oil and gas reservoir simulator (CMG software)
GEMINI	Geo-Engineering Modeling through Internet Informatics (software)
IT	Interference Test
IRIS	Incorporated Research Institutions for Seismology
KCC	Kansas Corporation Commission
KGS	Kansas Geological Survey
km	Kilometer
km2	Square kilometer
KU	University of Kansas
LAS	Log ASCII Standard (software)
MBO	Thousand barrels of oil
mD	millidarcys (a measure of permeability)
mi	Mile
mi2	Square mile
MMBO	Million barrels of oil
MMP	Minimum miscibility pressure
MPa	Mega Pascals
MRIL	Magnetic resonance imaging log
MSTB	Thousand stock tank barrels
MVA	Monitoring, verification, and accounting
NaCl	Sodium chloride
NETL	National Energy Technology Laboratory
NHSC	North Hugoton Storage Complex
NMR	Nuclear magnetic resonance
O	Oxygen
OPAS	Ozark Plateau Aquifer System
pH	Measurement of acidity or basicity of solution
psi	Pounds per square inch

PV Pore volume
PVT Pressure-volume-temperature
qPCR Quantitative polymerase chain reaction
RQI Reservoir quality index
Rs Gas–oil ratio
SO_4^{2-} Sulfate
Sr Strontium
SRB Sulfate reducing bacteria
UIC Underground Injection Control
USDW Underground sources of drinking water
WPAS Western

Table of Contents

Introduction

The Integrated CCS for Kansas project (ICKan) is a Phase I pre-feasibility study under DOE-NETL Carbon Storage Assurance Facility Enterprise (CarbonSAFE) program. The Kansas Geological Survey (KGS) and The University of Kansas (KU) together with a Carbon Capture and Storage (CCS) Coordination Team executed the study. The goal of Phase I activity under CarbonSAFE is to identify and critically evaluate challenges and opportunities for commercial-scale Carbon Capture and Storage (CCS) in Kansas. The objectives include identifying, evaluating, and addressing the major technical and non-technical challenges for implementing commercial-scale, CO_2 capture, transport, and secure geologic storage of 50 million tonnes CO_2 in Kansas.

This feasibility study examined three of Kansas' largest CO_2 point sources, nearby and distant storage sites, where an estimated storage capacity was equal or greater than 50 million tonnes, and prospective CO_2 transportation networks. Westar Energy's Jeffrey Energy Center--Kansas' largest coal-fired electrical generating facility--near St. Marys, Kansas served as the primary site because of its size (2.16 GigaWatt and 12.5 million metric tons of CO_2 emissions) and strategic location along the eastern margin of Kansas' aerially extensive and vertically stacked, reservoir complexes. Sunflower Electric Cooperative's Holcomb coal-fired plant near Garden City in southwest Kansas and one of Kansas' largest oil refineries, CHS Refinery, near McPherson in central Kansas were secondary sites. Because of the high cost of capture and compression from power plants and refineries, the study also considered ethanol plant sources where capture and compression costs are significantly lower.

The KGS undertook highly technical, sub-basinal evaluations of CO_2 storage building upon prior regional characterization studies conducted under DOE-NETL project DE-FE0002056. Risk assessment of the CO_2 storage sites was augmented through the use and testing of new models and tools developed by the DOE national laboratories under the DOE-NETL's NRAP (National Risk Assessment Partnership). Site-specific, risk assessments incorporated "lessons learned" by the KGS during the final EPA (Region 7) review of the Class VI geosequestration permit for storage of 26,000 tonnes of CO_2 within the Arbuckle saline aquifer at Wellington Field (DE-FE0006821). The success of the recent Class II CO_2 Enhanced oil Recovery (EOR) injection in the overlying Mississippian oil reservoir at Wellington, Kansas supports the viability of the stacked reservoir concept. The experience and knowledge gained established a foundation for planning to address post-injection site care, site closure, financial assurance, and long-long term liability.

The ICKan team consists of a number of industry partners that provided additional expertise in support of this project. The Linde Group, a multinational engineering company and the world's largest industrial gas company, evaluated the technical challenges and developed plans for CO_2 capture and transportation in Kansas. The Linde Group views Kansas as a strategic, midcontinent location for implementing an economically viable, anthropogenic-based, CO_2 source-to-sink network. Oil producers operating fields near the primary CO_2 sources were also Team members and included Berexco, Blake Exploration, Casillas Petroleum, Knighton Oil Company, and Stroke of Luck Energy and Exploration. They provided access to information from the CO_2 storage sites, are interested in economic utilization and storage of CO_2, and reflect a large and growing interest among the petroleum industry in CO_2-EOR for revitalizing Kansas' mature oil fields. Improved Hydrocarbon Recovery, with its history of managing large-scale reservoir characterization and modeling studies, including multiple projects administered by the KGS, supported the ICKan through project management and site technical evaluation. The law firm, DePew,

Gillen, Rathbun, and McInteer (DGRM), located in Wichita, Kansas assisted in this CCS effort providing expertise in energy, environmental, regulatory, business law, and public policy.

The Great Plains Institute (GPI) is a non-profit organization that works with diverse interests to promote both environmentally and economically sustainable energy technologies. In collaboration with other team members, GPI's role was to: 1) help foster public acceptance of the project, 2) develop a public input and education process that will take place in Phase II, 3) identify legal and regulatory obstacles and determine possible remedies, and 4) explore the impact of federal and state policies and incentives on project viability and economics.

The multi-disciplinary approach undertaken by ICKan created a plan that addresses regulatory, legislative, technical, public policy, commercial, and financial challenges for commercial-scale CCS in Kansas. Furthermore, the CCS Coordination Team offers a strategy that will bring rural and urban communities, state government, and academia together with industry to initiate and establish a viable path to CCS that will benefit the greater energy economy with cleaner air and water and new oil production with a reduced carbon footprint. The CCS Coordinating Team aims to guide decisions including adding members to augment the existing expertise. Selected storage sites were characterized and modeled where each be designed to safely store at least 50 million tonnes of CO_2 in stacked saline aquifer storage reservoirs beneath oil fields with potential for EOR.

Task 1.0: Project management and planning integrated CCS for Kansas (ICKan)

Authors who contributed to this task: Martin Dubois, Eugene Holubnyak, Susan Stover, Tandis Bidgoli, and Jennifer Hollenbach.

All project meetings were documented in project Quarterly Reports, which are published online at the ICKan project KGS web page (http://www.kgs.ku.edu/PRS/ICKan). All six published reports were composed with contributions from each team section lead to ensure compliance with DOE requirements. Each quarter, a summary of project activities was shared, as well as the latest findings and progress on each updated task. These reports can be accessed on the project website at http://www.kgs.ku.edu/PRS/ICKan/reports.html.

Regular meetings were held to convey project findings, ensure the project adhered to the project scope, evaluate and mitigate risk, and monitor resources on a timely basis. Scheduled events included site visits, annual CCUS Forum meetings involving all project stakeholders, all-team monthly meetings, as well as weekly internal meetings between subgroups as needed. A summary of discussion topics, as well as the meeting date and location, are provided in each quarterly report. A list of participants at key meetings and all individuals involved throughout the project is provided in the following section under Task 2.

Figure 1.1. Steam billows from Westar's three 800 Mw electrical generation units on a brisk February morning at the Jeffrey Energy Center in St. Marys, Kansas. Following the kick-off meeting for ICKan,, Yevhen (Eugene) Holubnyak, Petroleum Engineer, Kansas Geological Survey, Martin Dubois, Joint-PI, Improved Hydrocarbon Recovery, and Krish Krishnamurthy, head of Group R&D in the Americas for The Linde Group, visited two possible industrial sources for CO_2, Jeffrey Energy Center and the CHS refinery in McPherson, Kansas.

Information acquired during the project was shared via Quarterly Reports and published according to task under each publication. Supplementary information developed under DE-FE00029474 was uploaded to the NETL-EDX data portal per DOE requirements. EDX information includes Petrel models (shared via Petrel and rescue file format), model data inputs, and snapshots of analysis via images and supporting text. Details are organized by study area, including five potential sites evaluated: Davis Ranch/John Creek site in the Forest City Basin, and the Rupp, Patterson, Lakin and Pleasant Prairie sites in the North Hugoton Storage Complex. No private or patented material was generated during this study.

Integrated strategy/business plan for commercial scale CCS

Any business strategy for long-term safe CO_2 storage at a scale that would safely store 50 Mt CO_2 must consider the entirety of the endeavor as an integrated system. The three main components—1) capture and initial compression, 2) transportation, and 3) injection and storage—would likely operate as separate business entities, but their economical operations are intertwined. Additional complexities that are very possible are that the capture and compression facility may be a completely separate business from the CO_2 source and the injection site, if co-located with an existing oil field, might be operated by an entity other than the oil operator for that site.

Capture from ethanol plants

In the midcontinent region, aggregating CO_2 captured from multiple ethanol plants provides the most economical, and frankly, the only viable option for a CCS project of the scale envisioned by CarbonSAFE (see Task 6). The evaluations of CO_2 from coal-fired power plants or a refinery in this study suggest that the capture from these sources is cost prohibitive under current economic conditions, even when 45Q tax incentives are applied (see Tasks 5 and 6). We present two scenarios for capture from ethanol plants, one for 15 and the other for 34 plants. The ownership and financial structure of ethanol plants is varied, creating other complexities. They are owned by large and small corporations, farmer coops and LLCs, all having unique financial structures and differing abilities to make use of tax credits that could be afforded by 45Q or the California ethanol pricing benefits in their Low Carbon Fuel Standards (LCFS) program (see Task 6).

Tax and other incentives

CCS cannot work economically without financial support (subsidies), because no economic value is derived by the physical process of injecting CO_2 into geologic sites for permanent storage. Fortunately, 45Q tax credits were extended and expanded in 2018, making CCS economically viable, at least CO_2 from ethanol plants (see Task 6). Ethanol plants that have the ability to ship to California already see economic benefits under the LCFS program. The benefits could increase dramatically if they are able to decrease their carbon intensity (CI) by sequestering their CO_2 byproduct permanently.

CO_2 enhanced oil recovery (EOR) must also be a part of the plan

To achieve economies, and possibly provide supplemental pricing for CO_2 delivered for saline storage, shipping CO_2 for EOR must also be part of the business plan (see Task 6).

All entities must be economic (profitable)

The key, and challenge, for an integrated CCS system is to spread the benefits derived from 45Q and LCFS across all entities. The CO_2 source, capture and compression plant, pipeline company, the oil field operator and the injection and storage operator must all operate in a financially prudent manner. No matter who is able to actually take the financial credits, the benefits need to be distributed. A complex business plan needs to ensure this can happen and be flexible enough to change as legal, regulatory and public policy changes. Appendix A: Anticipated Business Contractual Requirements Necessary to Address Technical and Financial Risks is a good summary of the challenges and possible solutions to address the complex business of CCS.

Task 2.0: Establish a Carbon Capture and Storage (CCS) Coordination Team

The Phase I team structure was focused on a multidisciplinary group that could address the technical and non-technical challenges related to CCUS deployment in Kansas. Figure 2.1 depicts the team structure and briefly describes the roles and duties of each unit.

Organizational Chart
Integrated CCS for Kansas (ICKan)

Project Management & Coordination, Geological Characterization

Kansas Geological Survey, University of Kansas, Lawrence, Kansas
Yvehen "Eugene" Holubnyak, Co-PI—lead engineer, dynamic modeling
W. Lynn Watney, Co-PI—project leader, carbonate sedimentology/stratigraphy
Tandis Bidgoli, Joint-PI—structural geology, fault reactivation/leakage risks
K. David Newell, Co-PI—site characterization
John Doveton, Co-PI—log petrophysics
Susan Stover, Key Personnel—public outreach, stakeholder alignment, policy analysis
Mina FazelAlavi, Key Personnel—petrophysical and well test analyses
John Victorine, Key Personnel—data management, website, web-based tools
Jennifer Hollenbach—project coordinator

Improved Hydrocarbon Recovery, LLC, Lawrence, Kansas
Martin Dubois, Joint-PI—project manager, reservoir modeling, economic feasibility

CO_2 Source Assessments, Capture & Transportation, Economic Feasibility

Linde Group (Americas Division), Houston, Texas
Krish Krishnamurthy, Head of Group R&D—CO_2 sources, capture tech., and economics
Kevin Watts, Dir. O&G Business Development—CO_2 sources, transport., and economics

Policy Analysis, Public Outreach & Acceptance

Great Plains Institute, Minneapolis, Minnesota
Brendan Jordan, Vice President—policy & strategic initiatives, stakeholder facilitation
Brad Crabtree, V.P. Fossil Energy—policy and project development, strategic initiatives
Jennifer Christensen, Senior Associate—statutory and regulatory policy analysis
Dane McFarlane, Senior Research Analysist—analytics for policy research & development

Energy, Environmental, Regulatory, & Business Law & Contracts

Depew Gillen Rathbun & McInteer, LC, Wichita, Kansas
Charles Christian Steincamp, Attorney at Law—legal, regulatory, & policy analysis
Joseph Schremmer, Attorney at Law—legal, regulatory, & policy analysis

Figure 2.1. Organizational chart of the original ICKan Phase I team. Subrecipients to the KGS included Improved Hydrocarbon Recovery, Linde Group, Great Plains Institute, and Depew Gillen Rathbun & McInteer, LC.

The Phase I team hosted annual CCUS workshops with the intention of recruiting additional industry partners (oil, midstream, and ethanol industries) and stakeholders (regulatory, legislative, and NGOs). These efforts were successful and received strong support from the more than 100 guests who were invited to the meetings. Table 2.1 provides a complete list of attendees from the CCUS workshop on September 21, 2017, and the CCUS Forum on July 27, 2018. The CCUS Forum in 2018 included all Phase I team members and introduced the committed Phase II team. Presentations focused on efforts that would be central to the Phase II objectives and how the study would transition into this work in the near term.

Table 2.1a. List of attendees at the CCUS for Kansas Meeting in Wichita, Kansas, on September 21, 2017

First Name	Last Name	Title	Organization
Andrew	Duguid	Principal Engineer	Battelle
Dana	Wreath	VP	Berexco
Scott	Ball	VP	BOE Midstream
Fatima	Ahmad	Solutions Fellow	Center for Climate and Energy Solutions
Rick	Johnson	Process Engineering & Development Manager	CHS McPherson Refinery
Deepika	Nagabhushan	Energy Policy Associate	Clean Air Task Force
Roger	Erickson	Field Representative	Congressman Estes Ks 4th District
Keith	Tracy	President	Cornerpost CO_2 LLC
Joe	Schremmer	Attorney	Depew Gillen Rathbun & McInteer LC
Charles	Steincamp	Managing Partner	Depew Gillen Rathbun & McInteer LC
Kevin	Gray	Director, Innovation	Flint Hills Resources
Gary	Gensch	Consultant	Gary F. Gensch Consulting
Dan	Blankenau	President	Great Plains Energy Inc.
Dane	McFarlane	Senior Research Analyst	Great Plains Institute
Doug	Scott	Vice President	Great Plains Institute
Chuck	Brewer	President	GSI Engineering
Martin	Dubois	Owner	Improved Hydrocarbon Recovery, LLC
Greg	Krissek	CEO	Kansas Corn
Justin	Grady	Chief of Accounting and Financial Analysis	Kansas Corporation Commission
Jeff	McClanahan	Director, Utilities Division	Kansas Corporation Commission
Mike	Cochran	Chief of the Geology & Well Technology Section	Kansas Department of Health & Environment
Brandy	DeArmond	PG, Chief, Underground Injection Control	Kansas Department of Health & Environment - Bureau of Water
Tandis	Bidgoli	Assistant Scientist	Kansas Geological Survey
Yevhen	Holubnyak	Petroleum Engineer	Kansas Geological Survey
Rolfe	Mandel	Director	Kansas Geological Survey
Susan	Stover	Outreach Manager, Geologist	Kansas Geological Survey
Edward	Cross	President	Kansas Independent Oil & Gas Association
Jessica	Crossman	Professional Geologist	KDHE
Makini	Byron	Innovation Project Manager	Linde LLC
Krish R.	Krishnamurthy	Head of Group R&D	Linde LLC

Steve	Melzer	Owner	Melzer Consulting
Sarah	Bennett	MidCon Exploitation Manager	Merit Energy Company
Ryan	Huddleston	Engineer	Merit Energy Company
Martin	Lange	Engineer	Merit Energy Company
Frank	Farmer	General Counsel	Mississippi Public Service Commission
Leon	Rodak	VP Production	Murfin Drilling Company
Al	Collins	Senior Director Regulatory Affairs	Occidental Petroleum Corporation
Christian	McIlvain	Vice President, Denaturant and Carbon Dioxide	Poet Ethanol Products
Jeffrey	Brown	Research Fellow	Stanford Business School
Sarah	Forbes	Scientist	United States Department of Energy
Paul	Ramondetta	Manager of Exp. And Exploitation	Vess Oil Corp.
Scott	Wehner	Owner	Wehner CO_2nsulting, LLC
Dan	Wilkus	Director, Air Programs	Westar Energy, Inc.
Kim	Do	Finance Manager	White Energy
Matt	Fry	Policy Advisor	Wyoming Governor's Office

Table 2.1b. List of attendees at the CCUS Forum at Lawrence, Kansas, on July 27, 2018.

First Name	Last Name	Job Title	Company
Keith	Brock	Attorney	Anderson & Byrd, LLP
Scott	McDonald	Director of Biofuels Development	Archer Daniels Midland
Andrew	Duguid	Senior Engineer	Battelle
Keith	Tracy	President	Cornerpost CO_2, LLC
Charles	Steincamp	Managing Partner	Depew Gillen Rathbun & McInteer LC
Joseph	Schremmer	Lawyer	Depew Gillen Rathbun & McInteer, LC
Michael	Barger	EHS Manager	East Kansas Agri-Energy
Todd	Barnes	Environmental Specialist	East Kansas Agri-Energy
Bill	Pracht	CEO	East Kansas Agri-Energy
Doug	Sommer	Vice President of Operations	East Kansas Agri-Energy
Eric	Mork	Business Development	EBR Development, LLC
Jason	Friedberg	General Manager	ELEMENT, LLC
Neil	Wildgust	Principal CCS Scientist	Energy & Environmental Research Center
Dan	Blankenau	President	Great Plains Energy, Inc
Brad	Crabtree	Vice President	Great Plains Institute
Jess	Jellings	Event Planner	Great Plains Institute
Brendan	Jordan	Vice President	Great Plains Institute
Martin	Dubois	Owner	Improved Hydrocarbon Recovery LLC
Mike	Cochran	Chief, Geology and Well Technology Section	Kansas Bureau of Water
Ingrid	Setzler	Director Environmental Services	Kansas City Board of Public Utilities
Sue	Schulte	Director of Communications	Kansas Corn
Dwight	Keen	Commissioner	Kansas Corporation Commission

Jessica	Crossman	Deputy Chief, Geology and Well Technology Section	Kansas Department of Health and Environment
Michael	Chisam	President/CEO	Kansas Ethanol, LLC
Esmail	Ansari	Postdoctoral Researcher	Kansas Geological Survey
Tandis	Bidgoli	Assistant Scientist and PI	Kansas Geological Survey
Andrew	Hollenbach	Graduate Student	Kansas Geological Survey
Jennifer	Hollenbach	Project Coordinator	Kansas Geological Survey
Eugene	Holubnyak	Petroleum Engineer	Kansas Geological Survey
Rolfe	Mandel	Director	Kansas Geological Survey
Sahar	Mohammadi	Petroleum Geoscientist	Kansas Geological Survey
K. Dave	Newell	Assoc. Scientist	Kansas Geological Survey
Oluwole	Okunromade	Graduate Research Assistant	Kansas Geological Survey
Susan	Stover	Geologist, Outreach Manager	Kansas Geological Survey
Willard	Watney	Senior Scientific Fellow	Kansas Geological Survey
Dave	Heinemann	Member	Kansas Geological Survey Advisory Council
Mark	Schreiber	Representative	Kansas House of Representatives
Donna	Funk	Principal	KCoe Isom, LLP
Krish	Krishnamurthy	Head of Group R&D - Americas	Linde
Kevin	Watts	EOR Business Development Director	Linde
Sarah	Bennett	MidCon Exploitation Manager	Merit Energy Company
Martin	Lange	Sr. Technical Advisor	Merit Energy Company
Al	Collins	Senior Director Regulatory Affairs	Occidental Petroleum
Charlene	Russell	Vice President Low Carbon Ventures	Occidental Petroleum
Peter	Barstad	Policy Analyst	Office of Kansas Governor Jeff Colyer, M.D.
Andrew	Wiens	Chief Policy Officer	Office of Kansas Governor Jeff Colyer, M.D.
Marcus	Lara	Marketing Manager	Poet Ethanol Products
Tom	Sloan	State Representative	State of Kansas
Tiraz	Birdie	President	TBirdie Consulting, Inc
Mark	Ballard	Petroleum Engineer	Tertiary Oil Recovery Program, KU
Jyun Syung	Tsau	Director CO_2 Flooding & Sequestration	Tertiary Oil Recovery Program, KU
Anthony	Leiding	Director of Operations	Trenton Agri Products LLC
Sarah	Forbes	Scientist	U.S. Department of Energy
Kurt	Hildebrandt	Geologist	U.S. Environmental Protection Agency
Ben	Meissner	Physical Scientist	U.S. Environmental Protection Agency
Reza	Barati	Associate Professor	University of Kansas
Steve	Randtke	Professor	University of Kansas
Dana	Divine	Hydrogeologist	University of Nebraska Conservation and Survey Div.
Paul	Ramondetta	Manager of Exploration and Exploitation	Vess Oil Corporation
Scott	Wehner	Proprietor	Wehner CO_2nsulting, LLC
Greg	Thompson	Chief Executive Officer	White Energy

In an effort to establish a larger CCS Coordination team, the ICKan Phase I project partnered with Battelle on a Phase II proposal and was successfully awarded the Phase II CarbonSAFE program in Summer 2018, titled “Integrated Mid-Continent Stacked Carbon Storage Hub,” DE-FE0029264. Phase II officially kicked off on October 3, 2018. The Phase II team is led by Battelle Memorial Institute and includes Archer Daniels Midland Company (ADM), the Kansas Geological Society (KGS), the Energy and Environmental Research Center (EERC) at the University of North Dakota, Schlumberger, the Conservation and Survey Division (CSD) at the University of Nebraska-Lincoln (UNL) and others. The Phase II team has identified groups to fill in technical and non-technical areas from the Phase I team, as well as expand the involvement from potential sources and sinks in the Midwest. More details are described in the Phase II DE-FE0029264 project narrative.

Task 3.0: Develop a plan to address challenges of a commercial-scale CCS Project

This application presents three candidate sources and identifies three possible geologic complexes suitable for storage. Phase I work shall determine which are most feasible, and shall identify and develop a preliminary plan to address the unique challenges of each source/geologic complex that may be feasible for commercial-scale CCS (50+ million tonnes captured and stored in a saline aquifer). Reliable and tested approaches, such as Road mapping and related activities (Phaal, et al., 2004, Gonzales-Salavar, et al., 2016; IEA, 2013) shall be used to identify, select, and establish alternative technical and non-technical options based on sound, transparent analyses including monitoring for adjustment as the assessment matures.

(**Note:** Non-technical and technical challenges are discussed separately. Subtask 3.A. covers non-technical challenges for capture, transportation and injection, and geologic sites. Technical challenges for capture, transportation and injection, and geologic sites are covered in Subtasks 3.1, 3.2, and 3.3, respectively.)

Subtask 3.A: Develop a plan to address non-technical challenges of a commercial-scale CCS Project

Contributors Subtask 3.A include Susan Stover, Charles Christian Steincamp, Joseph Schremer, Brendan Jordan, Martin Dubois Jennifer Christensen, and Jennifer Hollenbach.

Overview

The ICKan Legal, Regulatory and Public Policy team (LRPP) comprises attorneys from Depew Gillen Rathbun & McInteer (DGRM), public policy experts from the Great Plains Institute, and the Kansas Geological Survey outreach manager/geologist. The LRPP team met with State and Federal regulators and industries and researched approaches taken in other states. Its work covered issues ranging from Class VI well permitting, pore space ownership, carbon capture in the public interest, and public utilities versus private contractors for CO_2 transportation and geologic storage. The team's discussion of possible contractual arrangements (Appendix A) addresses alternate legal and contractual requirements to address ownerships, liabilities, and financial arrangement. The LRPP team also devised a model statutory scheme to establish a CCS public utility (Appendix B).

3.A.1: Significant activities and accomplishments include the following:

1. Having supportive public policies in place is critical for the development of large-scale capture and storage projects in Kansas and the Midwest. The ICKan team took a proactive approach by informing the Kansas Governor's office about the U.S. DOE CarbonSAFE initiative, the concept of CCS and CCUS through enhanced oil recovery, and the potential positive impact on the Kansas economy. This led to strong support by Kansas Governor Jeff Colyer and his Chief of Public Policy, Andrew Wiens. Contacts and key outcomes are highlighted below:

   On behalf of the ICKan project, KGS Director Rolfe Mandel met with staff from Kansas Governor Sam Brownback's office in December 2017 and January 2018 to provide information about the possibilities of CCUS in Kansas and the importance of the passage of federal legislation that would extend and reform Section 45Q Tax Credit for Carbon Dioxide Sequestration. After Brownback's departure for a position in the Trump administration, and on the day he was sworn in (February 6), new Kansas Governor Jeff Colyer joined five other governors in signing a letter in support of the 45Q legislation and sending it to the eight leaders of the U.S. House of Representatives. The legislation passed in both houses and was signed into law on February 9.

2. In February 2018, Governor Colyer provided a letter of support for the CarbonSAFE Phase II project Integrated Midcontinent Stacked Carbon Storage Hub, which combined three Phase I projects, including ICKan.

3. Rolfe Mande and Martin Dubois, ICKan Joint-PI, met with Andrew Wiens, Chief of Public Policy for Governor Jeff Colyer, on April 25, 2018. They discussed the ICKan project, CCS and CCUS opportunities in Kansas, especially in light of the expansion of 45Q tax credits, and how Kansas public policy, the legislature and regulatory agencies could play a significant role in facilitating large-scale CO_2 storage and utilization in Kansas. This meeting and other communications led to engagement by the governor and his public policy staff, as summarized below:
    a. Wiens participated in the *CO2NNECT 2018: Carbon Capture Pathways to Clean Energy* conference *(https://co2nnect.net/)*, June 18–19, 2018, hosted by Wyoming Governor Mead.
    b. Governor Colyer joined five other governors in establishing the *Governor's Coalition on Carbon Capture* on June 19, 2018, to provide state executive leadership, focus and outreach on behalf of carbon capture policy and technology deployment.
    c. Wiens delivered a keynote address and he and Peter Barstad from the governor's public policy office participated in the *CCUS for Kansas* conference. The meeting, held August 15–16, 2018, was co-hosted by the Kansas Geological Survey's ICKan Project and the State CO_2-EOR Workgroup, representing 14 states. It was held in the Earth Energy and Environment Center on the University of Kansas campus in Lawrence.

4. The LRPP team gave multiple presentations in public settings to state agencies, legislators, industries, and other stakeholders and held private discussions with state agencies and others regarding legal, regulatory and public policy issues. Presentations covered policies currently in place, identified gaps, and discussed issues that may yet develop. Phase 1 meetings, presentations and discussions:

    a. Presentation on opportunities and challenges of CCS/CCUS to the Kansas Geological Society, October 3, 2018, Wichita (Stover, Holubnyak, Watney). Discussions covered the legal, regulatory and public policy landscape and the technical evaluations for commercial-scale geologic storage.

    b. Presentations at the Kansas Field Conference, August 15, 2018, in Abilene. Participants consisted of state legislators, state agency and program heads, and representatives of industry and non-profit organizations (Stover, Holubnyak).

    c. Presentation at the Kansas Independent Oil and Gas Association annual meeting August 14, 2018, in Wichita (Dubois).

    d. Presentation at the CCUS in Kansas forum July 26, 2018, in Lawrence (Schremmer), followed by a breakout group discussion on concerns and opportunities for CCUS, with focus on legal, regulatory or policy actions. Participants included Kansas Legislators, the EPA, oil and gas industries, ethanol industries, Kansas Corn Growers, Kansas Department of Health and Environment, and a Kansas Corporation Commissioner. Presentations from the forum are online: http://www.kgs.ku.edu/PRS/ICKan/index.html

    e. Meeting with Jeff McClanahan, Director of Utilities; Leo Haynes, Pipeline Safety; Justin Grady, economist; and a counselor for the Kansas Corporation Commission on May 29,

2018, in Topeka (Stover, Dubois, Schremmer, and Steincamp). The group discussed progress on CCS and new momentum with passage of improved 45Q tax credit. A major concern from the KCC was the economic impact to rate payers if carbon capture equipment is placed on the coal power electrical generating plant. The KCC has a responsibility to protect costs to rate payers.

f. Evaluation of successful approaches to Class VI applications, including a teleconference with Battelle (Andrew Duguid) and ADM (Scott McDonald), Midwest Geologic Sequestration Consortium, on their successful experience obtaining a Class VI well permit (Bidgoli, Holubnyak, Stover, 1/24/2018).

g. Continued discussions with state regulatory agencies Kansas Corporation Commission and Kansas Department of Health and Environment on CCS in Kansas and provided an update on CarbonSAFE Phase II plans (Rick Brunetti, Chief, Division of Air, Kansas Department of Health and Environment, January 5, 2018; Jeff McClanahan, Director, Division of Utilities, Kansas Corporation Commission, January 6, 2018; Ryan Hoffman, Director, Division of Conservation, Kansas Corporation Commission, January 12, 2018).

h. Meeting with EPA Region VII Administrator Jim Gulliford on November 8, 2017, to discuss CCS Research needs and Class VI permitting requirements (KGS Director Mandel, Bidgoli, and Stover).

i. Presentation at the CCUS for Kansas workshop on September 21, 2017, in Wichita (Steincamp). Co-hosted by the Kansas Geological Survey and the Great Plains Institute, the workshop brought together representatives from utilities (coal-fired power), refineries, oil and gas producers, ethanol producers, mid-stream pipeline companies, NGOs, policy makers, regulators, engineers and scientists. A state legislator and staff for Congressman Estes and Congressman Marshall participated. Presentations from the meeting are available online: http://www.kgs.ku.edu/PRS/ICKan/presentations.html

j. Meeting with the Kansas Department of Health and Environment Division Director and others on August 10, 2017, in Topeka, to review the study (Stover, Bidgoli, Holubnyak, and Dubois). The KDHE administers the UIC program (all except Class II wells) and regulates air quality.

5. Results of work from ICKan project were shared with regional and national initiatives dedicated to supporting deployment of carbon capture and utilization.
   a. Work by the Great Plains Institute and the Kansas Geological Survey on the economics and feasibility of regional CO_2 pipelines was sha
   State CO_2EOR Deployment Work Group, a partnership of state officials and industry stakeholders dedicated to expanding the carbon capture and storage industry. Research from the ICKan team was incorporated in a white paper published by that group that focused on the potential for carbon capture from the ethanol industry, "Capturing and Utilizing CO_2 from Ethanol: Adding Economic Value and Jobs to Rural Economies and Communities While Reducing Emissions."
   b. Research by the Great Plains Institute and the Kansas Geological Survey on regional CO_2 pipelines also has
   Initiative, a stakeholder partnership focused on planning and spurring construction of regional pipeline infrastructure.

3.A.2: Identify challenges and develop a plan to address challenges for CO_2 capture, transportation and injection

Discussions with stakeholders, regulators and others noted in the Activities and Accomplishments section above, included the non-technical issues associated with CO_2 capture, transportation, injection and storage. State legislators have expressed a willingness to introduce bills to support CCS and CCUS. Additional education and communication outreach on CCS and CCUS and its potential in Kansas with industry and stakeholders is an important next phase. It is critical to build a wide coalition of support and public acceptance. Challenges and possible solutions are identified below.

3.A.2.1: Capture

Opportunities: Although this study focused on CO_2 capture from Westar's Jeffrey Energy Center, the largest source of CO_2 in Kansas, representatives from CHS McPherson Refinery, Kansas City Kansas's Board of Public Utilities, and Sunflower Electric, all major generators of anthropogenic CO_2, have expressed interest in CCS. Sunflower Electric has a coal-fired plant at Holcomb, Kansas, which is located near potential geologic storage sites.

Ownership and Liability During Capture: Two models could address ownership and liability during capture. In one, a private business model, contractual arrangements would specify whether the CO_2 was owned by the business that generated it or the contractor that captured it. The contract would indicate responsibilities of each party, such as for maintenance and repair or liability for loss of CO_2. Under current statutes, the title to the CO_2 stream likely falls under K.S.A. 65-3418, vesting of title to solid waste, or K.S.A. 65-3442, vesting of title to hazardous waste. If CO_2 falls under the solid waste statute, the generator could ultimately be responsible for any risks associated with the CO_2 throughout the capture and transportation phases.

An alternative model would be to set up the CCS as a public utility for capture, transportation, injection and storage. A stand-alone public utility could handle capture of the CO_2 and then hand it off to the next public utility for transportation, or one public utility could cover multiple or all phases.

Cost: The cost of carbon capture from coal-fired utilities could put this energy source at an economic disadvantage compared to wind-, solar-, or nuclear-generated electricity in Kansas. The Southwest Power Pool dispatches the least expensive (in the short term) energy first, which typically is wind generated. However, coal-fired plants are still the largest source of energy for Kansas, supplying 38% of the electricity generated in 2017 (U.S. EIA, 2018). Without additional government support to defray the cost of the carbon capture or a national policy for a different cost evaluation criterion, the Kansas Corporation Commission Utilities Director McClanahan indicated he would have a responsibility to public utility rate payers and may not support it.

3.A.2.2: Transportation

Pipeline Infrastructure: Most CO_2 pipelines are built organically, responding to localized, economic opportunities to transport CO_2 from a source to an oil and gas field for enhanced oil recovery or, in a few cases, to dedicated (non-EOR) geologic storage. A comprehensive, interstate pipeline infrastructure with trunk lines is necessary to significantly scale up CO_2 transportation.

The regulatory authority that oversees pipeline safety depends on whether a pipeline is intrastate or interstate. Interstate pipeline safety is handled by the Department of Transportation Pipeline and Hazardous Materials Safety Administration. Intrastate pipeline safety and permitting is handled by the Kansas Corporation Commission.

Significant capital costs are required for an interstate CO_2 pipeline in the Midwest. The level of investment required may be accomplished through a public-private partnership. An economic study of an industry-only financed pipeline system questions whether it could be economically viable (Edwards and Celia, 2018).

Obtaining Right of Way is a non-trivial task, as each Kansas county may have its own procedures and individual landowners would need to be located and contacted and right-of-way leases obtained. If the CO_2 pipeline is determined to be a public utility, eminent domain would be an option, if necessary. A counselor with the Kansas Corporation Commission indicated a pipeline must be in the public interest to be considered a public utility.

Geologic Storage of Anthropogenic CO_2 in the Public Interest. The team discussed an option to recommend that the State of Kansas declare geologic storage of anthropogenic CO_2 to be in the public interest. That would make a CO_2 pipeline potentially eligible as a public utility pipeline.

Common Carrier Pipelines: The team discussed with stakeholders the possibility of designating a private pipeline as a common carrier. North Dakota, Minnesota and Colorado allow private pipelines to be common carriers, to provide that service without discrimination and at a reasonable cost.

Ownership and Liability During Transport: The CO_2 ownership could be established through a business model or a public utility model. A business model would involve a contract between private parties that assigned ownership, specified at which point that transfer occurred, and assigned risks to each party. The contract would specify costs for CO_2 treatment and processing, compression, and regulatory compliance such as LDAR (locating and repairing leaks along the pipeline system).

Under current statutes, the title to the CO_2 stream likely falls under K.S.A. 65-3418, vesting of title to solid waste, or K.S.A. 65-3442, vesting of title to hazardous waste. CO_2 would likely fall under the solid waste statute. If that is the case, the generator could be responsible for any risks associated with the CO_2 throughout the capture and transportation phases.

Using a public utility model, the utility would assume responsibility for transportation of CO_2; the same public utility potentially could also inject and geologically store the CO_2.

3.A.2.3: Injection and Storage

Class VI Well Permits: The Kansas Geological Survey's experience in obtaining a Class VI well permit from the EPA was a slow, intensive, and expensive process with several requests for additional tests and monitoring. The KGS sought a permit for a proposed pilot project with relatively small quantities of CO_2 to be injected. The KGS experience was not unique, as reflected in the very few numbers of approved Class VI well permits issued in the United States. The State of North Dakota sought and, after several years, received primacy for issuing Class VI well permits.

Suggestions for improving the well permitting process:

1. Establish different characterization, monitoring and insurance requirements for a pilot project with relatively low quantities of CO_2 to be stored versus a commercial-scale geologic storage site.
2. Streamline communications to allow more reviews and discussions between the applicant and the regional EPA office. In the KGS experience, all discussions and decisions were routed from the regional office through the EPA headquarters in Washington, D.C.
3. Re-evaluate the PISC (post-injection closure period) requirements. Currently post-closure monitoring is required for 50 years.
4. Have guidance performance-based monitoring. For example, low movement within the

parameters of modeled behavior over 10 to 15 years would likely indicate low risk.

Pore Space: Pore space ownership for geologic storage of carbon dioxide has been debated in the Kansas Legislature (House Committee on Energy, 2011; Joint Committee on Energy and Environmental Policy, 2011, 2012; Senate Natural Resources Committee, 2012). Kansas does not have a statute clarifying ownership. The states of Montana, North Dakota and Wyoming have all declared pore space ownership in statute. Two models could be used to establish pore ownership: Ownership could vest with the owner of the mineral right, or it could vest with the landowner. If ownership is vested with the landowner, policy makers would need to decide whether pore space ownership could be severed through sale or leasing. Pore space ownership is an issue when considering the potential for CO_2 migration off site as well as for storage compensation and liability. Kansas case law in the context of disposal of saltwater establishes that the surface owner owns the pore space.

Pooling of Pore Space: Kansas does not have statutes for the unitization of pore space for CO_2 storage. There is not compulsory pooling in Kansas. There are statutes for pooling of one or more oil and gas reservoirs in communication where pressure in one part of the pool would affect pressure throughout the pool (§ 55-1300 series). State approval for unitization of oil or gas reservoirs requires approval by the working interest owners that would pay at least 63% of the costs of the unit operation and have at least 75% of the production, and options for payment of costs by and profits to nonworking owners. For CO_2 storage, the level of approval by landowners may need to be reviewed to obtain sufficient reservoir space.

Ownership and Liability: The site injection and storage ownership could be established through a business model or a public utility model. Under a business model, a contract between private parties would establish ownership of and liability for the CO_2, indicate at which point that transfer occurs, and assign risks to each party. A public utility model may own the entire process.

A mix of the two models is also an option, wherein a private contractor would inject and store the CO_2. At post-injection site closure (PISC), the site would be monitored for a period of time, perhaps 10 years. If the CO_2 plume moved within model parameters during that time and met criteria upon which the state agreed, the site would be considered to have acceptably low risk. The closed site would then be transferred to the state for long-term stewardship. Several states have adopted this option, which was supported in the 2009 Midwestern Governors' Association CCS Inventory.

For the Kansas Corporation Commission to ultimately take ownership of a CCS site, the Carbon Dioxide Injection Well and Underground Storage Fund (K.S.A. 55-1638) must contain enough funds to cover such activities as monitoring and long-term remedial activities.

Kansas has a carbon dioxide reduction act (K.S.A. 55-1636), for which regulations were developed but later revoked. A statute that states carbon capture and geologic storage would be in the public interest would support development of a public utility model. Several states, including North Dakota (Chapter 38-22, 38022-01), have statutes declaring it is in the public interest to promote the geologic storage of carbon dioxide.

Subtask 3.1: Identify challenges and develop a plan to address challenges for CO_2 capture from anthropogenic sources

Contributors to Subtask 3.1 include Krish Krishnamurthy, Makini Byron and Martin Dubois.

The object of Phase I is to evaluate commercial-scale capture and storage (50+ million tonnes captured and stored in a saline aquifer). Although no time frame was defined by FOA15824 for the processing of 50 million tonnes, the ICKan project set 2.5 million tonnes/year over a 20-year period as a target.
In this section, we provide an overview of the three facilities evaluated for CO_2 capture, the technical

challenges unique to each and a preliminary plan to address the challenges. Plant configuration, operating conditions and preliminary engineering design plans are presented in Task 5 of this report.

Overview

Three candidate sources, two coal-fired power plants and steam methane reformers at a refinery were evaluated for their potential to economically capture 50 million tonnes of CO_2 (Figure 3.1). The Linde Group and other ICKan personnel made site visits to three of the potential CO_2 sources in Kansas—Jeffrey Energy Center, Holcomb Station, and CHS Refinery—to establish relationships with the operations personnel, familiarize them with the goals of the ICKan project, tour the facilities, and gain an understanding of the physical plant and operations.

- **Westar Energy Jeffrey Energy Center**, a large coal-fired power plant, is located in St. Marys, Kansas. The plant is composed of three separate 800 MWe (megawatt electric) units with annual CO_2 emissions on the order of 12.5 million tonnes. The units were built in the 1980s but fitted in the past decade with selective catalytic reduction (SCR) based NOx removal, activated carbon sorbent-based Hg removal and scrubber-based flue gas desulfurization (FGD). This plant is capable of delivering the entire CO_2 capture volume targeted for ICKan, 50 million tonnes, through partial carbon capture of flue gas from one of the three units (~350MWe).
- **Sunflower Electric Power Corporation's Holcomb Station** is a single 348 MWe_e unit (387 MVA; 0.9 PF) located in Holcomb, Kansas. This subcritical power plant began operation in 1983 and uses low sulfur, sub-bituminous coal from the Powder River Basin (PRB) in Wyoming. The plant is fitted with environmental controls including low-NO_X burners, over-fire air (OFA), a powdered activated carbon (PAC) injection system, a dry scrubber and baghouse. The Holcomb Station presents an opportunity to perform a full CO_2 capture installation that will deliver a total of 30 million tonnes of CO_2 for sequestration or utilization over a period of 20 years.
- **CHS, Inc. Refinery, McPherson, Kansas**. The largest potential single-point sources for CO_2 at CHS refinery in McPherson, Kansas, are two steam methane reformer (SMR) based hydrogen plants that yield approximately 760,000 tonnes of CO_2 per year (~30% of the ICKan project current annual target). The refinery also has other CO_2 emissions, mainly from boilers and fired heaters, that total approximately 624,000 tonnes/year. However, these sources are distributed throughout 27 locations within the refinery, with the largest (the CO boiler that treats the Fluid Catalytic Cracker (FCC) regenerator gas) producing just 150,000 tonnes/year. The potential volume of CO_2 capture is about one-third of that required to meet the 50Mt goal over a 20-year timeframe. However, it might be a significant contributor if considered as part of a multi-facility capture system.

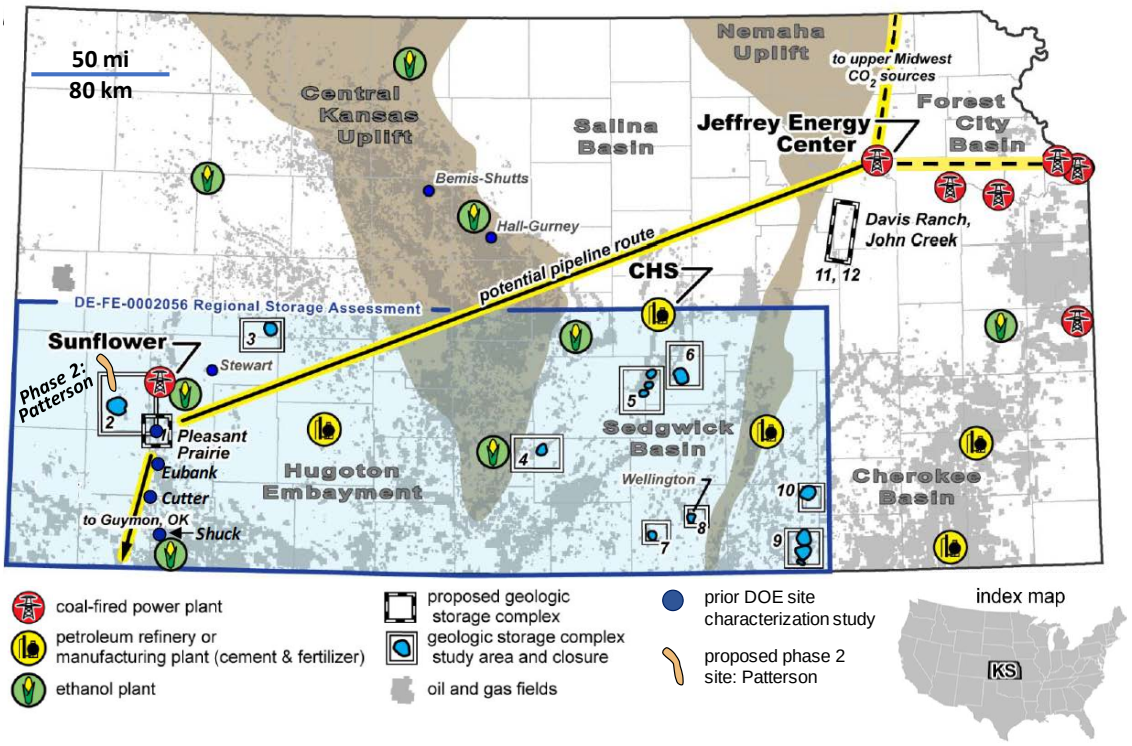

Figure 3.1. Kansas map showing location of the Patterson site, a variety of CO_2 sources, possible CO_2 pipeline routes, other possible CO_2 injections sites (numbered 1–12) identified in Watney et al. (2015) located inside the DE-FE0002056 study areas (blue), and oil fields (gray). The primary sources in this study are labeled. The figure is modified from ICKan proposal SF 424 R&R, 2016 (Watney et al., 2016).

Site Related Challenges

An in-depth discussion with the operations and facilities support staff at the three locations identified a number of key challenges that will need to be addressed for successful completion of project goals. Table 3.1 shows a summary of the challenges identified for CO_2 capture from this study's sources. The table also contains a preliminary action plan to address these challenges.

Table 3.1. Challenges and mitigations for CO_2 capture from identified anthropogenic sources

Location	Challenges	Mitigation Plans
Westar Jeffrey Energy Center	• Lack of baghouse may contribute to aerosol formation in flue gas and solvent carry-over/losses from the column.	• Measure particle size distribution and evaluate the impact of particles on amine carry-over. Make provisions toward reducing aerosol particles in the flue gas at source.
	• The long-term capacity of the power plant to use coal may be a concern due to cheap natural gas and increasing wind power generation.	• Continue to monitor fuel mix in Westar's energy portfolio. Select a carbon capture solution also applicable to natural gas emissions.
	• Heat recovery from identified waste heat sources present technical challenges for recycle.	• Thorough evaluation by Linde Engineering will determine appropriate heat exchanger design for feasible heat extraction.

Sunflower Holcomb Station	• Long-term power plant utilization may be low or variable due to dynamic market power pricing and competing sources of power generation such as cheap natural gas and/or renewables.	• Install a partial capture system that will meet anticipated minimum power plant utilization at turndown rate.
	• Maximum total CO_2 captured at full capacity (1.7Mt/yr) is unlikely due to electricity market conditions, falling short of the 50Mt project requirements.	• Combine CO_2 captured from nearby ethanol plants with CO_2 captured from power plant.
	• Because of the large PCC parasitic load (both steam and power demand), direct power purchase from the site may not be possible due to Kansas electricity regulations.	• Purchase wholesale power from the Southwest Power Pool (SPP) market at market rates. • Consider parasitic load mitigation alternatives such as a NGCC Cogeneration or a Packaged Air Boiler (PAB) system for low-pressure steam generation and auxiliary power. Both would generate excess power to be exported to the grid and may cover cost of installation.
	• Limited cooling water supply potential and strained waste water basin(s) capacity.	• Discuss viable options with the Kansas water authority, including closed loop cooling and air-cooling systems. These will require additional capital investment.
CHS Inc. Refinery	• Refinery CO_2 emissions distributed throughout facility and in small amounts and there is little opportunity to capture excess heat from current operations.	• Combine flue gas from the two reformers for option of largest scale capture. This flue gas (~ 300°F) will also provide waste heat that can be used by the capture process, if appropriate.
	• Total CO_2 emissions from plant does not meet project's target for sequestration and utilization over time period.	• Combination of SMR H_2 plants with other industrial capture including ethanol (fermentation) sources may provide improved overall economics.
	• Refinery is short on steam with sources distributed throughout the facility.	• Additional steam generation from a new gas-fired boiler is being considered for refinery needs as well as generation of low-pressure steam for solvent reclamation in capture process.
	• Availability of excess utilities for CO_2 capture is unfavorable – solvent-based technologies use steam for CO_2 regeneration, Pressure Swing Adsorption (PSA)/Vacuum Swing Adsorption (VSA) sorbent-based technologies require electric power to drive the compressor or vacuum pumps.	• The choice of CO_2 capture technology will take into account the availability of steam and power in the reformer as well as the economics of capture.

Additional Challenges
In addition to the site-related challenges listed in Table 3.1, other concerns must be addressed if large-scale CO_2 capture is to be realized at any of these sites. These challenges are multidimensional, overlapping with transportation and storage, and are therefore covered in other parts of the report, including in the Task 3 discussion of non-technical challenges, and in the overall implementation plan.

- Coal-fired power in Kansas, and throughout the Southwest Power Pool, has been substantially and increasingly displaced by wind power, creating concern about the long-term viability of the CO_2 sources. Economical, large-scale capture of CO_2 could help extend the life of the power plants to maintain diversity in the power portfolio.
- Jeffrey Energy Center could easily provide the volume of CO_2 required from a slip stream from one of its three 800 MWe generators. However, it is located several hundred miles from the more favorable injection sites. Nearby geologic sites—Davis Ranch and John Creek fields, 50 miles distant—appear to be capable of storing a maximum of 25Mt. Under certain conditions, there could be a case for CO_2 capture at 2.5Mt/yr, and transportation to a larger, regional trunk line.
- The maximum CO_2 that could be captured at the Holcomb Station facility (1.7Mt/yr) would fall short of the 50Mt target over a 20-year period. It would, however, meet the target if considered over a 30-year period. Holcomb Station is ideally located in close proximity to viable saline aquifer storage sites.

Summary
The team has identified three CO_2 emission sources that can potentially deliver the target CO_2 volumes for the ICKan EOR utilization/geological storage sites: two coal-fired power plants and one industrial emissions source. The feasibility of a commercial-scale CCS project at each site has been assessed, including the unique challenges and best fit technology solution. Though proven technologies can address each capture scenario, other factors such as the plant configurations, projected operating conditions, and regulatory uncertainty challenge the economic viability of a commercial CCS project at each of these sites. The team has created preliminary action plans to address these challenges and has discussed how these mitigations will advance the successful completion of project goals.

Subtask 3.2: Identify challenges and develop a plan to address challenges for CO_2 transportation and injection

Contributors to Subtask 3.2 include Martin Dubois and Dane McFarlane.

Subtask 3.2.1: Technical challenges for CO_2 transportation

Because large-scale coal-fired power plants, capable of supplying the requisite amount of CO_2 for a 50 Mt project, are distant to potential storage sites, pipelines are the only option for transporting large volumes of CO_2. Smaller, more disparate ethanol plant sources considered as alternatives or as a means to enhance the economics of a larger CO_2 transportation through economies of scale would also be best served by pipelines. Compressing CO_2 to a supercritical state and transporting it via pipelines is the most cost-effective manner in which to transport large volumes. Because of the long history (40+ years) of CO_2 transportation, and even a longer history of transporting high-pressure natural gas, there are no significant technical challenges to transporting CO_2 via pipelines. Non-technical challenges are covered separately in Subtask 3.A.

Subtask 3.2.2: Technical challenges for CO_2 injection

Similar to transportation, CO_2 injection into geologic reservoirs in a super critical state is proven technology after 40+ years in enhanced oil recovery. There are no significant challenges to the actual injection into saline aquifers. Non-technical challenges are covered separately in Subtask 3.A.

Subtask 3.3: Identify challenges and develop a plan to address challenges for CO_2 storage in geologic complexes

Contributors to Subtask 3.3 include Martin Dubois, Eugene Holubnyak, Tandis Bidgoli, Mina FazelAlavi, David Newell, and Jeffrey Jennings.

The KGS shall evaluate candidate geological complexes for technical risks (capacity, seal, faults, seismicity, pressure, existing wellbores), economics (location/distance, injectivity, availability), and legal (pore space rights, liability) and document the results in a plan.

Subtask 3.3.1: Overview

Two geologic complexes identified in the initial proposal as potential sites for storing >50 million tonnes (Mt) are the Pleasant Prairie field geologic site, considered the primary storage site in the proposal, and the Davis Ranch and John Creek fields, in the Forest City Basin storage complex (FCB), in combination, considered a secondary site (Figure 3.1). Preliminary capacity evaluation for the FCB site indicated it is probably not capable of storing >50Mt CO_2 (Bidgoli and Dubois, 2017a). In the process of evaluating the Pleasant Prairie site, four separate geologic structures were identified as each having potential for storing 50Mt. The four structures, aligned on the same regional geologic structure, are similar in size, have >100 ft of closure, and have similar geologic histories. The four potential sites—Rupp, Patterson, Lakin and Pleasant Prairie—are situated in what we have named the North Hugoton Storage Complex (NHSC) (Figure 3.2).

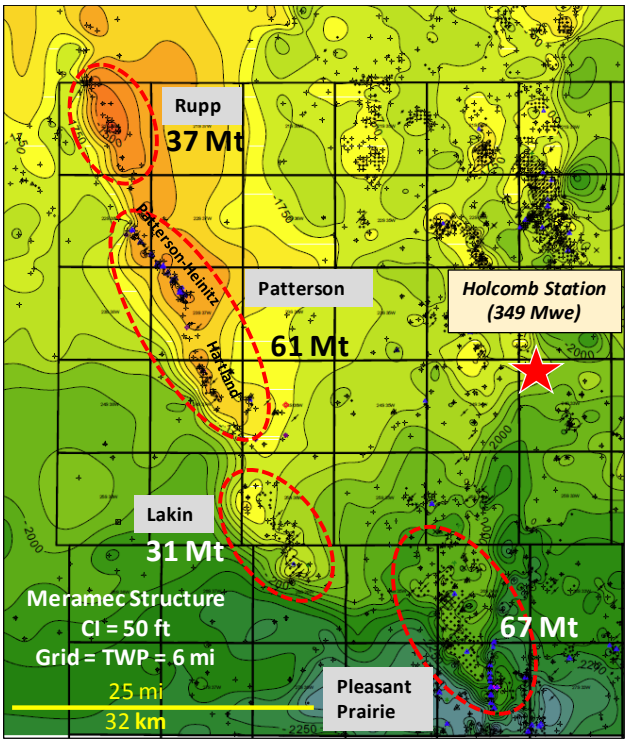

Figure 3.2. Location of four plausible storage sites within the North Hugoton Storage Complex. Map is the structure on the top of the Meramec (Mississippian). Patterson is the primary site for Phase II and the others are alternative sites. Annotations (e.g.: 61Mt) indicate volumes of CO_2 "stored" in numerical simulations of CO_2 injection.

Subtask 3.3.2: Capacity, injectivity and pressure

The Patterson site is one of several geologic sites that has been demonstrated by initial simulation analysis to be capable injecting and storing 50Mt of CO_2 in a 25- to 30-year timeframe (see Task 4 report). However, the analyses in this study are based on limited subsurface well, core, and injectivity data, and in the case of the Patterson, no seismic data. Considerable additional data need to be collected and technical analysis performed to validate the Patterson site. Key questions that need to be resolved are 1) the geometry of the Patterson site structure, hence potential volume of CO_2 stored, 2) injectivity in the target reservoirs, in particular in the Osage, and 3) integrity of the caprock and seals. The current model (see Task 4 report) was built without the advantage of having 3-D seismic to locate the bounding fault on the southwest side and knowing the overall geometry of the geologic structure. Questions remain about the injectivity and capacity at the site, particularly in the Osage. Closest core analysis in the Osage suggests low permeability, despite porosity in the range of 25–30%. There is currently no geo-mechanical nor capillary pressure data for the caprock seals for the reservoirs, although indirect data discussed below suggest that the seals are effective to the vertical migration of hydrocarbons and mixing of brines.

Depth and reservoir pressure are critical for reservoir storage injectivity and capacity, as well as risk of loss through seals, faults and potential wellbore integrity issues. Primary storage zones in the Patterson site, Osage, Viola and Arbuckle are at ideal depths (5,260–6,340 ft) and exhibit favorable reservoir pressures (Table 3.1). Depths are average depths at the Patterson site, reservoir pressures are based on sparse drill stem test data in the area, and reservoir temperatures are based on bottom hole temperature data from 1,734 well logs from a 16-township area around the Patterson site, adjusted upward by 5 degrees F to account for cooling effect from drilling.

Depths and temperature ensure CO_2 injected will be at conditions well above CO_2 supercritical state and at optimally high density, optimal for efficient use of storage space. The three targeted reservoirs are naturally under-pressured—the reservoir pressure is significantly below calculated hydrostatic pressure, assuming a brine density that yields a pressure gradient of 0.43 psig/foot of depth. The reservoir pressures are tied to their outcropping elevations on the Ozark Plateau, nearly 400 miles to the east (Watney et al., 2015). In reservoir simulations (see Task 4 report), the maximum injection pressure was purposely kept below hydrostatic pressure, and well below estimated rock fracture pressure calculated using a gradient of 0.75 psi/foot of depth (Table 3.1). Simulation injection pressures average 55% of calculated fracture pressure. The difference between injection pressure and current reservoir pressure (delta P) is 600 psi, aiding in the injectivity.

Reservoir pressures, temperatures and depth are ideal at the Patterson site. There is substantial room for increasing injection pressure if needed. Pressure is not likely to be a significant risk to the project.

Table 3.1. Patterson site targeted injection reservoirs and respective depths, properties and simulation maximum injection bottom-hole pressures (BHP). PSIG = pounds per square inch gauge; MD = measured depth; C = Celsius; F = Fahrenheit.

	Injection Interval		
Properties	**Osage**	**Viola**	**Arbuckle**
Reservoir Temperature (C/F)	60C (140F)	61C (142F)	62C (144F)
Formation Top (MD - ft)	5,260	5,500	5,740
Middle of Formation (MD - ft)	5,330	5,600	6,040
Formation Base (MD - ft)	5,400	5,700	6,340
Reservoir Pressure (psig)	1,650	1,700	1,800
Normal Hydrostatic Pressure (psig)	2,292	2,408	2,597
Estimated Fracture Pressure (psig)	3,998	4,200	4,530
Max. Injection BHP (psig)	2,250	2,300	2,400

Subtask 3.3.3: Seals and caprock

Subtask 3.3.3.1: General description of seals (caprock) and baffles

Protecting underground sources of drinking water (USDW) and/or escape of CO_2 the surface is a primary objective. The Patterson site is situated on the very edge of a major source of irrigation and drinking water in southwest Kansas, the High Plains aquifer, or the Ogallala (Figure 3.3).

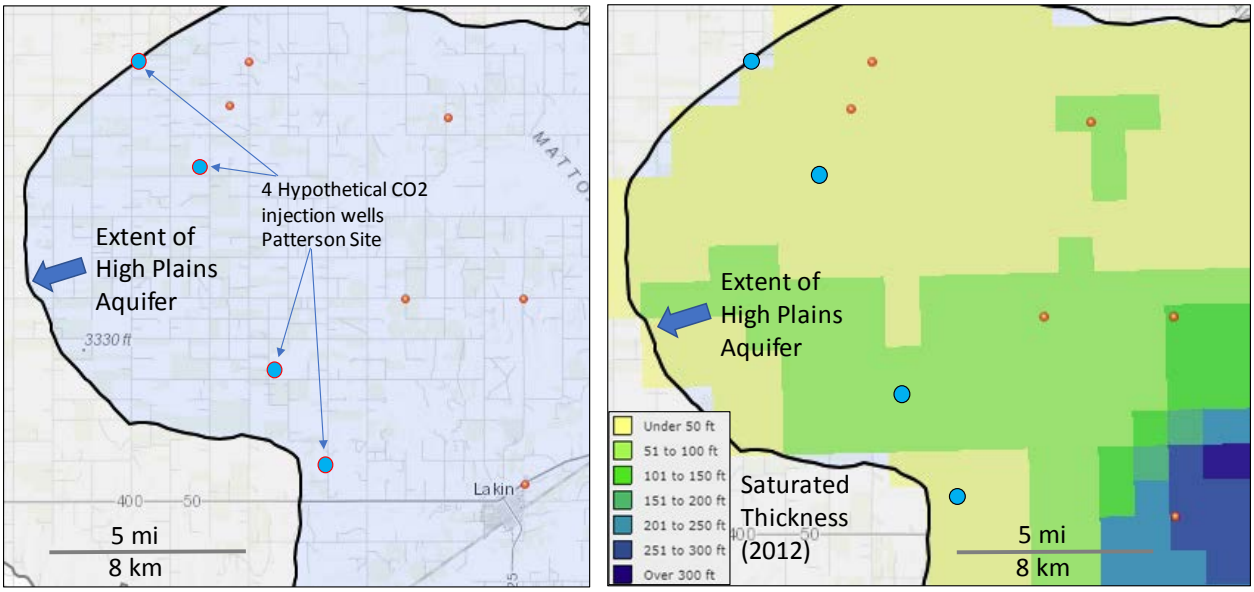

Figure 3.3. Plats showing the extent and thickness of water saturation in the Ogallala formation of the High Plains aquifer. The location of four hypothetical CO_2 injection wells in the Patterson site are shown as blue dots.

Multiple seals (caprock) and baffles above the three targeted saline aquifer storage zones, Mississippi Osage, Ordovician Viola, and Cambrian-Ordovician Arbuckle, could provide barriers to vertical migration of CO_2 (Figure 3.4). Tight carbonate intervals separate the three target zones and act as

caprock, or at a minimum, baffles, based on reservoir simulations. Statistics for the High Plain aquifer, caprock and saline aquifers are provided in Table 3.2.

Most of the stratigraphic column in the Patterson site can be traced across the midcontinent and from one basin to another. In Table 3.2, under the column labeled Extent, "Basin" means that the stratigraphic interval extends across the Anadarko Basin and Hugoton Embayment but is not present atop major structural features that separate basins such as the Central Kansas Uplift (Figure 3.1) due to erosion beneath unconformities. Most of the intervals identified as having basin-wide extents are also present in adjacent Salina and Forest City basins. "Inter-basin" intervals, in general, can be traced continuously from the Patterson site across major structural features from one basin to another.

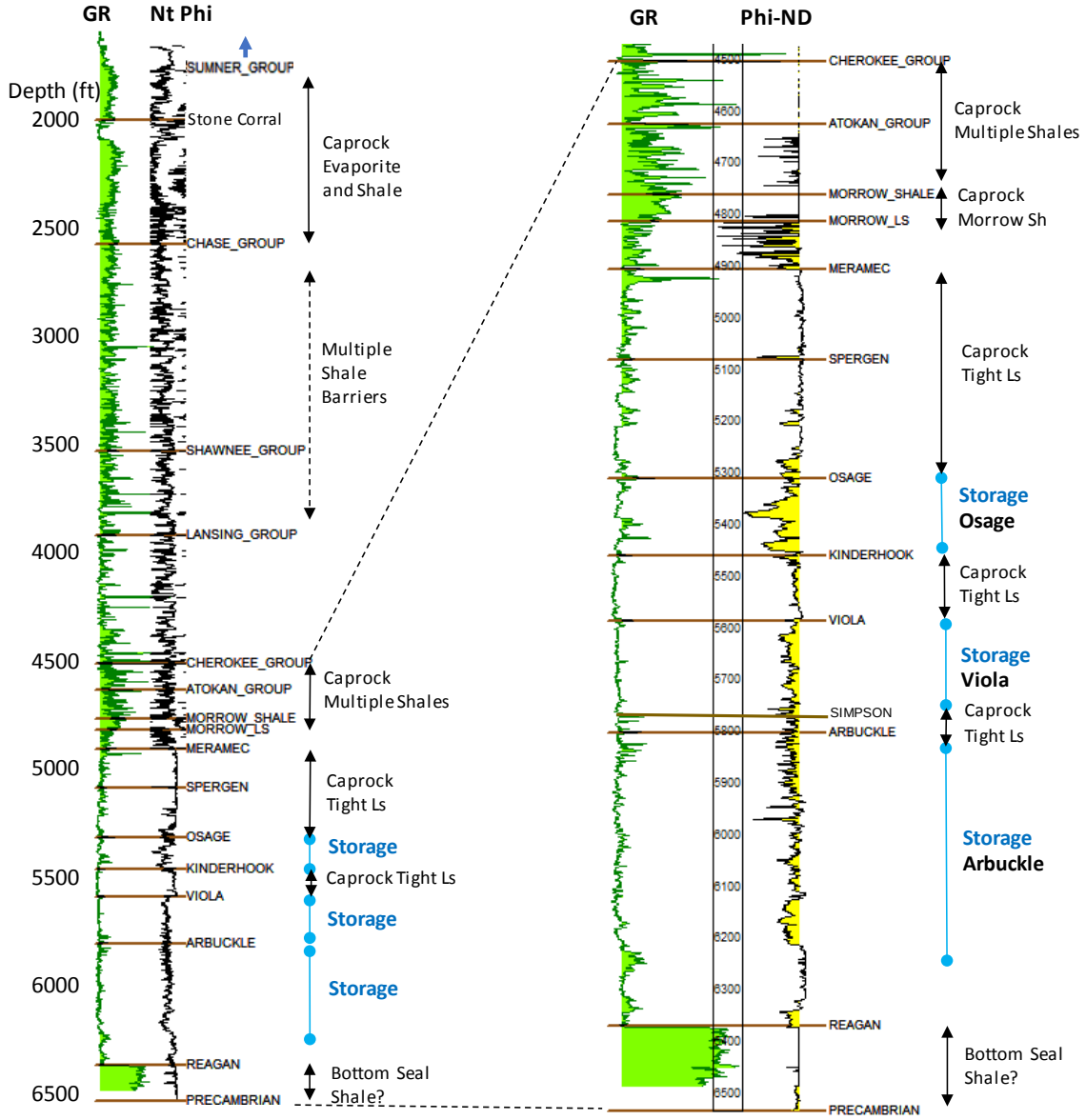

Figure 3.4. Stratigraphy of the Lower Paleozoic and proposed storage zones illustrated by a wireline log from a key well in the Patterson site, the Longwood Gas Unit #2 well. Tight carbonate baffles separate storage units from one another. Porous intervals (>8% porosity) are shaded yellow and shale intervals are shaded green. Left—full column from beneath surface casing to TD. Right—enlarged portion for details.

Table 3.2. Statistics for the High Plain aquifer, caprock and saline aquifers at the Patterson site.

Interval	Depth - top (ft)	Thickness	Depth Below USDW (ft)	Extent	Lithology
Base of Ogallala - *High Plains Aquifer - USDW*	250	0-100 ft saturated		Region	sand and conglomerate
Sumner Group	1,600	950	1,350	Basin	salt, anhydrite, shale
Upper Pennsylvanian	3,050	600	2,850	Inter-basinal	interbedded shale and limestone
Cherokee-Atokan	4,500	250	4,250	Inter-basinal	interbedded shale and limestone
Morrow Shale	4,750	50	4,500	Basin	shale
Meramec	4,900	180	4,650	Basin	tight limestone
Spergen-Warsaw	5,080	220	4,830	Basin	tight limestone
Osage *- Saline Aquifer*	5,300	150	5,050		porous cherty dolomite and limestone
Kinderhook	5,450	130	5,200	Basin	tight limestone
Viola *- Saline Aquifer*	5,580		5,330		porous cherty dolomite
Simpson	5,770	30	5,520	Basin	tight limestone. thin shale
Arbuckle *- Saline Aquifer*	5,800		5,550		porous cherty dolomite
Reagan	6,370	160	6,120	Basin?	shale, sandstone, granite wash
Precambrian	6,530		6,280	Inter-basinal	granite

From bottom to the top, a general description of the seals that would prevent vertical migration of CO_2 are given below:

- *Reagan*. Little is known about the Reagan, which separates the Arbuckle from the Precambrian granite, because of the very few well penetrations in the region, one of which is in the Patterson site model area.
- *Simpson and Kinderhook.* Low porosity and low permeable carbonate rocks separate the Arbuckle, Viola and Osage saline aquifers and are likely baffles, if not barriers, to vertical migration of CO_2.
- *Spergen, Warsaw and Meramec*. Approximately 450 feet of mostly tight (low porosity and permeability) cap the Osage-Viola-Arbuckle saline aquifer forming at a minimum a baffle, and possibly a caprock seal. In this long interval, there are scattered porous and permeable zones—the oil productive St. Louis C zone, for example—but they are demonstrated by the static geomodel to be discontinuous.
- *Morrow Stage.* The interval between the top of the Morrow to the top of the Meramec varies considerably in thickness, with the Mississippian-aged Chester limestone and sandstone

thickening off-structure and absent atop the structures due to erosion. The Morrow shale above the Chester is a regional seal for oil and gas reservoirs in the Morrow and Chester.

- *Cherokee Group and Atoka Stage.* Although thin, 5–10 ft, numerous basin to inter-basin scale shales in the Cherokee and Atoka groups could act in combination as seals, or at a minimum as baffles to vertical migration of CO_2.
- *Upper Pennsylvanian.* Similar to the Cherokee and Atoka, numerous basin- to inter-basin scale shales could act in combination as seals, or at a minimum as baffles, to vertical migration of CO_2.
- *Sumner Group (Permian).* Thick, laterally extensive (basin-wide), anhydrite and salt layers in the Sumner group form the ultimate seal for the basin. They are the top seal for the giant Hugoton and Panoma fields stretching across much of Southwest Kansas and the Oklahoma and Texas panhandles.

Subtask 3.3.3.2: Indirect evidence for effectiveness of seals

Physical measurements testing the soundness of the tight carbonate and shale seals in the Patterson project area, such as geomechanical and capillary pressure measurements are non-existent. However, there are several indirect lines of evidence supporting their ability to prevent the vertical movement of fluids.

Seals for oil and gas reservoirs—Oil and gas is produced from dozens of stratigraphic intervals in the Permian, Pennsylvanian and Mississippian spanning a gross interval of nearly 2,500 ft (2,600–5,100 ft). Production is from porous sandstone and carbonate reservoirs, all having effective caprock seals with at least regional lateral extents. The Morrow shale is the top seal for the oil trapped in the Morrow sandstone in the Patterson-Heinitz unit. It is also the top seal for the Chester sandstone reservoirs in the Pleasant Prairie, Eubank and Shuck fields, located 25–50 miles southeast of the Patterson site. In those fields the incised valley fill Chester sandstone is filled to the spill point where the reservoirs "cross" major structural features. The average oil and gas column height averages 120 ft (Dubois et al., 2015a, 2015b, 2015d), demonstrating the seal has capillary pressure properties to support a hydrocarbon height of a *very minimum* of 120 feet. The shallow Chase and Council Grove gas reservoirs are a part of the giant Hugoton and Panoma gas fields. Dubois et al. (2007) demonstrated that the Chase and Council Grove have a common free water level that supports a gas column height of 500 feet, sealed by the thick evaporite layers in the Sumner Group.

Caprock entry pressure and CO_2 column height inferred from KGS-Cutter #1 (science well)—The KGS-Cutter #1 well is a science well drilled as part of the KGS-managed DOE-funded project, Modeling CO_2 Sequestration in Saline Aquifer and Depleted Oil Reservoir to Evaluate Regional CO_2 Sequestration Potential of Ozark Plateau Aquifer System, South-Central Kansas (DE-FE0002056). A robust data set was collected in the well located approximately 50 miles southeast of the Patterson site, including extensive core and modern wireline well logs including nuclear magnetic resonance. Although 50 miles distant and the reservoirs and caprock being slightly deeper than they are in the Patterson site, the stratigraphic intervals of interest can be easily correlated and have similar properties (porosity and gamma-ray).

Capillary entry pressure was calculated using the NMR module of the petrophysics application Techlog^{TM}, a Schlumberger product. In a process described in more detail in Appendix E, capillary entry pressure was calculated by 1) a correlation that relates pore throat radius (r_{neck}) to R35 Winland (SPE-181305-MS) 2) NMR capillary pressure module where pore size (T2 distribution) is converted to pore

throat radius as a function of capillary pressure using a proportionally constant Kappa (K) according to the following relationship proposed by Volokin et al. (2001):

$$K = \frac{P_c}{T_2^{-1}} = \frac{2\sigma \cos\theta R_{pore}}{\rho r_{neck}}$$

Where,

K=Kappa
ρ=NMR surface relaxivity
σ = Interfacial tension
θ = Contact angle
r_{neck}= pore throat radius
R_{pore} = pore body radius

The minimum capillary entry pressure of cap-rock was then used to estimate the height of CO_2 column that can be trapped by cap-rock, also called sealed capacity. Therefore, the column of CO_2 determines whether CO_2 enters the cap-rock or not. The equation to estimate the height of CO_2 is:

$$h = P_e/(\rho_w - \rho_{CO2})g$$

Where,

h=Height of CO_2 column that can be trapped by cap-rock

P_e= Capillary entry pressure

ρ_w= Density of brine at formation P-T

ρ_{CO2}=Density of CO_2 at formation P-T

g= Gravity

Caprock intervals above the Osage and separating the Osage from the Viola were identified as having an entry pressure of 100 psi or greater, sufficient to hold a CO_2 column height of a calculated 367 feet. Shallower intervals at 5,000–5,100 feet in the Lower Pennsylvanian, a thousand feet above the Osage, appear to have equally high entry pressures.

Water geochemistry—Varying salinities between the main injection zones as well as with porous intervals above the Mississippi suggest that the target injection zones (Osage, Viola and Arbuckle) are isolated. There is likely no natural communication between them, nor communication with porous zones in the Upper Mississippi and shallower stratigraphic intervals. Water salinities from a total of 19 wells in the Pleasant Prairie, Lakin and Patterson site are from three sources: the Kansas Geological Survey on-line brine database, salinity analyses reported for water recovered in drill-stem tests, and salinity determined from geophysical well logs using the methodology outlined by Doveton (2004). Details of the analysis is provided in Appendix F.

Subtask 3.3.4: Existing wellbores

Information on wellbores penetrating the primary caprock units was compiled to assess the potential need for corrective action to prevent CO_2 leakage via surrounding wellbores. This included compilation of well type, construction, date drilled, location, total depth (Table 3.3). Although 419 wells were found to fully

penetrate the Sumner Group caprock (436 wells in Table 3.3, less the 17 cathodic protection wells), only 133 of these wells penetrate the Upper Pennsylvanian, Cherokee-Atoka and Morrow caprocks, and only seven wells penetrate the target storage zones in the Osage, Viola, and Arbuckle. Figure 3.5 shows the location of the wells within the Area of Interest, including the seven that penetrated at least to the Osage.

Table 3.3. Information on wellbores within the area of interest.

Well Type	Well Status	Well Count	Mean Total Depth (ft)	Total Depth Range (ft)	Mean Completion Year	Completion Years (Range)
Cathodic Protection	Unknown	17	161	50-300	2006	1999-2010
Dry Hole	Dry and Abandoned	59	4,675	860-5,928	1986	1941-2014
Shallow Gas	Producing*	234	2,956	2,584-5,190	1976	1946-2005
	Plugged and Abandoned	21	3,007	2,631-5,100	1970	1946-1993
	Shut In	33	3,304	2,675-6,534	1981	1975-2008
Oil	Producing	34	5,125	4,782-5,783	1987	1941-2005
	Plugged and Abandoned	7	5,025	4,760-5,190	1981	1941-2005
	Shut In	5	5,090	5,030-5,100	2000	1990-2013
Enhanced Oil Recovery - Injection	Active Injection	13	5,075	4,952-5,150	1994	1987-2016
	Plugged and Abandoned	0				
	Shut In	0				
Salt Water Disposal**	Active Injection**	10	4,686	2,600-6,500	1977	1956-2006
	Plugged and Abandoned	3	2,966	1,824-5,250	1963	1958-1963
	Shut In	0				

* Includes a handful of dry and abandoned deep, plugged back for shallow gas

** Includes 6500' City of Lakin Class V WDW

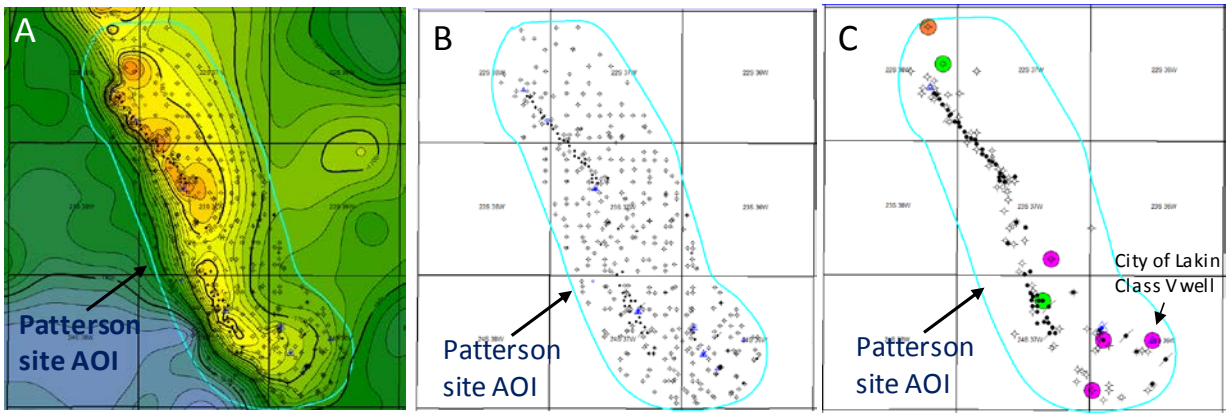

Figure 3.5. Plats showing wells within an area of interest (AOI) for the Patterson site. A. Plat showing the location of 419 wells within the AOI and the structure on top of the Meramec. B. Same plat without the structure map. Red well symbols are shallow gas wells. C. Plat showing the location of 133 wells that have penetrated at least through the top of the Morrow shale. Seven wells that penetrated the Osage are highlighted: Green—Osage only, orange—Osage and Viola, pink—Osage, Viola and Arbuckle.

Subtask 3.3.5: Faults and seismicity risks

3.3.5.1: Overview

A key challenge for commercial-scale injection and storage of CO_2 in Kansas and other parts of the central and eastern United States (CEUS) is the potential for injection-induced fault reactivation and seismicity. In recent years, such seismicity has been in the spotlight nationally and internationally, with the State of Oklahoma becoming the type example for the phenomenon. Since 2013, that seismicity has extended into southern and central Kansas. Between 2013 and the second quarter of 2017, two counties in south-central part of the state have experienced more than 2,500 earthquakes, with more than 100 of the events recorded as M 3.0 or greater (Figure 3.6). The largest of these earthquakes was the Milan M4.9 event on 12 November 2014, centered approximately 50 km SSW of Wichita, the most populous city in Kansas. The event had a shaking intensity (Modified Mercalli Intensity) of VII near the epicenter and was felt in states as far away as Alabama (>1,000 km; Figure 3.6).

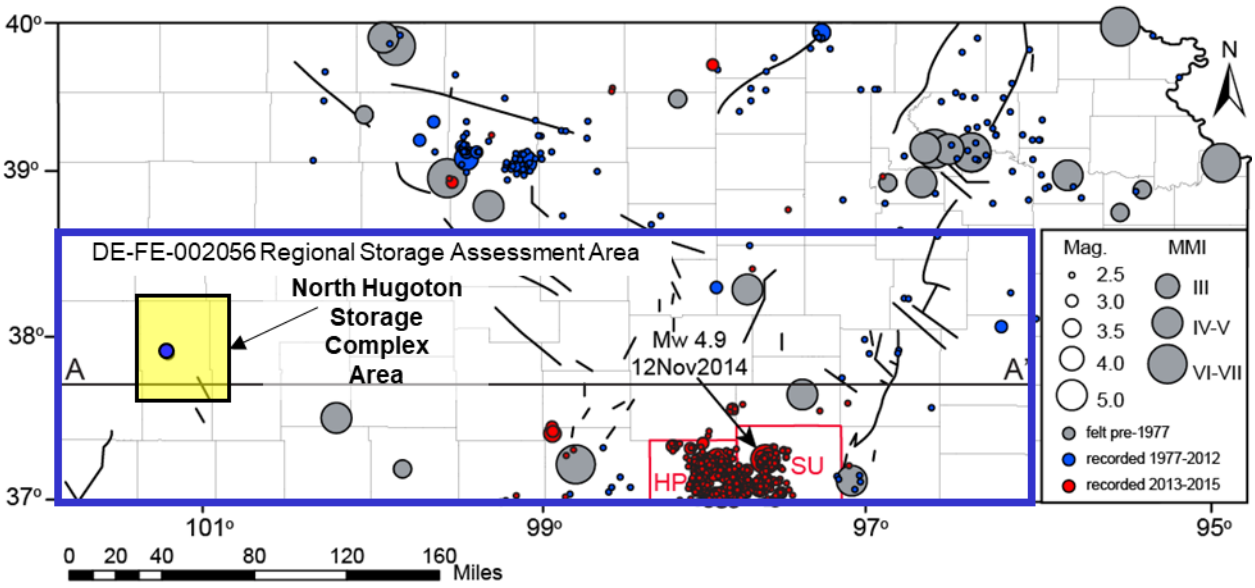

Figure 3.6. Map of Kansas showing historical (gray and blue) and recent earthquakes (red) and the North Hugoton Storage Complex area (yellow rectangle), the main focus of investigation for Phase I. Harper (HP) and Sumner (SU) counties, where recent (since 2013) seismicity is concentrated, are outlined in red. Black lines are NE-trending structures of the Nemaha Ridge-Humboldt fault zone and NW-trending structures of the central Kansas Uplift. Earthquakes from DuBois and Wilson (1978), Hildebrand et al. (1988), and USGS—National Earthquake Information Center.

The spatial and temporal association between the recent earthquakes and major injection operations into the Arbuckle Group, one of the target reservoirs in this study, has led the federal and state agencies, such as the USGS (Rubinstein et al., 2014; Benz et al., 2015; Ellsworth et al., 2015; Choy et al., 2016), Kansas Geological Survey (KGS; Bidgoli et al., 2015; Buchanan, 2015; Bidgoli and Jackson, 2017; Peterie et al., 2015; 2018), Oklahoma Geological Survey (Kroll et al., 2017; Walter, et al., 2017), and Oklahoma and Kansas Corporation Commissions, to conclude that these events are likely man-made or induced. Hazard mitigation steps are being taken through state-ordered reductions in disposal volumes (Langenbruch and Zoback, 2016; Yeck et al., 2017); however, large volume (>5,000 bbl/day) disposal is still active across much of the midcontinent. Thus, the potential for additional injection-induced earthquakes and their

associated effects/risks remains and is a critical issue for any commercial-scale injection operation within the State of Kansas.

For the North Hugoton Storage Complex, evidence of past seismicity in the vicinity of the Patterson site suggests that faults and associated seismicity are technical risks that must be addressed (Figure 3.6). The earthquake in question was a M3.0 earthquake that occurred on October 20, 1986. Though small, such an earthquake would likely be felt by any communities nearby. No additional seismicity has occurred since, suggesting that the earthquake may be a consequence of natural stresses in intraplate regions. However, further analysis is necessary to more robustly address risks associated with any subsurface faults and potential earthquakes.

3.3.5.2: Key technical and non-technical risks

Injection-induced fault reactivation and associated seismicity can be problematic for commercial-scale CO_2 injection and storage for a number of reasons. (1) Seismicity can pose a risk for CO_2 leakage through damage to seals that keep CO_2 in the subsurface. (2) Seismicity is likely a consequence of pore pressure changes that cause pre-existing faults to reactivate. Such pore pressure changes alter the stress state of faults and associated fractures and may leave them vulnerable to becoming leakage pathways or conduits for fluid flow. (3) Seismicity has the potential to damage well-bore casing, a common cause of fluid leakage at injection sites, and other critical infrastructure at or near injection sites. (5) Seismicity can pose a risk to the public, potentially damaging property and/or causing injury to people. (6) Seismicity, even small, low-magnitude earthquakes, can alter public perception and acceptance of a project.

Subtask 3.3.6: Economics

In comparison to the cost of CO_2 capture, compression and transportation to the Patterson injection site, the actual injection site capital and operating costs are relatively small on a $/tonne basis (see ”plans” at the end of this report’s sections covering Task 4, geologic sites; Task 5, sources; and Task 6, transportation). Reservoir modeling in Phase I (see Task 4) suggest that four injection wells are adequate if the complexity of multi-zone injection can be economically and technically managed. Whether fewer or more wells would be required should be determined to some level of certainty in Phase II. Regardless, the overall economic viability of a fully integrated CCS project (capture, compression, transportation, injection) are more dependent on the economics upstream of the geologic site and, importantly, the resolution of the non-technical challenges outlined in this report’s subtask 3.A.

Subtask 3.3.7: Risk mitigation plan

To address and mitigate the risks outlined above, it is necessary to complete detailed characterizations of potential injection/storage sites. Although much of these activities are covered under EPA’s site characterization guidelines for Class VI injection, critical elements to be evaluated for seismicity risks include developing a detailed understanding of the following:

1. injection reservoirs, baffles, and seals—their properties (porosity, permeability, saturations, etc.) and overall architecture, including lateral extents and stacking arrangement;
2. the area of interest (AOI), defined by injection activity, and likely spatial and temporal distribution of change in pressure;
3. subsurface faults and fractures, including their timing, spatial extents, and cross-cutting and fault juxtaposition relationships;

4. subsurface stresses, including stress orientation, stress magnitudes, and stress gradients (pore pressure, lithostatic stress, minimum horizontal stress, and maximum horizontal stress gradients);
5. stability of faults, including evaluation of reactivation potential and allowable thresholds for pore pressure increases; and
6. past earthquakes, including historical rates, magnitudes, and underlying causes.

In addition to these technical activities, early engagement and communication with the various stakeholders (e.g., local communities; local, regional, and state-level agencies; non-governmental organizations, etc.) through meetings, presentations, and literature may be helpful in mitigating issues associated with public perception and acceptance of a commercial-scale injection project and its potential hazards.

The degree to which each of the above items can be evaluated will, in large part, depend on the datasets available at the injection/storage site. Data needed for thorough investigation include:

1. 3-D seismic data to define the Patterson site structure's geometry for a more accurate estimation of the storage volume, map faults, fractures and possible karst sinkholes and their relations with the stratigraphy and underlying Precambrian basement;
2. drilling two wells to a depth of approximately 6,700 feet into the Precambrian basement and collecting extensive technical data;
3. collecting wireline logs (ideally modern log suites, including image and NMR logs) and core data (preferably full diameter core) to define reservoir and seal properties, including rock mechanical properties, and stress orientations; and
4. well test data (e.g., drill-stem, pressure fall-off, and step-rate tests) to characterize reservoir dynamic properties and reservoir pressures and stresses.

In the case of the North Hugoton Storage Complex and specifically the Patterson site, the lack of 3-D seismic data across the structure makes completion of the necessary tasks a challenge. Future evaluation under subsequent phases of the CarbonSAFE Program will require additional data to be collected across the site.

Task 4.0: Review storage capacity of geologic complexes identified in this proposal and consider alternatives

Contributors to Task 4 include Martin Dubois, Eugene Holubnyak, Tandis Bidgoli, Mina FazelAlavi, David Newell, Andrew Hollenbach, and Jeffrey Jennings.

Three candidate sources and two possible storage complexes were identified. Phase I work shall determine which are most feasible and will identify and develop a plan to address the unique challenges of each storage complex that may be feasible for commercial-scale CCS (50+ Mt captured and stored in a saline aquifer). Each location will be evaluated using NRAP models and the results shall be submitted to DOE.

Subtask 4.1: Review storage capacity of geologic complexes identified in this proposal and consider alternatives

In the proposal outlining this study we identified three possible sites in two geologic complexes that were in various stages of analysis. Each geologic complex appeared likely to meet the minimum 50 million tonnes CO_2 storage requirement. Post award, the sites were further analyzed and a survey of alternative geologic sites was conducted.

Subtask 4.1.1: Overview

Two geologic complexes identified in the initial proposal as potential sites for storing >50 million tonnes (Mt) are the Pleasant Prairie field geologic site, considered the primary storage site in the proposal, and the Davis Ranch and John Creek fields in the Forest City Basin storage complex (FCB), in combination considered a secondary site (Figure 4.1). Preliminary capacity evaluation for the FCB site indicated it is probably not capable of storing >50Mt CO_2 (Bidgoli and Dubois, 2017a). In the process of evaluating the Pleasant Prairie site, four separate geologic structures were identified as each having potential for storing 50Mt. The four structures, aligned on the same regional geologic structure, are similar in size and have >100 ft of closure and similar geologic histories. The four potential sites—Rupp, Patterson, Lakin and Pleasant Prairie—are situated in what we have named the North Hugoton Storage Complex (NHSC) (Figure 4.2).

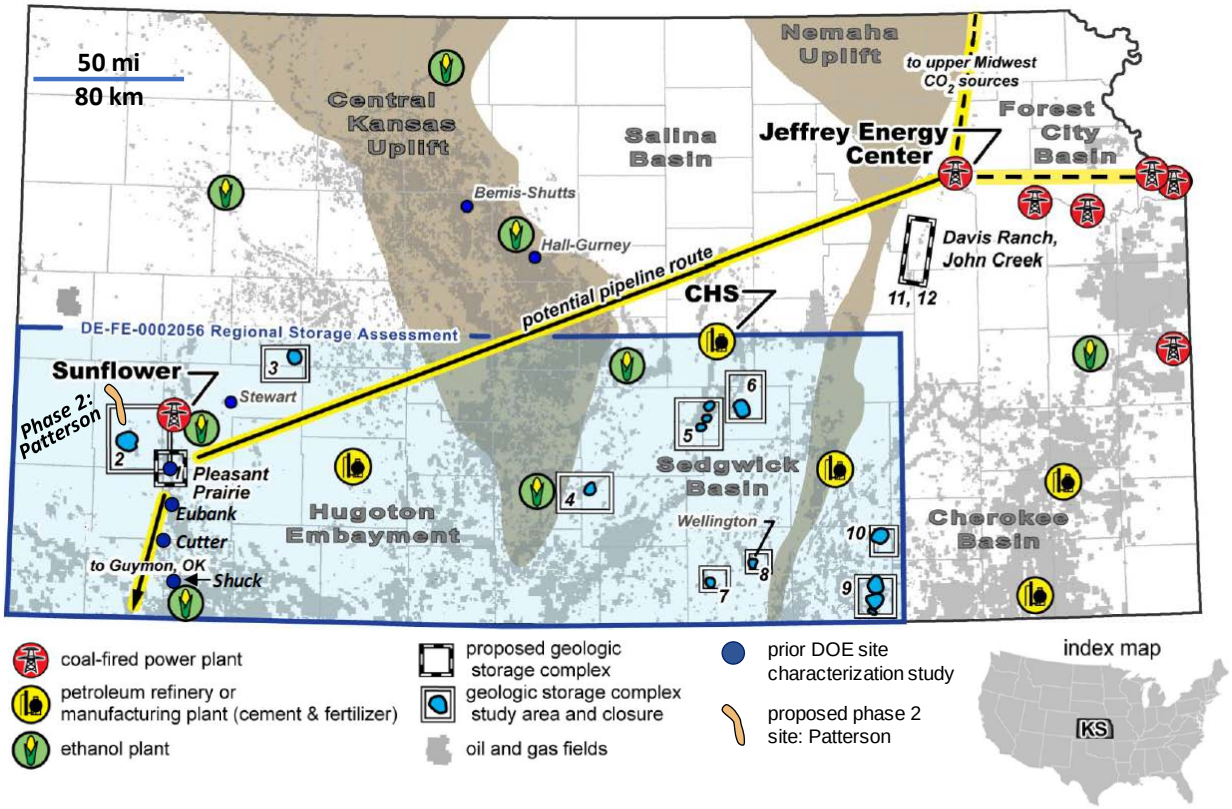

Figure 4.1. Kansas map showing location of the Patterson site, a variety of CO_2 sources, possible CO_2 pipeline routes, other possible CO_2 injection sites (numbered 1–12) identified in Watney et al. (2015) located inside the DE-FE0002056 study areas (blue), and oil fields (gray). The primary sources in this study are labeled. The figure is modified from ICKan proposal SF 424 R&R, 2016 (Watney, et al., 2016).

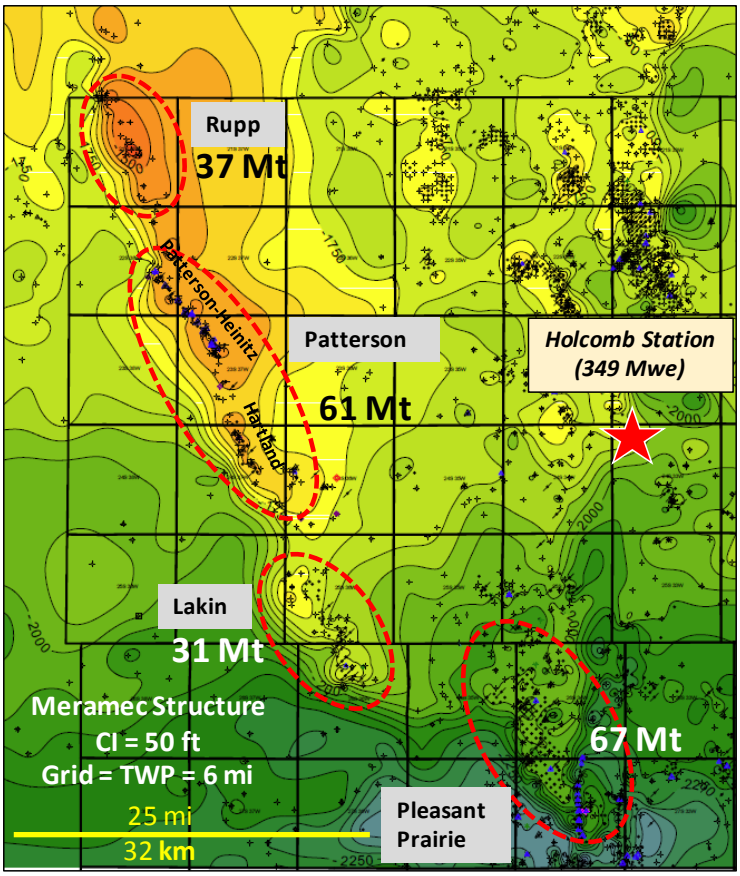

Figure 4.2. Location of four plausible storage sites within the North Hugoton Storage Complex. Map is the structure on the top of the Meramec (Mississippian). Patterson is the primary site for Phase II and the others are alternative sites. Annotations (e.g., 61Mt) indicate volumes of CO_2 "stored" in numerical simulation models in millions of tonnes.

Subtask 4.1.2: Process for determining potential Phase II sites

As mentioned above, we went into this study with two geologic complexes in mind, FCB and Pleasant Prairie, on the basis of prior DOE-funded Kansas Geological Survey studies and the proximity to coal-fired powerplant source industry partners. The study also evaluated alternative geologic sites to the two in the proposal. Early in the study, we determined that the FCB site, the Davis Ranch and John Creek fields, in combination, probably do not meet the >50Mt capacity standard (Bidgoli and Dubois, 2017a). The Pleasant Prairie site was determined by CO_2 injection simulation studies to have the capacity to store >50Mt CO_2 (Bidgoli and Dubois, 2018a, 2018b). However, the operator of the Pleasant Prairie Field determined that they and their business partners could not commit to Phase 2 operational and financial obligations that would be required. Thus, the Pleasant Prairie site could not be considered as a Phase 2 site. The operator supports our Phase 2 study, and provided a letter of support for the ICKan project in the successful proposal for Phase 2 submitted by Battelle (Integrated Midcontinent Stacked Carbon Storage Hub) with the Kansas Geological Survey as a partner.

Alternative sites were evaluated for capacity and willingness of oil field operators to participate in a Phase 2 project. A starting point were sites evaluated in an earlier DOE-funded study (DE-FE0002056) on regional saline aquifers (Watney et al., 2015) that identified 10 sites possibly capable of storing 50+Mt

CO_2 (Figure 4.3). Most of the sites were eliminated from consideration for a variety of reasons. The site numbered 2 did not meet the 50Mt minimum in the aforementioned study, sites 1 and 5 are in an area of significant seismic activity induced by high-rate injection of produced brines into the Arbuckle, sites 9, and 10 were given lower priority because of proximity Class I Arbuckle disposal wells with rising water levels, and site 3 was downgraded because of its proximity to an operating gas storage field. At sites 4 and 8, the structures are relatively small and storage reservoir shallow (~3,200 ft), and site 7 had very limited well control and no available seismic data needed to estimate the size of the geologic structure. Thus sites 4, 7, and 8 were downgraded. Site 6, the Lakin site, was characterized, modeled and a numerical simulation of CO_2 injection was performed, along with other potential sites in the NHC, the Rupp and Patterson (Figure 4.2).

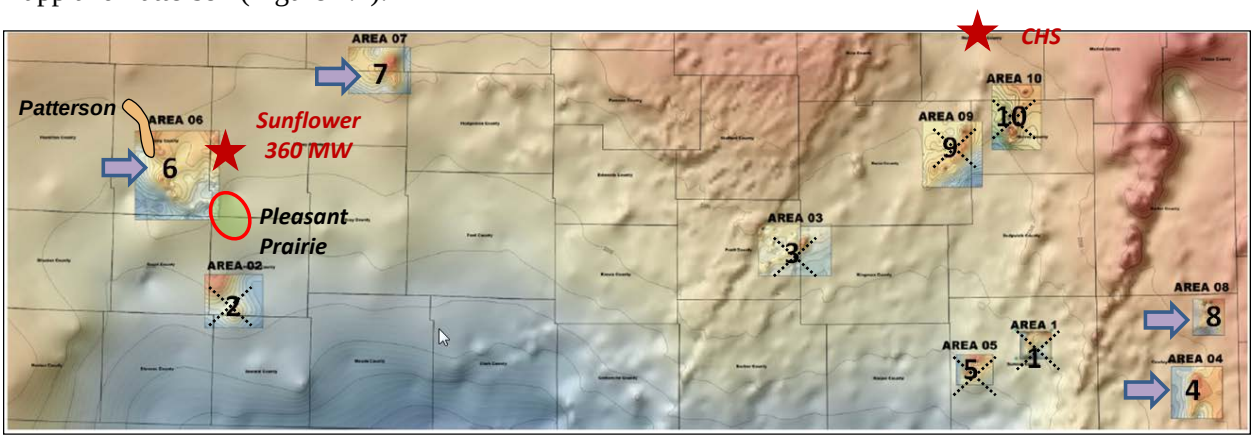

Figure 4.3: Location of 10 potential CO_2 storage sites (numbered) studied by Watney et al. (2015) and further evaluated in this study. Map is the structure on top of the Arbuckle. (Modified from Watney et al., 2015). Map area is the study area shaded blue in Figure 4.1.

Subtask 4.1.3: Results of high-level analysis for capacity at geologic sites

Site studies involving characterization, 3-D reservoir modeling and numerical simulation of CO_2 injection were performed on five potential geologic sites to estimate capacity for CO_2 storage. Results of those simulation are summarized in Table 4.1. Volume stored represent the amount of CO_2 injected in the initial, non-optimized numerical simulation exercises. Volumes could be significantly larger, particularly in the Rupp and Lakin sites, if the injection was for longer periods, more injection wells, injection under higher pressures, or with more optimal well siting. Details of the technical evaluation are available in quarterly reports referenced in Table 4.1.

Table 4.1. Results of initial numerical simulation for five geologic sites evaluated. Mt = millions of tonnes stored.

Storage Complex	Geologic Site	Volume Stored (Mt)	Injection Wells	Injection Zones	Years of Injection	References (Quarterly Reports)
North Hugoton Storage Complex	Rupp	36.6	4	Osage, Viola, Arbuckle	30	Q5—Bidgoli and Dubois, 2018b
	Patterson	60.7	4	Osage, Viola, Arbuckle	30	Q3—Bidgoli and Dubois, 2018a
	Lakin	30.8	3	Osage, Viola, Arbuckle	25	Q2—Bidgoli and Dubois, 2017b, and Appendix D
	Pleasant Prairie	67.4	3	Osage, Viola, Arbuckle	25	Q3—Bidgoli and Dubois, 2018a, and Q5—Bidgoli and Dubois, 2018b
Forest City Basin	Davis Ranch - John Creek	24.6	6	Simpson, Arbuckle	25	Q1—Bidgoli and Dubois, 2017a, and Appendix C to Q1

Subtask 4.2: High-level technical analysis of potential injection sites

Subtask 4.2.1: Introduction

After thorough screening and review of prior DOE-funded studies, a total of five potential sites were subjected to a more detailed analysis involving subsurface data gather from public and private sources, data preparation and reservoir characterization, 2-D geologic modeling, 3-D reservoir modeling, and numerical simulation of CO_2 injection for storage evaluation. The ultimate purpose was to determine the most feasible site for meeting a 50+Mt CO_2 storage target based upon both technical and non-technical criterion. In this portion of the report, we will discuss the technical aspects of the site chosen as most feasible, the Patterson site, located in the North Hugoton Storage Complex. Although there are other viable sites in the NHSC, notably the Pleasant Prairie site, Patterson was chosen as most feasible, in a large part, because of a strong business partner, Berexco, LLC. Also noteworthy is that the Patterson and the three other sites are within 40 miles of one of the CO_2 source partners in the project, Sunflower Electric's Holcomb Station (Figures 4.1 and 4.2).

In this report, we will focus on the Patterson site technical evaluation. Analysis of the three other sites listed in Table 4.1—the Rupp, Lakin, and Pleasant Prairie—followed similar workflows as that for the Patterson. See quarterly reports referenced in Table 4.1 for details for those four sites.

Subtask 4.2.2: Patterson site description

Subtask 4.2.2.1: Setting

The Patterson site is situated in southwest Kansas at the northern end of the giant Hugoton Gas Field in the Hugoton Embayment of the Anadarko Basin (Figure 4.4). The Patterson site comprises three closely-spaced oil pools, Patterson, Heinitz, and Hartland, aligned on a geologic structure (Figure 4.5) and is one of the four geologic sites in the NHSC. The four NHSC geologic sites are similar in that they have approximately 100 ft of structural closure, are located on a prominent northwest-southeast structural trend, have the same geologic history, and have the same saline aquifer reservoirs beneath them.

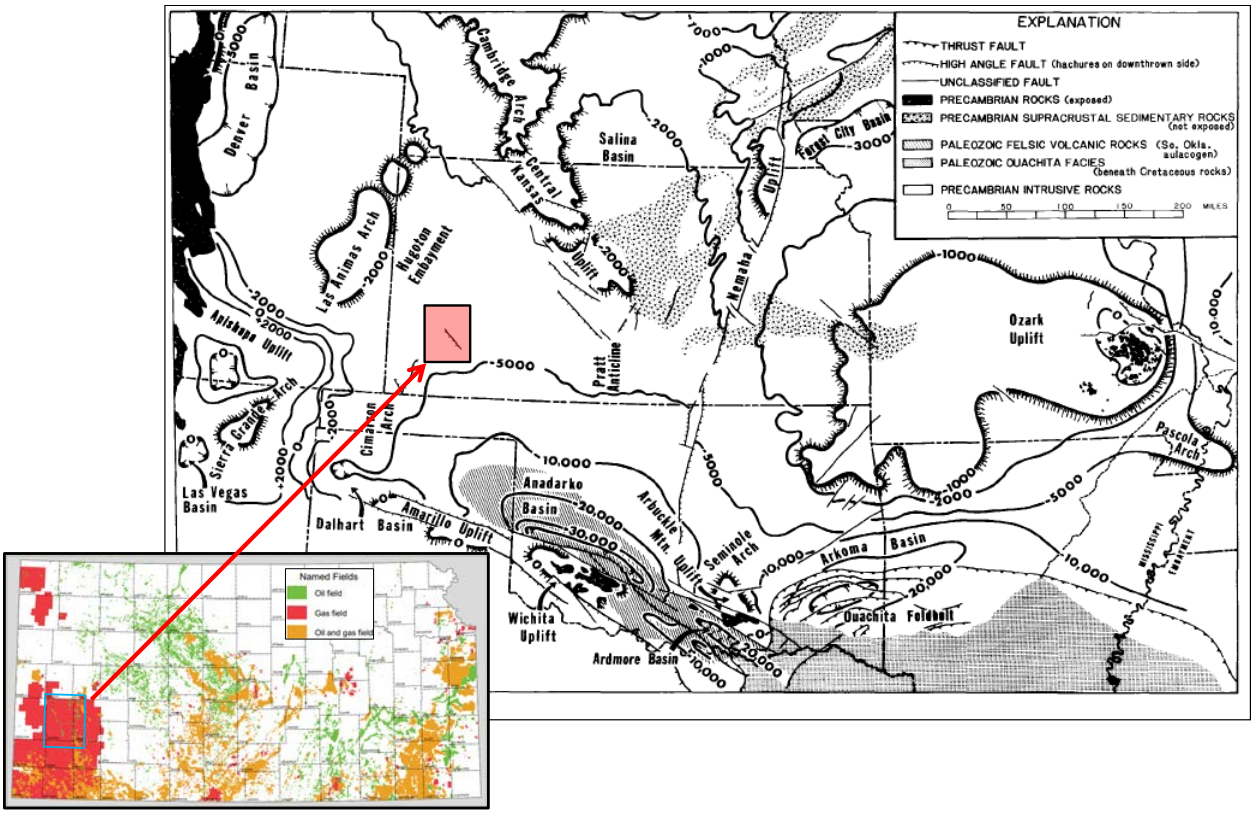

Figure 4.4. Locator map for North Hugoton Storage Complex (red-shaded box) showing Pre-Cambrian basement configuration (Rascoe and Adler, 1983). The red-shaded box is the area covered by the map in Figure 4.2. Inset map illustrates the oil and gas fields in Kansas in 2009 (http://www.kgs.ku.edu/PRS/petro/ogSheetMap.html).

Three stratigraphic intervals are considered for CO_2 storage—the Mississippian Osage, Middle-Ordovician Viola, and Cambrian-Ordovician Arbuckle—shown in stratigraphic charts in Figures 4.6 and 4.7. All three have regional lateral extent and appear to be separated by vertical barriers to fluid migration (Meramec, Kinderhook, and Simpson dense carbonate and thin shales). The Morrow shale (Pennsylvanian) on top of the Meramec (Mississippian) is a regional top seal for the oil and gas accumulations in the Mississippian, Morrow sandstone and Chester sandstone.

The Mississippi stratigraphy deserves additional discussion and explanation of how we have treated it for mapping and modeling purposes. The Mississippi-aged Chester Stage unconformably overlies the Meramec Stage. There is a major unconformity atop the Mississippi upon which the Morrow was deposited. The Chester thins atop structures throughout the NHSC due to erosions and in some areas has

been completely eroded and Morrow rests directly on Meramec. The lower Morrow section and the Chester similarly comprise interbedded limestone and shale making it difficult to correlate the contact between them when complicated by an unconformity. For mapping and modeling purposes, the Morrow and Chester have been lumped. The Mississippian-aged Meramec Stage comprises the Ste. Genevieve, St. Louis, Spergen (Salem), and Warsaw limestones. Because of an unconformity atop the Meramec and the major unconformity atop the Mississippian, it is not always clear whether the Ste. Genevieve or the St. Louis is the subcropping unit, so we chose to pick that top as the Meramec, rather than differentiate. The St. Louis C, the main producing zone in the Pleasant Prairie field, top was also picked but not used as a horizon in modeling.

Saline aquifer reservoirs in the Osage and Viola consist of thick (>100 ft), vertically continuous, laterally extensive porous carbonate, primarily medium-crystalline sucrosic dolomite with good intercrystalline porosity and varying amounts of chert. The Arbuckle storage reservoir consists of stacked thin beds of porous dolomite over the 570-foot-thick Arbuckle, separated by thin intervals of tight carbonate. Although they do not appear to be well-connected vertically, drill stem tests in the Arbuckle, albeit limited in number, prove otherwise with fluid recoveries averaging more than 2,000 feet of saltwater in one-hour flow tests.

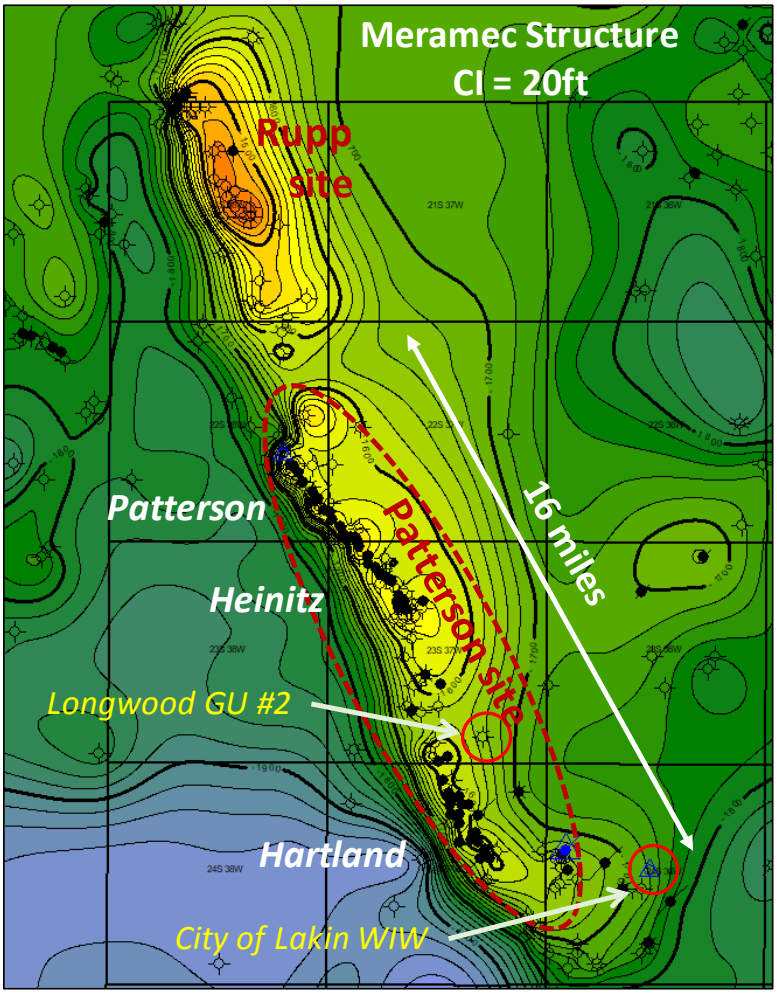

Figure 4.5. Structure map on top of the Meramec (Mississippi) covering the area modeled for the Rupp and Patterson geologic sites. Contour interval = 20 feet. Patterson site is outlined by the red dashed line.

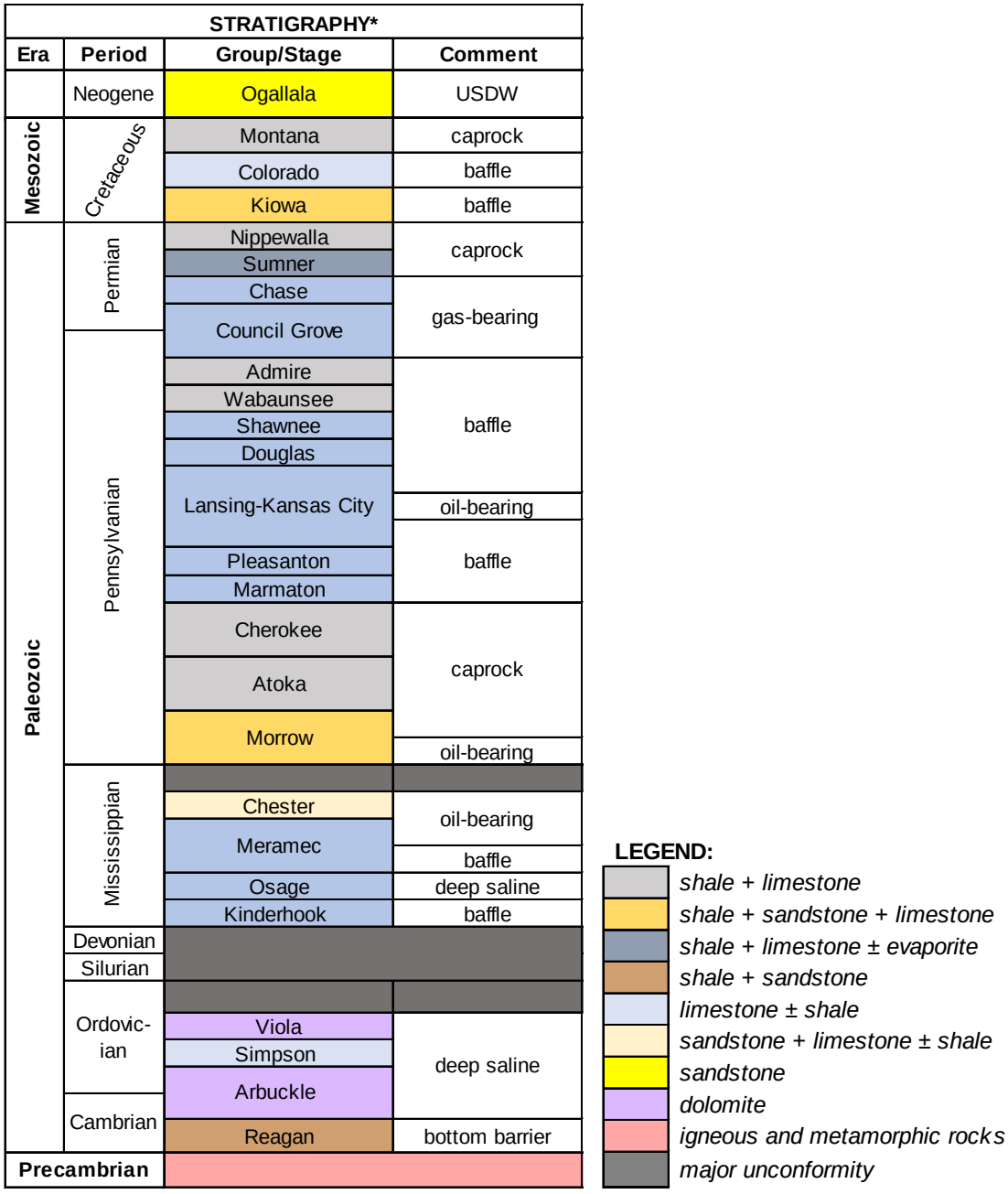

Figure 4.6. Generalized stratigraphic chart for the NHSC in southwest Kansas. Comments column shows oil and gas producing intervals in the area and regional barriers, caprock and baffles to vertical fluid flow. USDW = underground source of drinking water.

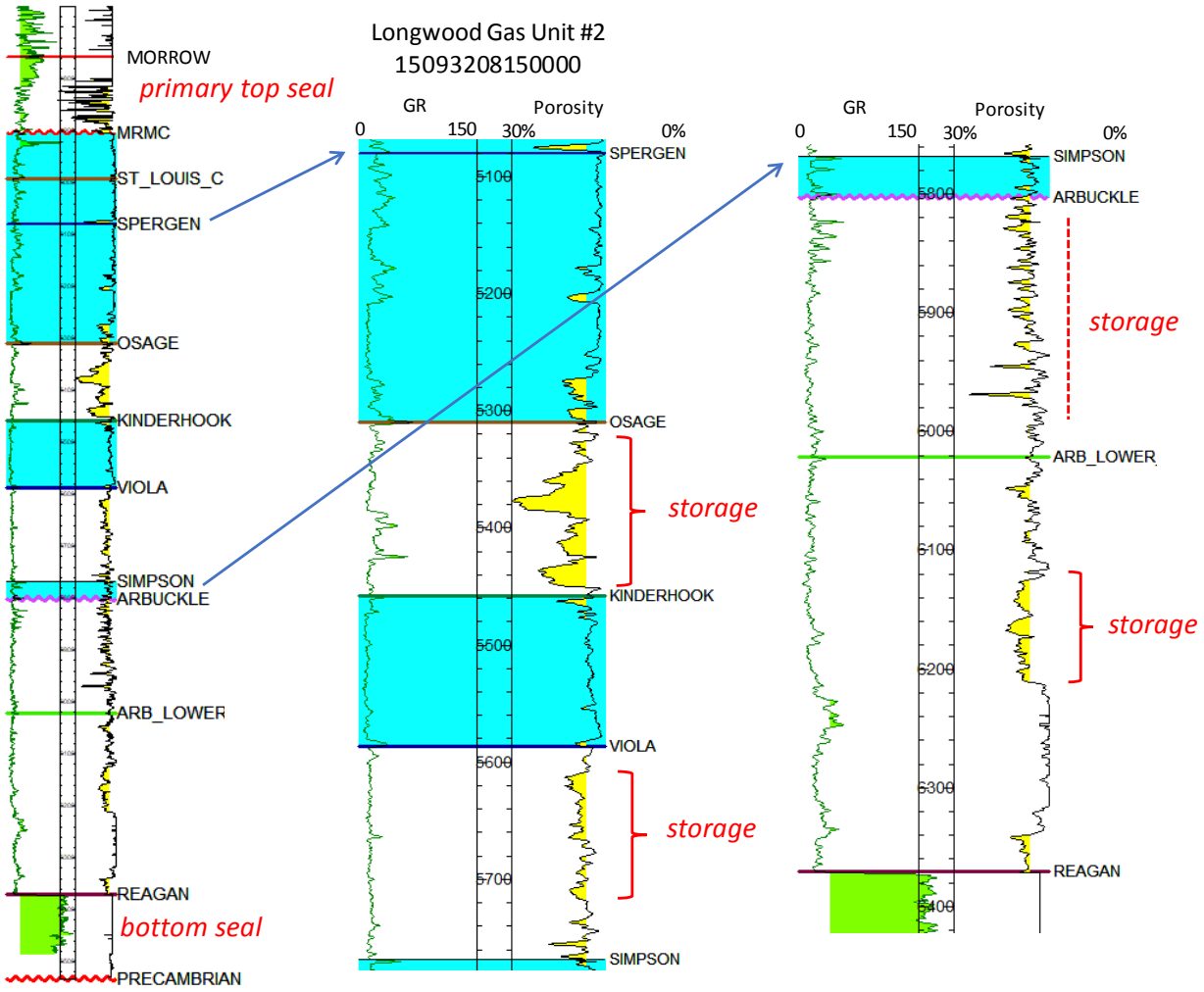

Figure 4.7. Stratigraphy of the Lower Paleozoic and proposed storage zones illustrated by a wireline log from a key well in the Patterson site, the Longwood Gas Unit #2 well (see Figure 4.5 for well location). Tight carbonate baffles separate storage units from one another (shaded blue). Porous intervals (>7% porosity) are shaded yellow and shale intervals are shaded green.

Subtask 4.2.2.2: Oil production history and CO_2 enhanced oil recovery potential

Oil has been produced in the Patterson site since 1966 with the discovery of the Patterson oil pool. A total of 7.3 million barrels of oil have been produced from the three pools through August 2018, most of it from the Morrow sandstone (Table A in Figure 4.8). The Morrow sandstone reservoir in the Patterson-Heinitz Unit (two fields unitized in 2010) has responded well to a waterflood installed in 2010 (Figure 4.8B and 4.8C). In all, 5.5 million barrels of oil have been produced from the combined Patterson and Heinitz before and after unitization, and an additional 1.2 million barrels of oil are expected from the waterflood (6.7 million barrels ultimate recovery). Because of the oil volume, reservoir conditions, solution-gas drive mechanism and being a successful waterflood, the Patterson-Heinitz Morrow reservoir is a candidate for CO_2 enhanced oil recovery (EOR).

In addition to the Patterson-Heinitz Unit, there are many other CO_2 EOR opportunities in southwest Kansas, four of which were part of a DOE-funded study (DE-FE0002056) conducted by the Kansas Geological Survey (Watney et al., 2015) and located within fifty miles of the Patterson site. The CO_2 EOR market for CO_2 could help the economics of transporting CO_2 to the Patterson site through economies of scale and the reduction of market risk. There would be the added benefit of concurrent CO_2 storage in the EOR projects. The four fields—Pleasant Prairie South (part of the Pleasant Prairie site), Eubank North Unit, Shuck, and Cutter—are similar in size and reservoir as the Patterson-Heinitz Unit, having produced a combined 23.6 million barrels of oil through 2014 from the Morrow and Chester (Mississippian) sandstones. Dubois et al. (2015c) estimated the ultimate recovery by primary and secondary (waterflood) of 25.4 million barrels and the potential CO_2 EOR recovery at 13 million barrels of oil. Their reservoir simulations estimate 5 Mt CO_2 would be stored in the oil reservoir in the process.

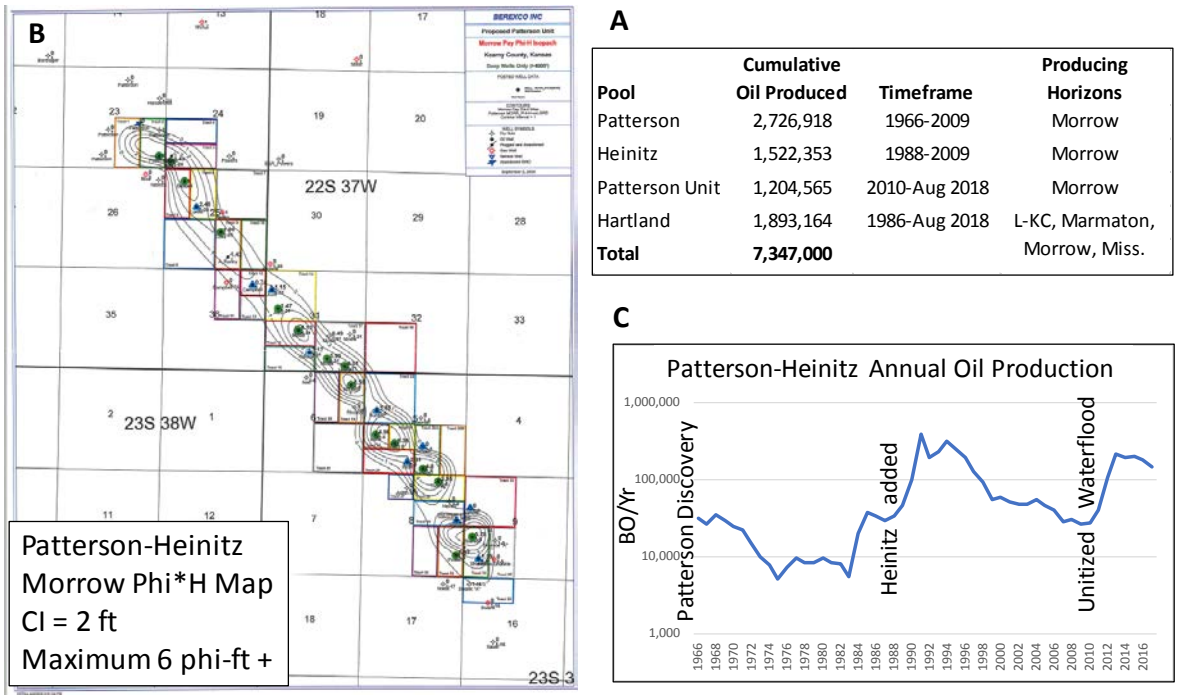

Pool	Cumulative Oil Produced	Timeframe	Producing Horizons
Patterson	2,726,918	1966-2009	Morrow
Heinitz	1,522,353	1988-2009	Morrow
Patterson Unit	1,204,565	2010-Aug 2018	Morrow
Hartland	1,893,164	1986-Aug 2018	L-KC, Marmaton, Morrow, Miss.
Total	**7,347,000**		

Figure 4.8. A—Table of oil produced and producing horizons at the Patterson site. B—Porosity (fraction) * thickness (H) map of the Morrow sandstone in the Patterson-Heinitz Unit. Map is courtesy of Berexco LLC, operator of the Unit. C—Annual oil production for the combined Patterson, Heinitz and Patterson-Heinitz Unit.

Subtask 4.2.3: Estimating CO_2 storage volume—building the static model

Storage volume was estimated by building a static geologic model on the basis of mainly public, but some well data from our industry partner, Berexco LLC, and then performing dynamic simulations of CO_2 injection into targeted reservoirs.

Subtask 4.2.3.1: Workflow for building 3-D static model

A simple, un-faulted 3-D static model was built for a 920 mi^2 (2,400 km^2) area and then a smaller area was cut out of the model for simulation (Figure 4.9). A large area with relatively coarse XY cells was required to capture enough data to model the reservoirs. Few wells in the region penetrate the target saline storage

intervals because they do not produce hydrocarbons and the oil and gas reservoirs are at shallower depths. The entire area shown in Figure 4.9 was modeled and a smaller area was cut out for simulating the Patterson and the Rupp in separate simulation exercises. The Lakin had been modeled and simulated separately, but data from the few useful wells in that area were incorporated in the Patterson and Rupp static model.

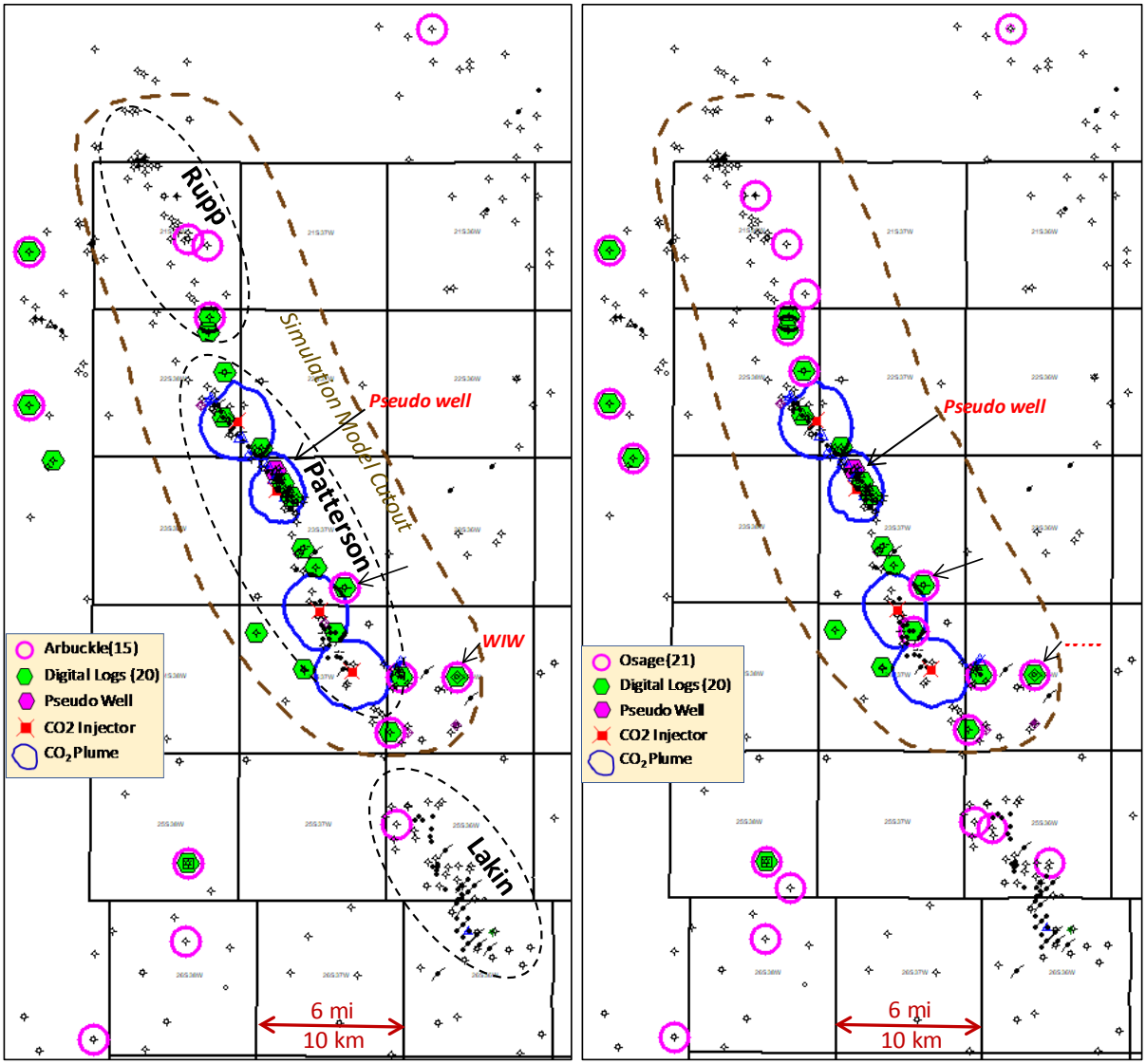

Figure 4.9. A. Plat showing locations of 363 "deep" wells and 4 hypothetical CO_2 injection wells and their CO_2 plume (blue polygons) based on simulations. The simulation model was cut out of the static model (brown dashed line). 15 wells that have penetrated the Arbuckle are circled. B. Same plat except the 21 circled wells are Osage penetrations.

A conventional workflow (Figure 4.10) for building a 3-D static model was deployed: 1) gather, prepare and analyze well-scale well data from public sources and operator-partner data, 2) build thirteen 2-D structure and isopach maps (grids) with Geoplus Petra™, 3) develop petrophysical relationships to estimate permeability knowing porosity, 4) import well headers, tops and digital well logs into Petrel™ for static model building, 5) build wireframe model using the imported 2-D grids as horizons making 12 zones and layering according to Table 4.2, and with 660 ft xy cells, 6) upscale porosity and GR to layer

scale, 7) develop porosity variograms for 10 of the 12 zones, excluding the Morrow and Reagan, and GR for the Arbuckle, and model porosity for the 10 zones using sequential Gaussian simulation and simple kriging for the GR in the Arbuckle, 8) calculate permeability at the upscale model by zone to reduce cell count, porosity—arithmetically, permeability—geometrically, 9) cut a smaller area around the Patterson and Rupp sites for simulation, and 10) export in rescue format.

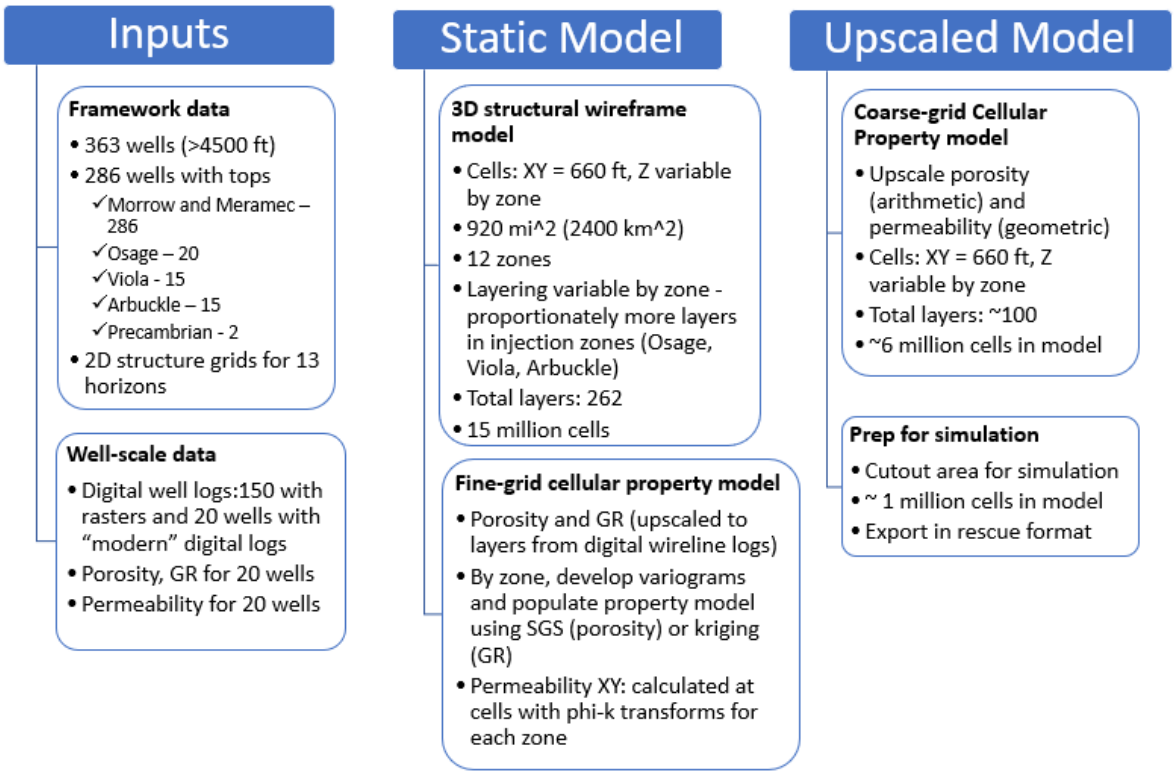

Figure 4.10. General workflow used for building the Patterson static model and preparing it for export for simulation.

Table 4.2. Zones and designated layering in the Patterson model.

Zone	Layer geometry		Mean H	Mean Layer H	Layer count
Morrow	Proportional	Conformable	150	10	15
Meramec	Follow Base	Unconformity	100	10	10
St Louis C	Proportional	Conformable	90	10	9
Spergen	Proportional	Conformable	110	10	11
Warsaw	Proportional	Conformable	120	10	12
Osage	Proportional	Conformable	150	5	30
Kinderhook	Proportional	Conformable	120	10	15
Viola	Proportional	Conformable	180	5	36
Simpson	Proportional	Conformable	35	5	7
Arbuckle (Upper)	Follow Base	Unconformity	160	5	32
Arbuckle (Lower)	Proportional	Conformable	350	5	70
Reagan	Proportional	Conformable	150	10	15
Precambrian	NA	NA			

Subtask 4.2.3.2: Well data

There are 363 wells deeper than 4,500 ft in the model area (Figure 4.9) and 1,952 shallow wells (<4,500 ft) that are not shown in Figure 4.9. The vast majority are shallow gas wells that have depths of less than 3,200 feet, that were completed in the Permian Chase and Council Grove Groups, and that are part of the shallow Hugoton-Panoma gas field. Of the 363 wells, 361 penetrate the top of the Meramec, but relatively few penetrate the prospective saline storage zones—Osage, Viola, and Arbuckle—because there is no production below the upper 150 feet of the Meramec. Raster log images were available for most wells in the immediate vicinity of the simulation model. Formation tops were picked for all wells with logs available having penetrations below the Meramec. Only 21 wells penetrated the Osage, 20 cut the Viola, and 14 penetrated the Arbuckle. Modern logs, having a minimum neutron and density porosity and gamma ray, were digitized for 20 wells yielding porosity coverage for the Osage (12 wells), Viola, (9 wells) and Arbuckle (8 wells). Although the data are sparse, porous intervals in the three candidate injection zones are laterally extensive. Because of porosity modeling difficulties in the immediate Patterson-Heinitz-Hartland area due to disparate data, especially in the Arbuckle, we needed to place a pseudo well half way between the Longwood GU-2 well and the next well with Arbuckle data 10 miles to the northwest. The pseudo well is essentially a copy of the Longwood GU-2 with minor adjustments due to changes in thickness in some of the zones.

Subtask 4.2.3.3: Petrophysics

Porosity input for the geomodel was the average of neutron and density porosity and gamma ray at the half-foot scale for the 20 wells with modern logs and the pseudo well (Figure 4.9) from the Morrow to total depth. Permeability was calculated in the geomodel using porosity-permeability transform equations derived from available empirical data.

Empirical data used in petrophysical analysis at the Patterson site include limited core data from the Longwood GU-2 well, engineering injection/falloff test in the City of Lakin WIW, both within the bounds of the reservoir simulation (Figure 4.9), and extensive core and NMR log data from Berexco KGS-Cutter 1 well, located 30 miles south of the Patterson site. Conventional core analysis for plugs and whole core in the Longwood well provide nearly full coverage in the Osage, but limited coverage in the Viola and Arbuckle. Initial porosity-permeability transform equations (Table 4.3) for the Osage were based on core from the Longwood well while transforms for all other zones (Meramec, Spergen, Warsaw, Kinderhook, Viola, Simpson and Arbuckle) were based on KGS-Cutter 1 data. Although the Arbuckle was split into two zones, upper and lower and porosity modeled separately, only one porosity-permeability transform was used to calculate permeability. No transform was derived for the Morrow and Reagan. The Morrow exhibits high vertical heterogeneity including shale (caprock) tight limestone and sandstone, and localized porous sandstone. For this simulation, the Morrow interval was generically treated as a caprock with very low permeability. There is only one penetration through the Reagan, and little else is known of this interval in the region. It was treated as a no-flow boundary in these simulations.

Table 4.3. Porosity-permeability transforms derived from empirical data used in the Patterson geomodel.

Zone	Permeability from Porosity (and GR for Arbuckle)
Meramec and St. Louis C	Kxy=87.768*Porosity^2.0923
Spergen	Kxy=212571*Porosity^4.377
Warsaw	Kxy=452218* Porosity ^5.0603
Osage	Kxy=331.31* Porosity ^2.9257
Kinderhook	Kxy=157.2* Porosity ^2.1019
Viola	Kxy=4160* Porosity ^3.2036
Simpson	Kxy=40647* Porosity ^3.7804
Arbuckle	Kxy=1000000000*GR ^(-4.84)* Porosity^(9.37*(GR^(-0.486))))

Porosity-permeability transform equations for six zones derived by cross-plotting porosity and Coates-based permeability from NMR digital log in the KGS-Cutter #1 well are shown in Figure 4.11. In the KGS-Cutter #1, the Coates-based NMR permeability was closely correlated with core permeability, validating the methodology (see Appendix E for documentation).

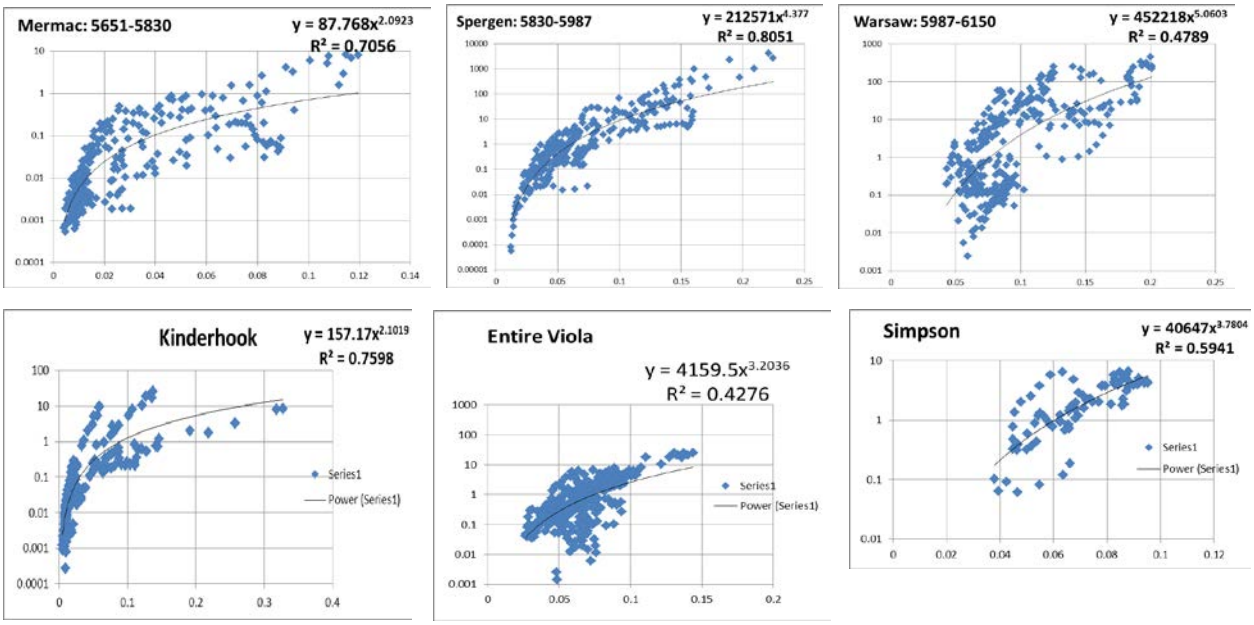

Figure 4.11. Coates-based permeability from NMR (validated by core perm) cross-plotted with log porosity.

Coates-based permeability from NMR in the KGS Cutter #1 well is an order of magnitude higher than core permeability in the Longwood GU-2 well for the same porosity value (Figure 4.12). Longwood GU-2 cross plot is core-derived permeability and log-derived porosity, while the KGS-Cutter #1 cross plot uses Coates-derived NMR permeability based on log porosity. The two plots have very similar data

configurations; however, there is an order of magnitude difference in permeability for a given porosity. Figure 4.12C illustrates the difference in permeability in a wireline log format.

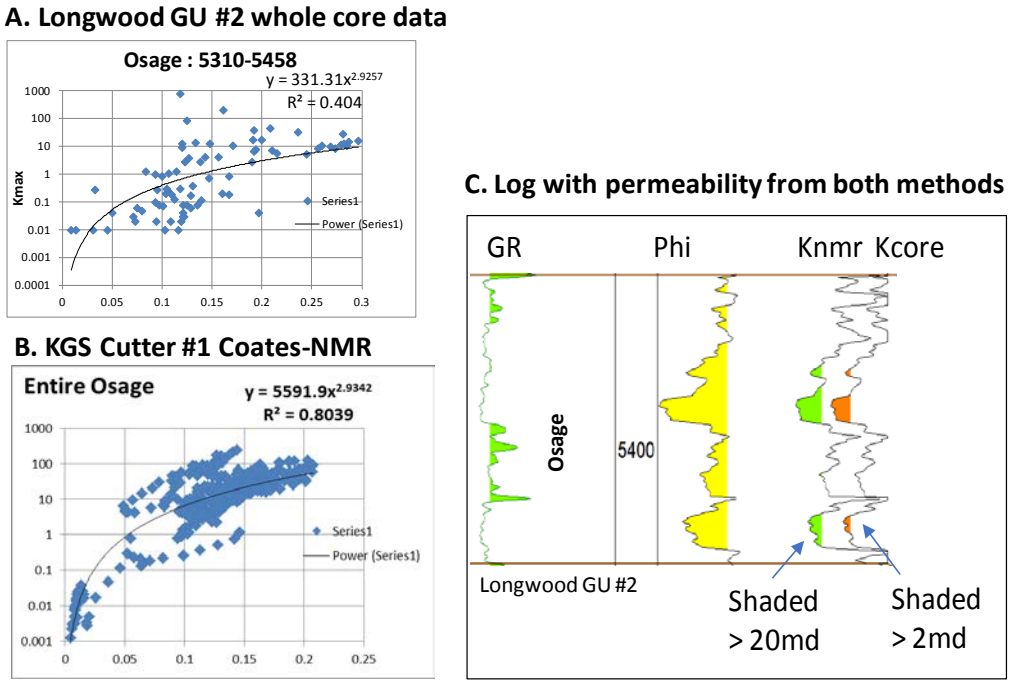

Figure 4.12. Porosity and permeability cross plots for two wells (A and B). C. Longwood GU-2 well log with permeability calculated based on log porosity (average neutron and density porosity) using transform equations from A and B.

Adjustments (increases) to permeability were made in the simulation model for the Osage and Arbuckle. The adjustments are justified by reservoir performance data demonstrating that reservoir-scale permeability data are significantly greater than matrix permeability at the core scale. Six miles east of the southernmost simulated CO_2 injection well, the maximum injection rate in the City of Lakin Class I well injection/falloff test in the Arbuckle was 4,831 barrels of water per day on a vacuum. The calculated average permeability is 1.43 Darcy over a 690 ft interval, a thousand times the average permeability using the transform in Table 4.3. The permeability transform based on core data for the Osage in Table 4.3 is less than $1/10^{th}$ that of a transform based on the KGS-Cutter #1 data, both likely to be significantly lower than reservoir-scale data. Merit Energy obtains >2,000 barrels of water per day per well from the Osage water supply wells for its Victory field area just southeast of the NHSC area, requiring much greater permeability than the average of 1.34 mD for core data from the Longwood #2 well.

Subtask 4.2.3.4: Three-dimensional static model

A single 3-D cellular model covering both the Rupp and Patterson geologic sites was constructed using the workflow discussed in detail above. Figure 4.13 is a view from the southeast of the fine-grid permeability model before upscaling. There is a known fault with nearly vertical offset, down to the southwest, that bounds the structure to the southwest. The exact location of the fault is not known because of the lack of seismic data. Discussion of faulting is covered later in this report. In this phase, the mapping and modeling was performed without inserting the fault or faults. The 3-D model and cross section

illustrate the continuous nature of the permeable intervals in the proposed injection zones, Osage, Viola, and Arbuckle. It also shows the low permeability in the Meramec, Spergen and Warsaw intervals above the Osage.

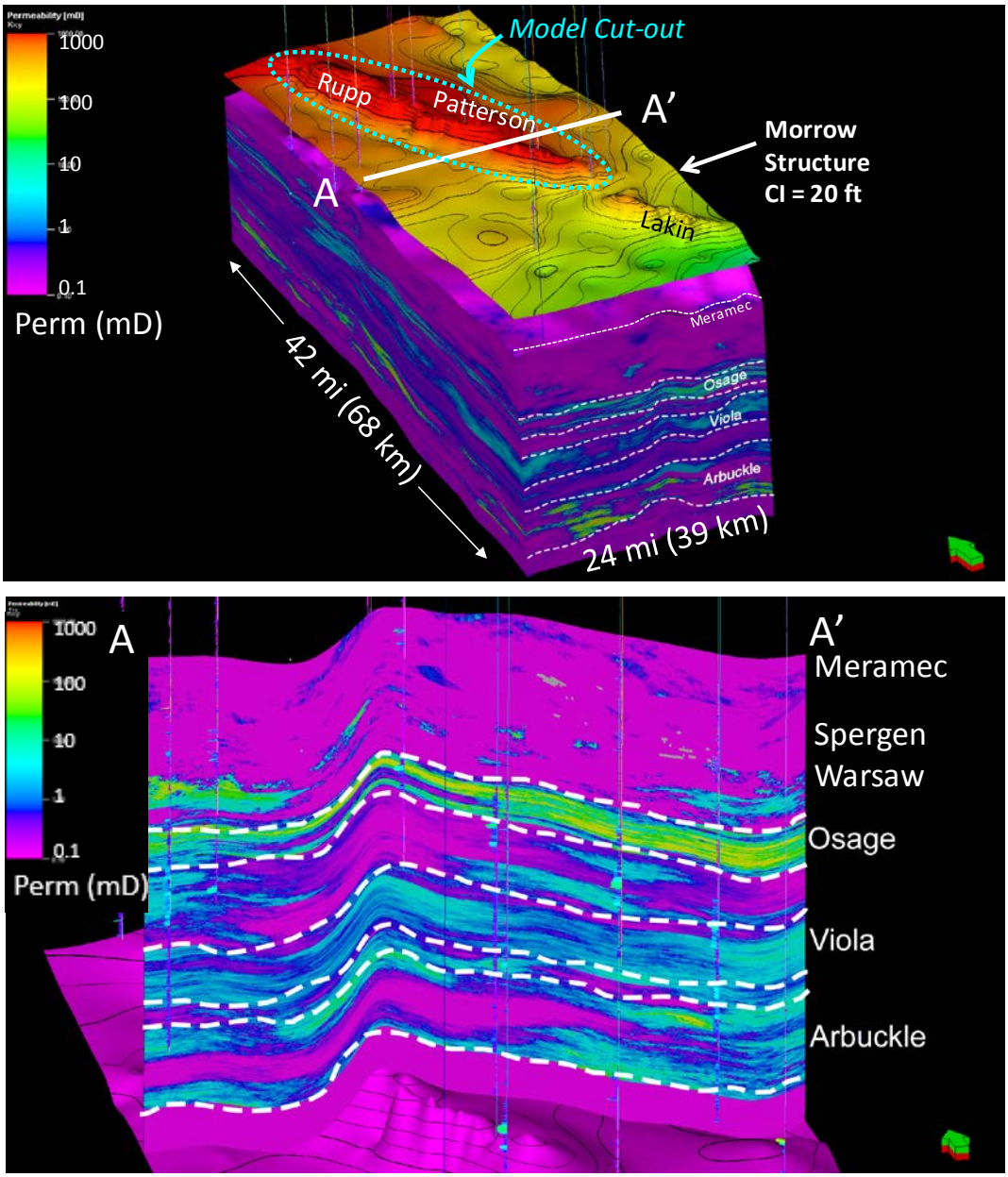

Figure 4.13. Upper figure—3-D volume of permeability from the top of the Meramec to basement. The map above the cube is the top of the Morrow; its color does not reflect permeability. Area of model cut out for the Patterson simulation is indicated by the dashed ellipse. Lower figure—A-A' cross section through the permeability model in the upper figure. Map at the base of the cross section is the top of the basement.

Subtask 4.2.4: Estimating CO_2 storage volume—running the dynamic model

The key objectives of the dynamic modeling were to determine the volume of CO_2 stored, resulting rise in pore pressure and the extent of CO_2 plume migration in the Patterson field structure. Simulations were conducted using the Computer Modeling Group (CMG) GEM simulator, a full equation of state compositional reservoir simulator with advanced features for modeling the flow of three-phase, multi-component fluids that has been used to conduct numerous CO_2 studies (Chang et al., 2009; Bui et al., 2010).

Subtask 4.2.4.1: Initial reservoir conditions and simulation constraints

The initial conditions specified in the reservoir model are specified in Table 4.4. The simulations were conducted assuming isothermal conditions. Although isothermal conditions were assumed, a thermal gradient of 0.008 °C/ft was considered for specifying petrophysical properties that vary with layer depth and temperature such as CO_2 relative permeability, CO_2 dissolution in formation water, etc. The original static pressure in the injection zone was set to reported field test pressures and the Arbuckle pressure gradient of 0.48 psi/ft was assumed for specifying petrophysical properties. Perforation zone was set at top 35 ft in all three injection intervals: Osage, Viola, and Arbuckle. Injection rate was assigned according to maximum calculated based on well tests and reservoir properties. Boundary conditions were selected as open Carter-Tracy aquifer with leakage allowed.

Table 4.4. Model input specification and CO_2 injection rates.

Injection Interval	**Osage**	**Viola**	**Arbuckle**
Temperature	60 °C (140 °F)	61 °C (142 °F)	62 °C (144 °F)
Pressure	1,650 psi (11.38 MPa)	1,700 psi (11.5 MPa)	1,800 psi (11.72 MPa)
Max. BHP	2250 psi ()	2300 psi	2400 psi
TDS	100 g/l	140 g/l	180 g/l
Formation Top	5,260 ft	5,500 ft	5,740 ft
Formation Base	5,400 ft	5,700 ft	6,340 ft
Perforation Zone	110 ft	200 ft	150 ft
Injection Period	30 years	30 years	30 years
Number of wells	4	4	4
Injection Rate	3,050 T/day	1,400 T/day	1,080 T/day
Total CO_2 injected	33.5 MT	15.3 MT	11.8 MT

Four wells were completed in the main part of the Patterson structure and were “perforated” in the Mississippi Osage, Viola, and Arbuckle. No flow boundary conditions were specified above and below the injection zones as indicated by brine chemistry. CO_2 was injected at rates determined by the petrophysical conditions at each injection site and within each perforated interval. The lateral boundary conditions were set as an infinite-acting Carter-Tracy aquifer (Dake, 1978; Carter and Tracy, 1960) with leakage.

Subtask 4.2.4.2: Simulation results

Figure 4.14 shows the maximum lateral migration of the CO_2 plume approximately 100 years after cessation of CO_2 injection activities at Patterson Field. The plume grows rapidly during the injection phase and is largely stabilized 20–30 years after the end of injection period. CO_2 travels throughout the reservoir for an additional several years and enters stabilization phase after several years post injection commencement. A significant amount of CO_2 (~30%) is dissolved in water over the period of 50 years past injection commencement.

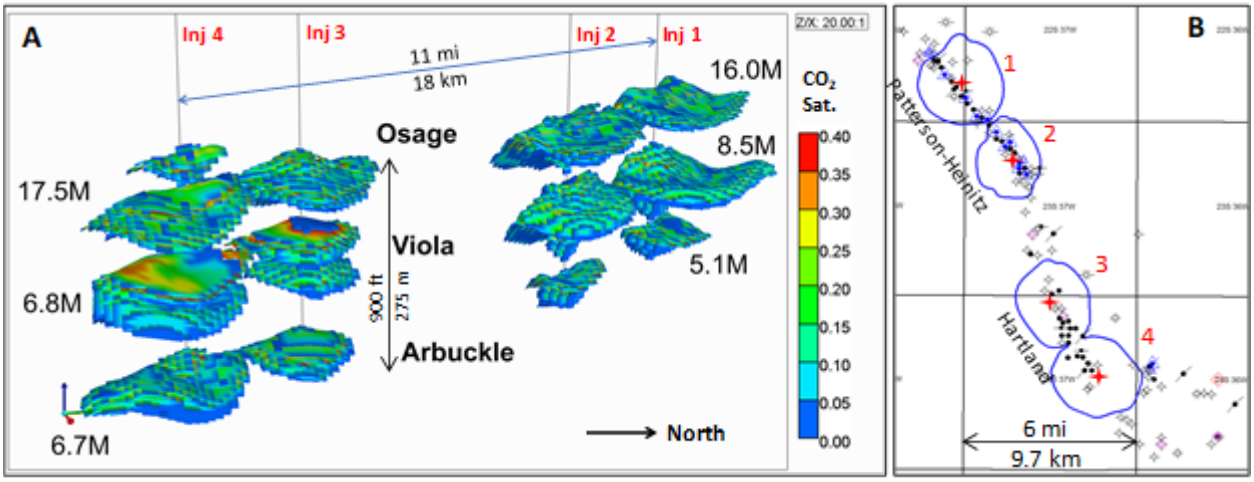

Figure 4.14. Dynamic simulation results showing CO_2 plumes after vertically stacked injection in the Arbuckle, Viola, and Osage. A. 3-D view of CO_2 plumes in stacked saline aquifers with CO_2 volume stored for each plume (million tonnes). B. Plate showing aerial extent of plumes for the four injectors and 132 wells that penetrate the Morrow caprock (~4,800 ft)

Figure 4.15 presents the distribution of reservoir pore-pressure at the maximum point of CO_2 injection. The pressure increases are estimated to be below 500 psi on commencement of injection and then pressure gradually drops after the commencement of the injection as the capillary effects are overcome. The pressure decreases to almost pre-injection levels after approximately 15–20 years, as illustrated in Figure 4.16.

Figure 4.17 illustrates modeled cumulative injection volumes obtained via injection by four injection wells completed at Osage, Viola, and Arbuckle intervals. Maximum combined injection rate for four wells modeled for the Patterson site is 5,800 metric tonnes/day. The cumulative injected CO_2 estimate for the Patterson site is 60.7 M metric tonnes; however, the injection strategy could be optimized to inject even higher amount of CO_2 at this site.

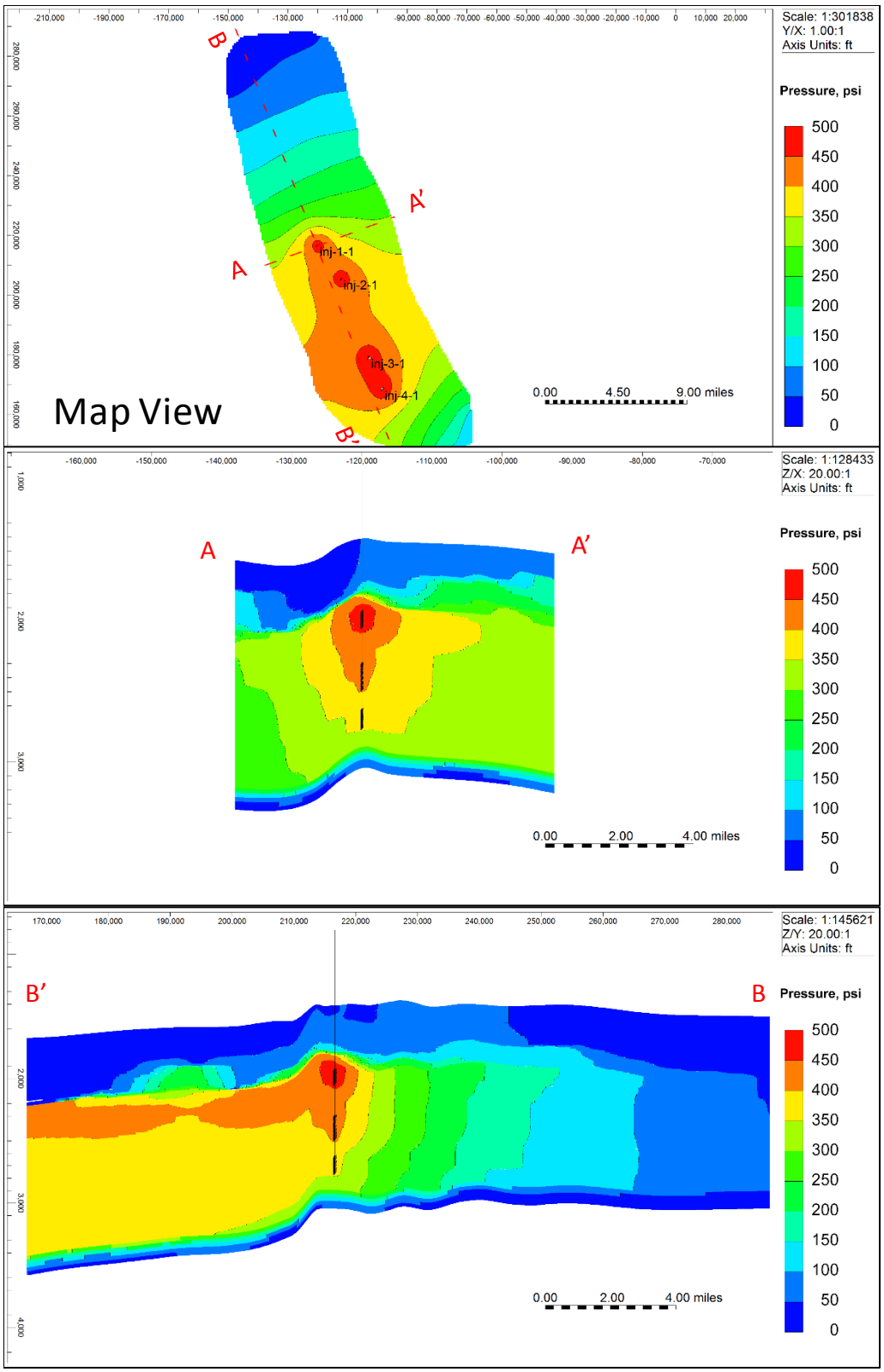

Figure 4.15. Maximum reservoir pressure increases as a result of CO_2 injection.

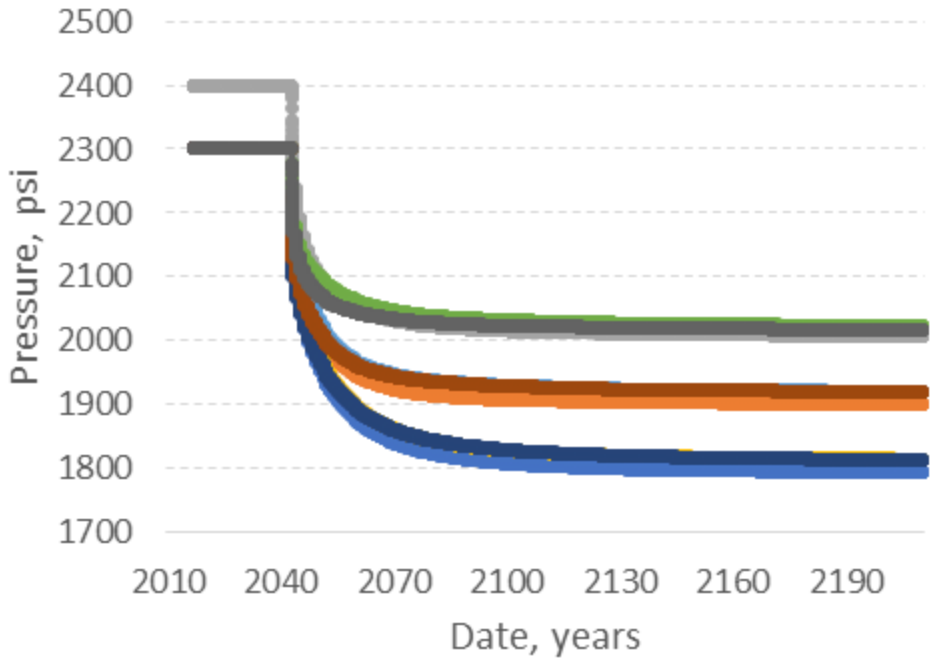

Figure 4.16. Bottom-hole pressure profiles for CO_2 injection in four wells and three injection intervals.

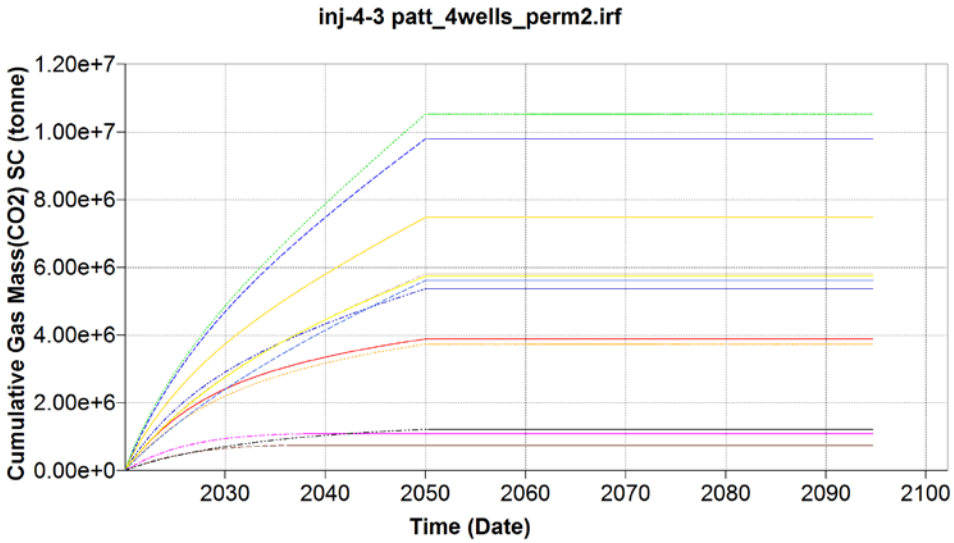

Figure 4.17. Cumulative CO_2 injection volumes in four wells and three injection intervals.

Subtask 4.2.4.3: Summary/Discussion

For CO_2 injection simulations at the Patterson site, four wells were placed in close proximity to the apex of the linear closed structure where there was higher porosity and permeability indicated in the 3-D static model in the three storage zones, the Osage, Viola, and Arbuckle (Figure 4.1). A fully compositional simulation using CMG Gem software was performed. Injection was restricted to a delta P of 600 psi above reservoir pressure and a maximum of 2,400 psi in the Arbuckle, approximately equal to hydrostatic pressure and 2,100 psi under fracture pressure (assuming 0.75 psi/ft). Daily injection rates were 1.6, 1.3,

1.5, and 1.4 kilotonnes/day for 30 years, storing 60.7 million tonnes. Maximum plume diameter averages 2.9 miles (4.6 km) 100 years after injection ceased.

This presented scenario is a conservative estimate and the performance of the dynamic model could be further improved. For example, it is possible to optimize well locations and increase the number of injectors; perforations could also be placed more strategically and perforated intervals could be extended to decrease injection pressures; and delta injection pressure could be increased to 600 psi. Stated measures would allow injecting much larger volumes of CO_2 in a safe manner without increasing potential risks.

Subtask 4.2.5: Faults and seismicity risks in the North Hugoton Storage Complex

Subtask 4.2.5.1: Overview

Documenting subsurface faults and lineaments, present-day stresses, brine disposal trends and seismicity risk in the North Hugoton Storage Complex (NHSC) is a part of a larger, more regional study conducted by the Kansas Geological Survey and reported in more detail in Appendix H. That study covers more than 40 counties (29 complete; 14 partial) in the southern part of the state, where oil and gas production is most active and where available data are concentrated (Figure 4.18). The area of analysis also corresponds to areas covered by prior Department of Energy-sponsored projects, in particular the regional storage assessment area covered by award DE-FE0002056.

The rapid rise in seismicity in Kansas and other parts of the central and eastern United States (CEUS) is without precedent and has quickly changed the hazard landscape for injection activities in the state, including for commercial-scale injection of CO_2. A major challenge for stakeholders in Kansas is that subsurface faults and stresses are not well known, making it difficult to properly site new injection wells or make decisions regarding operations of existing wells (e.g., Class I and II wastewater injection wells).

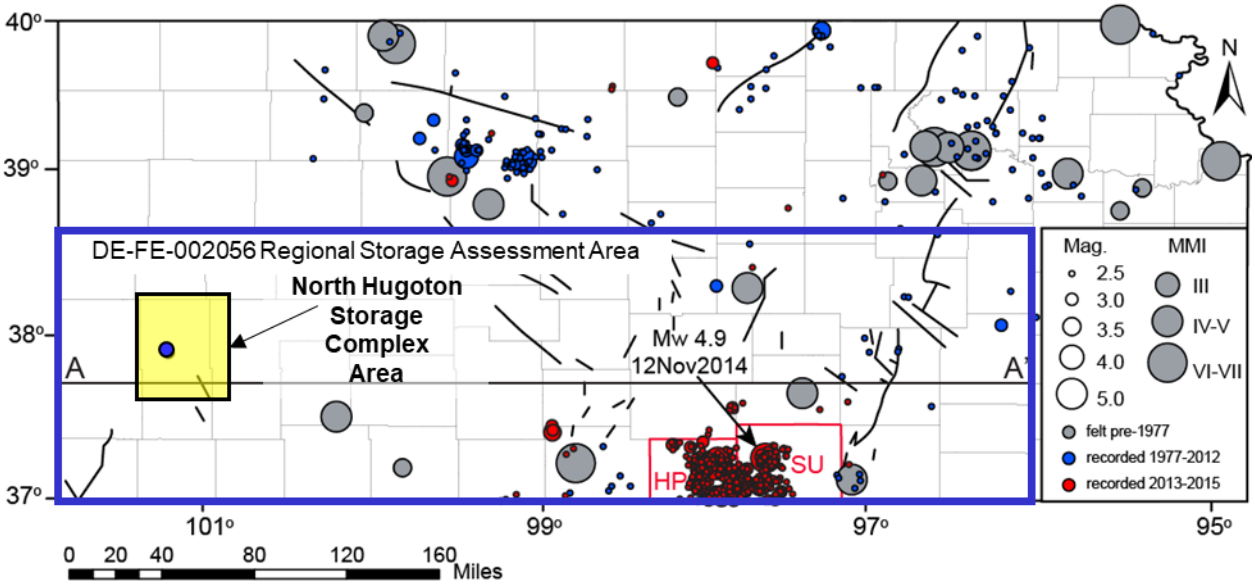

Figure 4.18. Map of Kansas showing historical (gray and blue) and recent earthquakes (red) and the North Hugoton Storage Complex area (yellow rectangle), the main focus of investigation for Phase I. Harper (HP) and Sumner (SU) counties, where recent (since 2013) seismicity is concentrated, are outlined in red. Black lines are NE-trending structures of the Nemaha Ridge-Humboldt fault zone and NW-trending structures of the central Kansas Uplift.

Earthquakes from DuBois and Wilson (1978), Hildebrand et al. (1988), and USGS—National Earthquake Information Center.

New structure contour maps of 18 major stratigraphic boundaries were used to map potential faults. The maps were constructed from a dense sampling of stratigraphic tops, established from the KGS's well database. To identify potential faults, a range of surface analysis methods were used (e.g., slope, aspect, curvature, etc.). To identify faults that have the highest risk for failure, we mapped in situ stress orientations and magnitudes using well log (e.g., image, caliper, dipmeter) and test data (e.g., leak off, interference, step rate test data) and performed slip and dilation tendency analysis. The resulting fault maps and stress data were used to assess the reactivation potential of faults, that when evaluated in conjunction with brine disposal data, can be used to flag areas at risk for injection-induced earthquakes.

Subtask 4.2.5.2: Subsurface lineaments and faults

Several lineaments were documented in the North Hugoton Storage Complex (Figure 4.19). The lineaments predominantly trend NNW and bound structural closures that make the oil and gas fields in the area. A few WNW- and NE-trending lineaments were also documented across the storage complex area. The lineaments, overall, are poorly identified in the Arbuckle through Mississippian stratigraphic surfaces (Figure 4.20) and well documented in the surfaces from Cherokee Group through Blaine Formation (Figure 4.21), which likely relates to quality of the structure contour maps for those horizons related to data density. Deeper stratigraphic boundaries have few tops constraining them and may cause grids to be oversmoothed, increasing the potential for missed faults/lineaments.

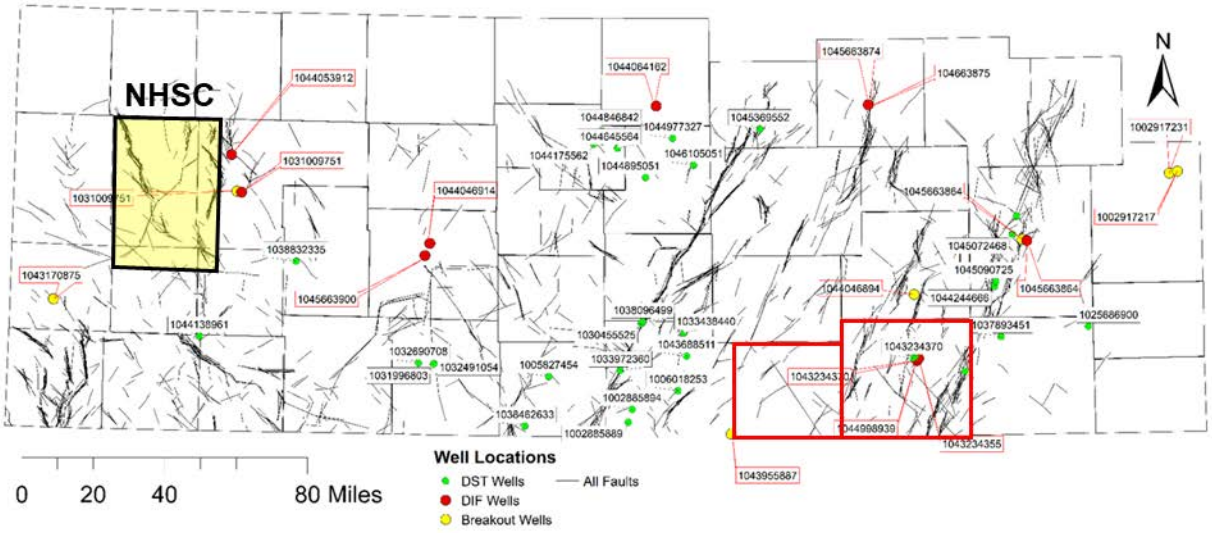

Figure 4.19. Composite map of lineaments documented from surface to the Cambrian-Ordovician. Note the dominant NNE and NNW structural trends. Locations and KID (KGS unique ID number) of wells used for analysis of in situ stresses are shown as colored circles (green—DST [drill stem test], red—DIF [drilling induced fracture], yellow—wellbore breakout). Black outline defines the North Hugoton Storage Complex (NHSC). Red outlines are Harper (west) and Sumner (east) counties.

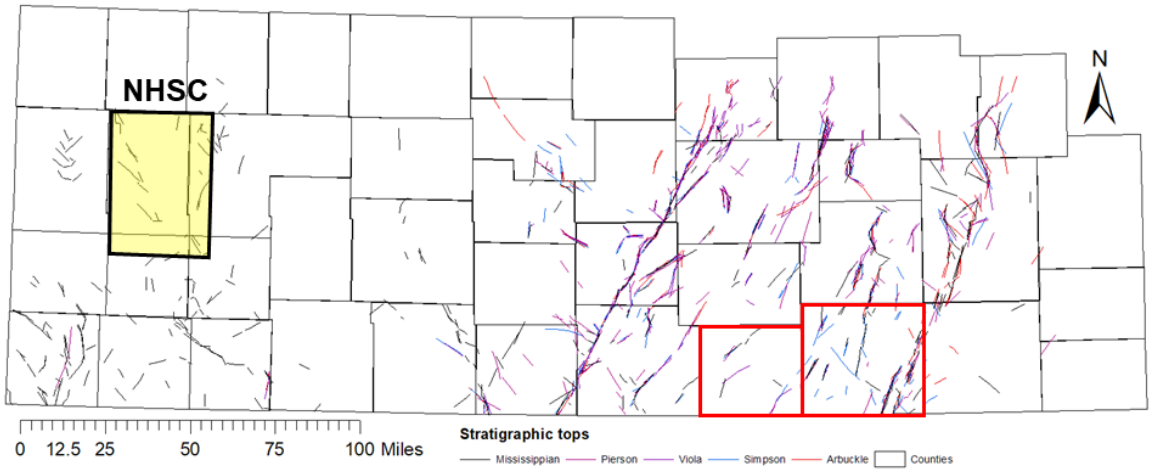

Figure 4.20. Mapped lineaments from the Arbuckle through the Mississippian. Black outline defines the North Hugoton Storage Complex (NHSC). Red outlines are Harper (west) and Sumner (east) counties.

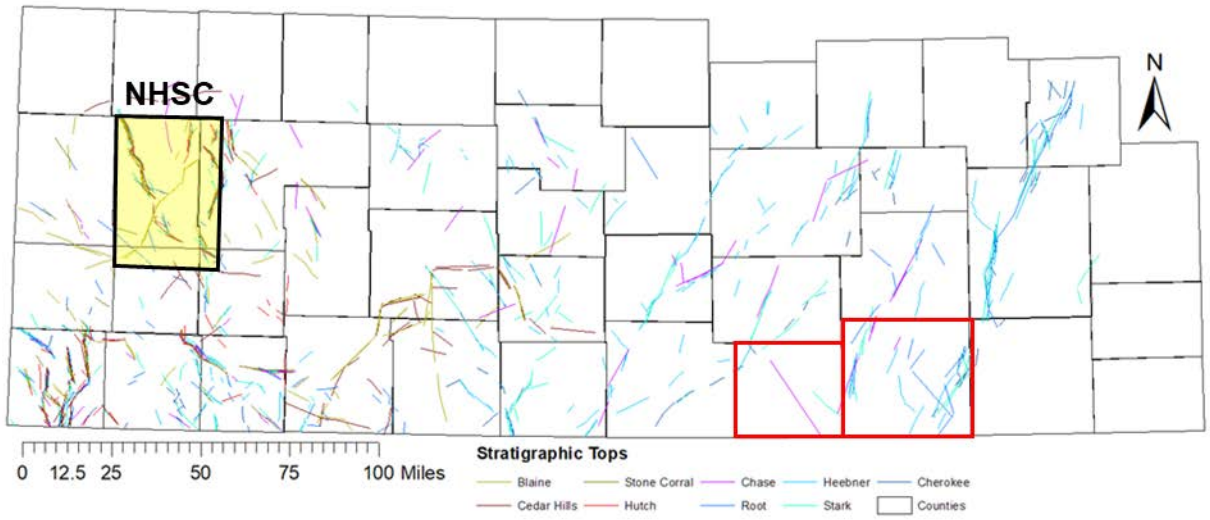

Figure 4.21. Mapped lineaments from the Cherokee Group through the Blaine Formation. The lineament density increases westward through the stratigraphic column and tracks with data density. Lineaments visible in the top Arbuckle surface remain present into the Heebner Shale and partially into the Root Shale. Black outline defines the North Hugoton Storage Complex (NHSC). Red outlines are Harper (west) and Sumner (east) counties.

Subtask 4.2.5.3: Stress orientations and magnitudes

To determine the orientation of present-day stresses, 14 image and 7 caliper logs were studied for borehole breakouts and drilling-induced fractures using standard criteria (e.g., Heidebach et al., 2010). Well locations and the data-type are shown in Figure 4.22. Although none of the data wells are located within the NHSC, five wells representing all three data types—breakouts, drilling induced fractures and drill stem tests—are located in adjacent counties.

The maximum stress orientation follows a trend of ENE-WSW (Figure 4.23). The total range was 060–090°, with an average of 075–080°. The minimum stress orientation follows a trend of NNW (Figure 4.23) and, as expected, is roughly orthogonal to the maximum stress direction. Overall, stress orientations

determined by this study agree well with stress orientations from other studies in this part of the U.S. midcontinent (e.g., Dart, 1990; Holland, 2013; Alt and Zoback, 2015).

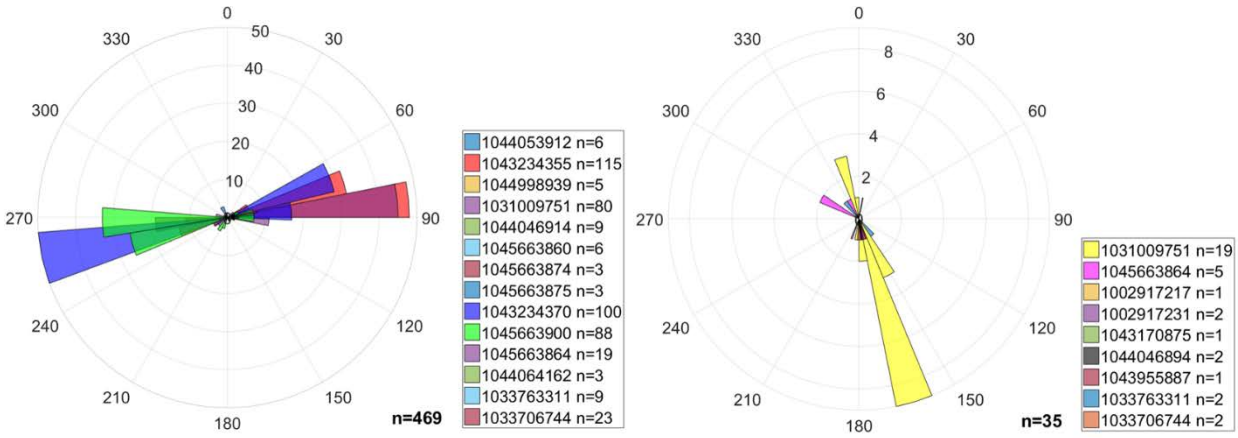

Figure 4.22. (Left) Drilling-induced fracture orientations from 14 wells within the larger study area, identified by their Kansas unique well identification number or KID. Wells having KID ending in 912, 751, and 875 are near the NHSC. (Right) Borehole breakout orientations from 9 wells in the larger study area, labeled by KID. Wells having KID ending in 751 and 875 are near the NHSC.

Stress magnitudes were estimated using well log and test data across the region. Pore fluid pressures were determined from shut-in or stabilization pressures obtained from drill stem tests (DSTs; Figure 4.23). Vertical stress gradients were estimated using the average calculated density, which ranged from 2.4–2.5 g/cm^3 across much of the study area. However, an average density of as high as 2.65 g/cm^3 was documented in the southwestern part of the study area. A density of 2.45 g/cm^3 was used to a depth of 1.5 km, which is average depth to Precambrian basement in the region. At depths greater than 1.5 km, a density of 2.75 g/cm^3 was used. A stress magnitude versus depth graph was created with these values and used to calculate Sv at 5 km depth, a typical hypocentral depth for induced earthquakes in the state of Kansas (Figure 4.23). SHmin and SHmax gradient values for normal faulting regimes were estimated at 15.4 MPa/km and 26 MPa/km, respectively. Strike-slip faulting regimes had SHmin and SHmax gradient values of roughly 26 and 60 MPa/km respectively.

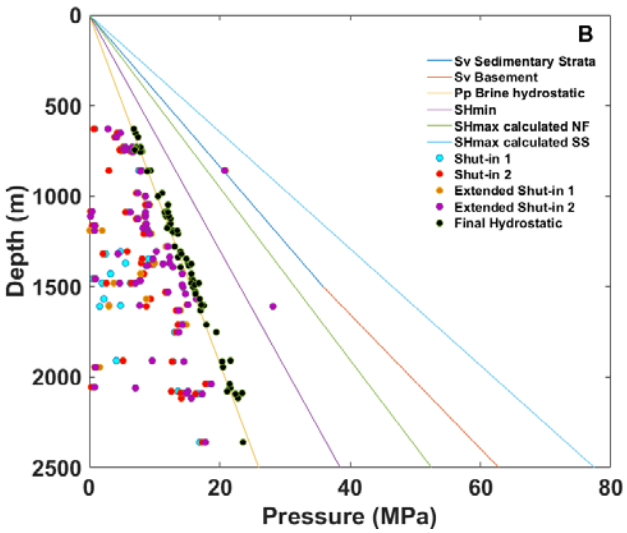

Figure 4.23. Stress gradients based on well-log-based average densities, drill-stem test data, and estimations from the stress polygon (Zoback et al., 2003).

Subtask 4.2.5.4: Fault slip and dilation tendency analysis

To analyze slip tendency, the mapped lineaments were imported into 3DStress. Magnitudes for Sv (130 MPa), Shmin (77 MPa), and SHmax (295 MPa) at 5 km depth were derived from stress gradients. The analysis presumed a strike-slip stress state (SHmax>Sv>Shmin) and the largest value for SHmax, so that lineaments with any potential for reactivation were aggressively identified. Results from the slip tendency analysis are shown in Figure 4.24 for SHmax oriented 075°. Slip tendency values ranged from 0 to 0.72, with lineaments at or above 0.6 at a critical state.

For the North Hugoton Storage Complex, the slip tendency analysis suggests that most of the documented lineaments are stable under current stress states and reservoir conditions. The majority of the lineament are green and blue, corresponding to a slip tendency of <0.5. Such faults can accommodate increases in pore pressure without failing.

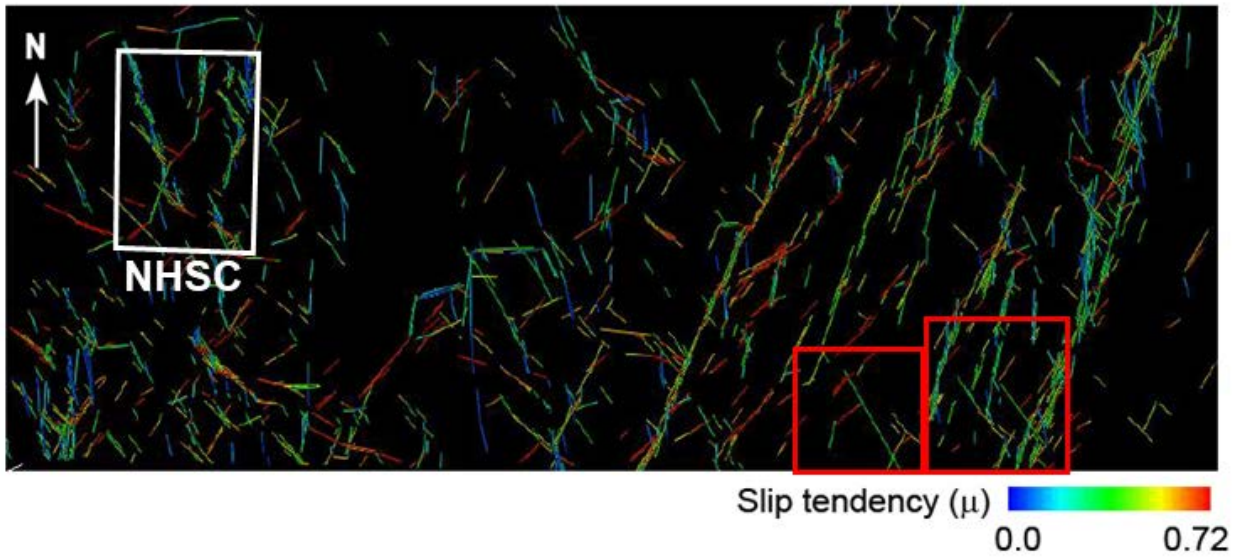

Figure 4.24. Slip tendency of mapped lineaments (as shown in Figure 4.19). Lineaments with NE and NW strikes (red) are critically stressed under the presumed stress state and are most likely to reactivate with small changes in pore fluid pressure with injection. N-striking faults (blue) are stable and may accommodate large pore fluid pressure increases. White outline defines the North Hugoton Storage Complex (NHSC). Red outlines are Harper (west) and Sumner (east) counties.

Subtask 4.2.5.5: Validation of results

Comparison of the results with 3-D seismic reflection data volumes are encouraging. The mapped features correspond with similarly oriented faults recognized in higher resolution datasets in the Pleasant Prairie, Cutter, and Wellington fields, where mostly pre-Pennsylvanian motion is evident. The Pleasant Prairie field seismic data (Figure 4.25) is located in the southern part of the North Hugoton Storage Complex, and the Cutter field is 40 miles to the south.

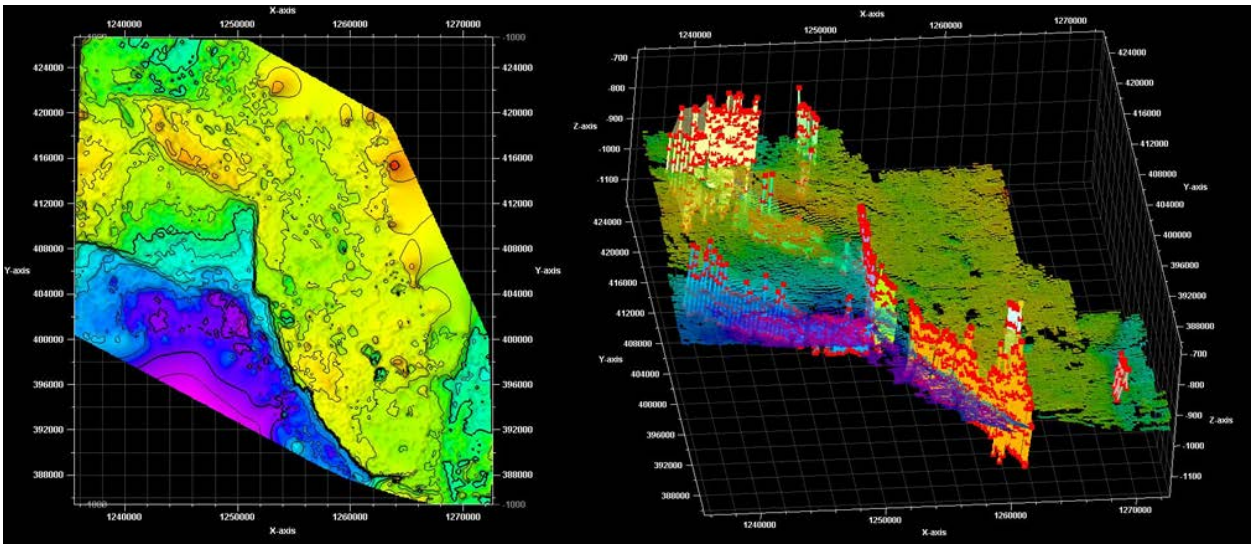

Figure 4.25. Faults documented in 3-D seismic reflection data over the Pleasant Prairie field in the southern part of the North Hugoton Storage Complex. Left figure is a grid of the time structure map on the Top Arbuckle horizon. Right shows line interpretation of surface and documented faults, shown as fault sticks that define the 3-D fault planes.

The slip tendency analysis, when paired with the disposal trends for Kansas counties, demonstrates that the combination of optimally oriented lineaments (faults) with high rates of injection explains the recent increase in seismicity observed in the south-central part of the state, particularly in Harper County. Although there may be some well-oriented structural features in the North Hugoton Storage Complex, overall reductions in disposal volumes in most of these counties contributes to a lower chance of such structures reactivating in the near future. This observation paired with below hydrostatic conditions for target injection reservoirs, Osage, Viola and Arbuckle, mean that large pore pressure increases, like those observed in the southern and central part of the state, are less likely to occur.

Subtask 4.3: Compare results using NRAP tools

The team used The National Risk Assessment Partnership (NRAP) tools to perform high-level technical sub-basinal evaluations of CO_2 storage, building on previous regional characterization of the same stacked storage complex in southern Kansas conducted under DOE-NETL project DE-FE0002056. Risk assessment of the CO_2 storage sites was also performed using NRAP tools. The results obtained with NRAP tools were compared with modeling and other evaluation techniques performed with conventional methods. The results obtained with NRAP tools were very similar or comparable to results obtained by conventional methods. More detailed explanation of methodologies and results is provided in the Appendix G.

Team used NSealR to quantify and assess the leakage risk of injected CO_2 into the Arbuckle, Osage and Viola groups in the Patterson Field. Simpson shale, Kinderhook and Spergen-Meramec are the caprock barriers for the Arbuckle, Viola and Osage, respectively. The main barrier is the thick, non-permeable limestone, Meramec-Spergen, overlying the Osage. Additionally, the Morrow shale, the seal for southwest Kansas petroleum reservoirs, acts as the ultimate barrier. The seal assessment results for the Morrow shale and Meramec limestone, the topmost seal barriers, show that the risk of CO_2 leakage through primary caprocks is very low.

The NRAP Integrated Assessment Model (IAM) for Carbon Storage (CS) (NRAP-IAM-CS) tool was used to account for key geological parameters to model long-term leakage behavior to the groundwater aquifer or atmosphere through the legacy wellbores and caprock. It was determined that legacy wellbores and their cement permeability pose the highest leakage risk.

Using Reservoir Evaluation (REV) and NETL CO_2 –SCREEN the team estimated CO_2 storage potential in the Patterson area and CO_2 plume size and pressure plume size (Figure 4.26). These results were compared to results obtained via dynamic simulations performed using CMG GEM software. REV tool allowed for obtaining metrics such as CO_2 plume size and pressure plume size. These metrics are useful for determining the post injection fate of the carbon dioxide such as the post shut-in decay rate of pressure, plume growth rate in a long-term period, and maximum pressure increase at the shut-in time. NETL CO_2 –SCREEN verified storage capacities suggested by dynamic modeling and supports the hypothesis that it is possible to inject larger volumes of CO_2 into Patterson structure (Figure 4.27).

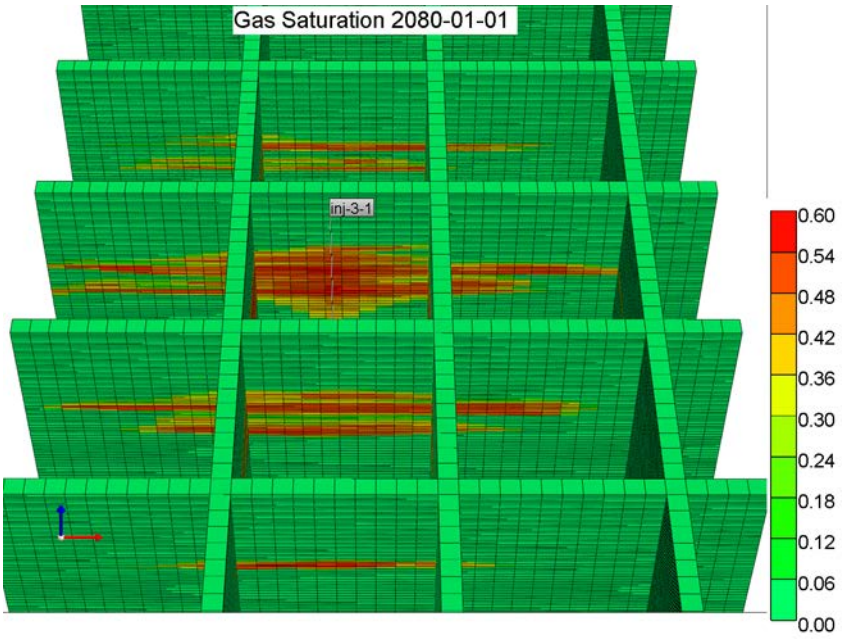

Figure 4.26: Projected grid blocks from corner point to the Cartesian grid. The figure shows the CO_2 plume in the Osage formation after 60 years (30 years of injection).

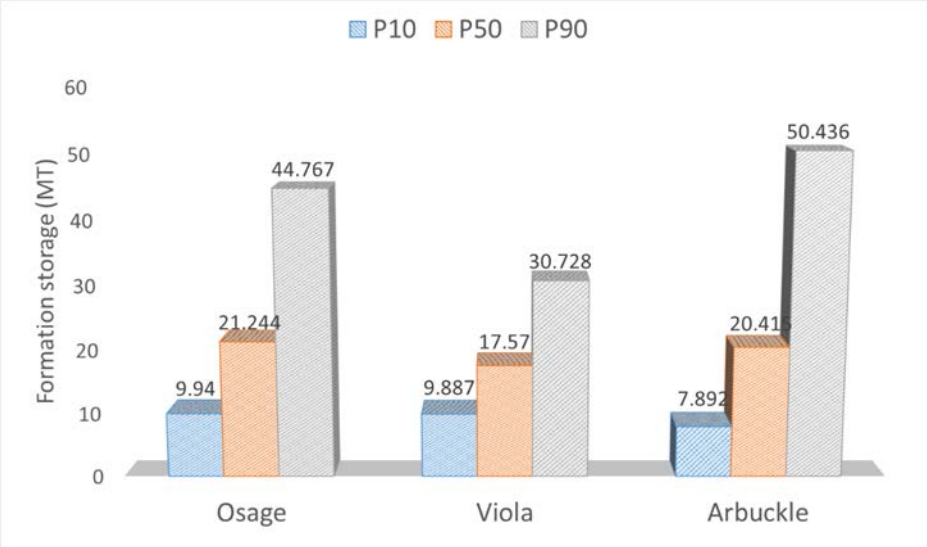

Figure 4.27: Formation capacity for the formations in the Patterson area.

Subtask 4.4: Preliminary plan for implementation

If saline storage is considered as a primary route for CCS in Kansas, then it is necessary to take into account UIC Class VI requirements in order to estimate potential operational and permitting costs. KGS and Berexco have a prior exposure to the permitting process through a Wellington pilot test project. The following are considerations of basic MVA and site closure requirements:

40 CFR §146.93(a) requires that the owner or operator of a Class VI well prepare, maintain, and comply with a plan for post-injection site care and site closure. 40 CFR §146.93(a)(2) requires this plan to include the following information:

1. The pressure differential between pre-injection and predicted post-injection pressures in the injection zone(s);
2. The predicted position of the carbon dioxide plume and associated pressure front at site closure as demonstrated in the area of review evaluation required under §146.84(c)(1);
3. A description of post-injection monitoring location, methods, and proposed frequency;
4. A proposed schedule for submitting post-injection site care monitoring results to the director pursuant to §146.91(e); and,
5. The duration of the post-injection site care timeframe and, if approved by the director, the demonstration of the alternative post-injection site care timeframe that ensures non-endangerment of USDWs.

The monitoring activities prescribed by the EPA would continue during the post-injection phase to meet the post-injection site care (PISC) requirements of 40 CFR §146.93. Both direct and indirect data will be acquired during the post-injection period.

Direct data is acquired in the injection well and the monitoring wells in target formation (injection and monitoring intervals). Upon cessation of injection, the most recently acquired data and modeling results will be reviewed with respect to the most recent PISC plan. Depending on the rate and extent of plume movement observed during the injection phase, the frequency and spatial extent of the monitoring

activities may be modified, and the PISC plan may be resubmitted to the EPA director for review and approval. If the preliminary plans do not need to be altered, there will be no modification to the monitoring plan and the well and sampling locations/frequencies will be maintained.

If significant differences between observed and model-simulated plume and pressure front are noted during the post-injection period, and if these differences are deemed to have the potential to alter the basis for the permit, the model will be recalibrated, and revised plume and pressure projections will be obtained. The existing post-injection monitoring plan will be reviewed along with the latest model projections, and the testing/monitoring plan will be adjusted and provided to the EPA for review to ensure accurate tracking of the plume/pressure front in support of eventual site closure. If necessary, this process of data acquisition and model refinement/projections may continue to determine whether or not the injected CO_2 poses any threat to the USDW. Once a determination of no negative impacts to the USDW is made, an application for site closure will be filed with the EPA director.

The following activities will have to be carried out before requesting site closure:

1. A 3-D seismic survey might be acquired over the area of interest or equivalent to area of review.
2. The new 3-D data will be interpreted and compared with the baseline survey to detect the presence of CO2 outside the expected plume containment area as modeled by reservoir simulation studies.
3. The non-seismic MVA data and its analyses conducted during the post-injection phase will be integrated with the newly acquired 3-D seismic data to validate the absence of CO_2 outside the containment strata, thus confirming that future leakage risks are minimal to non-existent.
4. All monitoring data and other site-specific data will be accounted for and used in the simulation model to demonstrate to the EPA in the form of a report that the pressures have abated, that the plume growth has slowed, and that no additional monitoring is needed to ensure that the storage project does not pose a danger to USDWs. If the EPA does not approve the demonstration, an amended plan will be submitted to the director for continuing PISC until a demonstration of safe site closure is made and approved by the director.
5. Well plugging and site restoration.
6. Report outlining operational and closure activities

Injection site cost estimates

Cost estimates for the full life-cycle of a large-scale CCS project at the Patterson site are shown in Table 4.5. In this hypothetical scenario at the Patterson, following additional data collection and full site characterization, four CO_2 injections wells would be drilled and 50Mt CO_2 would be injected into saline formations over a period of 25 years, followed by 50 years of monitoring. Approximate costs for drilling, characterization, site infrastructure, surface facilities, MVA, insurance, and financial responsibility are presented in the Table 4.5. These costs are based on estimations and direct quotes obtained for a Wellington pilot test and more detailed outlined is presented in the report submitted to DOE (Watney et. al, 2017). For instance, the cost of drilling and equipping of one operational injection well was estimated at ~$1.1M. Moreover, the number and equipment of deep monitoring wells will depend on the decision from the EPA; however, for our purposes we assumed that four injection wells at the site would have three dedicated monitoring wells. We assume costs for 2D lines and 3D seismic based on the Patterson site aerial extent and current acquisition and processing rates. Four shallow monitoring wells would be drilled for each injection well. The cost of insurance was estimated for Wellington Field, might change with time, and will depend on site specific risks. It is important to note that financial responsibility could be demonstrated by different methods and is specific to a company that is seeking UIC Class VI permit.

The site characterization and cost of effort directed towards obtaining UIC Class VI permit were assumed based on experience with Wellington project.

Table 4.5. Costs estimated for CO_2 storage site preparation, UIC Class VI wells permitting, operations and closure.

ITEMIZED ESTIMATED COSTS		**$million**
Site characterization (3D, science wells)		5
MVA equipment and baseline		2
Legal and regulatory		2.5
Pore space and security bond		16
Infrastructure	Surface equipment	1.5
	4 Injection wells	4.8
	3 deep monitoring wells	2.4
	12 shallow monitor wells	0.2
	Total upfront cost	**34.4**
Annual operating costs	Injection wells	1.5
	MVA	2
Closure and post closure	CapEx for plugging	1.2
	Annual MVA	0.5

ESTIMATED COSTS / TONNE	**$million**	**$/tonne**
Capital costs	35.6	$0.71
Operating costs (25 years)	87.5	$1.75
Post closure monitoring (50 years)	25	$0.50
Combined cost per tonne		**$2.96**

Based on 25 years of injection, 2 Mt/yr, and 50 years of postclosure monitoring

Task 5.0: Perform a high-level technical CO_2 source assessment for capture

Contributors to Task 5 include Krish Krishnamurthy, Makini Byron and Martin Dubois.

An assessment of the capture technologies best suited for efficiency, addressing the concerns of the electric utilities and their operating requirements and economic needs will be performed.

***Note:** Reporting on the study of the three CO_2 sources does not fit well within the rigid structure of the proposal. We have modified the reporting structure slightly:*

- *Subtask 5.1. Determined best technology for capture and provide vital information for all three facilities*
- *Subtask 5.2. Preliminary engineering designs and options for each of the three facilities, presented separately.*
- *Subtask 5.3. Preliminary plan including economics and discussion around the options made possible by sources in the project.*

Subtask 5.1: Review current technologies and CO_2 sources of team members and nearby sources using NATCARB, Global CO_2 Storage Portal, and KDM

Solvent based technologies for post-combustion capture are the leading candidates for large-scale capture and would be the most likely option at the **Westar Energy Jeffrey Energy Center and Sunflower Electric's Holcomb Station** coal-fired power plants. The Linde-BASF novel amine-based technology for post combustion capture removes more than 90% of the CO_2 from all or part of the flue gas (Krishnamurthy, 2016). With the successful completion of the pilot campaign at the National Carbon Capture Center (NCCC) in 2016, the Linde-BASF system has achieved a Technology Readiness Level (TRL) of 6 (U.S. Department of Energy, 2012), and demonstrated significant improvements to the performance, efficiency and the cost of electricity when compared to today's state of the art capture systems (see Process Flow Diagram in Figure 5.1, Bostick et al., 2017). As with all solvent-based technologies, this process requires steam for solvent regeneration and power for rotary equipment and CO_2 compression. The preliminary design options for each site will consider options for optimizing the generation of steam and/or power for the capture facility.

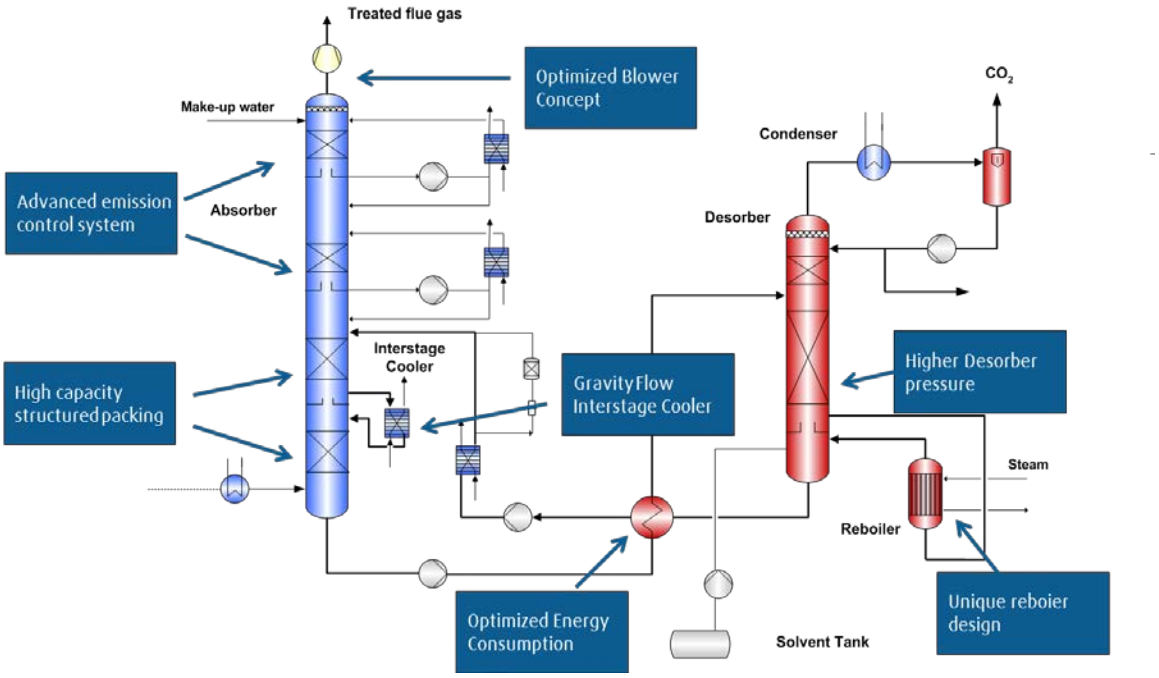

Figure 5.1. Linde-BASF novel amine-based PCC technology: Optimized for reduced parasitic energy need and low capital expenditures (from Krishnamurthy, 2016).

Options for industrial CO_2 capture at the **CHS Refinery SMR-based hydrogen reformers** can be either solvent-based, sorbent-based or membrane applications. Solvent based post-combustion capture from the reformer furnace flue gas will result in maximum CO_2 emissions reduction (~90% of total emissions from SMR H_2 plants (Krishnamurthy, 2017). Sorbent based (pressure or vacuum swing adsorption – PSA, VSA) capture from syngas or purge gas are likely technology options for partial capture (~50-60% of total SMR H_2 plant emissions) as they are more cost effective than solvent based due to relatively smaller capture capacity (Krishnamurthy, 2017). Figure 5.2 shows three potential configurations for carbon capture from the reformer.

1. Process side from H_2 PSA purge gas: Low pressure, higher CO_2 concentration: PSA/VSA, FlashCO_2, Membranes. Power requirements of 280 kWh/t CO_2 (kilowatt-hour/ton CO_2) captured
2. Combustion side (furnace; 100%): Low pressure, low concentration – Solvent based. Power requirements of 130 kWh/t CO_2 captured. Steam requirements of 1.2 – 1.3 t/t CO_2 (ton/ton CO_2) captured
3. Process side CO_2 removal from syngas (~60-70%): Medium pressure, low CO_2 concentration – applicable technologies include solvents, PSA/VSA and integrated membrane.

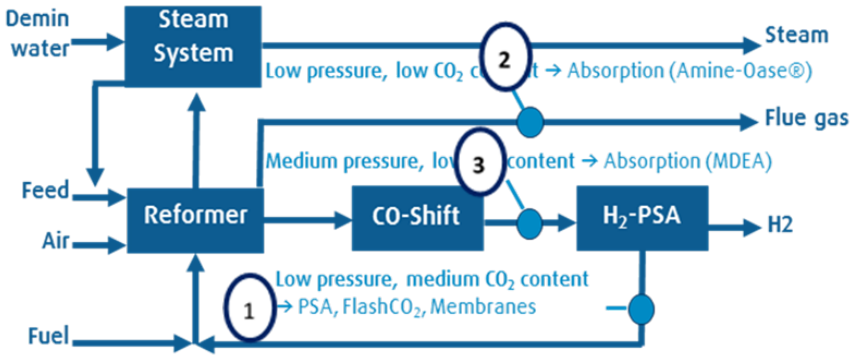

Figure 5.2. CO_2 capture in steam-methane reformer (SMR) based H2 plants: Solvent, PSA/VSA & membrane applications

Data and results of preliminary engineering designs discussed in Subtask 5.2 are presented in Table 5.1.

Table 5.1. Vital data and preliminary design for CO_2 capture at the three potential sources studied, utilizing the Linde-BASF amine-based PCC technology. MTPD = metric tons per day.

	Westar's Jeffrey Energy Center	**Sunflower's Holcomb Station**	**CHS Inc.'s Refinery**
Flue Gas			
Flow Rate, (MT/hr.) wet	2,063	1,191	363
Composition, (mol %) dry	CO_2 (13.2%) O2 (6.3%)	CO_2 (11.3%) O2 (2.5%)	CO_2 (19.1%) O2(2.7%)
Capture plant Capacity, (MW_e)	583 (~73% of Unit 1)	348 (100% of Unit)	~100 (100% of available flue gas)
Flue Gas Pressure, (bar)	1.01 (atmospheric)	1.01 (atmospheric)	1.01 (atmospheric)
Flue Gas Temperature, (◦C)	60	60	149
Product Gas			
Captured CO_2, (MTPD)	7,500	4,600	1,872
Capture Efficiency, (%)	90	90	90
Product Purity, (mol %)	99.7+ (<100ppmv O2) (<100ppmv H2O)	99.7+ (<100ppmv O2) (<100ppmv H2O)	99.7+ (<100ppmv O2) (<100ppmv H2O)
Product Pressure, (bar)	150	150	150
Product Temperature, (◦C)	<40	<40	<40
Utility Requirements			
Regenerator LP Steam, (MTPD)	8,640	4,600	2,184
Electrical Power, (MW)	40.4	24.5	9.6
Cooling Water, (m3/hr) x 1000	36	21.3	9
Plant Configuration			
Plot Size, m x m (PCC + compression/drying)	130 x 150	60 x 90	60 x 90
Absorber Height, (m)	60-75	60-75	60-75
Stripper Height, (m)	30-40	30-40	30-40

Subtask 5.2: Determine novel technologies or approaches for CO_2 capture

Standalone reports covering preliminary design and economic studies for each of the three potential CO_2 sources are presented in Subtask 5.2.

Subtask 5.2.1: Preliminary design and economic analysis for carbon capture at the Westar Energy Jeffrey Energy Center

5.2.1.1: Conceptual Design and Technical Feasibility

A preliminary design and economic analysis were completed to determine the feasibility of implementing the Linde-BASF amine-based technology for post-combustion capture (Figure 5.1) at the Westar Energy Jeffrey Energy Center (JEC), a large coal-fired power plant located in St. Marys KS. Table 5.2 presents a high-level overview of the design parameters. Figure 5.3 displays a 3D model view of the proposed PCC plant at the Westar's Jeffrey's Energy Center with a coarse indication of the plot size.

Table 5.2. High-level overview of the results for the proposed CO_2 source. MTPD = metric tons per day.

	Westar's Jeffrey Energy Center
Flue Gas	
Flow Rate, (MT/hr.) wet	2,063
Composition, (mol %) dry	CO_2 (13.2%), O_2 (6.3%)
Capture plant Capacity, (MW_e)	583 (~73% of Unit 1)
Flue Gas Pressure, (bar)	1
Flue Gas Temperature, (◦C)	60
Product Gas	
Captured CO_2, (MTPD)	7,500
Capture Efficiency, (%)	90
Product Purity, (mol %)	99.7+ (<100ppmv O2) (<100ppmv H2O)
Product Pressure, (bar)	150
Product Temperature, (◦C)	<40
Utility Requirements	
Regenerator LP Steam, (MTPD)	8,640
Electrical Power, (MW)	40.4
Cooling Water, (m3/hr) x 1000	36
Plant Configuration	
Plot Size, m x m (PCC + compression/drying)	130 x 150
Absorber Height, (m)	60-75
Stripper Height, (m)	30-40

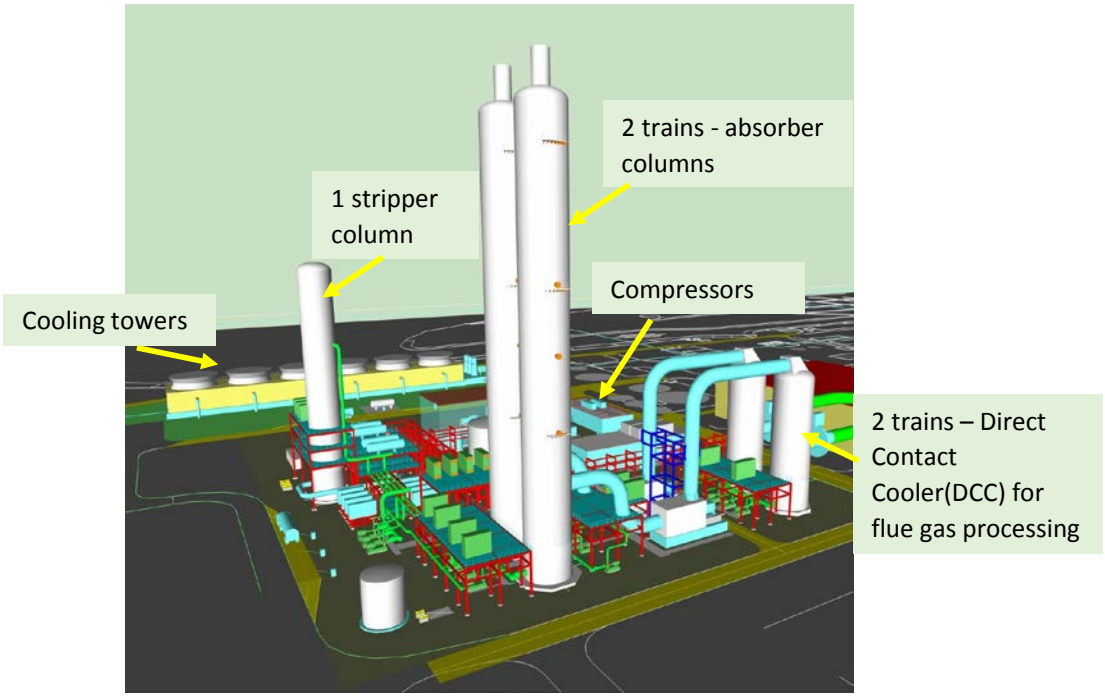

Figure 5.3. 3-D model of Linde-BASF post combustion capture plant designed for Westar's Jeffrey Energy Center. Based on a target capture rate of 7,500 metric tonnes per day of captured CO_2, 360 tonnes/hour of low pressure (LP)steam is required for solvent regeneration in the Linde-BASF post combustion carbon capture system using a novel amine solvent called OASE® blue. To reduce the specific energy consumption of the process and the operating costs for the large-scale solvent-based CO_2 capture project under consideration, a detailed engineering analysis of waste heat recovery options at the plant was performed.

The team approach for the engineering analysis was as follows:

- Determine low pressure steam requirement based on target CO_2 capture rate and estimate thermal energy required for LP steam generation
- Calculate waste heat recovery potential range and configuration options for an 800 MW_e unit at Jeffrey Energy Center (JEC)
    - for different assumed coal moistures, up to 30%
    - to prevent acid condensation of SO_2 and SO_3 in flue gas
- Determine thermal energy required for other uses within power plant
- Calculate the reduction in power production based on waste heat extraction
- Highlight other challenges for proposed heat recovery.

Three potential locations for waste heat extraction that could be used to generate steam for regeneration of the solvent in the stripper were identified and are illustrated in Figure 5.4:

1. The flue gas upstream of the FGD (flue gas desulfurizer) which is around 350-400°F. The FGD operates at around 100°F.
2. The flue gas leaving the selective catalytic reactor (SCR) for NOx removal at 832°F
3. Fly ash leaving the boiler at a high temperature and collecting in an ash removal hopper.

The available heat that could potentially be obtained from the three heat recovery options was used to calculate the amount of LP steam that could be generated under each scenario. The results are given in Table 5.3, along with the challenges that each option presents.

Table 5.3. Results from the analysis of waste heat extraction and utilization options at Westar's Jeffrey Energy Center.

	Waste Heat Recovery Option	**LP steam from waste heat (tonnes/hour)**	**Challenges for Heat Extraction**
#1	Flue Gas Upstream Flue Gas Desulfurizer	42	Low flue gas temperatures can cause acid condensation of SOx, which would require more expensive materials of construction
#2	Downstream Selective Catalytic Reactor (SCR) but upstream Activated Carbon Filter (ACI)	613	Some of this thermal energy is required for preheating air for coal combustion
#3	Fly Ash Waste Heat Recovery	< 1	Solid/gas heat exchange is a technical challenge. Significant capex required for low thermal energy extraction.

The results indicate that option 2 presents the most attractive option for the Jeffrey Energy Center. This opportunity has the potential to provide >100% of thermal energy required for the carbon capture plant's LP steam generation needs. The other two options 1 and 3 are not able to meet the full LP steam load of the PCC However, to fully understand the feasibility of this option, the total cost of heat recovery and utilization (CAPEX + OPEX) would need to be compared with the cost of utilizing steam from the existing IP-LP (intermediate pressure to low pressure) crossover at 700◦F. This is the current method for obtaining LP steam for solvent generation in post-combustion capture (PCC) plants, although it affects the power plant efficiency and reduces the total power production.

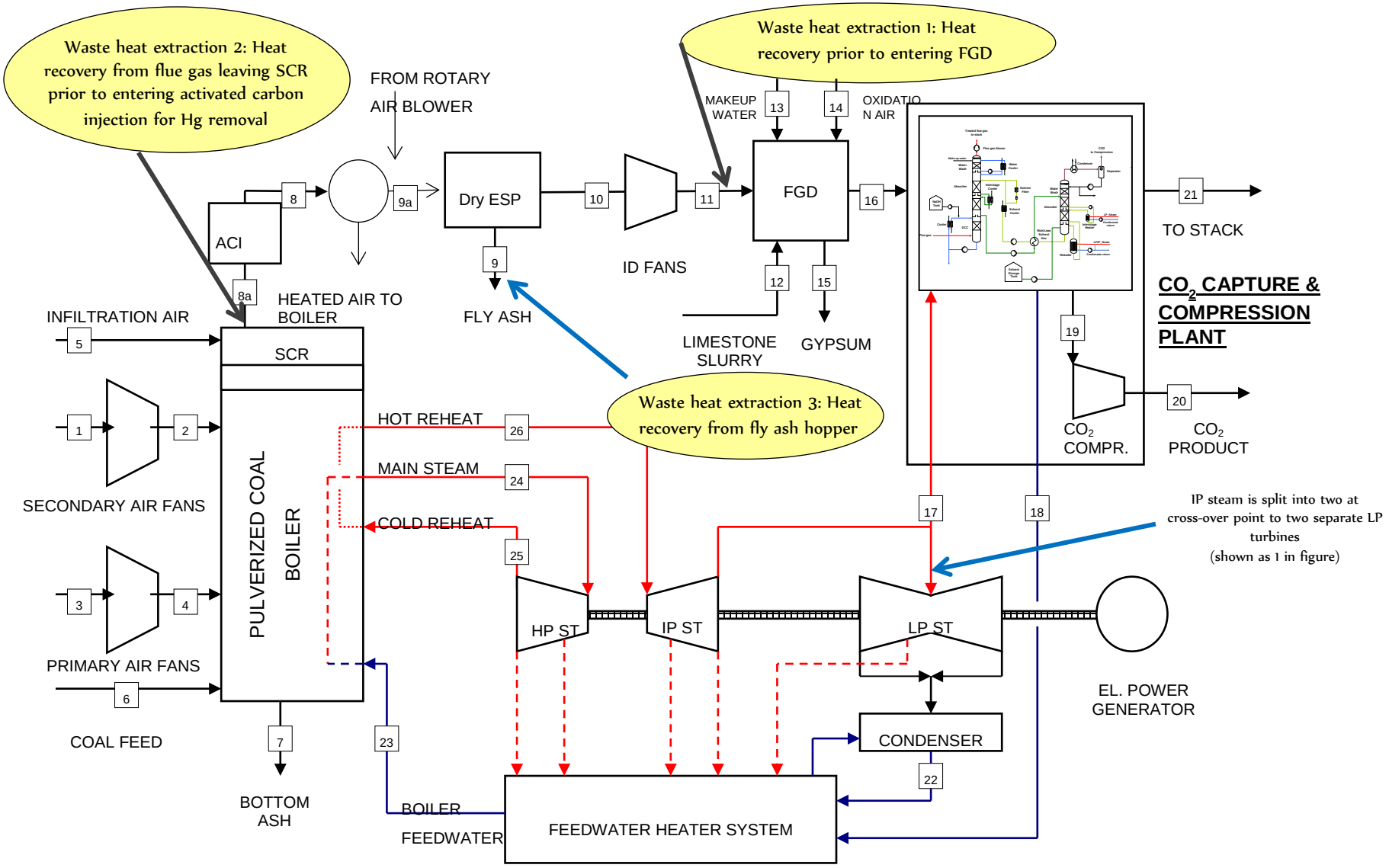

Figure 5.4. Block Flow Diagram of power plant showing potential sources of waste heat for extraction and use in PCC plant to generate low pressure steam.

5.2.1.2: Preliminary Techno-Economic Analysis

A preliminary economic analysis was conducted to evaluate a range of likely costs of capture based on the solvent-based Linde-BASF PCC technology at the Jeffrey Energy Center. The team considered cost sensitivity to capital costs of equipment, steam and power demand and costs, and options for waste heat recovery at the power plant.

Because the power plant does not change its size or produce more steam for CO_2 capture, Linde has calculated the reduction in the electrical output of the plant due to the repurposing of steam for solvent regeneration. This loss in power output is included in the parasitic electrical energy demand and increases it from 40.5 MW to 95.3 MW. Since the cost of power is typically lower than the cost of steam, this approach favors the cost of captured CO_2. The matrix of variables considered is shown below in Table 5.4.

Table 5.4. Matrix of variables investigated for carbon capture costs at the Jeffrey Energy Center.

		Upside	**Base**	**Downside**
Capital Costs		-25%	0%	+25%
Power plant parasitic electrical loss	kWh/t CO_2	305	305	305
Cost of power	$/MWh	$44.3	$44.3	$65.0

The results of the sensitivity analysis are given in Table 5.5 as a range of cost per tonne of CO_2 captured. In the best-case scenario, the costs of CO_2 capture at the Jeffrey Energy Center meets the DOE target for retrofit of existing pulverized coal (PC) plants with carbon capture ($45/t CO_2). If the power plant waste heat can be effectively recovered and utilized in the capture plant, this would offset the PCC parasitic load and further reduce the cost of CO_2 to $42/t CO_2. Linde has shown that under certain configurations for a greenfield site, their solvent-based technology with BASF can be as low as $40/t CO_2 (Bostick et al., 2017).

Table 5.5. Range of costs for CO_2 capture using the Linde-BASF solvent-based carbon capture technology at the two sources of anthropogenic CO_2.

		Cost of Capture	
Facility	Capture Rate	Best Case	Worst Case
	tonnes/annum	/tCO_2	/tCO_2
Jeffrey Energy Center	2,687,500	$45	$68

Subtask 5.2.2: Preliminary design and economic analysis for carbon capture at the Sunflower Electric Holcomb Station

5.2.2.1: Conceptual Design and Technical Feasibility

A preliminary design and economic analysis were completed to determine the feasibility of implementing of implementing the Linde-BASF amine-based technology for post-combustion capture (Figure 5.1) at the Sunflower Electric Power Corporation -Holcomb Station, Holcomb, Kansas. Table 5.6 presents a high-level overview of the base case design parameters. Figure 5.5 displays a 3-D model view of the proposed PCC plant at the Sunflower's Holcomb Station with a coarse indication of the plot size.

Table 5.6. Preliminary design for CO_2 capture at Sunflower Holcomb power plant.

	Case 1 – Integrated PCC at Sunflower Holcomb Power Plant
Flue Gas	
Flow Rate, (MT/hr) wet	1,191
Composition, (mol %) dry	CO_2 (11.3%), O_2 (2.5%)
Capture plant Capacity, (MW_e)	348 (100% of Unit)
Flue Gas Pressure, (bar)	1.01 (atmospheric)
Product Gas	
Captured CO_2, (MTPD)	4,600
Capture Efficiency, (%)	90
Product Purity, (mol %)	99.7+ (<100ppmv O_2), (<100ppmv H_2O)
Product Pressure, (bar)	150
Product Temperature, (◦C)	<40
Utility Requirements	
Regenerator LP Steam, (MTPD)	4,600
Electrical Power, (MW)	24.5
Cooling Water, (m^3/hr) x 1000	21.3

Based on a target capture rate of 4,600 metric tonnes per day of captured CO_2, 190 tonnes/hour of low pressure (LP)steam is required for solvent regeneration in the Linde-BASF post combustion carbon capture system using a novel amine solvent called OASE® blue. The capture plant would also need 24.5 MW of power for rotary equipment and compression of CO_2 product. Several scenarios were investigated to determine the lowest cost option for providing auxiliary power and steam to the capture plant. These cases are described below.

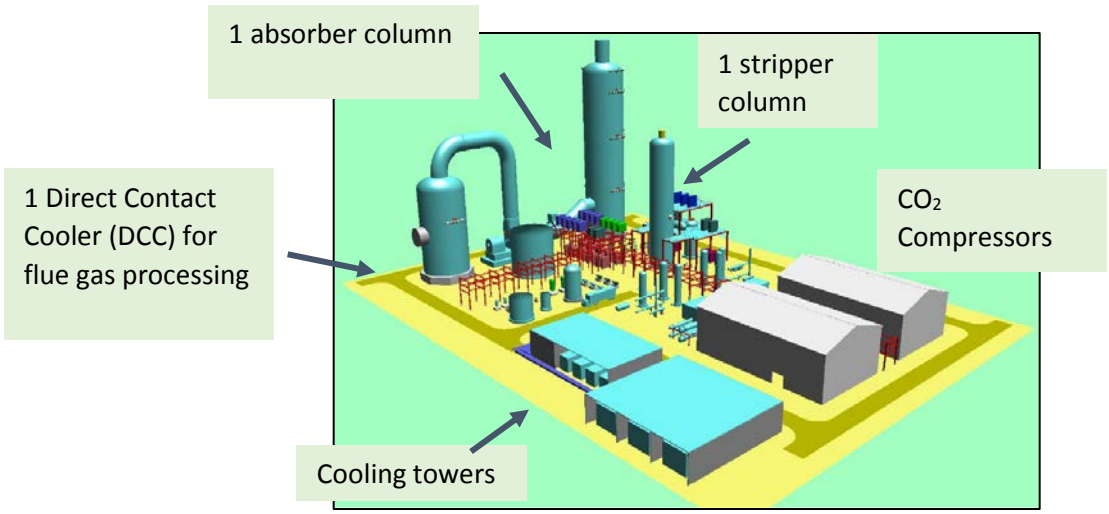

Figure 5.5. 3-D model of Linde-BASF post combustion capture plant.

- **Case 1a: Integrated capture—**The low-pressure steam needed for solvent regeneration in the PCC plant is taken from the intermediate pressure to low pressure cross-over point within the power plant steam cycle (Figure 5.6). The auxiliary electricity required for the PCC plant and CO_2 compression is drawn from the grid.
- **Case 1b: Integrated partial capture—**This case is similar to Case 1a, but the capture plant capacity is set at 70% of the total power plant capacity

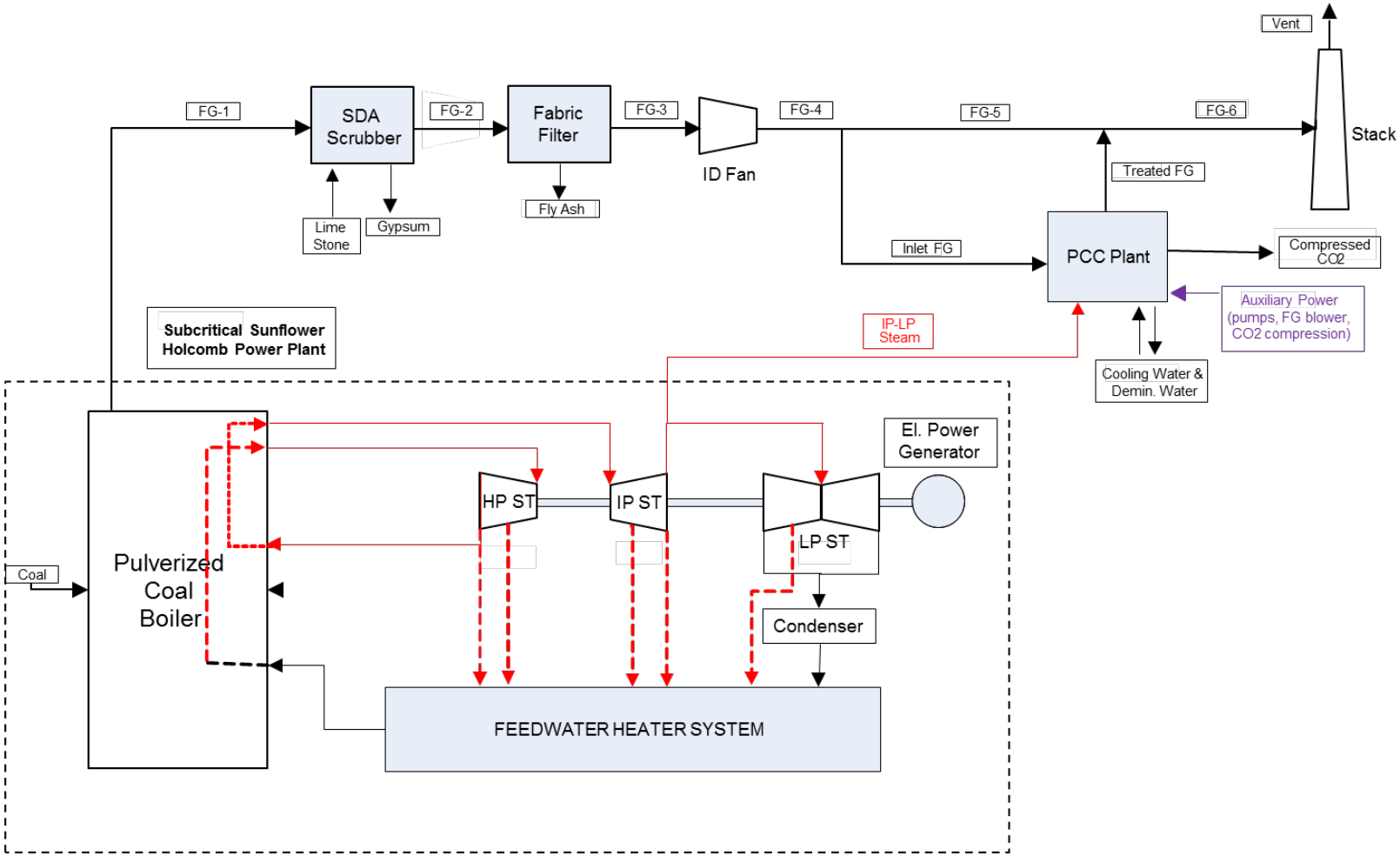

Figure 5.6. Simple block diagram illustrating Case 1: Sunflower Holcomb Station Subcritical Power Plant integrated with Post-Combustion CO_2 Capture (PCC) Plant.

- **Case 2: NGCC Cogeneration (NGCC) –** A natural gas fired combined-cycle cogeneration plant can be built to provide both the low-pressure (LP) steam needed for solvent regeneration and the auxiliary power required for the PCC plant operation and CO_2 compression (Figure 5.7). When configured to meet the PCC LP steam demand, a standard NGCC plant produces an excess amount of power above what is required for the PCC. This excess power requires export to the grid.

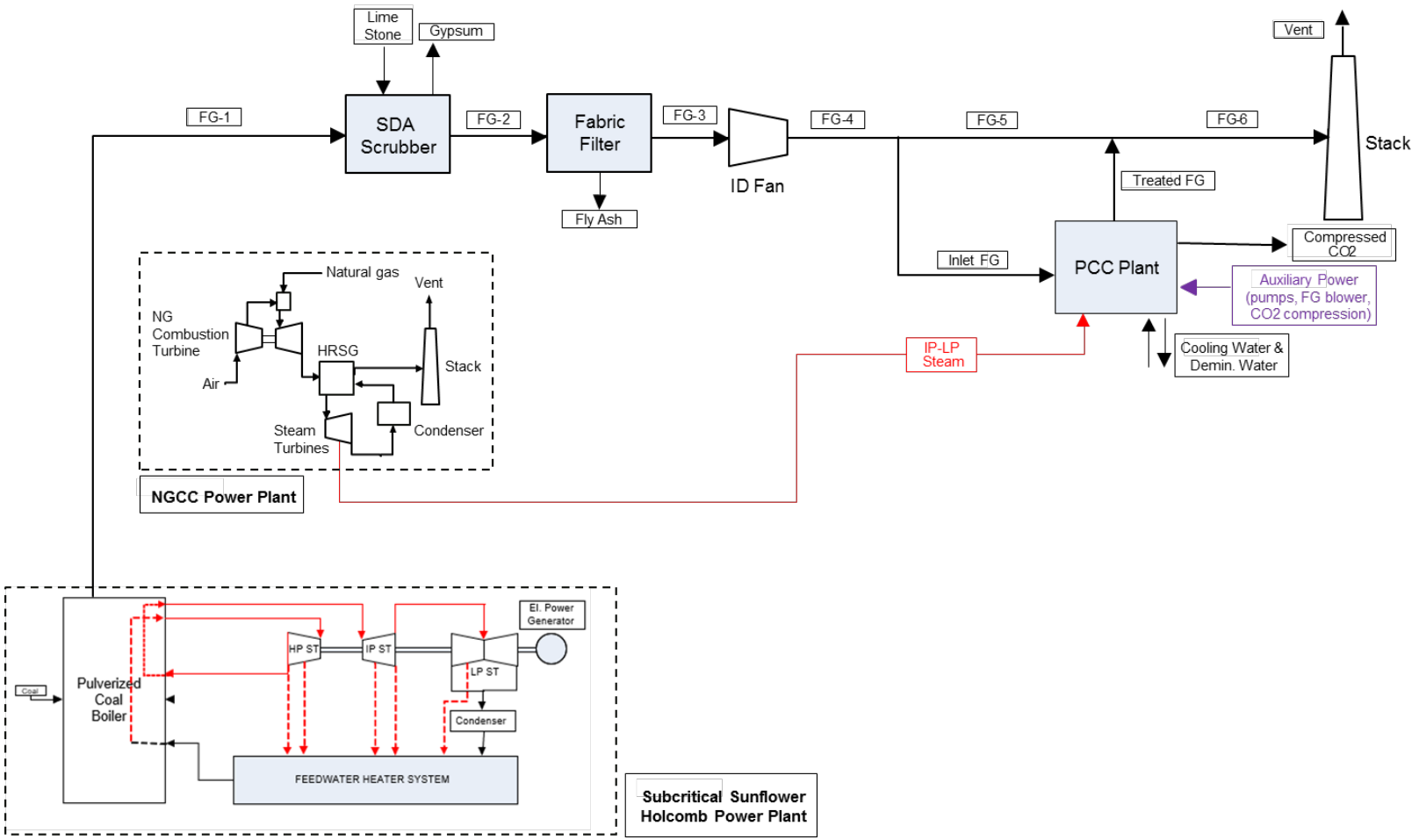

Figure 5.7. Simple block diagram illustrating Case 2: Sunflower Holcomb Station Subcritical Power Plant with Natural Gas Combined Cycle (NGCC) plant to provide steam and power for PCC plant.

- **Case 3: Packaged air boiler cogeneration (PAB) –** A packaged air boiler and steam turbine system can be installed to provide both the low-pressure steam needed for solvent regeneration and the auxiliary power required for the PCC plant operation and CO_2 compression (Figure 5.8). A dedicated cooling tower is installed for the boiler. The capacity of the packaged boiler/steam turbine system is designed to cover the PCC plant maximum demand and minimize the generation of excess power.

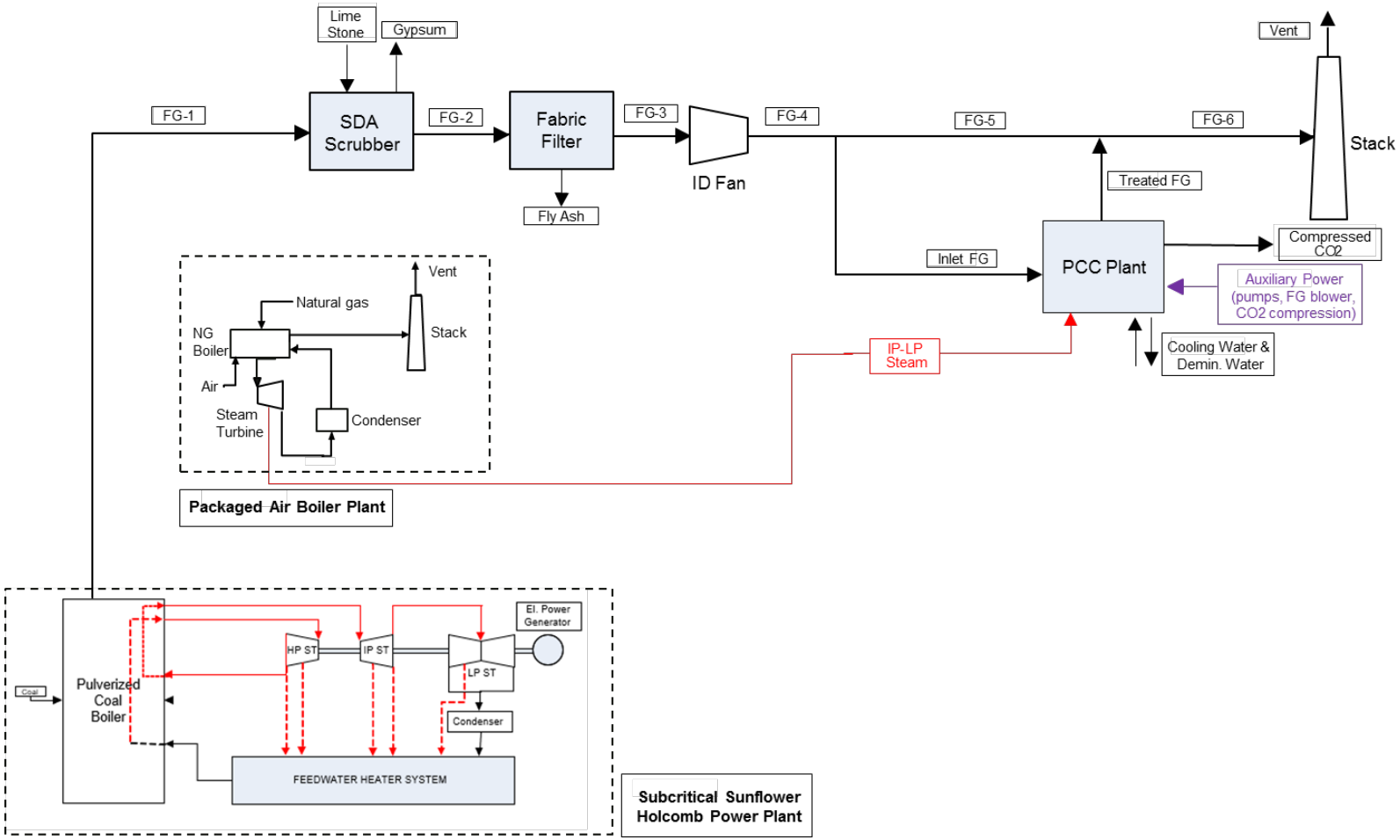

Figure 5.8. Simple block diagram illustrating Case 3: Sunflower Holcomb Subcritical Power Plant with NG-Fired Packaged Air Boiler (PAB) to provide steam and power for PCC plant.

The four cases presented require power for the PCC plant for steam required for solvent regeneration and CO_2 compression. Power, and/or steam could be derived from the existing plant, reducing the plant's output (Cases 1a and 1b) or by adding NGCC cogeneration (Case 2) or packaged air boiler (Case 3). The overall effects for the four cases presented are illustrated in Table 5.7.

Table 5.7. Effect of PCC steam and power demand on power plant and grid resources.

	Case 1a	**Case 1b**	**Case 2**	**Case 3**
Power plant net power (MW_e)	331	336	348	348
Auxiliary power taken from grid (MW_e)	24.5	17.2	0	0
Excess power available to grid (MW_e)	0	0	121	3.2
Natural gas fuel feed rate, (MT/hr)	0	0	17.6	15.1
Additional capital required for steam and power generation	No	No	Yes	Yes

5.2.2.2: Preliminary Techno-Economic Analysis

An economic sensitivity analysis was performed around the parameters that can affect the cost of CO_2 under these different scenarios. The PCC capital cost was found to have the largest effect on the cost of captured CO_2. Table 5.8 shows the range in the cost per ton of captured CO_2 for PCC capital costs that are +40% and -25% of the base price. In addition, the team also investigated the effect of the costs of integration, the cost of providing steam and power using an NGCC or PAB/turbine system, the life of the PCC plant, the cost of power, the cost of natural gas, and the cost of water.

Table 5.8. Range of costs for CO_2 capture using the Linde-BASF solvent-based carbon capture technology for the four cases considered.

	Cost of Capture	
Facility	Best Case	Worst Case
	$/tCO$_2$	$/tCO$_2$
Case 1a	46	72
Case 1b	50	79
Case 2**	35	61
Case 3	46	71

The case for cogeneration of steam and power with a natural gas combined-cycle power plant can present an economical alternative for captured CO_2. However, the extent of this benefit is risky, as it depends on factors outside of the control of the PCC technology supplier. These include:

- ***The availability of natural gas:*** although natural gas is used onsite in an auxiliary boiler, the project is not aware of any current mechanism that would allow use of that existing natural gas infrastructure for the PCC plant. In addition, land use in the area for any new natural gas infrastructure is constrained,
- ***The ability to sell excess power of 121 MW:*** due to the extreme penetration of wind resources near the site and the federal programs which support the increase in penetration, the dispatch of natural gas-based electricity may be disadvantaged,

- ***And, the market cost of excess power.*** The economic analysis assumed that this power could be sold at market rates of $40/MWh. However, given the dynamics of power pricing and the fact that the current Southwest Power Pool (SPP) market allows negative power pricing during periods of excess production and low load conditions, this may be an optimistic projection for an average selling price over the life of the project.

Case 3 also cogenerates steam and power. However, the packaged air boiler/steam turbine system can be optimized to minimize or eliminate the excess power generated.

DISCLAIMER: Except for the specific representations made by Sunflower regarding its Holcomb Station facility, The Linde Group ("Linde") and the Kansas Geological Survey-The University of Kansas ("KGS"), disclaim that it is relying upon or has relied upon any other representations that may have been made by Sunflower, and acknowledge and agree that Sunflower has specifically disclaimed and does hereby disclaim any such other representation made by Sunflower; and agree that Sunflower did not contribute to, nor does Sunflower validate, the analysis or results of the study.

Subtask 5.2.3: Preliminary design and economic analysis for carbon capture at the CHS, Inc. refinery, McPherson, Kansas

5.2.3.1: Conceptual Design and Technical Feasibility

A preliminary design and economic analysis were completed to determine the feasibility of implementing carbon capture at the CHS, Inc. refinery in McPherson, Kansas. Due to the large volumes of CO_2 targeted for sequestration as part of the ICKan project, the team chose to evaluate the Linde-BASF amine-based technology for post-combustion capture (Figure 5.1) of the combined flue gas from two steam methane reformer (SMR) based hydrogen plants (Figure 5.9)**.**

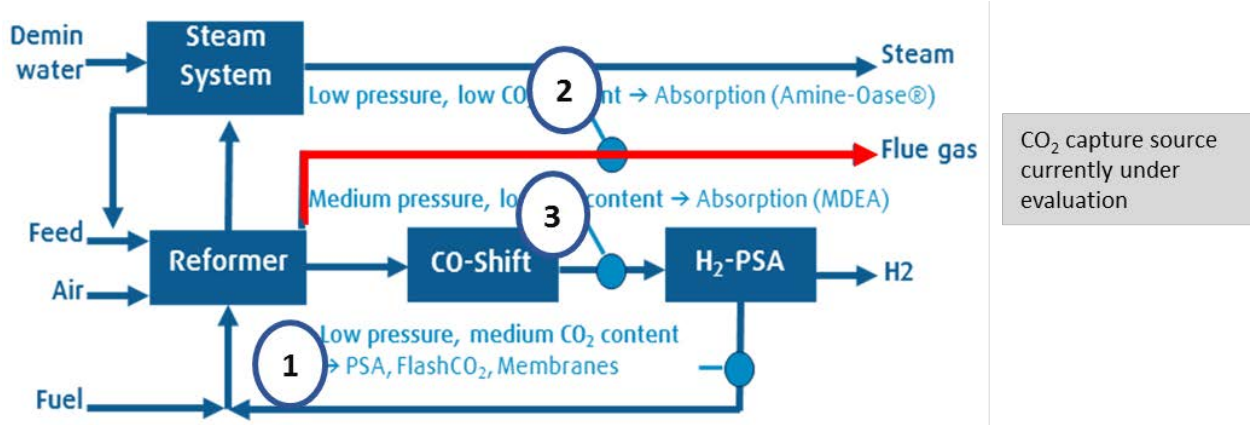

Figure 5.9. CO_2 Capture in Steam-methane reformer (SMR) based H2 plants: Solvent, PSA/VSA & membrane applications.

The refinery has advised the team to design a capture system for the current operating capacity of the plant (40 mmscfd and 42 mmscfd), despite the potential for future expansion or improvement projects. This is preferable since the reformers are not always run at 100% capacity at the same time. Table 5.9

presents a high-level overview of the design parameters. Figure 5.10 displays a 3-D model view of the proposed PCC plant at the Westar's Jeffrey's Energy Center with a coarse indication of the plot size.

Table 5.9. High-level overview of the results for the proposed CO_2 source. MTPD = metric tons per day.

	CHS Inc.'s Refinery
Flue Gas	
Flow Rate, (MT/hr.) wet	363
Composition, (mol %) dry	CO_2 (19.1%), O_2(2.7%)
Capture plant Capacity, (MW_e)	~100 (100% available flue gas)
Flue Gas Pressure, (bar)	1
Flue Gas Temperature, (◦C)	60
Product Gas	
Captured CO_2, (MTPD)	1,872
Capture Efficiency, (%)	90
Product Purity, (mol %)	99.7+ (<100ppmv O2) (<100ppmv H2O)
Product Pressure, (bar)	150
Product Temperature, (◦C)	<40
Utility Requirements	
Regenerator LP Steam, (MTPD)	2,184
Electrical Power, (MW)	9.6
Cooling Water, (m3/hr) x 1000	9
Plant Configuration	
Plot Size, m x m (PCC + compression/drying)	60 x 90
Absorber Height, (m)	60-75
Stripper Height, (m)	30-40

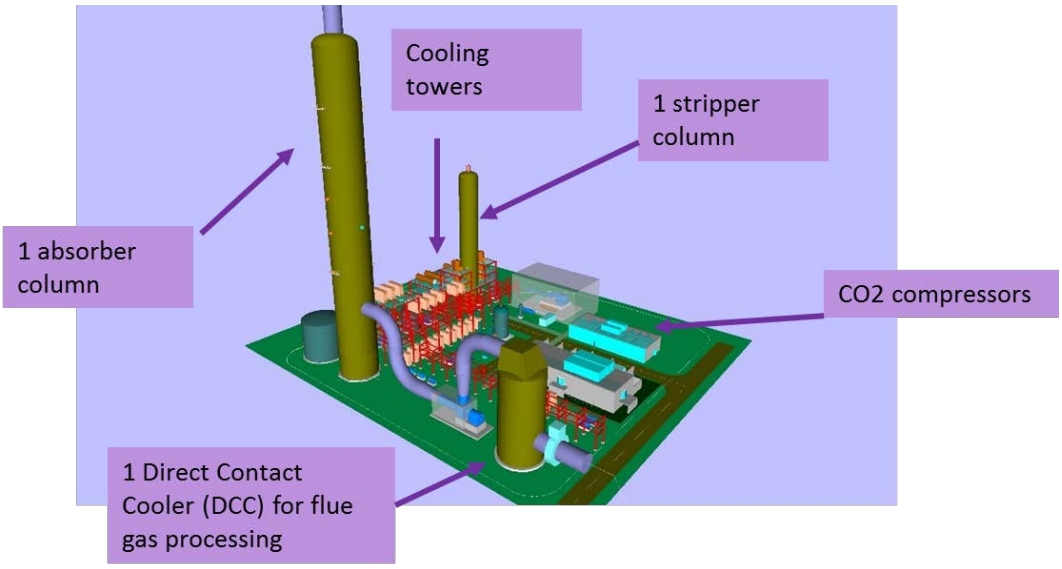

Figure 5.10. 3-D model of Linde-BASF post combustion capture plant designed for CHS refinery.

The refinery is short on steam and the sources are distributed throughout the facility. For solvent-based PCC to be feasible at this site, a new gas-fired boiler would need to be built to generate the low-pressure steam required for solvent regeneration. Adsorption-based technologies, although they do not require steam, do require electric power to drive the compressor or vacuum pumps. The current cost of electricity at the refinery is $0.04425/KWH. The cost of a new boiler system and its components for the generation of low-pressure steam is estimated at $10MM.

5.3.3.2: Preliminary Techno Economic Analysis

A preliminary economic analysis was conducted to evaluate a range of likely costs of capture based on the solvent-based Linde-BASF PCC technology. The team considered cost sensitivity to capital costs of equipment, costs of installation, steam and power demand and costs, and options for waste heat recovery at the power plant. The matrix of variables considered for the CHS refinery is shown below in Table 5.10.

Table 5.10. Matrix of variables investigated for carbon capture costs at the CHS refinery.

		Upside	**Base**	**Downside**
Capital Costs		- 40%	0%	0%
Carbon capture electrical demand	kWh/t CO_2	123	123	135
Carbon capture steam demand	t steam/ hr	91	91	100
Cost of power	$/MWh	$44.3	$44.3	$65.0
Cost of steam	$/ t steam	$11.1	$11.1	$13.5

The results of the sensitivity analysis are given below as a range of costs (Table 5.11). The results indicate that solvent-based carbon capture at the CHS refinery is less economically attractive than at a power plant. For better economics, other capture options such as membrane-based technologies or PSA/VSA-based technologies, should be evaluated.

Table 5.11. Range of costs for CO_2 capture using the Linde-BASF solvent-based carbon capture technology at the CHS refinery.

		Cost of Capture	
Facility	Capture Rate	Best Case	Worst Case
	tonnes/annum	/tCO_2	/tCO_2
CHS SMR refinery	670,800	$60	$94

Subtask 5.3: Develop an implementation plan and strategy for cost effective and reliable carbon capture

An optimal CCS plan and strategy that best represents the holistic operating environment and requirements of the CO_2 sources will be developed. The team shall develop a means to ensure a mechanism to update and adapt to new disruptive technologies and possibly accommodate them in the design document.

5.3.1: Implementation plan

Having three potential capture sites provides multiple options and flexibility in the overall project implementation plan that integrates capture, transportation and geologic storage, discussed in a later section. One of the primary drivers is the cost of CO_2 capture. Preliminary economic analyses were conducted to evaluate a range of likely costs of capture for each facility based on high-level preliminary engineering designs. Table 5.12 shows the range in the cost per ton of captured CO_2 for PCC capital costs that are +40% and -25% of the base price. See Subtask 5.2 report for complete description of the design for each facility or case. Economic analysis was conducted using a proprietary DCF-based Linde finance model with the following assumptions:

- Required IRR – 10%
- Project life – 20 years
- Cost assumptions used a combination of industry best practices and publicly available information
- All parasitic power costs for steam generation and compression are included at retail price
- CO_2 output is 99%+ pure and at 150 bar

Table 5.12. Preliminary cost estimates for CO_2 capture and compression at three facilities.

Facility	**Capture Rate (tonnes/annum)**	**Best Case ($/tCO$_2$)**	**Worst Case ($/tCO$_2$)**
Jeffrey Energy Center	2,687,500	$45	$67
Holcomb Station, Case 1a	1,679,000	$46	$72
Holcomb Station, Case 1b	1,175,300	$50	$79
Holcomb Station, Case 2	1,679,000	$35	$61
Holcomb Station, Case 3	1,679,000	$46	$71
CHS SMR refinery	670,800	$60	$94

Based on cost estimates alone, capture from the steam reformers at the CHS refinery are at a distinct disadvantage. High costs coupled with relatively low CO_2 volumes, well under the target of 50Mt over the life of a project, likely rule this facility out. The estimated cost of capture for the Jeffrey Energy Center and Holcomb Station Cases 1a, 2, and 3 are at or below the DOE target for retrofit of existing pulverized coal (PC) plants with carbon capture ($45/t CO_2). Either or both (JEC and Holcomb) could be part of a large-scale integrated system outlined in the overall implementation plan.

Task 6.0: Perform a high-level technical assessment for CO_2 transportation

Contributors to Task 6 include Martin Dubois and Dane McFarlane.

Note: *Rather than covering transportation alone, the Task 6 report includes economic analyses of several fully integrated systems for CO_2 capture, compression and transportation from sources to injection sites (in Subtask 6.3). Because there is currently no infrastructure capable of transporting CO_2 from sources to injections sites in Kansas, the economics of a wholly integrated system, including capture, initial compression and delivery to the injection site via pipeline, must be evaluated.*

Subtask 6.1: Review current technologies for CO_2 transportation

Because large-scale coal-fired power plants, capable of supplying the requisite amount of CO_2 for a 50 Mt project, are distant to potential storage sites, pipelines are the only option for transporting large volumes of CO_2. Smaller, more disparate ethanol plant sources considered as alternatives or as a means to enhance the economics of a larger CO_2 transportation through economies of scale would also be best served by pipelines. Compressing CO_2 to a supercritical state and transporting it via pipelines is the most cost-effective manner in which to transport large volumes. Because of the long history (40+ years) of CO_2 transportation, and even a longer history of transporting high-pressure natural gas, there are no significant technical challenges to transporting CO_2 via pipelines. Non-technical challenges are covered separately in Task 3.

Subtask 6.2: Determine novel technologies or approaches for CO_2 transportation

Because the transportation of CO_2 by pipeline for EOR has been occurring for 40+ years, the technology is considered "off-the-shelf." However, transporting large volumes of CO_2 considerable distances for CCS in saline aquifers in the continental United States is something new and presents economic challenges. A novel approach that should be considered in the ICKan project and possibly in other CCS locales is to lower the cost of transportation of CO_2 destined for saline aquifer storage by transporting it in pipeline systems carrying CO_2 for EOR, thereby decreasing the overall transportation costs. In a case discussed in Subtask 6.3, 2.5 Mt/yr CO_2 from a coal-fired power plant would connect to a large-scale pipeline that might transport 9.85 Mt/yr CO_2 exclusively from ethanol plants. Expansion of the trunk line would benefit the carrier by reducing transportation costs of the ethanol CO_2, and, possibly more important, diversify the systems sources.

Gains in efficiency in capital costs are directly related to carrying capacity. Pipeline capacity is a function of the cross-sectional area of the pipe, which is a function of the square of the radius. Doubling the radius increases the cross-sectional area by a factor of four. Capacity is not directly proportional to the cross-sectional area because throughput losses due to friction as a percent of capacity is inversely proportional to pipe size. There are definite economies of scale when compared to throughput for pipe, but less so for labor, right-of-way, surge tanks, pump stations and control systems, some of which are nearly fixed regardless of pipe size. Operating costs also gain efficiencies in scale in all areas of operations and maintenance except for electricity to run the pump stations.

Efficiencies gained by scale are demonstrated by data in Table 6.1 and Figure 6.1. Data on costs are from the modified NETL Transport Cost Model, discussed more thorough in Subtask 6.3. The table and figure compare costs for varying pipe sizes for 200-mile long pipelines. Assumptions include 80% capacity efficiency, four pump stations, and a 2,000psi inlet pressure and 1,400 psi pressure at the outlet. Capital costs per tonne of CO_2 vary significantly with pipe size. In comparing the increase in diameter from 8-

inch to 16-inch, capital costs increase 1.9x ($150 to $286 million) but the model predicts capacity to increase 5.3x (1.06 to 5.63 Mt/year). Annual operating expense are predicted to decrease from $2.39 to $1.04 per tonne, a 56% decrease on a per-tonne basis. It is noteworthy that the modified NETL Transport Cost Model may over-estimate costs for smaller pipelines, especially 4-inch lines.

Table 6.1. CO_2 volumes transported by pipe diameter and modeled capital costs (CapEX) and annual operating expense (OpEX). Mt = million metric tonnes.

Length (miles)	CO_2 Volume (Mt/yr)	Diameter (inches)	CapEX ($million)	Annual OpEX ($million)	CapEX/tonne ($/tonne-yr)	OpEX ($/tonne)
200	0.17	4	$113	$1.89	$667	$11.10
200	0.50	6	$130	$2.12	$259	$4.24
200	1.06	8	$150	$2.54	$141	$2.39
200	3.05	12	$201	$3.98	$66	$1.31
200	5.63	16	$286	$5.86	$51	$1.04
200	10.06	20	$384	$9.09	$38	$0.90
200	16.10	24	$508	$13.49	$32	$0.84
200	28.80	30	$706	$22.74	$25	$0.79

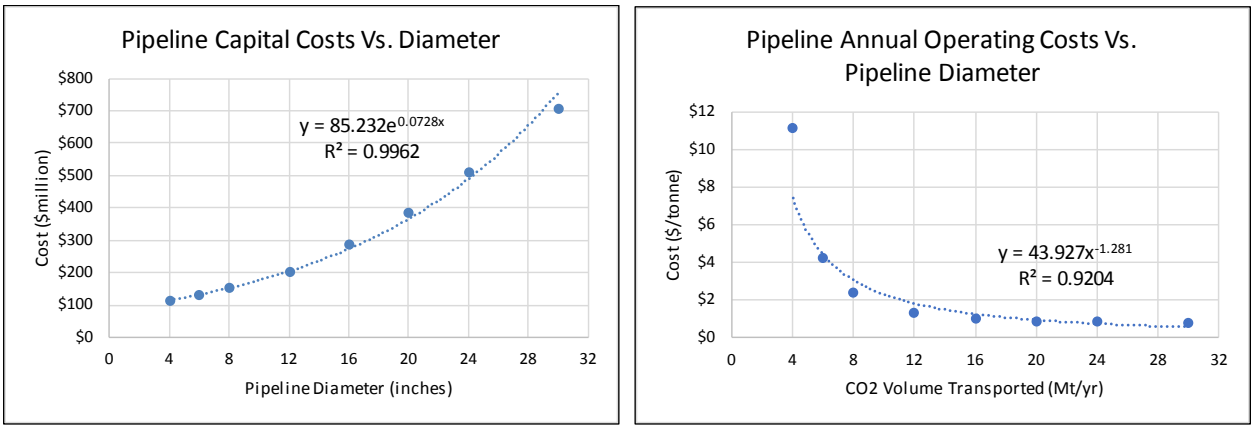

Figure 6.1. Data from Table 6.1 cross-plotted.

Subtask 6.3: Develop a plan for cost-efficient and secure capture and transportation infrastructure

6.3.1: Introduction

Understanding the economics of and exploring options and strategies to transport CO_2 from large-scale anthropogenic sources in the most optimal manner is a key component of the ICKan project. Because large-scale coal-fired power plants (e.g.: Jeffrey Energy Center) are distant to potential storage sites, pipelines are the only option for transporting large volumes of CO_2. However, pipelines have extremely high capital costs that negatively impact the overall costs and feasibility for CCS projects. The ICKan project considers the option of reducing the net costs for CO_2 transported for CCS by combining CO_2 captured from power plants with CO_2 destined for EOR operations in a larger system.

6.3.2: Modeling pipeline costs

We identified the National Energy Technology Laboratory's (NETL) CO_2 Transport Cost Model (Grant et al., 2013; Grant and Morgan, 2014) as a resource for estimating the technical requirements and costs of CO_2 transport through pipelines. In test runs, the model capital cost estimates compared well against pipeline cost estimates prepared by pipeline engineering firms in McPherson (2010) and that of a privately funded feasibility study in another, unrelated project. The capital costs estimated by the NETL cost model compare well with an industry rule-of-thumb, $100,000/inch-mile, except for small diameter pipes (4 inch) where cost model estimates are consistently higher. Advantages to using the NETL model are that it breaks down capital costs, provides annual operating costs and is simple to run. A disadvantage for our project is that it calculates only one segment at a time. The NETL model calculates costs by pipeline segment based on inputs such as pipeline length, annual CO_2 volume, input/outlet pressure, capacity factor, and number of booster pumps. Model output includes capital costs for materials, labor, right-of-way negotiations, CO_2 surge tanks, pipeline control systems, and pumps. Operational costs include pipeline O&M, equipment and pumps, and electricity costs for pumps, by segment. Calculations are done through both spreadsheet formulas and more complex Excel Visual Basic for Applications (Excel VBA) functions.

To evaluate costs from multiple sources, the ICKan project requires the assessment of pipeline networks composed of multiple trunk segments and many feeder lines connected to individual CO_2 sources; however, the original NETL model calculates specifications and costs for only one pipeline at a time. To streamline the process of calculating many pipeline network segment costs, Great Plains Institute (GPI), an ICKan partner, created additional Excel VBA macro functionality to interact with the NETL cost model. More details on the modifications and use of this tool are in Dubois et al. (2017) and Appendix I. Without changing or modifying the NETL spreadsheets or VBA code in anyway, GPI created a VBA macro that collects inputs from a list of pipeline segments, inputs the parameters for each segment, and records the model outputs for each segment individually. The cost outputs are then summed for the systemwide costs. Model inputs and outputs are summarized in Table 6.2. Model costs are in 2011 dollars, the model default.

Table 6.2. Model inputs and outputs. Abbreviations: MT/yr = million tonnes/year, psig = pounds per square inch gauge, ID = inside diameter, ROW = right of way, O&M = operations and maintenance.

Inputs (by segment)	**Outputs (by segment)**
length (miles)	minimum pipeline ID (inches)
number of booster pumps	pipeline nominal diameter (inches)
annual CO2 transport capacity (MT/yr)	materials costs
capacity factor	labor costs
input pressure (psig)	ROW-damage costs
output pressure (psig)	miscellaneous costs
change in elevation (feet)	CO2 surge tanks costs
	pipeline control system costs
	pump costs
	Total capital cost
	pipeline O&M
	other equipment and pumps O&M
	electricity costs for pumps
	Total annual operating expenses

Inputs for ICKan pipeline models

1. Pipeline lengths—We first determined the most logical pipeline path based on source size and location and the market location (EOR or storage site) and plotted straight-line segments and measured segment lengths using ESRI ArcGIS geographic information system mapping program. Segment lengths were multiplied by a factor of 1.1 to approximate additional routing requirements. Ethanol plant locations were derived from Energy Information Agency (EIA) tables (DOE-EIA, 2017).
2. Number of booster pumps—An iterative process was used to determine the optimal number of booster pump stations by comparing costs. There is a trade-off between pipe diameter and pipeline costs (smaller with more pumps) and the capital and operating expense of pump stations.
3. Annual CO_2 transport capacity—Determined by Linde Group specifications for Jeffrey Energy Center, Holcomb Station and CHS Refinery. Ethanol CO_2 production was set at 90 percent of plant fermenter-sourced potential based on nameplate ethanol production volumes derived from EIA tables (DOE-EIA, 2017). Ethanol production converted to CO_2 at the rate of 6.624 pounds CO_2 per gallon of ethanol (Dubois et al., 2002).
4. Pipeline capacity factor—used the default (80%).
5. Input and output pressures—2,000 psig and 1,400 psig. This is the pressure of CO_2 when it enters the system (input) and exits at the injection sites (output). It is also the pressure drop allowed in the model between pump stations.
6. Change in elevation—used the default, no net change in elevation. There is a gradual rise in elevation from east to west approaching 1,500–2,000 feet.

6.3.3: Costs of capture and initial compression

The cost of capture and compression for coal-fired power plants and a refinery's methane reformer was thoroughly discussed in the Task 5 report. The Linde Group, and ICKan partner, estimated cost for capture and compression to150 bar (2200 psi) for Jeffrey Energy Center (2.5 Mt/yr), Holcomb Station (1.7 Mt/yr) and CHS Refinery (0.67 Mt/yr) at a cost range by facility of $45–$67/tonne, $46–$72/tonne, and $60–$94/tonne, respectively. The cost/tonne includes both capital and operating expenses over a 2-year construction and 20-year operating life, including a 10% cost of capital (or ROI).

(Note: The following discussion of capital and operating costs for CO_2 from ethanol plants was taken directly from the Appendix to the State CO_2-EOR Deployment Work Group's white paper: Capturing and Utilizing CO_2 from Ethanol (State CO_2-EOR Deployment Work Group, 2017). Dane McFarlane, Great Plains Institute, and Martin Dubois, Improved Hydrocarbon Recovery, LLC, and ICKan project Joint-PI, are the authors of the Appendix and the Technical Evaluation of the Ethanol Opportunity section of the white paper).

Estimating the capital and operating costs for CO_2 capture, compression, and dehydration (CCD) from fermenters in an ethanol plant is problematic because of the paucity of publicly available data. There are currently only three commercial-scale ethanol plant operations that process and deliver CO_2 via pipelines for injection into geologic targets, two for EOR and the other for saline storage, and capital expenditures (CapEX) and operating expenses (OpEX) are not publicly available for the three privately operated facilities. For this study, we relied on CapEX estimates from two DOE-funded projects (McPherson, 2010, and Leroux, 2017) and data sourced from a publicly available presentation covering a third DOE-funded project (McKaskle, 2016). These data were augmented and adjusted by input from trusted sources with direct project experience. A simple linear regression equation was derived by cross-plotting CapEX estimates and ethanol plant size in millions of gallons per year (MGY) for the three examples:

*CapEx ($Million) = 0.15*Plant Size [million gallons per year (MGY)] + 9*

Capital costs for 55 and 200 MGY plants are estimated at $17 and $39 million respectively, and they typically emit 400 and 1,480 tonnes/day, respectively, of capturable CO_2 from the fermentation process. On a cost per daily-tonne of CO_2 basis, costs are approximately $43,000 and $26,000 per daily-tonne, respectively, for the 55 and 200 MGY plants.

Operating expense for capture, compression, and dehydration from ethanol plants in this study is $8.58 per tonne processed. Operating costs are derived from the two DOE final reports (McPherson, 2010, and Leroux, 2017) and are applied in a linear fashion for all CO_2 volumes. By far, the largest contributor to OpEx is energy costs, which are directly proportional to CO_2 volumes compressed. There would be economies of scale for larger-sized plants but these savings could not be quantified from the data available. Both CapEx and OpEx for capture, compression, and dehydration operations deserve significant additional study and refinement but are considered adequate for this study.

In the cases involving ethanol plants, where we estimated the capital costs and operating costs as described above, the cost per tonne for CapEx and OpEx for both the ethanol plant and pipeline components were calculated. In the case of the power plant sources, the Linde Group provided costs that combined capture and compression into a single value. Table 6.3 summarizes pipeline statistics and cost estimates for the six scenarios presented in this report, including pipeline CapEx using an industry rule-of-thumb—$100,000/inch-mile for comparison with that calculated by the modified NETL Cost Model. Annual OpEx for the pipelines are from the cost model but for the ethanol plants are calculated at $8.58/tonne.

Table 6.3. Summary of pipeline statistics and estimated costs in $millions ($M). The first four scenarios listed are for power plant capture and do not include costs for capture. The next two scenarios (ethanol plants) have a line for Capture and Compression costs (Cap./Comp). MT = million tonnes.

Capture/Transport Scenario	Component	CO2 Vol./yr (MT)	Pipe Diameter (inches)	Length (miles)	CapEX - $100k/inch-mile ($M)	CapEX - cost model ($M)	Annual OpEX ($M)
1. Holcomb Station to Patterson	Pipeline	1.67	8	25	$20	$42.2	$1.3
2. JEC to Davis Ranch/John Creek	Pipeline	2.5	12	50	$60	$72.9	$1.8
3. JEC to Patterson Site	Pipeline	2.5	12	323	$388	$320	$5.1
4. JEC to Trunk Line	Pipeline	2.5	12	167	$200	$166	$2.4
5. 34 ethanol plants to Permian Basin	Pipeline	9.85	4-20	1546	$1,821	$1,857	$47
	Cap./Comp.					$809	$85
6. 15 ethanol plants to SW Kansas	Pipeline	4.3	4-12	737	$613	$642	$16.2
	Cap./Comp.					$364	$36.5

6.3.4: Tax incentives through Section 45Q

Section 45Q of the Internal Revenue Service code was expanded and extended as part of the federal budget bill signed into law on February 9, 2018. Section 45Q was set to expire, and its extension through 2035, increase in the tax credit value, and lowering the qualifying threshold CO_2 is pivotal for the improvement of economics for CCS through saline aquifer storage and CCUS through EOR. Tax credits increased from $10/metric ton to $35 for CO_2 stored in qualified EOR reservoirs and from $20/metric ton to $50 for saline aquifer storage. The escalation of credits is in Table 6.4. Highlights of the revised version of Section 45Q, listed below, are compiled from the budget bill document, S.1535, and Walzer (personal communication, 2018) and Crabtree (personal communication, 2018):

- Capture projects must begin construction before February 9, 2025.
- Lowered the qualifying threshold for CO_2 credits to a facility to 100,000 metric tons per year.
- Credits may be claimed for 12 years from first date of CO_2 capture.
- Credits may be claimed by capture facility, may be transferred to the storage facility, but may not be directly transferred to the transporter.
- 2017 tax credits are $12.83/tonne for EOR and $22.66/tonne for saline storage.
- Credits escalate linearly through 2026 to $35 for EOR and $50 for saline storage and is flat through 2035, except for an adjustment for inflation.
- Credits are adjusted for inflation after 2026.
- CO_2 must be injected into a qualified EOR project in a secure geologic storage or injected and sequestered in a secure geologic storage (saline storage).

Year	EOR	Saline
2017	$12.83	$22.66
2018	$15.26	$25.70
2019	$17.76	$28.74
2020	$20.22	$31.77
2021	$22.68	$34.81
2022	$25.15	$37.85
2023	$27.61	$40.89
2024	$30.07	$43.92
2025	$32.51	$46.96
2026 - 2035	$35.00	$50.00

Table 6.4. 45Q tax credits in $/tonne, without inflation adjustments available after 2026.

An initial interpretation of the law would indicate that the tax credits may not be taken by the pipeline component. However, in reality, the pipeline system would benefit indirectly by being able to charge a higher tariff for the transportation. In the economic analysis that we present here, we evaluate the system as a whole. For simplicity, the credits are either "taken" by the pipeline (power plant source cases) or split between the ethanol plants and the pipelines (ethanol plant source cases).

6.3.5: Economics for capture, compression and transport of CO_2

Going into this project, we were certain that capturing anthropogenic CO_2 from a single coal-fired power plant, large enough to supply 50 Mt, and transporting it to a single geologic site with sufficient capacity to store 50 Mt safely, and doing so economically, would take some creative thinking. Determining the cost of transportation via pipelines and evaluating whether there could be opportunities to join coal-fired power CO_2 destined for saline aquifers with larger-scale ethanol CO_2 pipeline infrastructure headed for EOR for mutually advantageous economies of scale.

6.3.5.1: Pipeline systems analyzed

We used the modified NETL CO_2 Transport Cost Model, to calculate detailed breakdowns of capital and operating costs for multiple CO_2 pipeline systems, from simple to complex. Details for all of the variations and general history of the body of work can be found in the quarterly reports (Q1–Q4), poster presented at the DOE-NETL Annual Technology meeting (Dubois et al., 2017), the ethanol CO_2 white paper (State CO_2-EOR Deployment Work Group, 2017), Dubois and McFarlane (2018), and Appendix I to this final report. In this final report, we will discuss six key systems that were evaluated:

1. Holcomb Station to Patterson storage site (Figure 6.2)
    - 25-mile pipeline, 8-inch pipeline
    - Directly connects the Holcomb Station 384-MWe coal-fired power to the Patterson site
    - Deliver 1.67 Mt/yr with full capture

2. Jeffrey Energy Center to Davis Ranch/John Creek storage site (Figure 6.2)
    - 50-mile, 12-inch pipeline

- Directly connects one of three of Jeffrey Energy Center's 800-MWe coal-fired power plants to the Davis Ranch/John Creek storage site
- Deliver 2.5 Mt/yr with partial capture from one plant

3. Jeffrey Energy Center (JEC) to Patterson storage site (Figure 6.2)
    - 323-mile, 12-inch pipeline
    - Purposely passes by the CHS refinery and Lyons ethanol plant
    - Directly connects one of three of JEC's 800-MWe coal-fired power plants to the Patterson storage site
    - Deliver 2.5 Mt/yr with partial capture from one plant

4. Jeffrey Energy Center to main trunk line of the 34-ethanol plant system (Figure 6.2)
    - 167-mile, 12-inch pipeline
    - Connect one of JEC's power plants' CO_2 with the main trunk line in case 5
    - Deliver 2.5 Mt/yr with partial-capture from one plant

5. 34 ethanol plants to Permian Basin (Figure 6.2)
    - 1,546-mile system with gathering, feeder and main trunk lines requiring 4-inch to 20-inch pipe
    - Gathers all CO_2 available from 34 of the larger ethanol plants in Iowa, Nebraska and Kansas, a combined 3,643 MGY capacity, ranging in size from 55 to 300 MGY (0.15 to 0.81 Mt/yr CO_2), assuming 90% of plant ratings.
    - Deliver 9.85 Mt/yr to a connection point in the Texas Panhandle-NE New Mexico area, and ultimately to markets for EOR in the Permian Basin.
    - The system could "drop off" sufficient CO_2 to the Patterson site to meet the 50Mt target for storage in saline aquifers.

6. 15 ethanol plants to SW Kansas (Figure 6.3)
    - 737-mile system with gathering, feeder and main trunk lines requiring 4-inch to 12-inch pipe
    - Gathers all CO_2 available from the 15 of the larger ethanol plants in Nebraska and Kansas combining for 1,575 MGY capacity, ranging in size from 55 to 300 MGY (0.15 to 0.81 Mt/yr CO_2), assuming 90% of plant ratings.
    - Deliver 4.3 Mt/yr to Kansas primarily for EOR in central and southwest Kansas.
    - The system could deliver sufficient CO_2 to the Patterson site to meet the 50Mt target for storage in saline aquifers.

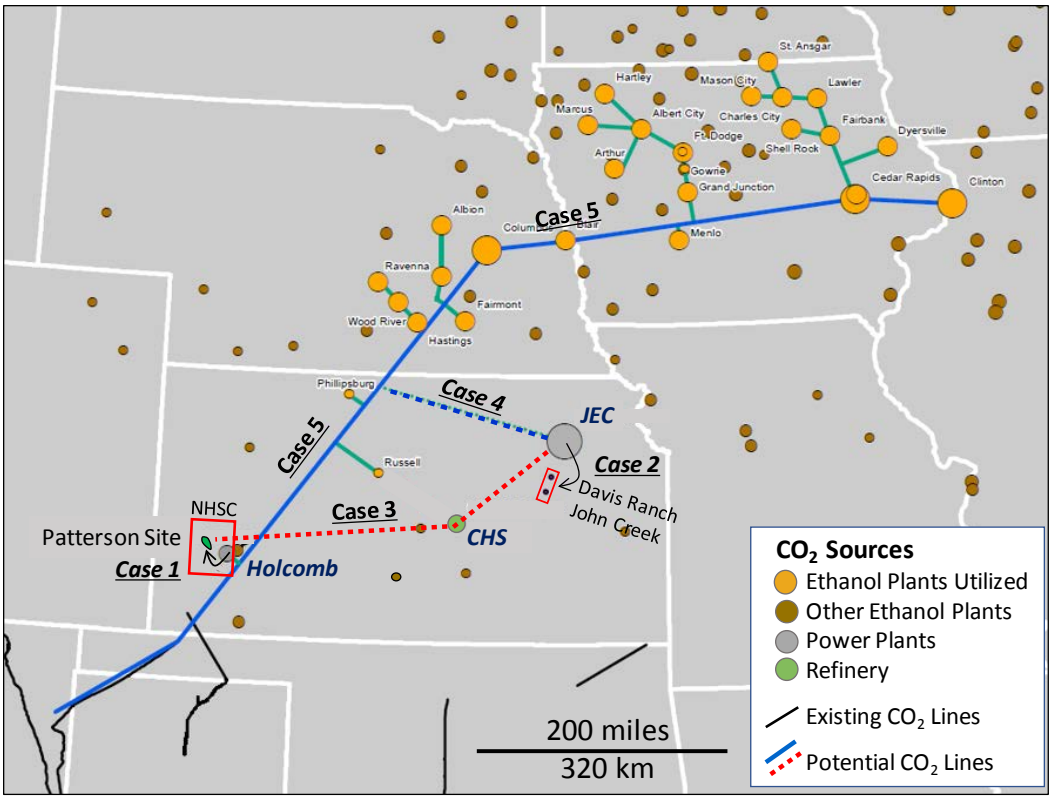

Figure 6.2. Map of pipeline locations in Cases 1–5 with respect to CO_2 sources and existing pipeline infrastructure. Cases 1 and 2 are short lines, not readily displayed at the figure scale, and connection between source and injection site are indicated by an arrow. Bubbles are sized in proportion to CO_2 resource. *Modified after State CO_2-EOR Deployment Workgroup, 2017.*

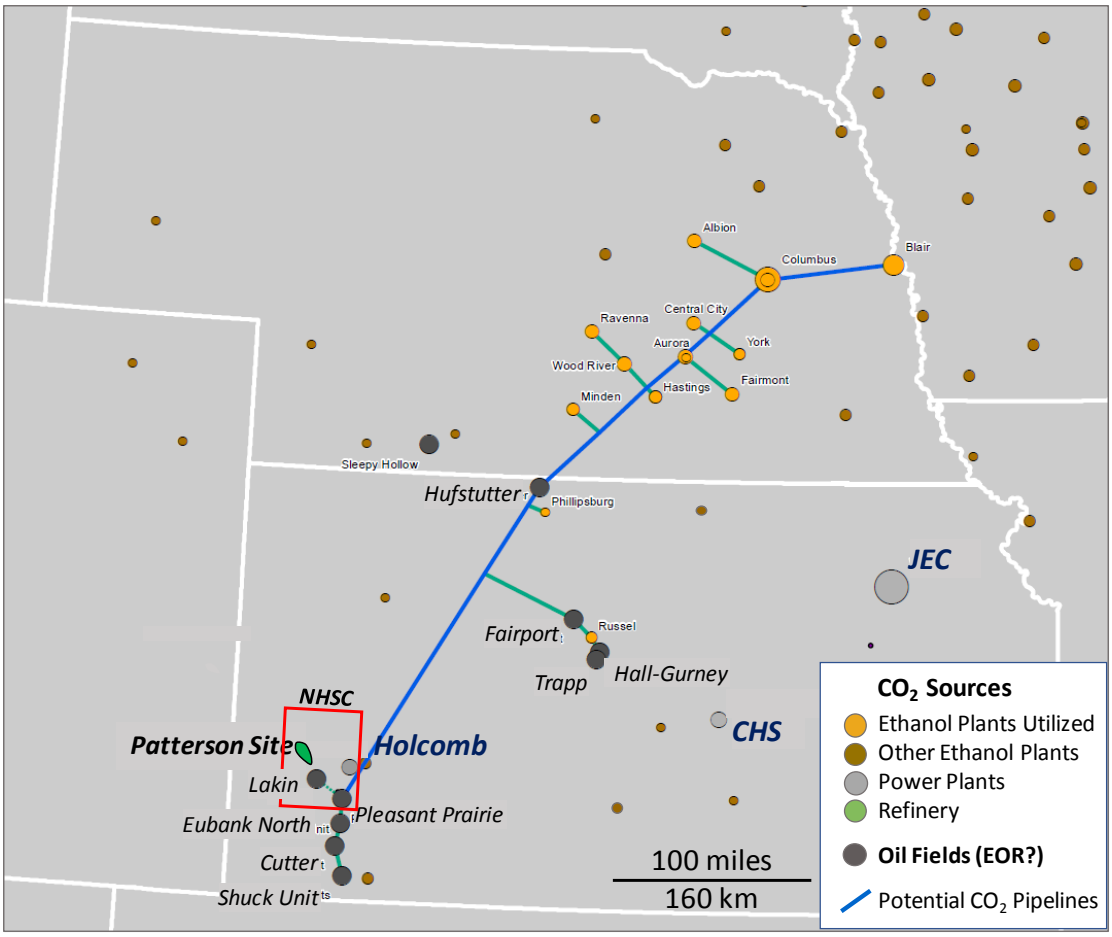

Figure 6.3. Map of pipeline locations in Case 6 with respect to CO_2 sources, existing pipeline infrastructure, and potential CO_2 EOR fields (labeled). Bubbles are sized in proportion to CO_2 resource. *Modified after State CO_2-EOR Deployment Workgroup, 2017.*

6.3.5.2: Economic analysis

High-level, simple economic analyses were performed on the six cases presented, and more. Rather than calculating the rate of return for a project, we took the approach of calculating the CO_2 price (cost) on a per tonne basis that would be required to cover operations and capital costs, given a specified cost of capital, and a specified project life. The cost of capital is the return on investment (ROI) that investors would require to build and operate the project. For the analysis, we assumed the following:

- Cost of capital—two cases: 6.67% and 10%
- Project life—two years construction, 20 years of operation, and no residual value
- Construction begins January 1, 2022, and capture and injection starts on January 1, 2024
- Project initiation—operates at full capacity from day one of operations
- No inflation factored in
- Tax incentives—three cases: no incentives, 45Q for EOR, 45Q for saline aquifer storage with incentives for the first 12 years of operations

A simple Excel-spreadsheet calculator was used for the economic analysis. In a single column, capital costs were evenly divided between years 1 and 2 as negative values, followed by 20 years of cash flow from operations. We then used Excel's Net Present Value function and Goal Seek function to determine

the annual net cash flow during the 20-year operating period that is required to provide for a specified IRR on the initial capital investment. Using Goal Seek, set Net Present Value (sum of the 22-year project cash flow column) = 0 for the given IRR (6.7% or 10%) by having Goal Seek change the Net Annual Cash Flow. The cost or price per tonne is the Net Annual Cash Flow divided by the annual CO_2 volume in tonnes.

Economic model results were converted to the cost per tonne of CO_2 delivered via pipeline to the injection site at 1,400 psig. Table 6.5 presents a summary of the results for the six scenarios. There are three lines per scenario, the first with no tax incentive and the next with 45Q EOR tax incentive and 45Q saline aquifer storage tax incentives applied, reducing costs. Pipeline costs for a 6.67% ROI (no tax incentive applied, are shown for comparison, however, a 10% ROI is more realistic in today's market. Reduction of interest rates from 10% to 6.67% would reduce the cost for CO_2 an average of 19%.

45Q tax credits have a 12-year limit, and thus were applied for both EOR and saline aquifer cases for the first 12 years of operations. The credits average $34.38 for EOR and $49.24/tonne for the saline aquifer case. However, tax credits lower the average delivered cost of CO_2 for the 20-year operations period to $27/tonne for EOR and $39/tonne for saline aquifer, less than what one might expect. The difference is due to the time-value of money in the Net Present Value calculation. In Cases 1–4, the tax credits were applied to the pipeline entity, while in Cases 5 and 6 they were applied to the pipeline and ethanol plants in proportion to their capital costs.

Table 6.5. Pipeline statistics and summary of CO_2 costs per tonne for six scenarios. Negative numbers (red) indicate negative costs or "profit" derived from 45Q tax credits. MT = million tonnes.

	Pipeline Statistics				6.67% ROI	10% ROI		
Scenario	CO2 Vol./yr (MT)	Line Diameter (inches)	Length (miles)	Tax Credit Status	Pipeline Costs ($/tonne)	Pipeline Costs ($/tonne)	Capture costs ($/tonne)	Delivered Cost* ($/tonne)
1. Holcomb Station to Patterson	1.67	8	25	No 45Q	$3.21	$3.92	$46-$71	$50
				45Q EOR		($23.33)	$46-$71	**$23**
				45Q Saline		($35.15)	$46-$71	$11
2. JEC to Davis Ranch/John Creek	2.5	12	50	No 45Q	$3.47	$4.30	$45-$67	$49
				45Q EOR		($22.95)	$45-$67	**$22**
				45Q Saline		($34.78)	$45-$67	$10
3. JEC to Patterson Site	2.5	12	323	No 45Q	$14.21	$17.83	$45-$70	$63
				45Q EOR		($9.41)	$45-$70	$36
				45Q Saline		($21.24)	$45-$70	$24
4. JEC to Trunk Line**	2.5	12	167	No 45Q	$7.27	$9.15	$45-$73	$54**
				45Q EOR		($18.10)	$45-$73	$27**
				45Q Saline		($29.93)	$45-$73	$15**
5. 34 ethanol plants to Permian Basin	9.85	4-20	1546	No 45Q	$22.69	$28.03	$18.71	$47
				45Q EOR		$9.05	$10.44	**$19**
				45Q Saline		$0.81	$6.86	$8
6. 15 ethanol plants to SW Kansas	4.3	4-12	737	No 45Q	$18.14	$22.40	$19.13	$42
				45Q EOR		$5.02	$9.27	**$14**
				45Q Saline		($2.53)	$4.99	**$2**

** Delivered costs for Scenarios 1-4 use the lowest capture costs from Capture Costs column.*

*** Trunk line tariff ($1-$5 / tonne) for transportation 200 miles from intersection with Trunk to the Patterson site should be added to overall costs.*

Feeding CO_2 from large power plants that is destined for saline storage into a larger pipeline system supplying CO_2 for EOR would reduce overall costs for both and would be beneficial to the large power plant derived CO_2. However, in the JEC to Patterson site ICKan case, the potential cost savings will not be sufficient for the project to have positive economics.

CO_2 delivered from JEC to the Patterson site through a line that would join a larger system (Case 4) and on to Patterson through the larger system in Case 6, as depicted in Figure 6.2, could reduce transportation costs by $4/tonne, or possibly as much as $8/tonne (Table 6.6) when compared to transporting it directly to Patterson (Case 3). Adding JEC's 2.5 Mt/yr to the larger system near Phillipsburg and transporting it 200 miles southwest to the Patterson site would require an increase in pipe diameter for that section from 20-inch to 24-inch, sized to carry 12.35 Mt/yr, for the 200-mile segment. Theoretically, the costs for CO_2 moved in the 200-mile segment of the larger system would be reduced by $1.05/tonne. Assuming the operator of the larger system charged the JEC CO_2 a tariff equal to the amortized cost to ship ($4.67), the addition of the tariff to the cost to get it to the larger system trunk line ($9.15) would result in a savings of $4.01/tonne over case 3, a direct line to the Patterson site. Although this may be unrealistic, the larger system operator might provide a bonus as an inducement for the JEC CO_2, because it would provide the benefit of source diversification. If the bonus were equal to the savings on the EOR CO_2 (9.85 Mt*$1.05/tonne = $10.34 million/year), it would amount to another $4.14/tonne savings to the JEC CO_2. Regardless of the potential savings, the estimated minimum cost for CO_2 captured and delivered from JEC to the Patterson for saline aquifer storage, after 45Q credits, is approximately $16/tonne, a cost a storage site operator could not afford to pay.

Table 6.6. Possible savings and tariffs associated with concept of merging systems for economics.

Economic improvement with scale *($/tonne)*	
$5.72	Cost to move 9.85 Mt over 200 miles in a 20-inch line
$4.67	Cost to move 12.35 Mt over 200 miles in 24-inch line
$1.05	Savings for the "other" 9.85 Mt/yr over 200 miles ($10.34M/yr)
Savings for JEC CO_2 after tariff paid to large system in case 6 *($/tonne)*	
$9.15	JEC to Trunk line (case 4)
$4.67	Tariff for 200 miles in trunk
$13.82	JEC to trunkline + tariff
$17.83	JEC direct to Patterson site (case 3)
$4.01	Savings through the Trunk line option
Savings for JEC CO_2 if bonus is paid by large system in case 6 *($/tonne)*	
$4.14	Possible bonus of $10.34M for the 2.5Mt transported.
$0.53	Possible lower tariff through bonus
$8.15	Savings through the Trunk line option, bonus included

6.3.5.3: Discussion

Because there is currently no infrastructure capable of transporting CO_2 from sources to injection sites in Kansas, the economics of a wholly integrated system, including capture, initial compression and delivery to the injection site via pipeline, must be evaluated. For economic feasibility, the CO_2 needs to be delivered to the injection site at a price that the operator of the injection site would be willing to pay. For a saline aquifer site, under today's market condition, that price would be something less than zero – the operator would need to be paid to inject and store the CO_2 under the economic scenarios presented here where the tax credits are absorbed by the source capture and transportation system. In the analyses presented in this report, there are no scenarios where the integrated systems for saline aquifer storage are

economically feasible. The closest to being economic, within $2, is Case 6, CO_2 from 15 ethanol plants, delivered to southwest Kansas (e.g., Patterson site).

Four of the six cases evaluated (1, 2, 5, and 6) could be economically feasible for EOR. In these cases, an EOR operator may be able to afford to pay the prices highlighted in yellow in Table 6.5. Under current market conditions an EOR operator could pay approximately $23/tonne for CO_2 delivered to their site at 1,400 psig. The market value of CO_2 for EOR is tied to oil prices, is priced on peer mcf and is approximately 2% of the West Texas Intermediate (WTI) posted price (Melzer, personal communication, 2018). At a WTI price of $60/barrel, CO_2 value is $1.20/mcf, or $22.80/tonne.

For CO_2 saline storage, the economics look especially bleak for CO_2 from coal-fired power, even when the injection sites are relatively close to the source (Cases 1 and 2), the lowest costs for capture within the range of costs projected are assumed, and after 45Q credits are applied. Of the six scenarios presented in this report, the lowest delivered CO_2 cost for saline storage is that from ethanol plant scenarios (Cases 5 and 6). In Case 6, where CO_2 from 15 ethanol plants is captured, CO_2 for saline storage (Patterson) is projected to cost $2/tonne.

6.3.5.4: Possible enhancements

The economic analysis performed in this study assumed current market conditions, without considering possible future public policy and regulatory changes at the federal and state level. Nor did this study consider improvements in the economies in solvent-based recovery systems for power plant flue gas through generational improvements as these capture systems are built with regularity. Nor did it consider plausible additional incentives to ethanol plants through California's Low Carbon Fuel Standards (LCFS), administered by the California Air Resources Board (CARB). The ethanol industry already participates in the California markets where ethanol receives a higher price based on its lower carbon intensity. If ethanol plant's carbon intensity is lowered further through storage through EOR or saline aquifer storage, the value captured would be significant, possibly even more that provided by 45Q tax incentives. Potential value from plausible future enhancements are listed in Table 6.7.

Table 6.7. Three possible public policy or regulatory changes and their potential impact on the delivery price for CO_2.

Reduction in delivered CO_2 cost ($/tonne)	EOR	Saline Aquifer
Policy/regulatory change to extend the 45Q credit period from 12 to 20 years (life of project)	$7	$10
Policy/regulatory change that would allow for 6.67% cost of capital through loan guarantees or other mechanisms	$3-$6	$3-$6
LCFS benefits to ethanol facilities	Very significant	Very significant

Any of the enhancements would significantly improve EOR prospects and make Case 6 for saline storage economic. If any two enhancers came to fruition, several of the saline aquifer storage cases could be economic, possibly even capture from coal-fired power plants. LCFS benefits cannot be applied to power generation but could significantly benefit ethanol plants if the legal and regulatory requirements can be successfully navigated.

6.3.6: Conclusions and implementation plan

Under current market conditions, taking into account public policy, finance options, and 45Q tax credits, the only option for economically feasible, fully integrated CCS project in the midcontinent is capture from a large number of ethanol plants in Nebraska and Kansas and transporting it to southwest Kansas for saline storage. The system outlined in Case 6 (Table 6.5), 15 ethanol plants in Nebraska and Kansas, could deliver 4.3 Mt/year CO_2 to southwest Kansas, 2 to 2.5 Mt to the saline aquifer storage in the Patterson site and 1.8 to 2.3 Mt for EOR in several fields, especially those in southwest Kansas within and near the NHCS.

Five fields identified in the NHSC could readily take 1.8 to 2.3 Mt/yr for EOR. They include the Patterson Morrow waterflood and the Chester and Morrow waterfloods in four fields studied for EOR by Dubois et al. (2015c) as part of a DOE-funded study (DE-FE0002056). The four fields in that study—Pleasant Prairie South (part of the Pleasant Prairie site), Eubank North Unit, Shuck, and Cutter—are similar in size and reservoir as the Patterson-Heinitz Unit produce from the Morrow and Chester (Mississippian) sandstones. Operators of four of the five fields that have signed support letters for our successful Phase II application are all engaged, and one, Berexco LLC, operates the Patterson site as well as one of the other fields.

Economics—Table 6.5 suggests that if all 4.3 Mt CO_2 were delivered for saline storage, the cost would be $2/tonne (after 45Q credits), close but unaffordable. That same scenario could deliver CO_2 for EOR at a cost of $14/tonne, $9/tonne under market value. It may be possible that the $9/tonne could be enough to offset the shortfall destined for the CO_2 saline aquifer storage. This would seem reasonable because the saline aquifer market would provide diversity in the market and economies of scale gains for the pipeline.

CarbonSAFE Phase II and the next plan—The KGS-led ICKan project joined Battelle, the lead institution, and the Energy and Environmental Research Center (EERC) in pooling their Phase I projects in Nebraska with the Kansas ICKan project for a single project covering Nebraska and Kansas. The project, Integrated Midcontinent Stacked Carbon Storage Hub, was successful in its bid under DE-FOA-0001450, and the project (DOE—$9.6 million, Total—$13.3 million) kicked off in September, 2018. The project will evaluate the feasibility of capturing CO_2 from ethanol plants for storage in saline aquifer reservoirs in Nebraska (Sleepy Hollow field) and Kansas (Patterson site). Capture from coal-fired power plants from Nebraska and Kansas also will be evaluated.

Task 7.0: Technology Transfer

The KGS maintained and continually updated the ICKan project website. The website can be accessed at: http://www.kgs.ku.edu/PRS/ICKan/index.html. This page provides links to all Quarterly Reports, presentations, publications, and relevant project activities. All data developed by the project was shared internally on a secure cloud drive. Relevant data have been uploaded to EDX per DOE deliverables. Uploaded data include Petrel models from all study areas, including Patterson, Lakin, and Forest City Basin. Models and input parameters are provided in rescue file format for accessibility as well as snapshots of the analysis via images and text.

Public presentations were given frequently at conferences, technical talks, and similar academic events. A summary of all public presentations and publications is below. These presentations can be accessed at: http://www.kgs.ku.edu/PRS/ICKan/presentations.html.

Bibliography of presentations and publications

(*indicates funded student or postdoctoral scholar)

Manuscripts

1. *Ansari, E., Bidgoli, T. S., and *Hollenbach, in preparation, History matching pressure in the Arbuckle Group aquifer to manage midcontinent seismicity: Science Advances.
2. *Ansari, E., Bidgoli, T. S., and *Hollenbach, A., in revision, Accelerated fill-up of the Arbuckle Group aquifer and links to US midcontinent seismicity: Journal of Geophysical Research—Solid Earth.
3. State CO_2–EOR Deployment Work Group, Capturing and Utilizing CO_2 from Ethanol: Adding Economic Value and Jobs to Rural Economies and Communities While Reducing Emissions: White paper, December 2017.

Conference Abstracts

1. *Hollenbach, A., Bidgoli, T. S., *Ansari, E., and Victorine J., in review, Modeling the structure, porosity, and permeability of the Arbuckle Group in south-central Kansas: AAPG ACE 2019, San Antonio, TX.
2. *Ansari, E., Bidgoli, T. S., and *Hollenbach, A., 2019, History matching pressure in the Arbuckle Group aquifer to manage midcontinent seismicity: GSA Joint Section Meeting, Manhattan, KS.
3. *Hollenbach, A., Bidgoli, T. S., *Ansari, E., and Victorine J., 2019, Simulating injection-pressure response with real-world data and a high-resolution model of the Arbuckle Group, south-central Kansas: GSA Joint Section Meeting, Manhattan, KS.
4. *Ansari, E., Bidgoli, T. S., and *Hollenbach, A., 2018, The role of pressure diffusion in U.S. midcontinent seismicity: AAPG ACE 2018, Salt Lake City, UT.
5. *Ansari, E., Bidgoli, T. S., and *Hollenbach, A., 2018, Statistical analysis of Arbuckle pressure and static fluid level: Geological Society of America, South-Central Section Meeting 2018, Little Rock, AR.
6. *Ansari, E., Bidgoli, T. S., *Hollenbach, A., and Nolte, K. A., 2018, Interplay between pore pressure and elastic stress induces US midcontinent seismicity: AGU Fall Meeting, Washington, D.C.
7. *Hollenbach, A., Bidgoli, T. S., and *Ansari, E., 2018, Investigating the link between brine disposal practices and induced seismicity in Kansas and Oklahoma: AAPG ACE 2018, Salt Lake City, UT.
8. *Hollenbach, A., Bidgoli, T. S., *Ansari, E., and Nolte, K. A., 2018, Evaluating controls on US

midcontinent seismicity through modeling of wastewater injection into the Arbuckle Group aquifer: AGU Fall Meeting, Washington, D.C.

9. *Hollenbach, A., Bidgoli, T. S., *Ansari, E., and Nolte, K. A., 2018, A spatio-temporally constrained volumetric threshold for inducing seismicity in the midcontinent, USA: Geological Society of America Annual Meeting 2018, Indianapolis, IN.
10. Holubnyak, E., Birdie, T., Bidgoli, T. S., and Hollenbach, J., 2018, Methodology for capacity estimation for waste disposal and carbon management: AAPG ACE 2018, Salt Lake City, UT.
11. Bidgoli, T. S., Dubois, M., Watney, W. L., Stover, S., Holubnyak, Y., *Hollenbach, A., *Jennings, J. C., and Victorine, J., 2017, Is commercial-scale CO_2 capture and geologic storage a viable enterprise for Kansas?: AAPG Midcontinent Section Meeting 2017, Oklahoma City, OK.
12. Dubois, M., McFarlane, D., and Bidgoli, T. S., 2017, CO_2 Pipeline Cost Analysis Utilizing a Modified FE/NETL CO_2 Transport Cost Model Tool: Mastering the Subsurface Through Technology Innovation, Partnerships and Collaboration: Carbon Storage, Oil and Natural Gas Technologies Review Meeting, DOE-NETL Annual meeting, August 1–3, 2017, Pittsburgh, PA
13. *Hollenbach, A., Bidgoli, T. S., and Dubois, M., 2017, Evaluating the Feasibility of CO_2 Storage through Reservoir Characterization and Geologic Modeling of the Viola Formation and Arbuckle Group in Kansas: AAPG Midcontinent Section Meeting 2017, Oklahoma City, OK.
14. *Jennings, J. and Bidgoli, T. S., 2017, Identifying Areas at Risk for Injection-Induced Seismicity through Subsurface Analysis: An Example from Southern Kansas: AAPG Midcontinent Section Meeting 2017, Oklahoma City, OK.

Presentations

1. Ansari, E. and Bidgoli, T. S., 2018 Mastering the Subsurface Through Technology Innovation, Partnerships and Collaboration: Carbon Storage, Oil and Natural Gas Technologies Review Meeting, DOE-NETL, “Integrated CCS for Kansas,” 08/18.
2. Bidgoli, T. S. and Holubnyak, E., Eastern Kansas Oil and Gas Association—Mid Year Meeting “Integrated Carbon Capture, Utilization and Storage for Kansas,” 05/08/18 (Invited).
3. Bidgoli, T. S., Boone Pickens School of Geology, Oklahoma State University, “What’s shaking Kansas? Causality assessment approaches for injection-induced earthquakes,” 04/27/18 (Invited).
4. Bidgoli, T. S., KU Environment Engineering Conference, “Integrated CCS for Kansas,” 04/15/18 (Invited).
5. Newell, K. D., Bidgoli, T. S., Doveton, J. H., and Whittemore, D., 2017, Water Quality and Movement in Saline Aquifers in Kansas: Governor’s Conference on the Future of Water in Kansas, November 9, 2017, Manhattan, KS.
6. Bidgoli, T. S. and Dubois, M., 2017, Mastering the Subsurface Through Technology Innovation, Partnerships and Collaboration: Carbon Storage, Oil and Natural Gas Technologies Review Meeting, DOE-NETL, “Integrated CCS for Kansas,” 08/01/17.
7. Bidgoli, T. S. and Holubnyak, E., Oklahoma Corporation Commission, Arbuckle web conference, 7/6/17 (Invited).
8. Hollenbach, J., and Bidgoli, T. S., Stanford Center for Carbon Storage Annual Meeting, “Integrated Carbon Capture & Storage for Kansas,” May 11, 2018, Palo Alto, CA.
9. Dubois, M., and McFarlane, D., CCUS Forum “Economics for CO_2 Capture, Compression, and Transportation in the Mid-Continent,” July 27, 2018, Lawrence, KS.
10. Dubois, M., KIOGA—CCUS Opportunities. “CO_2 Capture and Utilization, a Genuine Opportunity for Kansas Operators,” August 13, 2018, Wichita, KS.
11. Dubois, M., Capturing Value from Biogenic CO_2, “Ethanol CO_2 for EOR, History, Challenges, and

Opportunity," August 2, 2017, Des Moines, IA.

12. Holubnyak, Y., Kansas Geological Society Workshop, "Challenges and Opportunities for Carbon EOR and Storage in Kansas," October 3, 2018, Wichita, KS.
13. Holubnyak, Y., CCUS Forum, "Introduction to Carbon Capture, Storage, and Utilization," July 27, 2018, Lawrence, KS.
14. Holubnyak, Y., Kansas Geological Survey Field Conference, "Introduction to CCUS in Kansas," August 15, 2018, Abilene, KS.
15. Stover, S., Kansas Geological Society Workshop, "Legal and Regulatory Topics of CCUS in Kansas," October 2, 2018, Wichita, KS.

Conclusions

Results of the Integrated CCS for Kansas pre-feasibility study indicate that large-scale CO_2 capture, transportation and storage in saline aquifers in Kansas is both technically and economically feasible and deserving of further study. Based on the technical work on multiple geologic sites their appear to be up to four sites within the North Hugoton Storage Complex (NHSC) in Southwest Kansas where >50 million tonnes CO_2 could be injected over a 25- to 30-year period and safely stored in a set of stacked saline aquifer reservoirs at ideal depths of 5200-6400 ft. The saline aquifers (Mississippian Osage, Ordovician Viola, and Cambrian-Ordovician) are overlain by oil reservoirs that are likely candidates for CO_2 Enhanced Oil recovery (EOR). Of the four possible sites in the NHSC, the Patterson site was chosen as the primary site for a CarbonSAFE Phase II project. Patterson was chosen because the operator of the overlying fields, Berexco, is a long-term trusted partner of the Kansas Geological Survey (KGS), having participated in several DOE-funded studies with the KGS, it has EOR opportunities in overlying reservoirs, and most of the prospective injection site is already unitized.

Capture, compression and transportation of large volumes of CO_2 can be done so economically in the region, particularly in light of the extension and expansion of 45Q tax credits in February 2018. Without these tax credits of up to $35/tonne for CO_2 stored during EOR and $50/tonne if stored in a saline aquifer reservoir, and can be captured for a 12-year period, saline aquifer storage is not economically feasible. CO_2 aggregated from multiple ethanol plants in network of small-diameter gathering pipelines that tie to a main trunk line for delivery to the market is the most economic scenario. CO2 EOR likely to be needed as part of the integrated system for economies of scale (pipeline) and, potentially, providing additional subsidy for saline aquifer injection through CO2 sales. High capture costs at the two power plants and refinery in this study make them non-economic options without further subsidy that could be possible in a large regional pipeline system.

Legal, regulatory, public policy aspects of a project of the scale envisioned will require significant, if not radical changes at the State level. In particular, legislation at the State level that would regulate capture, transportation, injection and storage as a public utility and allow eminent domain to be utilized for pipeline ROW and pooling of pore space would help resolving key obstacles to large-scale CCS. Streamlining the Class VI well process and/or establishing State primacy is extremely important if CCS is to become commercial. Well-orchestrated public outreach is critical for support of State regulatory changes, and for public acceptance, particularly in light of increased injection well induced seismicity in south-central Kansas and general public dissent over pipeline construction.

The KGS-led ICKan project joined Battelle, the lead institution, and the Energy and Environmental Research Center (EERC) in pooling their Phase I projects in Nebraska with the Kansas ICKan project for a single project covering Nebraska and Kansas. The project, Integrated Midcontinent Stacked Carbon Storage Hub, was successful in its bid under DE-FOA-0001450, and the project (DOE—$9.6 million, Total—$13.3 million) kicked off in October 2018. The project will evaluate the feasibility of capturing CO_2 from ethanol plants for storage in saline aquifer reservoirs in Nebraska (Sleepy Hollow field) and Kansas (Patterson site).

References

Alt, R. C., and Zoback, M. D., 2015, A detailed Oklahoma stress map for induced seismicity mitigation: AAPG ACE 2015, Denver, Colorado.

Bajura, R. A., Palmer, F. D., Beck, R. A., and Clemente, F., 2012, Harnessing coal's carbon content to advance the economy, environment, and energy security: National Coal Council.

Benz, H. M., McMahon, N. D., Aster, R. C., McNamara, D. E., & Harris, D. B. (2015). Hundreds of earthquakes per day: The 2014 Guthrie, Oklahoma, earthquake sequence: Seismological Research Letters, 86(5), 1318-1325

Bidgoli, T., and Dubois, M., 2017a, Integrated CCS for Kansas (ICKan) (DE-FE0029474): Quarterly Report 1, submitted July 31, 2017. http://www.kgs.ku.edu/PRS/ICKan/2017/Aug/Q1_7-31-2017.pdf. Accessed 1/2/2019

Bidgoli, T., and Dubois, M., 2017b, Integrated CCS for Kansas (ICKan) (DE-FE0029474): Quarterly Report 2, submitted October 31, 2017. http://www.kgs.ku.edu/PRS/ICKan/2017/Dec/Q2_11-01-2017.pdf. Accessed 1/2/2019

Bidgoli, T., and Dubois, M., 2018a, Integrated CCS for Kansas (ICKan) (DE-FE0029474): Quarterly Report 3, submitted March 9, 2018. http://www.kgs.ku.edu/PRS/ICKan/2018/March/Q3_3-9-2018_Finalv2.pdf. Accessed 1/2/2019

Bidgoli, T., and Dubois, M., 2018b, Integrated CCS for Kansas (ICKan) (DE-FE0029474): Quarterly Report 5, submitted July 17, 2018. http://www.kgs.ku.edu/PRS/ICKan/2018/July/Q5_7-17-2018_FINAL.pdf. Accessed 1/2/2019

Bidgoli, T. S., Holubnyak, Y., and FazelAlavi, M., 2015, Evaluating potential for induced seismicity through reservoir-geomechanical analysis of fluid injection in the Arbuckle saline aquifer, south-central Kansas: AAPG ACE Abstract, Spring Meeting.

Bidgoli, T. S., and Jackson, C., 2017, Operational practices and their influence on injection-induced earthquakes: Lessons learned from a statewide survey of brine disposal in Kansas: AAPG ACE 2017, Houston, Texas.

Bostick, D., Stoffregen, T., and Rigby, S., 2017, Final techno-economic analysis of 550 MWe supercritical PC power plant CO_2 capture with Linde-BASF advanced PCC technology: USDOE Office of Fossil Energy, Clean Coal and Carbon. https://www.osti.gov/scitech/servlets/purl/1338328. Accessed 6/27/2017.

Brownlee, M. H., and Sugg, L. A., 1987, East vacuum Grayburg-San Andres unit CO_2 injection project: development and results to date: In SPE Annual Technical Conference and Exhibition, Society of Petroleum Engineers.

Buchanan, R. C. (2015). Increased seismicity in Kansas: The Leading Edge, 34(6), 614-617.

Bui, L. H., Tsau, J. S., and Willhite, G. P., 2010, Laboratory investigations of CO_2 near-miscible application in Arbuckle Reservoir: SPE Improved Oil Recovery Symposium held in Tulsa, Oklahoma, 24–28 April 2010, SPE Publication 129710.

Carey, W., 2017, Probability distributions for effective permeability of potentially leaking wells at CO_2 sequestration sites; NRAP-TRS-III-021-2017: NRAP Technical Report Series, U.S. Department of Energy, National Energy Technology Laboratory, Morgantown, West Virginia, 28 p. DOI: 10.18141/1433164.

Carter, R. D., and Tracy, G. W., 1960, An improved method for calculating water influx: Petroleum Transactions, AIME, vol. 219, p. 415–417.

Chang, K. W., Minkoff, S. E., and Bryant, S. L., 2009, Simplified model for CO_2 leakage and its attenuation due to geological structures: Energy Procedia, v. 1, p. 3,453–3,460.

Choy, G. L., Rubinstein, J. L., Yeck, W. L., McNamara, D. E., Mueller, C. S., and Boyd, O. S., 2016, A rare moderate-sized (Mw 4.9) earthquake in Kansas: Rupture process of the Milan, Kansas, earthquake of 12 November 2014 and its relationship to fluid injection: Seismological Research Letters, doi:10.1785/0220160100.

Dake, L. P., 1978, Fundamentals of Reservoir Engineering, Chapter 9, Elsevier Scientific Publishing Co., 1978.

Dart, R. L., 1990, In situ stress analysis of wellbore breakouts from Oklahoma and the Texas Panhandle: U.S. Geological Survey Bulletin 1866-F, Department of the Interior, U.S. Geological Survey.

DOE-EIA (U.S. Dept. of Energy, Energy Information Administration), 2017, Ethanol plans: EIA-819M Monthly Oxygenate Report, March 27, 2017.

Doveton, J. H., 2004, Applications of estimated formation water resistivities to brine stratigraphy in the Kansas subsurface: Kansas Geological Survey, Open-File Report 2004-22, 20 p.

Dubois, M., and McFarlane, D., 2018, Economics for CO_2 capture, compression, and transportation in the Mid-Continent, Second CCUS for Kansas forum, co-sponsors: Kansas Geological Survey and State CO_2-EOR Work Group, University of Kansas, Lawrence, Kansas, July 26, 2018.

Dubois, M., McFarlane, D., and Bidgoli, T. S., 2017, CO_2 pipeline cost analysis utilizing a modified FE/NETL CO_2 transport cost model tool, mastering the subsurface through technology innovation, partnerships and collaboration: Carbon Storage, Oil and Natural Gas Technologies Review Meeting, DOE-NETL Annual meeting, August 1–3, 2017, Pittsburgh, Pennsylvania.

Dubois, M. K., Byrnes, A. P., Carr, T. R., Bohling, G. C., Bhattacharya, S., and Doveton, J. H., 2007, Hugoton Asset Management Project (HAMP): Hugoton Geomodel Final Report: Kansas Geological Survey Open-File Report, 2007-6, 11 chapters. http://www.kgs.ku.edu/PRS/publication/2007/OFR07_06/index.html

Dubois, M. K., White, S. W., and Carr, T. R., 2002, Ethanol production and CO_2 enhanced oil recovery: a model for environmentally and economically sound linked energy systems: Proceedings 2002 AAPG Annual Meeting, Houston, Texas, p. A46. Kansas Geological Survey Open-File Report 2002-6. http://www.kgs.ku.edu/PRS/Poster/2002/2002-6/index.html Accessed 7/1/2017.

Dubois, M. K., Williams, E. T., Hedke, D. E., Senior, P. R., and Youle, J. C., 2015a, Pleasant Prairie South reservoir characterization, modeling and simulation; *in* W. L. Watney, PI, Final Report for DOE Award Number: DE-FE0002056, Modeling CO_2 Sequestration in Saline Aquifer and Depleted Oil Reservoir to Evaluate Regional CO_2 Sequestration Potential of Ozark Plateau Aquifer System, South-Central Kansas, p. IV260-IV342.

Dubois, M. K., Williams, E. T., Youle, J. C., and Hedke, D. E., 2015b, Eubank North Unit reservoir characterization, modeling and simulation; *in* W. L. Watney, PI, Final Report for DOE Award Number: DE-FE0002056, Modeling CO_2 Sequestration in Saline Aquifer and Depleted Oil Reservoir to Evaluate Regional CO_2 Sequestration Potential of Ozark Plateau Aquifer System, South-Central Kansas, p. IV118-IV260.

Dubois, M. K., Williams, E. T., Youle, J. C., and Hedke, D. E., 2015c, Potential for CO_2 storage and enhanced oil recovery in four southwest Kansas oil fields, an extended abstract; *in* W. L. Watney, PI, Final Report for DOE Award Number: DE-FE0002056, Modeling CO_2 Sequestration in Saline

Aquifer and Depleted Oil Reservoir to Evaluate Regional CO_2 Sequestration Potential of Ozark Plateau Aquifer System, South-Central Kansas, p. IV1-IV19.

Dubois, M. K., Williams, E. T., Youle, J. C., and Hedke, D. E., 2015d, Shuck Field Chester incised valley fill reservoir characterization, modeling and simulation; *in* W. L. Watney, PI, Final Report for DOE Award Number: DE-FE0002056, Modeling CO_2 Sequestration in Saline Aquifer and Depleted Oil Reservoir to Evaluate Regional CO_2 Sequestration Potential of Ozark Plateau Aquifer System, South-Central Kansas, p. IV343-IV501.

DuBois, S. M., and Wilson, F. W., 1978, List of earthquake intensities for Kansas, 1967–1977: Environmental Geology Series 2, Kansas Geological Survey, 56 p.

Edwards, R. W. K., and Celia, M. A., 2018, Infrastructure to enable deployment of carbon capture, utilization, and storage in the United States: PNAS, v. 115, no. 38. http://www.pnas.org/content/115/38/E8815.

Ellsworth, W. L., Llenos, A. L., McGarr, A. F., Michael, A. J., Rubinstein, J. L., Mueller, C. S., and Calais, E. (2015). Increasing seismicity in the US midcontinent: Implications for earthquake hazard: The Leading Edge, 34(6), 618-626.

Gonzales-Salavar, M.A. Venturnini, M. Poganietz, W-R. Finkenrath, M. Kirsten, T. Acevedo, Spina, P.R., 2016, Development of a technology roadmap for bioenergy exploitation including biofuels, waste-to-energy and power generation and CHP: Applied Energy, v. 180, p. 338-352.

Goodman, A., Hakala, A., Bromhal, G., Deel, D., Rodosta, T., Frailey, S., Small, M., Allen, D., Romanov, V., Fazio, J., Huerta, N., McIntyre, D., Kutchko, B., and Guthrie, G., 2011, U.S. DOE methodology for the development of geologic storage potential for carbon dioxide at the national and regional scale: International Journal of Greenhouse Gas Control, v. 5, no. 4, p. 952–965. https://doi.org/10.1016/j.ijggc.2011.03.010.

Goodman, A., Sanguinito, S., and Levine, J. S., 2016, Prospective CO_2 saline resource estimation methodology: Refinement of existing US-DOE-NETL methods based on data availability: International Journal of Greenhouse Gas Control, v. 54, part 1, p. 242–249. https://doi.org/10.1016/j.ijggc.2016.09.009.

Grant, T., and Morgan, D., 2014, FE/NETL CO_2 transport cost model: National Energy Technology Laboratory. DOE/NETL-2014/1667. https://www.netl.doe.gov/research/energy-analysis/analytical-toolsand-data/co2-transport. Accessed 6/28/2017.

Grant, T., Morgan, D., and Gerdes, K., 2013, Carbon dioxide transport and storage costs in NETL studies: Quality Guidelines for Energy Systems Studies: DOE/NETL-2013/1614, 22 p.

Heidbach, O., Tingay, M., Barth, A., Reinecker, J., Kurfeb, D., and Muller, B., 2010, Global crustal stress pattern based on the World Stress Map database release 2008: Tectonophysics, v. 482, p. 2–15.

Hildebrand, G. M., Steeples, D. W., Knapp, R. W., Miller, R. D., and Bennett, B. C., 1988, Microearthquakes in Kansas: Seismological Research Letters, v. 59, p. 159–163.

Holland, A. A., 2013, Optimal fault orientations within Oklahoma: Seismological Research Letters, v. 84, no. 5, p. 876–890.

Holubnyak, E., and Dubois, M., 2018, Integrated CCS for Kansas (ICKan) (DE-FE0029474): Quarterly Report 6, submitted October 16, 2018. http://www.kgs.ku.edu/PRS/ICKan/2018/Dec/Q6_10-16-18_SIGNED.pdf. Accessed 1/2/2019.

Huerta, N. J., and Vasylkivska, V. S., 2016, Well Leakage Analysis Tool (WLAT) user's manual: NRAP Technical Report Series, U. S. Department of Energy, National Technology Laboratory, Morganotwn, West Virginia.

IEA (International Energy Agency), 2013, Technology Roadmap – Carbon capture and storage: 2013 Edition, 63 p.

King, S., 2016a, Reservoir Evaluation and Visualization (REV) tool user's manual, Version: 2016.

King, S., 2016b, Reservoir Reduced-Order Model – Generator (RROM-Gen) Tool User's Manual, Version: 2016.11-1.2.

Krishnamurthy, K. R., 2017, Linde carbon capture technologies for power and SMR based H_2 plants: Development & commercialization and techno-economic assessment: Integrated CCS for Kansas (ICKan) Kick-off Meeting. February 14, 2017.

Krishnamurthy, K. R., 2016, Slipstream pilot plant demonstration of an amine based post-combustion capture technology for CO_2 capture from coal-fired power plant flue gas: 2016 NETL CO_2 Capture Technology Meeting. August 8–12, 2016. https://www.netl.doe.gov/File%20Library/Events/2016/c02%20cap%20review/2-Tuesday/K-Krishnamurthy-Linde-Amine-Based-Process-Technology.pdf. Accessed 6/27/2017.

Kroll, K. A., Cochran, E. S., and Murray, K. E., 2017, Poroelastic properties of the Arbuckle Group in Oklahoma derived from well fluid level response to the 3 September 2016 Mw 5.8 Pawnee and 7 November 2016 Mw 5.0 Cushing Earthquakes: Seismological Research Letters, v. 88, p. 963–970, https://doi.org/10.1785/0220160228.

Krushin, J. T., 1997, Seal capacity of nonsmectite shale: Seals, Traps, and the Petroleum System, v. 67, p. 31–47. Retrieved from http://search.datapages.com/data/specpubs/mem67/ch03/ch03.htm.

Langenbruch, C., and Zoback, M. D., 2016, How will induced seismicity in Oklahoma respond to decreased saltwater injection rates?: Science Advances, v. 2, e1601542, doi: 10.1126/sciadv.1601542.

Langston, M. V., Hoadley, S. F., and Young, D. N., 1988, Definitive CO_2 flooding response in the SACROC unit: In SPE Enhanced Oil Recovery Symposium, Society of Petroleum Engineers.

Leroux, K., 2017, Integrated carbon capture and storage for North Dakota ethanol production, final report for DOE Project # DE-F0024233, May 31, 2017.

Lindner, E. N., 2016, NRAP Seal Barrier Reduced-Order Model (NSealR) tool user's manual, Version: 2016.11-14.

McKaskle, R., 2016, Trimeric Corporation, insights into costs of CCS gained from the IBDP: 2016 Midwest Carbon Sequestration Science Conference, May 17, 2016.

McPherson, B., 2010, Integrated mid-continent carbon capture, sequestration & enhanced oil recovery project, final report for DOE Project # DE-FE-0001942, August 31, 2010.

NETL, 2010, Carbon dioxide enhanced oil recovery: Untapped domestic energy supply and long term carbon storage solution: National Energy Technology Laboratory, Pittsburgh, Pennsylvania.

Peterie, S. L., Miller, R. D., Intfen, J., Bidgoli, T., & Buchanan, R. (2015). A geologically-based approach to mitigate potentially induced seismicity in Kansas: In SEG Technical Program Expanded Abstracts 2015 (pp. 4871-4876). Society of Exploration Geophysicists.

Peterie, S. L., Miller, R. D., Intfen, J. W., & Gonzales, J. B. (2018). Earthquakes in Kansas Induced by Extremely Far‐ Field Pressure Diffusion: Geophysical Research Letters, 45(3), 1395-1401.Phaal, et al., 2004, R., Farrukh, C.J.P., Probert, D.R., 2004, Technology roadmapping – A planning framework for evolution and revolution: Technology Forecasting and Social Change: v. 71, p. 5-26. Peterie, S.L., Miller, R.D., Intfen, J., Bidgoli, T., and Buchanan, R., 2015, A geologically based approach to mitigate potentially induced seismicity in Kansas: SEG Technical Program Expanded Abstracts 2015, p. 4871-4876.

Rascoe, B., Jr., and Adler, F. J., 1983, Permo-Carboniferous hydrocarbon accumulations, Mid-Continent, U.S.A.: AAPG Bulletin, v. 67, p. 979–1,001.

Rubinstein, J., Ellsworth, W., Llenos, A., and Walter, S., 2014, Is the recent increase in seismicity in Kansas natural?: American Geophysical Union Fall Meeting.

State CO_2-EOR Deployment Work Group, 2017, Capturing and utilizing CO_2 from ethanol: Adding economic value and jobs to rural economies and communities while reducing emissions (white paper). https://www.betterenergy.org/blog/capturing-utilizing-co2-ethanol-adding-economic-value-jobs-rural-economies-communities-reducing-emissions/. Accessed December 12, 2018.

Stauffer, P., Chu, S., Tauxe, C., and Pawar, R., 2016, NRAP Integrated Assessment Model-Carbon Storage (NRAP-IAM-CS) Tool User's Manual, Version: 2016.11-1.1; NRAP-TRS-III-010-2016: NRAP Technical Report Series, U.S. Department of Energy, National Energy Technology Laboratory: Morgantown, West Virginia, 64 p.

U. S. Department of Energy, 2012, 2012 technology readiness assessment overview: Clean Coal Research Program, U.S. Department of Energy, Office of Fossil Energy. https://www.netl.doe.gov/File%20Library/Research/Coal/energy%20systems/gasification/TRA-Overview-Report_121112_FINAL_1.pdf. Accessed 6/27/2017.

U.S. EIA, 2018, Independent statistics & analysis, Kansas state profile and energy estimates: U.S. Energy Information Administration, https://www.eia.gov/state/?sid=KS.

Volokin Y., Looyesttijn, W., Slijkerman, F., and Hofman, J., 2001, A Practical Approach to Obtain Primary Drainage Capillary Pressure Curves from NMR Core and Log Data, Petrophysics, Vol. 42. No. 4; p. 334-343.

Walter, J. I., J. C. Chang, and P. J. Dotray (2017). Foreshock seismicity suggests gradual differential stress increase in the months prior to the 3 September 2016 Mw 5.8 Pawnee earthquake: Seismological Research Letters, 88(4), 1-8, doi:10.1785/0220170007.

Watney, W. L. et al., 2015, Modeling CO_2 sequestration in saline aquifer and depleted oil reservoir to evaluate regional CO_2 sequestration potential of Ozark Plateau aquifer system, south-central Kansas, final report, Award Number: DE-FE0002056, submitted October 2, 2015, 4,867 p.

Watney, W. L. et al., 2016, Integrated CCS for Kansas (ICKan) SF 424 R&R, application for federal assistance, Phase I—Integrated CCS pre-feasibility study activity under CarbonSAFE, DOE-NETL FOA 1584.

Watney, L., Holubnyak, Y., Hollenbach, J., Bidgoli, T., Fazelalavi, F., Doveton, J., Victorine, J., Birdie, T., Nolte, A., Tsoflias, G., Graham, B., Wreath, D., Bruns, J., and Blazer, B., 2017 Small Scale Field Test Demonstrating CO_2 Sequestration In Arbuckle Saline Aquifer And By CO2-EOR At Wellington Field, Sumner County, Kansas. United States: N. p. Web. doi:10.2172/1420310.

Yeck, W. L., Hayes, G. P., McNamara, D. E., Rubinstein, J. L., Barnhart, W. D., Earle, P. S., and Benz, H. M., 2017, Oklahoma experiences largest earthquake during ongoing regional wastewater injection hazard mitigation efforts: Geophysical Research Letters, v. 44, p. 711–717. https://doi.org/10.1002/2016GL071685.

Zoback, M. D., Barton, C. A., Brudy, M., Castillo, D. A., Finkbeiner, T., Grollimund, B. R., Moos, D. B., Peska, P., Ward, C. D., and Wiprut, D. J., 2003, Determination of stress orientation and magnitude in deep wells: International Journal of Rock Mechanics and Mining Sciences, v. 40, p. 1,049–1,076.

Appendix A: Anticipated business contractual requirements necessary to address technical and financial risks

Charles C. Steincamp[1] and Joseph A. Schremer[2]
[1,2] Depew, Gillen, Rathburen & McInteer, LC, Wichita, Kansas

What business contractual requirements this project will require depends, in the first instance, on the business model for CCS the project ultimately embraces. Experience in other states suggests two potential general models: the public utility model and the private party model. In the public utility model, the transportation, disposal, and storage of CO_2 would be accomplished by one or more public utilities. Variations of the model may include a single public utility that is responsible for capture, transportation, disposal, and storage of captured CO_2, or separate utilities individually responsible for transportation and storage. Under a private party model, separate private firms would independently conduct the capture, transportation, disposal, and storage of CO_2.

The business contractual requirements necessary to address project risks would be greater under a private party model because custody of the CO_2 would potentially change hands among a succession of persons. Whereas under a public utility model, and particularly where a single public utility conducts all operations downstream of the generator, the number of persons involved in the chain of custody would be fewer. Regardless of which model ultimately emerges in this project, the business contractual requirements we anticipate to fully address technical and financial project risks fall into five broad categories: (1) capture, (2) transportation, (3) disposal and storage, (4) long-term liability, and (5) title to CO_2. We will survey the likely business contractual requirements in each category below.

I. Capture

Under either a public utility or private party paradigm, there are conceivably two alternative business arrangements for capture of CO_2. Either the generator will install, operate, and maintain the capture technology at the generation facility, or a third-party contractor will do so. There are few, if any, contractual considerations in the former scenario because the generator will bear all of the risks associated with capture. Where capture is conducted by a third-party, however, a contractual relationship between generator and capture contractor will need to address the risks of technical failure. In particular, the parties' contract must allocate the responsibility for maintenance and repairs, and the liability associated with system failure. System failure liability could include civil penalties for violation of applicable air permits and costs of plant downtime caused by a system failure. A full understanding of the potential technical and financial risks of capture is possible only after a thorough study of the methods and technology under Phase II. Additionally, any contractual relationship between a generator and capture contractor will need to address compensation for the contractor's services and title and responsibility for the captured CO_2 (the latter concern is addressed in section V, below).

II. Transportation

Once the CO_2 is sequestered at the generation plant, it will need to put into a pipeline for transportation to the ultimate storage site. The possible business models for pipeline transportation of CO_2 are myriad, especially under a private party model, and accordingly it is impossible at this stage to precisely anticipate, or briefly summarize, all of the contractual considerations that could arise. It is reasonable to predict the following issues.

Generator and transporter will need to agree on whether title and responsibility for the CO_2 is transferred and, if so, where the transfer occurs. This is addressed in section V, below.

Assuming the CO_2 remains the generator's property, the parties will need to price the transportation. The price will likely include charges for maintenance, treatment and processing, compression, and regulatory compliance (e.g., LDAR), incurred by the transporter. The price may vary based on either the volume delivered to the pipeline, the distance the CO_2 is transported, any potential gas quality issues that may need to be addressed, or a permutation of these factors. Alternatively, if the generator sells the CO_2 to the transporter, the parties will need to price the CO_2. Any pricing mechanism would likely begin with the prevailing market price for CO_2 (if any) and deduct costs of transportation.

The parties will allocate liability for shrinkage or loss of the CO_2 stream during transportation. How parties allocate this risk may depend on which retains title to the CO_2. This could include regulatory fines, penalties, and response costs.

The parties will allocate the technical risks associated with quality of the CO_2. These risks may include the pH balance of the CO_2 stream, as well as the presence of other impurities or contaminants which may be present, and its possible effects on the physical line. In addressing this issue, the parties are likely to adopt gas-quality criteria in their contract that the CO_2 must satisfy as a condition to transportation through the pipeline.

Under one possible business model, portions of the CO_2 stream may be diverted for sale to third parties for various industrial applications, notably tertiary oil recovery. Sales of CO_2 to third parties will involve contracts which both transfer title to the CO_2 and allocate the risks of subsequent transportation and application of the CO_2. The sale of portions of the CO_2 stream may also effect contractual relations between the transporter and generator if title to the CO_2 remains with the generator.

The transporter and the owner of the pipeline facility may be separate entities under some business models. In this case, there would be a contractual relationship between the two allocating the costs and risks of use of the physical pipeline.

The owner of the pipeline will obviously need to first construct the line. The construction process would begin with right-of-way acquisition, which will entail consensual easement agreements with landowners as well as easements obtained by condemnation.

III. Disposal and Storage

The contractual considerations surrounding disposal and storage of captured CO_2 begin with acquisition of rights in storage formation. Kansas law appears to hold that title to subsurface pore space remains with the surface estate despite severance of the mineral estates. *See Dick Props., LLC v. Paul H Bowman Tr.*, 43 Kan. App. 2d 139, Syl. ¶ 6, 221 P.3d 618 (2010). Lacking clear legal authority for this proposition, however, contracts for the acquisition of rights in the storage formation may need to address pore-space ownership among the various surface and mineral estate owners to reduce the risk of the disposal and storage firm committing pore-space trespass. Further, because storage formations may span many acres of surface land, it is usually necessary to obtain consent and transfer of rights from numerous owners of contiguous land. The public utility model is an attractive vehicle for such purposes because a utility can possess the power to condemn the rights of contiguous landowners for storage purposes. Absent statutory authority in Kansas for condemnation of saline storage formations, disposal and storage firms would need to obtain contractual agreements with all owners of the contiguous acreage needed for a storage formation. The significant associated costs would be contractually allocated among the disposal and storage firms and the titleholder of the CO_2 (likely the generator).

Disposal will require a regulatory permit for a Class VI Underground Injection well. In Kansas, this is administered through the U.S. Environmental Protection Agency. Class VI disposal well regulations, effective since 2011, have six phases of regulations and monitoring, from amalgamation of storage rights to post-closure long term monitoring. Contractual agreements will need to clarify whom is applying for what phases, whom is responsible for the costs associated with meeting the performance standards of the permit, and for providing the financial assurance to protect or remediate a drinking water source, if necessary.

The separate acts of disposal and storage may not be conducted by one firm under some business models. Consequently, where the two activities are undertaken independently of one another, a contractual relationship will need to exist between the two firms. The relationship will need to address compensation, liability for plugging and abandonment of injection wells, and liability for leakage including proximate property damage and personal injury. These risks could arise in a number of foreseeable scenarios including migration or escape of CO_2 into adjacent geologic formations or formations underlying land not included in the storage site (which we refer to as "pore-space trespass"), accidental release of CO_2 into formations bearing underground drinking water, and even accidents from the pressurized pipeline transportation or injection of gaseous CO_2. Under some circumstances, this may include the cost of regulatory compliance, fines, and penalties. These same risk allocations will need to be made between the disposal firm and the transporter under a contractual relationship governing delivery of the CO_2 at the tail end of the pipeline.

Whichever party or parties among generator, transporter, disposal firm, and storage firm, bears the risks of casualty loss from leakage will likely seek to reduce or eliminate these risks throuOnri nciz One (of several) possible contractual insurance arrangements may involve the penultimate custodian of the CO_2 (most likely the storage firm) purchasing a policy of casualty or general liability insurance covering operation of the storage site under which the generator is additional named insured. The costs of such an insurance policy would likely be allocated between the primary and additional insureds through the price charged for storage (or, alternatively, the price paid for the CO_2 by the storage firm).

IV. Storage Site Closure and Long-Term Liability

Several states have codified a procedure by which the state ultimately takes responsibility for monitoring and liability of a closed storage site. Kansas does not appear to have adopted such a procedure; consequently, storage firms and generators would need to contractually limit their long-term liability for closed storage sites, likely through private insurance. The most likely form of insurance would be a single ' premium tail or cost cap policy. It is unclear, however, whether there is an insurance market for long-term risks associated with closed CO_2 storage sites. For the project to be feasible, it is probable a statutory regime shifting responsibility for monitoring and long-term liability to the state would need to be passed. The specific long-term risks associated with a closed CO_2 storage field are similar to those associated with an operational site (e.g., pore-space trespass, drinking water contamination, and pressurized injection wells and surface equipment).

V. Title to CO_2

Underpinning all of the preceding categories of business contractual requirements is title to the CO_2 stream. Kansas has two pertinent statutes. K.S.A. 65-3418 governs vesting of title to solid waste. Solid waste is a broadly defined statutory term that likely encompasses captured CO_2. Under the statute, title to the solid waste vests in the owner of the solid waste_(the generator). The solid waste remains property of the generator, and the generator remains liable for the waste, notwithstanding any contractual arrangements between the generator and third parties. However, title to the solid waste is transferred to the resource recovery facility (the storage facility so long as the storage is conducted in accordance with

applicable law. If, however, the storage is not properly operated, liability for the CO_2 rests with the storage facility and the generator. K.S.A. 65-3442 sets forth a similar risk-allocation scheme for hazardous waste.

Because the solid waste transfer statutes likely apply to captured CO_2, the generator is likely to be ultimately responsible for risks associated with the CO_2 throughout the capture and transportation phases of the CO_2 stream. The storage firm will become liable for the CO_2 stream upon receipt but will probably share that liability with the generator. Therefore, the generator is likely to purchase private insurance, naming the generator as an additional insured, and price the costs of such insurance into its compensation for storage services (or, under a model in which the storage firm purchases the CO_2, price the costs into the consideration paid for the CO_2).

Appendix B: Draft statutes to address statutory challenges related to CCS in Kansas: Draft statute amendments

Charles C. Steincamp[1] and Joseph A. Schremer[2]
[1,2] Depew, Gillen, Rathburen & McInteer, LC, Wichita, KS

K.S.A. _____

_____. Ownership of pore space.

(a) The ownership of all pore space in all strata below the surface lands and waters of this state is declared to be vested in the several owners of the surface estate.

(b) A conveyance of the surface estate in real property shall pass all the estate of the grantor's interest in the pore space in all strata below the surface of such real property unless the intent to pass a less estate shall expressly appear or be necessarily implied in the terms of the grant.

K.S.A. § 17-618

17-618. Eminent domain, exercise by sundry corporations and partnerships.

Lands may be appropriated for the use of macadam-road, plank-road, hospital corporation or association, telegraph and telephone corporations, electric, hydraulic, irrigating, milling and manufacturing corporations using power, oil companies, geologic carbon storage utilities, pipeline companies, and for the piping of gas in the same manner as is provided in ***K.S.A. 26-501*** to ***26-516***, inclusive, and any macadam-road, plank-road, telegraph and telephone corporations, hydraulic, irrigating, oil company, geologic carbon storage utility, pipeline company, gas company, partnership holding a certificate of convenience as a public utility issued by the state corporation commission, milling or manufacturing corporation using power desiring the right to dam or take water from any stream, to conduct water in canals or raceways or pipes, or to conduct compressed air in pipes, or to conduct oil in pipes or conduct gas in pipes, or transmit power or communications by shafting, belting, or belting and pulleys, or ropes and pulleys, or by electrical current, or by compressed air, may obtain such right or the right-of-way for all necessary canals, raceways, pipes, shafting, belting and pulleys, ropes and pulleys or wires or cables in manner as aforesaid; and such canals, raceways, pipes, shafting, belting, belting and pulleys, ropes and pulleys or wires or cables may be laid, carried or stretched on, through or over any land or lot, or along or upon any stream of water, using so much of the water thereof as may be needed for any of the purposes aforesaid, or through any street or alley or public ground of any city of the second or third class: Provided, That

no such canal or raceway shall be located through any street or alley or any public ground of any city without the consent of the municipal authorities thereof: Provided further, That it shall be unlawful for any person or corporation to locate or construct any irrigating canal or raceway along or upon any stream of water or take and use the water of any stream in such manner as to interfere with or in any wise hinder, delay or injure any milling or irrigating improvements already constructed or located along or upon any stream of water, or to diminish the supply of water flowing to or through any established irrigating canal: Provided further, That in case of the erection of a dam, the report of the commissioners, instead of defining the quantity and boundaries of the land overflowed, shall designate particularly the height of such dam.

K.S.A. § 55-_____

55-_____. Definitions

As used in this act

(a) "underground storage" shall mean storage in a subsurface stratum or formation of the earth;

(b) "carbon dioxide" shall mean carbon dioxide gas produced from anthropogenic sources;

(c) "native gas" shall mean gas which has not been previously withdrawn from the earth;

(d) "geologic carbon storage utility" shall mean any person, firm or corporation authorized to do business in this state and engaged in the business of storing carbon dioxide by means of injection into underground storage, within or through this State for beneficial use or ultimate storage and disposal;

(e) "commission" shall mean the state corporation commission.

(f) "pore space" shall mean openings between or within geologic material under surface lands whether natural or artificially created, which may be referred to as voids or interstices.

(g) "underground carbon dioxide storage facility" shall mean a facility storing carbon dioxide in subsurface pore space.

K.S.A. § 55-_____

55-_____. Public interest and welfare.

The underground storage of carbon dioxide promotes protecting the health, safety and property of the people of the State, and preventing escape of carbon dioxide into the atmosphere and pollution of soil, and surface and subsurface water detrimental to the public health or to plant, animal and aquatic life and promotes the public interest and welfare of this state.

Therefore in the manner hereinafter provided the commission may find and determine that the underground storage of carbon dioxide as hereinbefore defined is in the public interest.

K.S.A. § 55-_____

55-_____. Appropriation of certain property.

Any geologic carbon storage utility may appropriate for its use for the underground storage of carbon dioxide fee simple absolute in all surface and mineral interests in any subsurface stratum or formation in any land which the commission shall have found to be suitable and in the public interest for the underground storage of carbon dioxide, and in connection therewith may appropriate such other interests in property as may be required adequately to examine, prepare, maintain and operate such underground carbon dioxide storage facility. The right of appropriation hereby granted shall be without prejudice to the rights of the owner of said lands or of other rights or interests therein to drill or bore through the underground stratum or formation so appropriated in such manner as shall comply with orders, rules and regulations of the commission issued for the purpose of protecting underground storage strata or formations against pollution and against the escape of carbon dioxide therefrom and shall be without prejudice to the rights of the owner of said lands or other rights or interests therein as to all other uses thereof.

K.S.A. § 55-_____

55-_____. Underground storage of carbon dioxide; certificate of commission; notice and hearing; assessment of costs; disposition of moneys.

(a) Any geologic carbon storage utility desiring to exercise the right of eminent domain as to any property for use for underground storage of carbon dioxide shall, as a condition precedent to the filing of its petition in the district court, obtain from the commission a certificate setting out findings of the commission:

(1) That the underground stratum or formation sought to be acquired is suitable for the underground storage of carbon dioxide and that its use for

such purposes is in the public interest; and

(2) the amount of recoverable oil and native gas, if any, remaining therein.

(b) As a condition to issuing any such certificate, the commission shall require that:

(1) the applicant post a bond in an amount the commission determines is sufficient to assure the costs of plugging all injection wells and completing all reclamation work required by the commission, and complying with all permits, rules, and regulations of the commission applicable to the proposed underground storage project for the life of the project; and

(2) purchase and maintain a policy or policies of liability insurance covering any damage injected carbon dioxide may cause, including damage caused by carbon dioxide that escapes from the underground storage facility. Such policy or policies shall provide limits of not less than $_____. Such policy or policies shall be maintained continually until such time as the commission shall issue a certificate of project completion covering the underground storage facility pursuant to ***K.S.A. 55-1211***, and amendments thereto.

(c) The commission shall issue no such certificate until after public hearing is had on application and upon reasonable notice to interested parties in accordance with the provisions of the Kansas administrative procedure act. Subject to the provisions of ***K.S.A. 55-1636 et seq.***, and amendments thereto, the applicant shall be assessed an amount equal to all or any part of the costs of such proceedings and the applicant shall pay the amount so assessed.

(d) All provisions of ***K.S.A. 66-106***, ***66-118a***, ***66-118b***, ***66-118c***, ***66-118d***, ***66-118e***, ***66-118j*** and ***66-118k***, and amendments thereto, shall be applicable to all proceedings of the commission under this act, inclusive, and amendments thereto.

(e) The state corporation commission shall remit all moneys received by or for it for costs assessed under this section to the state treasurer in accordance with the provisions of ***K.S.A. 75-4215***, and amendments thereto. Upon receipt of each such remittance, the state treasurer shall deposit the entire amount in the state treasury to the credit of the carbon dioxide injection well and underground storage fund created by ***K.S.A. 55-1638***, and amendments thereto.

(f) A certificate issued under this section may be assigned by the owner thereof to a third party who as determined by the commission complies with all the terms and conditions of such certificate and such transfer is approved following notice and hearing before the commission.

K.S.A. § 55-_____

55-_____. Eminent domain procedure.

Any geologic carbon storage public utility, having first obtained a certificate from the commission as hereinbefore provided, desiring to exercise the right of eminent domain for the purpose of acquiring property for the underground storage of carbon dioxide shall do so in the manner provided in ***K.S.A. 26-501*** to ***26-516***, inclusive. The petitioner shall file the certificate of the commission as a part of its petition and no order by the court granting said petition shall be entered without such certificate being filed therewith. The appraisers in awarding damages hereunder shall also take into consideration the amounts of recoverable oil and native gas remaining in the property sought to be appropriated and for such purposes shall receive as prima facie evidence of such amounts the findings of the commission with reference thereto.

K.S.A. § 55-_____

55-_____. Sale of state-owned lands for underground storage of carbon dioxide; conditions.

The director of the state department of administration, with the approval of the state finance council, may sell to a person, firm or corporation lands owned by the state of Kansas for the underground storage of carbon dioxide by such person, firm or corporation. All such sales shall be on such terms and conditions as the director of the state department of administration, with the approval of the state finance council, shall prescribe. Every such sale shall describe the subsurface stratum or formation in such lands which is to be utilized for such storage. Any sale made pursuant to the provisions of this section shall be without prejudice to the rights of the state as the owner of such lands, or any lessee of the oil and gas rights thereof, to develop other subsurface strata or formations so leased in such manner as will comply with existing or hereafter promulgated rules and regulations of the state corporation commission issued for the purpose of protecting underground carbon dioxide storage stratum or formation.

All proceeds of such sales shall be remitted to the state treasurer in accordance with the provisions of ***K.S.A. 75-4215***, and amendments thereto. Upon receipt of each such remittance, the state treasurer shall deposit the entire amount in the state treasury to the credit of the carbon dioxide injection well and underground storage fund created by ***K.S.A. 55-1638***, and amendments thereto.

K.S.A. § 55-_____

55-_____. Plat map of location of underground carbon dioxide storage facility required.

The owner of an underground carbon dioxide storage facility shall provide to the state corporation commission a plat map identifying the location of such facility and a description of the geological formation or formations to be used for storage.

K.S.A. § 55-_____

55-_____. Property rights to injected carbon dioxide gas established.

(a) Title to carbon dioxide produced from a discrete source and reduced to possession shall remain with the generator until transferred to the owner of a carbon dioxide storage facility unless title to such carbon dioxide is expressly transferred by contract or other written instrument. Transporters of carbon dioxide shall be common carriers unless expressly agreed.

(b) In no event shall such carbon dioxide be subject to the right of the owner of the surface of such lands or of any mineral interest therein, under which such carbon dioxide storage facility lies, or of any person, other than the owner of the carbon dioxide storage facility, to produce, take, reduce to possession, vent, release, allow escape, either by means of the law of capture or otherwise, waste, or otherwise interfere with or exercise any control over such carbon dioxide.

Nothing in this subsection shall be deemed to affect the right of the owner of the surface of such lands or of any mineral interest therein to drill or bore through the underground storage fields, sands, reservoirs and facilities in such a manner as will protect such fields, sand, reservoirs, environment and facilities against pollution and the escape of the carbon dioxide being stored.

(c) The owner of the carbon dioxide storage facility, such owner's heirs, successors and assigns shall have the right to compel compliance with this section by injunction or other appropriate relief by application to a court of competent jurisdiction.

(d) While the carbon dioxide storage facility owner holds title to injected carbon dioxide, the owner shall be liable for any damage the carbon dioxide may cause, including damage caused by carbon dioxide that escapes from the storage facility.

(e) Carbon dioxide produced from a discreet source and reduced to possession that is disposed of in ways other than in accordance with this act shall remain the property of the generator and the generator shall be liable for any damage the carbon dioxide may cause and to provide for lawful injection or management of the carbon dioxide. It shall not constitute a defense to the generator that the generator acted through an independent contractor in the transportation or disposal of the carbon dioxide.

(f) Nothing herein shall be construed to prevent the owner of a carbon dioxide storage facility from transferring title to the carbon dioxide or the carbon dioxide storage facility by contract to a third party.

K.S.A. § 55-_____

55-_____. Certificate of project completion; release; transfer of title and custody.

(a) Not less than ten (10) years after carbon dioxide injections into an underground carbon dioxide storage facility end and upon application by the owner of such facility, the commission may issue a certificate of project completion following public notice and hearing. The commission shall establish notice requirements for this hearing.

(b) The certificate may be issued only upon a showing by the applicant that:

(1) The applicant is in full compliance with all laws governing the underground carbon dioxide storage facility.

(2) The applicant has resolved all pending claims regarding the underground carbon dioxide storage facility.

(3) That the underground carbon dioxide storage facility is reasonably expected to retain the carbon dioxide stored in it.

(4) That the carbon dioxide in the underground carbon dioxide storage facility has become stable. Stored carbon dioxide is stable if it is essentially stationary or, if it is migrating or may migrate, that any migration will be unlikely to cross the boundary of the subsurface stratum of formation in which the carbon dioxide is stored.

(5) That all wells, equipment, and facilities to be used in the postclosure period are in good condition and retain mechanical integrity.

(6) That the applicant has plugged wells, removed equipment and facilities, and completed all reclamation work as required by the commission.

(c) Once a certificate is issued under this section:

(1) All right, title, and interest in and to the underground carbon dioxide storage facility and to the stored carbon dioxide transfers, without payment of any compensation, to the state. Title acquired by the state includes all rights and interests in, and all responsibilities and liabilities associated with, the stored carbon dioxide and the underground carbon dioxide storage facility.

(2) The applicant and all persons who generated, transported, or injected any carbon dioxide into the underground carbon dioxide storage facility are released from all regulatory requirements associated with the underground carbon dioxide storage facility.

(3) Any bonds posted by the applicant must be released.

(4) Monitoring and managing the underground carbon dioxide storage facility is the state's responsibility to be overseen by the commission until such time as the federal government assumes responsibility for the long-term monitoring and management of such facility.

K.S.A. § 66-104(h)

(h) The term "public utility" shall also include an entity engaged in the transportation or storage of carbon dioxide as those terms are defined in K.S.A. 55-_____.

Appendix C: Technical analysis of the Forest City Basin geologic complex: Davis Ranch and John Creek Fields

Martin K. Dubois[1], Yevhen Holubnyak[2], Andrew Hollenbach[3], Fatemeh FazelAlavi[2], Dave Newell[2]
[1] Improved Hydrocarbon Recovery, LLC, [2] Kansas Geological Survey, [3] University of Kansas

ABSTRACT

The two largest oil fields in relatively close proximity to Kansas' largest coal-fired power plant, Jeffrey Energy Center, comprise the Forest City Basin Complex. A high-level technical analysis was conducted on the two fields, the Davis ranch and John Creek fields to determine the volume of CO_2 that could be stored and the rate at which CO_2 could be injected into two saline aquifers, Simpson sandstone (3,250 ft) and Arbuckle dolomite (3,350 ft), beneath the producing horizons. The analysis followed a standard work flow including 1) gathering and processing basic well and engineering data, 2) stratigraphic and structural 2-D mapping, 3) petrophysical studies, 4) building a 3-D cellular property model that was then upscaled for simulation, and 5) simulating injection and storage in a dynamic model. It was determined that the two fields that make up the Forest City Basin storage complex, the Davis Ranch and John Creek fields, in combination, are unlikely to be capable of storing 50 million tonnes (Mt) of CO_2, the targeted storage volume. Although injection rates are adequate averaging 2,700 tonnes/day, the dynamic simulation projects a total of 24.6 Mt stored over a 25-year period. Initial work on evaluating the vertical seals, comparing the geochemistry of the reservoir brines, suggests that the target CO_2 injection zones, the Simpson and Arbuckle, are isolated from each other as well as from overlying strata. Additional risk evaluations have been postponed because of the apparent shortfall in reservoir capacity.

INTRODUCTION

The Forest City Basin (FCB) geologic complex is one of two geologic complexes identified as potential sites for storing >50 million tonnes (Mt) CO_2 as part of the Integrated CCS for Kansas (ICKan), contract number DE-FE0029474 under the DOE/NETL CarbonSAFE program. The other geologic complex is the Hugoton complex. The Pleasant Prairie field (Hugoton complex), numbered 1 in Figure 1, is the subject of a separate study. The subjects of this study are the Davis Ranch and John Creek fields, located in Wabaunsee and Morris Counties in northeast Kansas and numbered 11 and 12 in Figure 1.

The Davis Ranch and John Creek fields (FCB complex), numbered 11 and 12 in Figure 1, were chosen for this study largely due to their proximity to the Jeffrey Energy Center, the largest CO_2 source in Kansas located 40–50 miles to the northeast. The two fields are the largest oil fields in the Forest City Basin with the Davis Ranch having produced 9.1 million barrels (mmbo) of oil from the Kansas City and Hunton, but primarily from the Viola since it was discovered in 1949, and the John Creek having produced 10.3 mmbo from the Viola since its discovery in 1953. The Simpson Sandstone and the Arbuckle (dolomite) are saline aquifers lying beneath the producing intervals and are potential targets for CO_2 storage (Figure 2).

Technical evaluations of the two saline aquifers beneath the oil producing horizons were performed using publicly available data supplemented with data provided by the two field operators, Davis Ranch—Blake Production Co., and John Creek—Blake Production Co. and Knighton Oil Co.

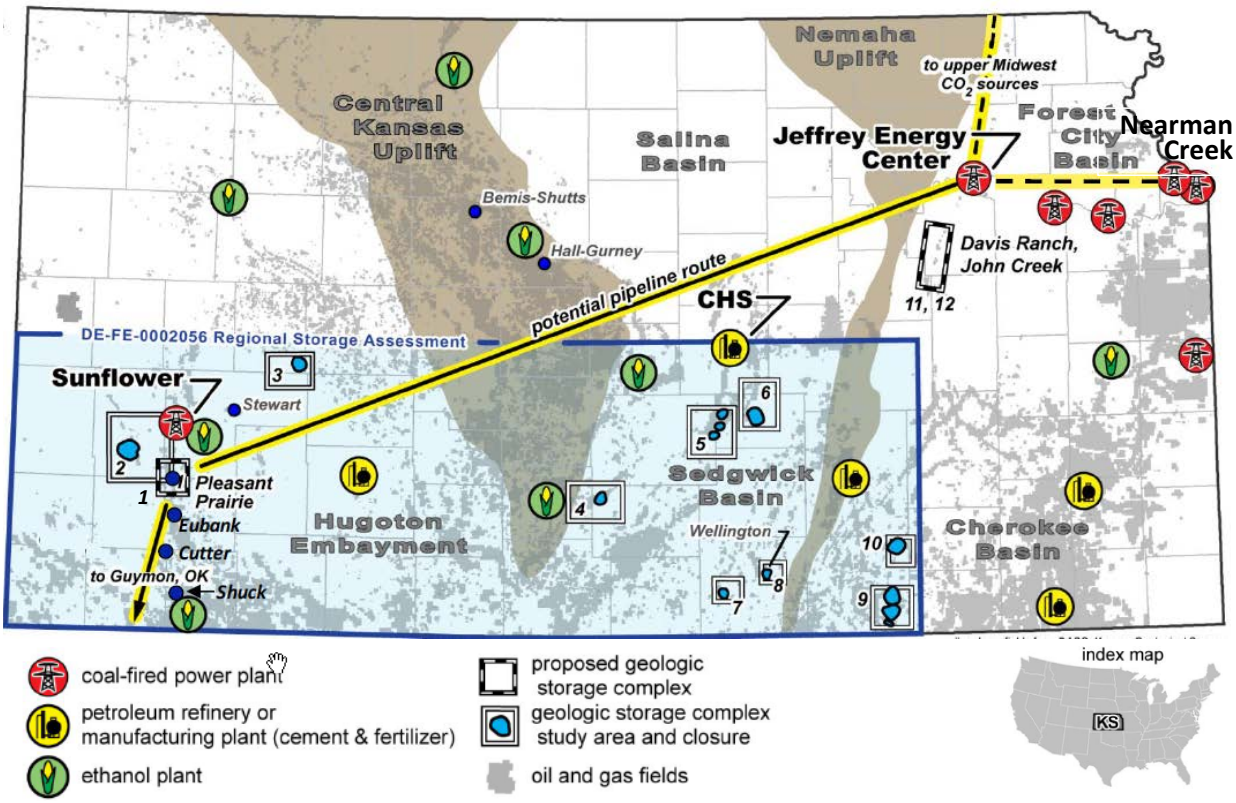

Figure 1. Kansas map showing possible CO_2 injections sites (numbered 1–12), CO_2 sources, possible CO_2 pipeline routes, DE-FE0002056 study areas (blue), and oil fields (modified from ICKan SF 424 R&R, 2016).

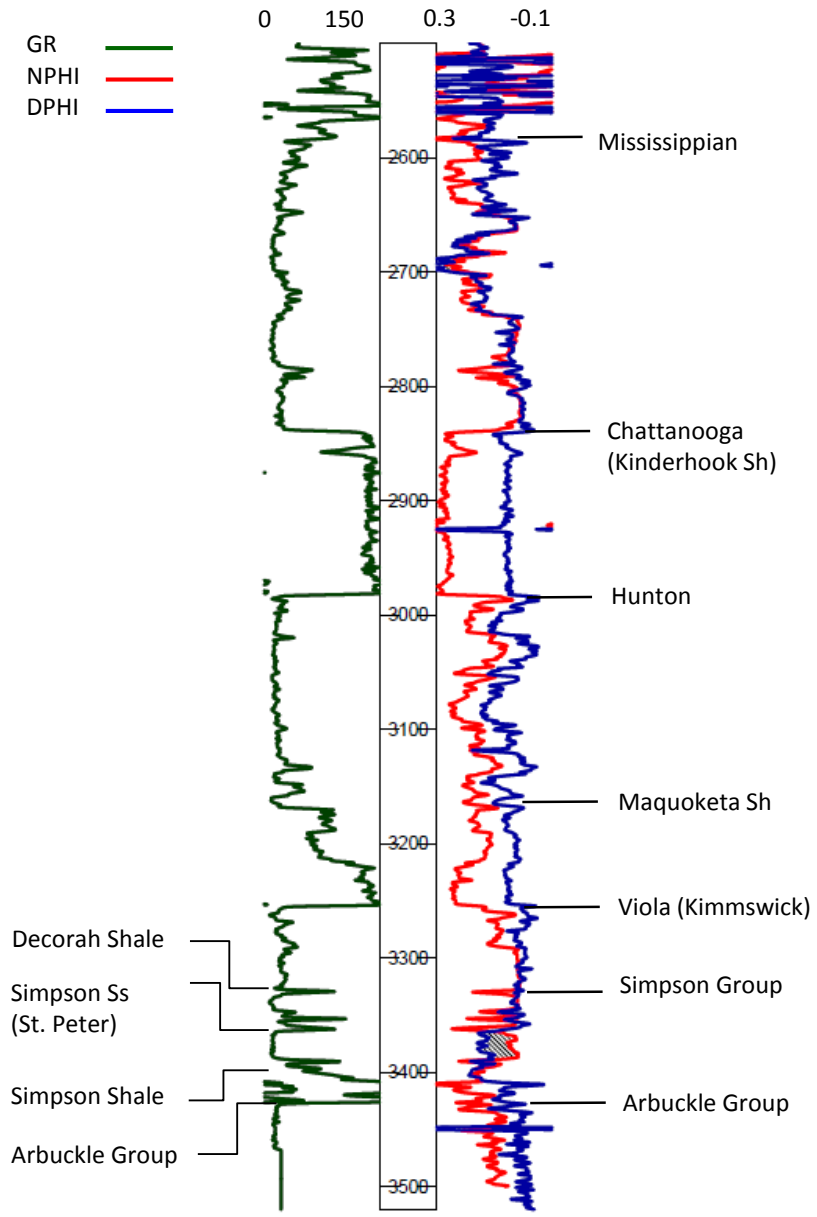

Figure 2. Generalized stratigraphic column for the Davis Ranch and John Creek area. Wireline log is from the Conoco, Inc. #1 Fisher Grace well in Morris County, Kansas (API 15-127-2045). Abbreviations included GR—natural gamma ray radiation in API counts, NPHI—neutron porosity expressed in decimal, DPHI—density porosity expressed in decimal.

STATIC MODEL CONSTRUCTION

A simple, un-faulted 3-D static model was built for a 418 mi^2 (1082 km^2) area (Figure 3) and then smaller areas were cut out of the model for simulation A standard workflow (Figure 4) for building a 3-D static model was deployed: 1) gather, prepare and analyze well-scale well data from public sources and operator-partner data, 2) build 2-D structure and isopach maps with Geoplus Petra™, 3) develop petrophysical relationships to estimate permeability knowing porosity, 4) build a larger-area 3-D static property model populated with porosity and permeability for the Simpson Sandstone and Arbuckle, 5) upscale the model to reduce cell counts for simulation, and 6) cut out and export smaller field-scale

models for simulating the two fields.

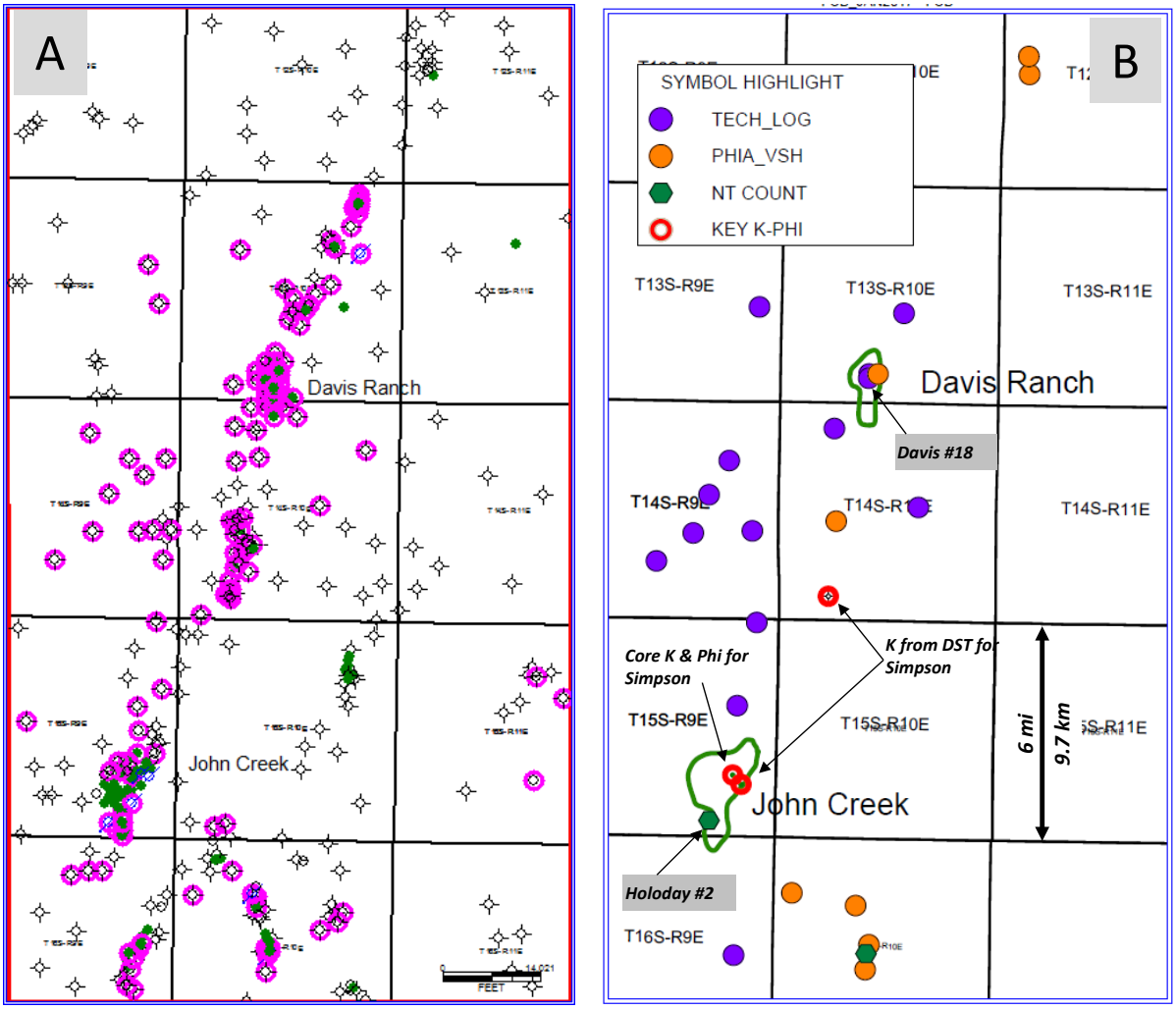

Figure 3. Davis Ranch and John Creek modeled area. A. 518 wells in the model with raster image logs available for 145 wells (circled). B. Solid-fill symbols are wells with digital logs (25) and the open circles are wells with Simpson Sandstone permeability estimated from drill stem tests (2) and core permeability (1).

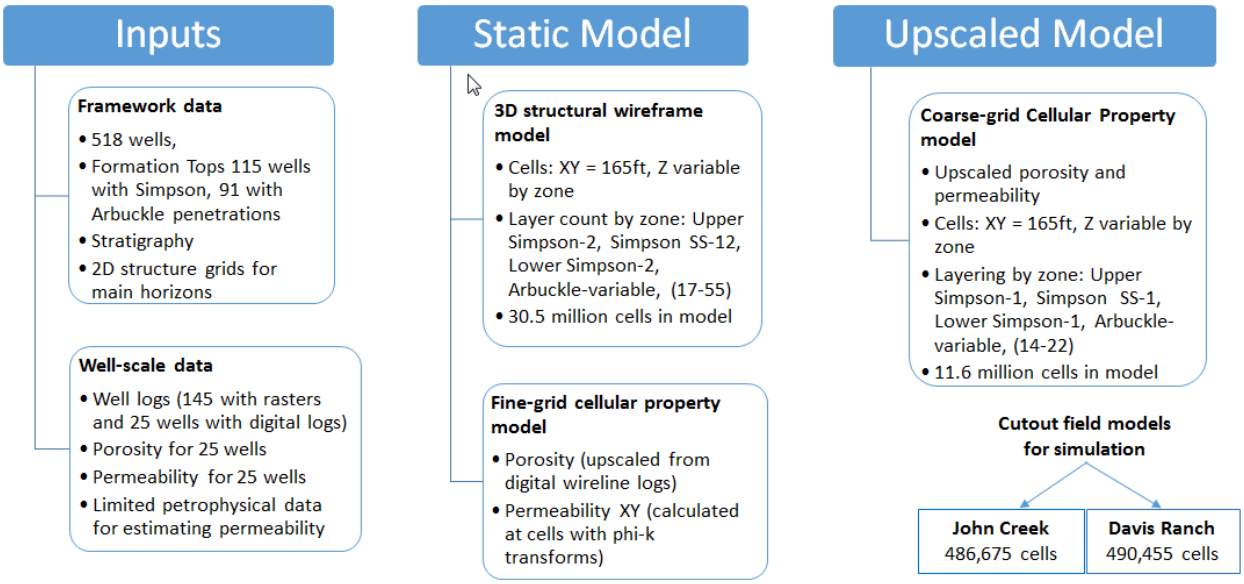

Figure 4. Workflow diagram describing data used and fine and coarse grid model statistics.

Data collection and analysis

The data for the static model was collected from the Kansas Geological Survey and Robert F. Walters Digital Library. Model framework and well-scale data were gathered in the form of well header information (e.g., operator information or well name and number), locations, formation tops, and wireline logs in the form of image files. The data were then analyzed in Petra™ geologic software application.

There are 518 wells in the model area (Figure 3). Of these, 387 wells contain formation top data including manually picked tops from the depth-calibrated wireline log images (rasters) at 145 wells. Because the Viola is the main producing horizon in the study area, the deeper Simpson Sandstone is only locally productive, and the Arbuckle is non-oil bearing, most wells stop in the Viola. Thus, fewer tops are available for mapping the deeper horizons (Table 1). Figures 5a through 5f illustrate the distribution of wells with tops by formation in descending order. Figure 3 identifies the wells with rasters, and Figure 4 identifies the 25 wells with digital logs used to model porosity and permeability.

Formation Top	Count
Any Formation	387
Hunton	130
Viola	358
Decorah	77
Upper Simpson Group	77
Simpson Sandstone	115
Lower Simpson Group	55
Arbuckle	91
Base Arbuckle (or est. Base Arb.)	11

Table 1. Formation tops available in modeled area by stratigraphic zone in descending order.

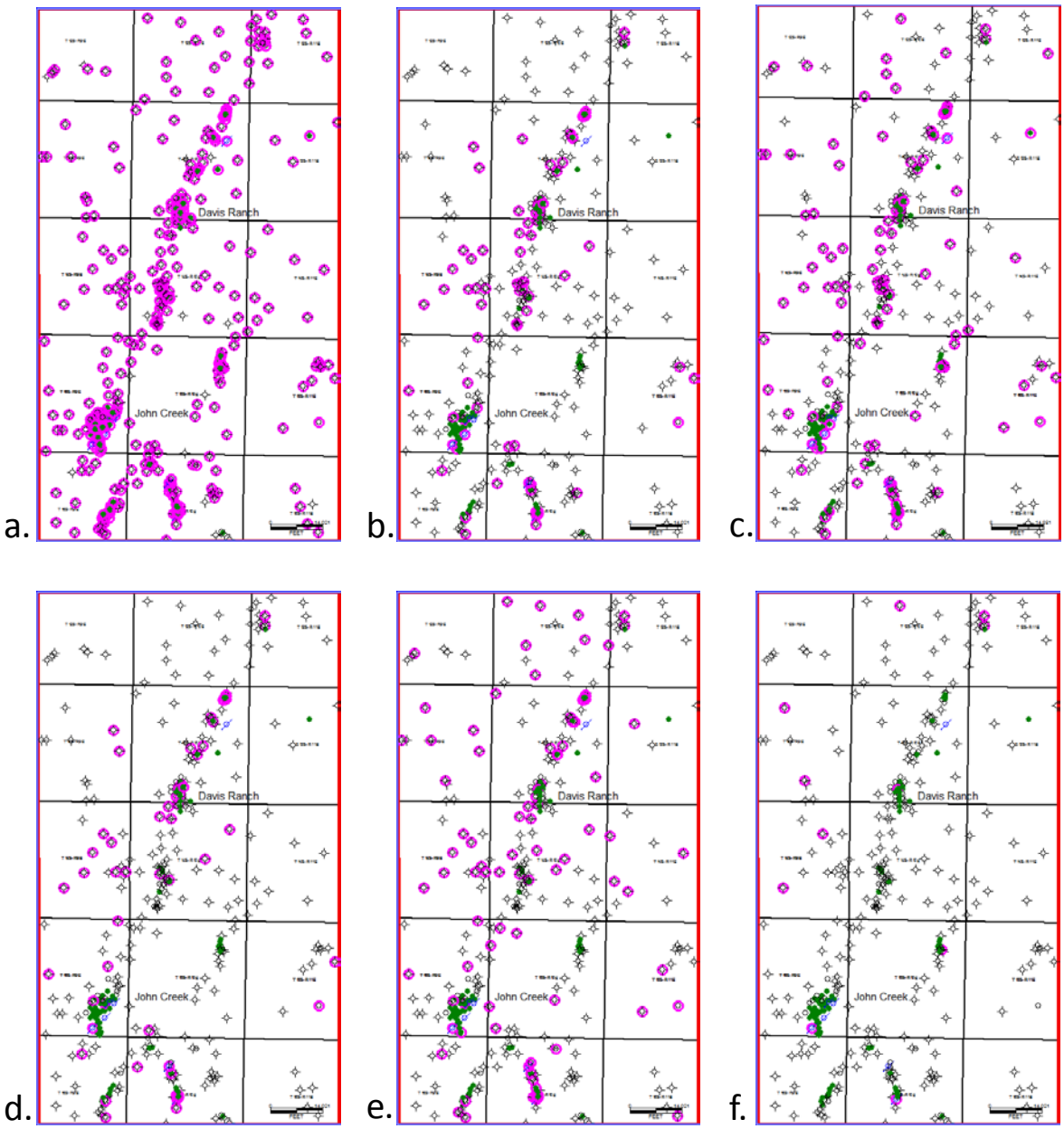

Figure 5. Formation tops available in the modeled area. a. Viola 358, b. Upper Simpson Group 77, c. Simpson Sandstone 115, d. Lower Simpson Group 55, e. Arbuckle 91, f. Base Arbuckle or estimated Base Arbuckle 11.

2-D Structure Mapping

2-D Structure Maps were generated in Petra™ and then exported to Petrel™ for 3-D modelling. A formation structure map (grid) for the Viola Formation (most tops control), was gridded from the tops data and manually input control points using a minimum curvature surface style with no faults. The structural surfaces for the zones below the Viola were generated by using grid-to-grid operations. Isopachs were gridded downward between tops to be mapped. In a sequential manner, the isopach grids were subtracted from the overlying structural grid, beginning with the

Viola (structure - isopach = next lower structural grid), until the structure of all targeted injection zones and seal intervals were gridded. Bounding structural surfaces for the Viola, Upper Simpson, Simpson Sandstone, Lower Simpson, and Arbuckle zones were generated by this process. The project grids, well header information, tops data, and digital porosity logs, were checked for quality and then exported from Petra™ to Petrel™.

3-D High Fine-Grid Cellular Structural Model

A 3-D skeletal grid was created in the model with four zones Upper Simpson, Simpson Sandstone, Lower Simpson, and Arbuckle zones, bounded by 2-D surfaces generated in Petra™. X-Y cell dimensions were set at 165X165 ft. The zones were layered as described below, to form cell z-values along the pillars of this skeletal grid.

Fine Grid Layering

The zones were layered in the model and are summarized in Table 2 and presented in Figure 6. The Simpson zones were layered proportionally and as a result cell height varies depending on zone thickness. The Arbuckle layers were set at 4 ft thicknesses from the base Arbuckle and as a result cell height is generally fixed to 4 ft, with the number of layers in the model varying dependent on the zone thickness. The cell height is "generally" fixed because while the layer/cell height does not vary from 4 ft, the layers crop out against the overlying Simpson Group (Figure 6), and a resulting number of cells have cell heights less than 4 ft thick. The Simpson zones layered proportionally consist of the Upper Simpson Group (2 layers), Simpson Sandstone (12 layers), and the Lower Simpson Group (2 layers). The Arbuckle, layered in 4 ft thick layers from the base Arbuckle, has 17–55 layers (average of 31 layers). The number of layers, number of cells, and cell height by zone for the fine and coarse cellular model are summarized on Table 2.

a) Fine Model

	Layers	Cell Height (ft)	# of cells in model (millions)
Upper Simpson Group	2	8.8-17.01 (avg = 13.66)	0.86
Simpson Sandstone	12	1.44-6.80 (avg = 3.78)	5.2
Lowers Simpson Group	2	3.79-15.83 (avg = 8.46)	0.86
Arbuckle	17-55 (avg = 31.36)	0-4 (avg = 3.93)	23.6
Totals for Model	33 -71	na	30.5

b) Coarse Model

	Layers	Cell Height (ft)	# of cells in model (millions)
Upper Simpson Group	1	17.59-34.02 (avg = 27.32)	0.43
Simpson Sandstone	3	5.77-27.20 (avg = 15.11)	1.3
Lower Simpson Group	1	7.57-31.66 (avg = 16.92)	0.43
Arbuckle	7-22 (avg = 12.8)	0-10 (avg = 9.59)	5.5
Totals for Model	12-27	na	7.6

Table 2. Static model statistics for fine- and coarse-grid models, layering, cell height, and cell count by zone.

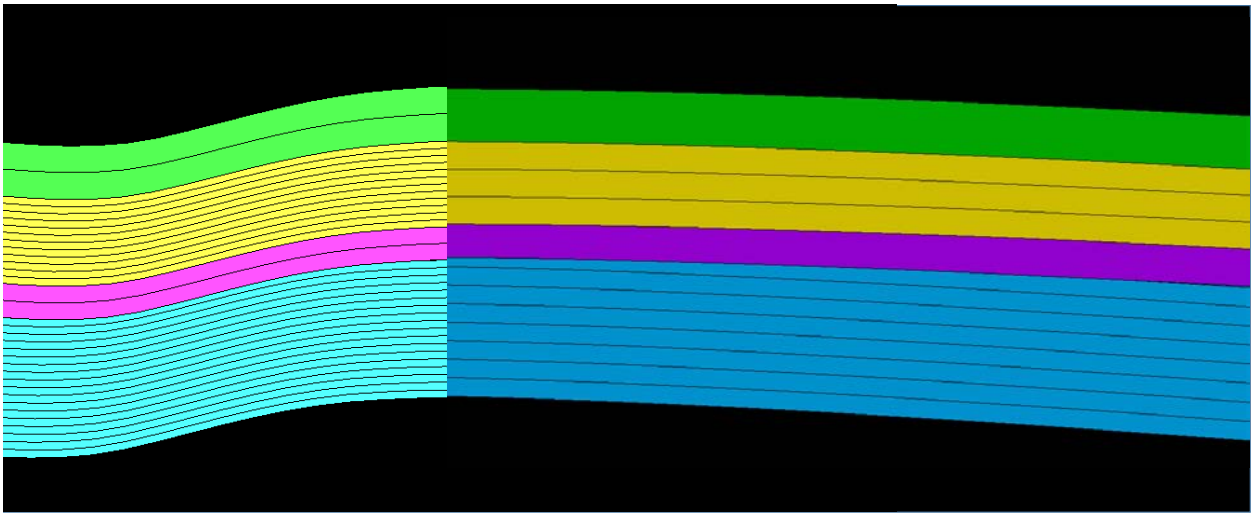

Figure 6. Skeletal grid layering by zone in the fine grid (left) and coarse grid (right).

Petrophysical Properties

In the fine-grid model, porosity from 25 digitized wireline logs was upscaled to layer scale using an arithmetic average. The Schlumberger Gaussian random function simulation© method was used to model zone porosity between wells with wireline logs. The simulation used a default spherical variogram model with a sill of 0.99 and range of 500 ft. Porosity distribution at the well log scale, upscaled to the cells at the well and the full model are very similar as illustrated in Figure 7.

Permeability was then calculated at each cell using porosity-to-permeability transform functions described in the petrophysics section. Permeability for the Simpson formation was calculated using the exponential function where porosity units are in percent:

$$(3.1549)\ e^{(\text{Porosity}*0.2021*100)}.$$

Permeability of the Arbuckle was calculated using the power function where porosity is in decimal fraction:

$$(840.11)\ *(\text{Porosity})^{(1.3289)}.$$

Permeability of the seals (upper and lower Simpson Group) were assigned .000001 mD for simplicity during simulation. Porosity and permeability for both fields are illustrated in Figure 8.

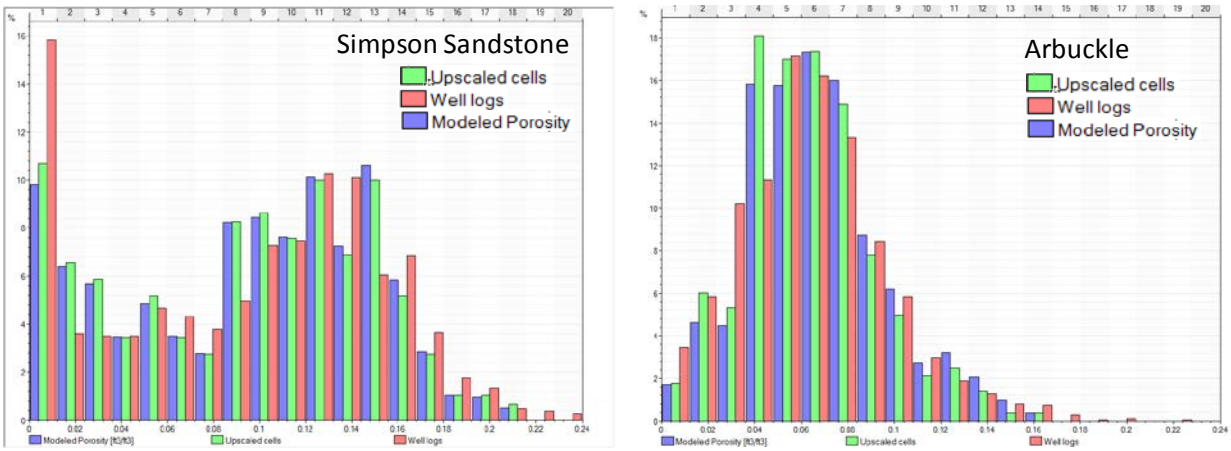

Figure 7. Porosity at three scales for the Simpson Sandstone and Arbuckle zones in the fine-grid model. Y-axis (% of volume) is from 0 to 16% for the Simpson and 0 to 18% for the Arbuckle. X-axis (porosity in decimal fraction) ranges from 0 to 0.24 in both charts.

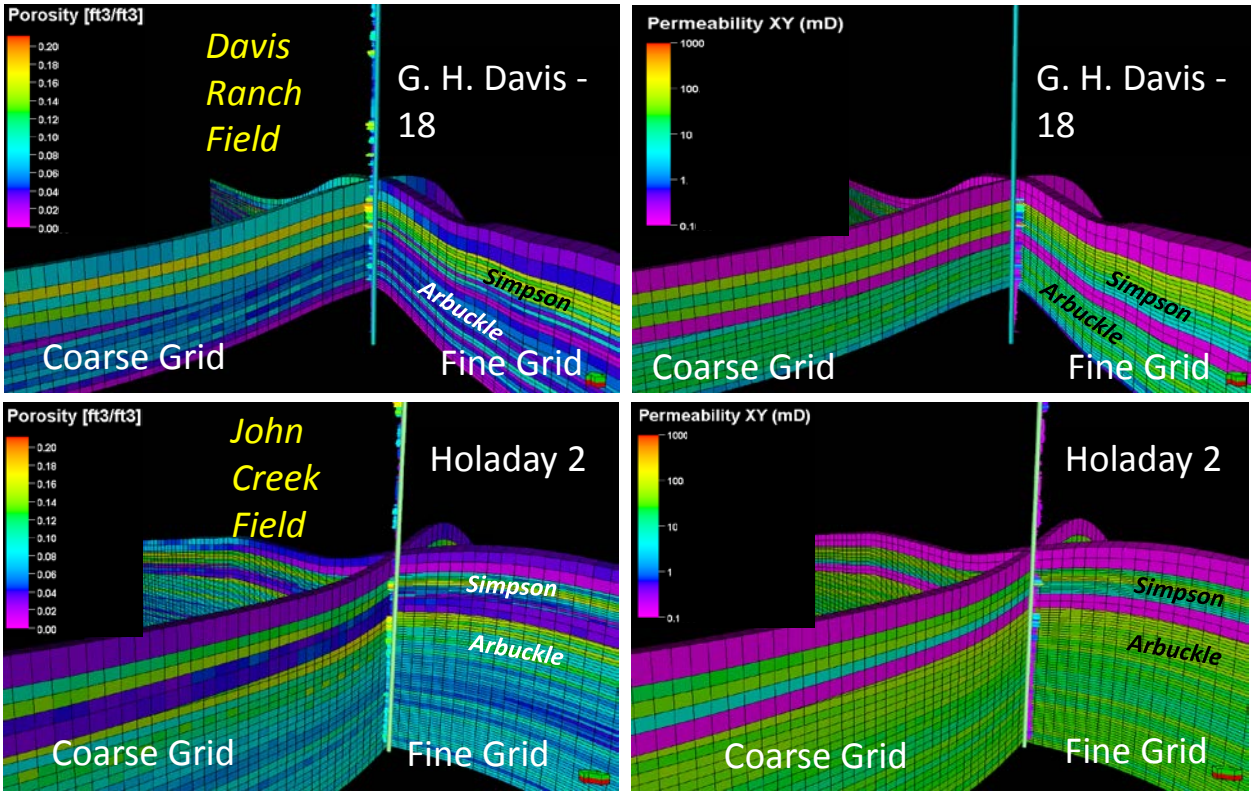

Figure 8. Intersecting cross sections demonstrating porosity and permeability Fence Diagrams of the Fine and Coarse Grid at key wells. VE=10.

Coarse-Grid Cellular Model for Simulation

Coarse Grid Layering

The Simpson zones were layered proportionally and consist of the Upper Simpson Group (1 layers), Simpson Sandstone (3 layers), and the Lower Simpson Group (1 layers). The Arbuckle, layered in 10 ft thick layers from the base Arbuckle, has 7–22 layers (average of 12.8 layers). The number of layers, cell height, and number of cells by zone for the coarse cellular model are summarized in Table 2.

Petrophysical properties upscaled to coarse-grid model

Porosity was upscaled to the coarse-grid model using volume-weighted arithmetic averaging algorithm. Permeability was upscaled using volume-weighted geometric averaging. Histograms of porosity in the Simpson Sandstone and Arbuckle for the coarse and fine grid models are compared in Figure 9.

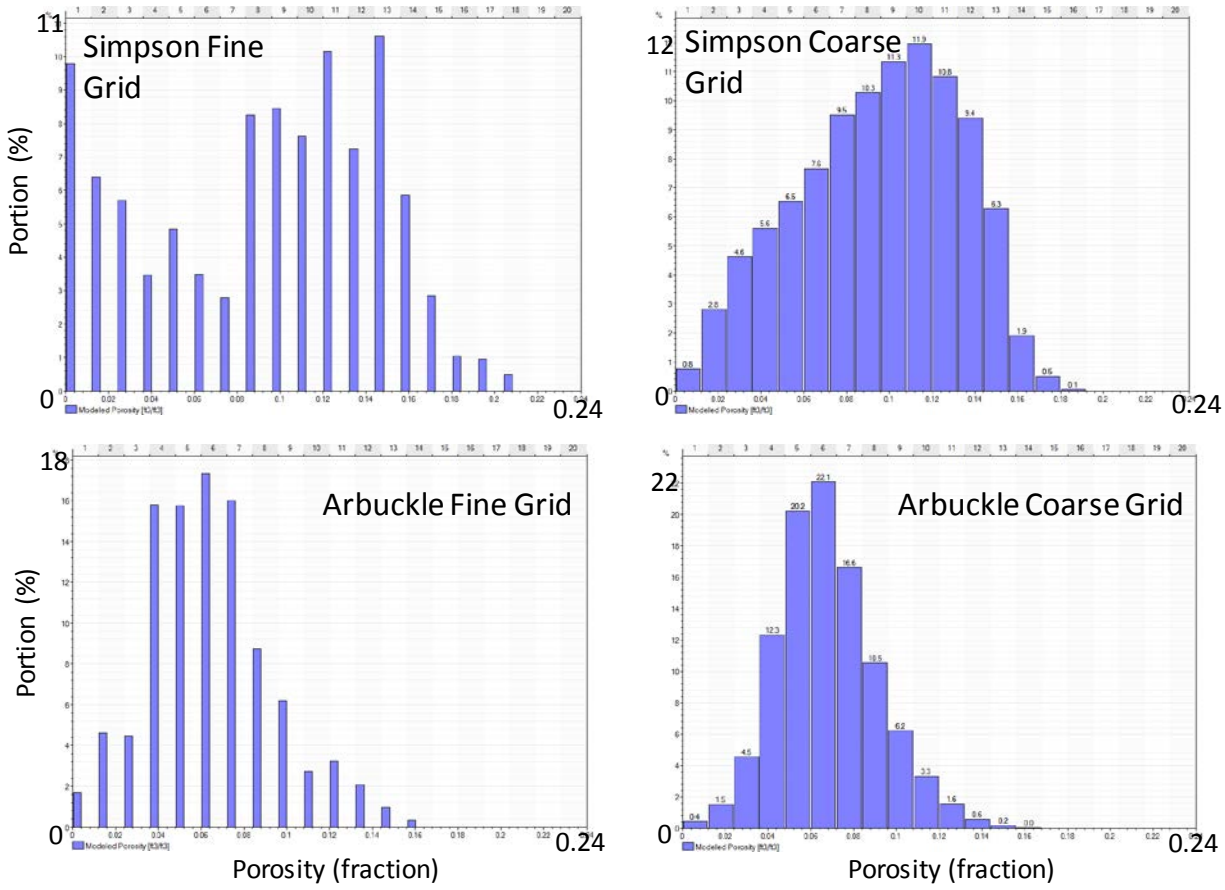

Figure 9. Porosity histograms for the Simpson and Arbuckle zones for the fine and coarse grid models.

Volumetric calculations

This section and Table 3 summarize the results of the volumetric calculations for the Simpson Sandstone and Arbuckle in the John Creek and Davis Ranch fields.

A spill point at sea-level -1,970 ft was identified for the Simpson Sandstone of the Davis Ranch. The corresponding volume of pore space in the resulting closed structure within the Simpson Sandstone was calculated at 466,010,389 cubic feet.

A spill point at sea-level -2,035 ft was identified for the Arbuckle of the Davis Ranch. The corresponding volume of pore space in the resulting closed structure within the Simpson Sandstone was calculated at 213,354,154 cubic feet.

A spill point at sea-level -1,850 ft was identified for the Simpson Sandstone of the John Creek. The corresponding volume of pore space in the resulting closed structure within the Simpson Sandstone was calculated at 432,322,891 cubic feet.

A spill point at sea-level -1,915 ft was identified for the Arbuckle of the John Creek. The corresponding volume of pore space in the resulting closed structure within the Simpson Sandstone was calculated at 583,916,632 cubic feet.

The total combined pore volume calculated in the Simpson Sandstone and Arbuckle of both fields is 1,695,604,066 cubic feet.

	Spill Point (SSTVD)	Bulk volume (billion ft^3)	Pore Volume (billion ft^3)	Pore RB (million)
Davis Ranch				
Simpson Sand	-1970	3.95	.466	83
Arbuckle	-2035	4.55	.213	38
John Creek				
Simpson Sand	-1850	3.85	.432	77
Arbuckle	-1915	6.18	.584	104
Totals				
Simpson Sand		7.8	0.898	160
Arbuckle		10.73	0.797	142
		18.53	**1.695**	**302**

Table 3. Modeled reservoir pore volumes by zone and field, and combined.

Field Extraction and Export

In both the Davis Ranch and John Creek fields, an irregular boundary larger than the modelled spill point was selected, and the two models were cut to make two separate models (Figures 10 and 11).

The two models were then exported under Rescue format.

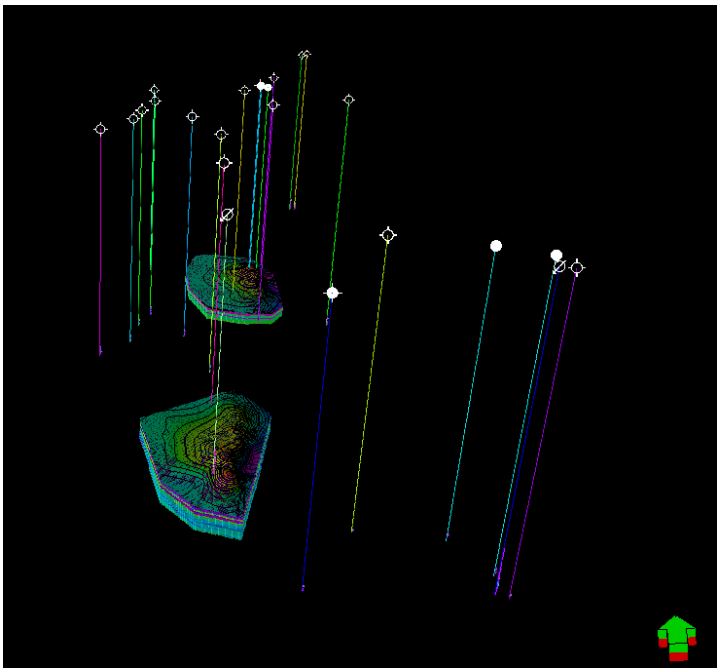

Figure 10. John Creek (lower, south) and Davis Ranch model extraction in relation to the 25 wells with digitized log data. Vertical exaggeration = 10X.

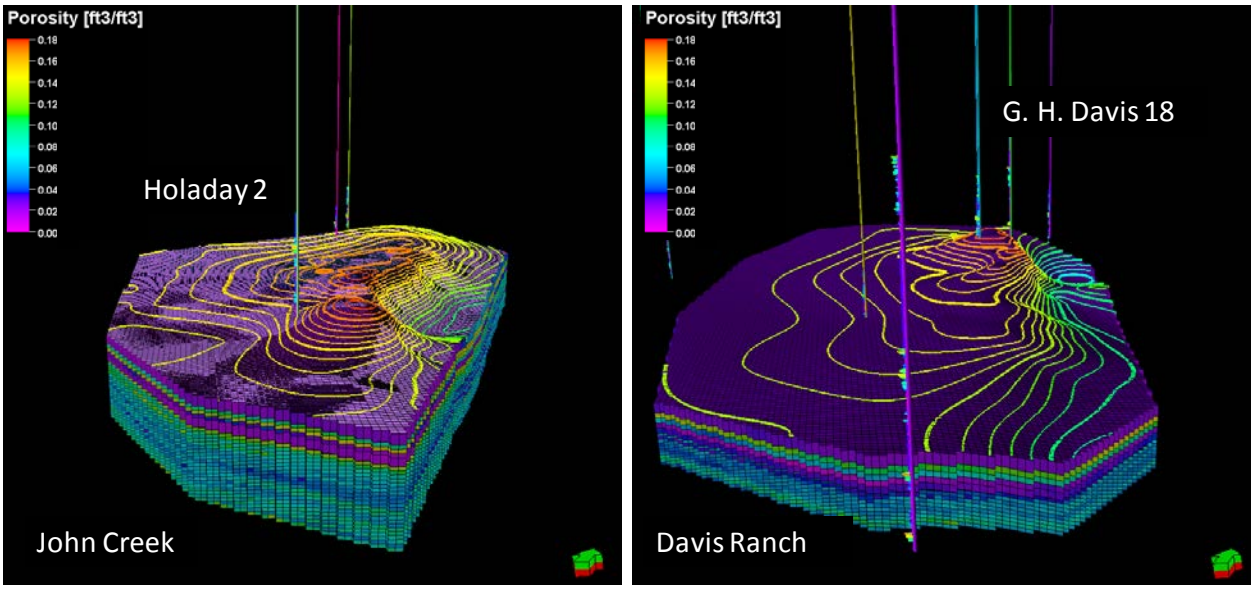

Figure 11. John Creek (lower, south) and Davis Ranch model extraction with key 25 wells. Vertical exaggeration = 10X, contours = 10 ft.

PETROPHYSICS

Porosity from wireline logs

Although petrophysical work in the study area was constrained by very limited data we are confident the main properties, porosity and permeability, are well characterized in the Simpson and Arbuckle. Because most of the drilling took place in the 1950s, there are a limited number of wells with modern logs (neutron and density porosity, GR and resistivity) that penetrated the target injection zones. The distribution of 23 wells fitting that criteria are shown in Figure 3 and denoted in Tech_Log and Phi_Vsh. Total porosity was calculated using Techlog™ multi-mineral module for 15 wells (purple dots) and average neutron-density porosity corrected for shale volume was used for the other eight wells (orange dots). Neutron count logs from two wells were calibrated for porosity in two wells, including a key well, the Holoday #2, the deepest penetration in the Arbuckle (216 ft). Simpson average porosity is about 13% v/v and Arbuckle has a mean porosity of 5% v/v.

Permeability estimation

Two independent empirically based methods for estimating permeability in the Simpson were deployed, with both having similar results (Table 4). For the Arbuckle, two different (from the Simpson) independent, empirically based methods were evaluated with similar results. A third method, described below, yielded lower permeabilities and was not considered. Transform functions for estimating permeability were derived from the data for the Simpson and Arbuckle (Figure 12) and applied to the log-calculated porosity in the 25 key wells at the half-foot scale.

	Average K (mD)	h (ft)	Kh (mD-ft)
Simpson			
Core Analysis (Lucy B Kiefer 4)	105	23	2415
DST Buildup (Vincent 1)	56	25	1400
DST Buildup (Eldridge 4))	182	25	4550
Arbuckle			
Injectivity Index	18	198	3564
Neural Network (Holoday 2)	13	198	2574
Neural Network (Davis 18)	19	60	1140
Neural Network (Warren 1)	27	64	1728

Table 4. Permeability for the Simpson Sandstone and the Arbuckle. Abbreviations: K—permeability, h—height, mD—millidarcies, and DST—drill stem test.

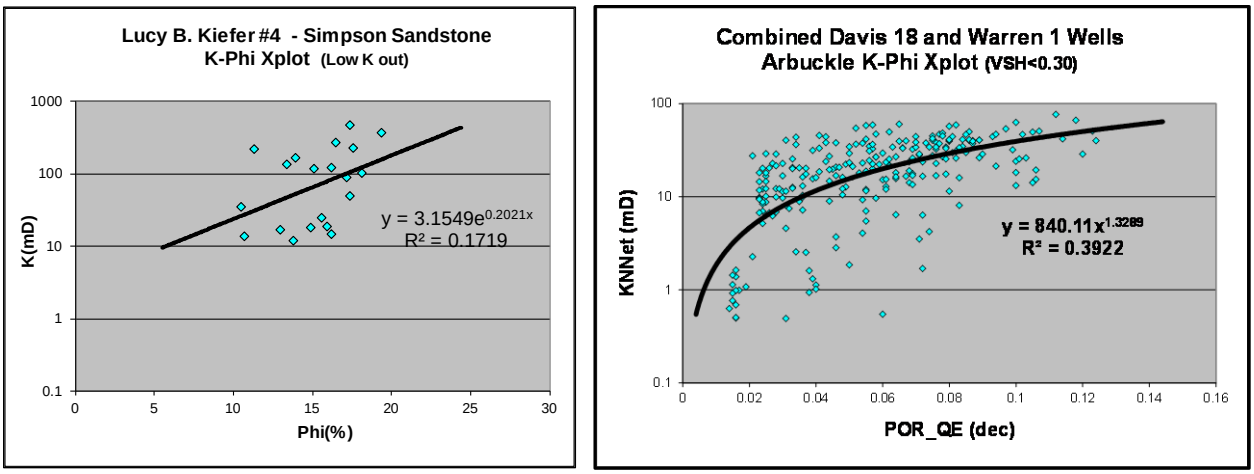

Figure 12. Porosity–permeability transform equations by regression for Simpson Sandstone and Arbuckle. Permeability for the Arbuckle was estimated using a neural network approached described in a later sub-section.

Simpson permeability

Two types of data for permeability in the Simpson were available, conventional core analysis and drill stem tests (DST) (locations in Figure 3). Routine core data were available for the Simpson group in Lucy B. Kiefer #4. Core permeability was plotted against core porosity for the Simpson sand and the exponential function was fit to the data (Figure 12).

DST in three wells were digitized and analyzed in Simpson sand. These wells are: Lucy B Kiefer 4 (well with core data), Vincent 1 and Eldridge 4. Lucy B Kiefer #4 well is next to the Vincent 1 well in the John Creek field, and the Eldridge 4 is six miles to the northeast (Figure 3). Permeability estimates for the three Simpson DSTs are summarized in Table 5.

Well name	K	h	Kh	Pressure
	mD	ft	mD.ft	psia
Lucy B	75	23	1726	1181
Vincent 1	55.6	25	1391	1093
Eldridge 4	134	25	3350	1052

Table 5. DST analysis results for Lucy B Kiefer 4, Vincent 1 and Eldridge 4.

DST in Lucy B Kiefer 4 and Vincent 1 were old (1950s vintage) and generally of poor quality. The more recent DST data for the Eldridge 4 may be more reliable. Raster images of the older, unscaled DST charts were digitized and time and pressure axes were estimated as best possible. The Eldridge 4, a more recent DST was of high quality and results are considered accurate. Average permeability from core in Permeability in Simpson ranges from 55-134 mD from DST results, Table 5. DST analysis plots are in Figures 13, 14 and 15.

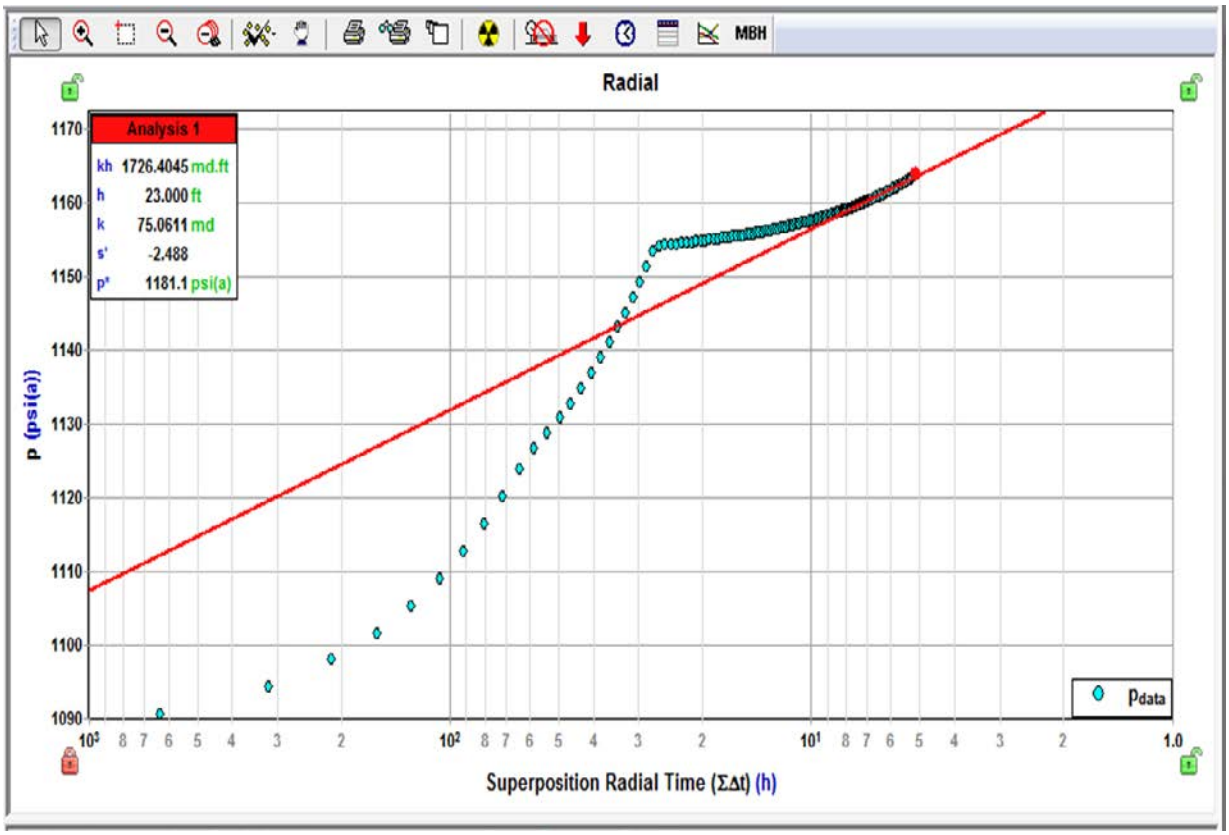

Figure 13. DST analysis in Lucy B Kiefer #4

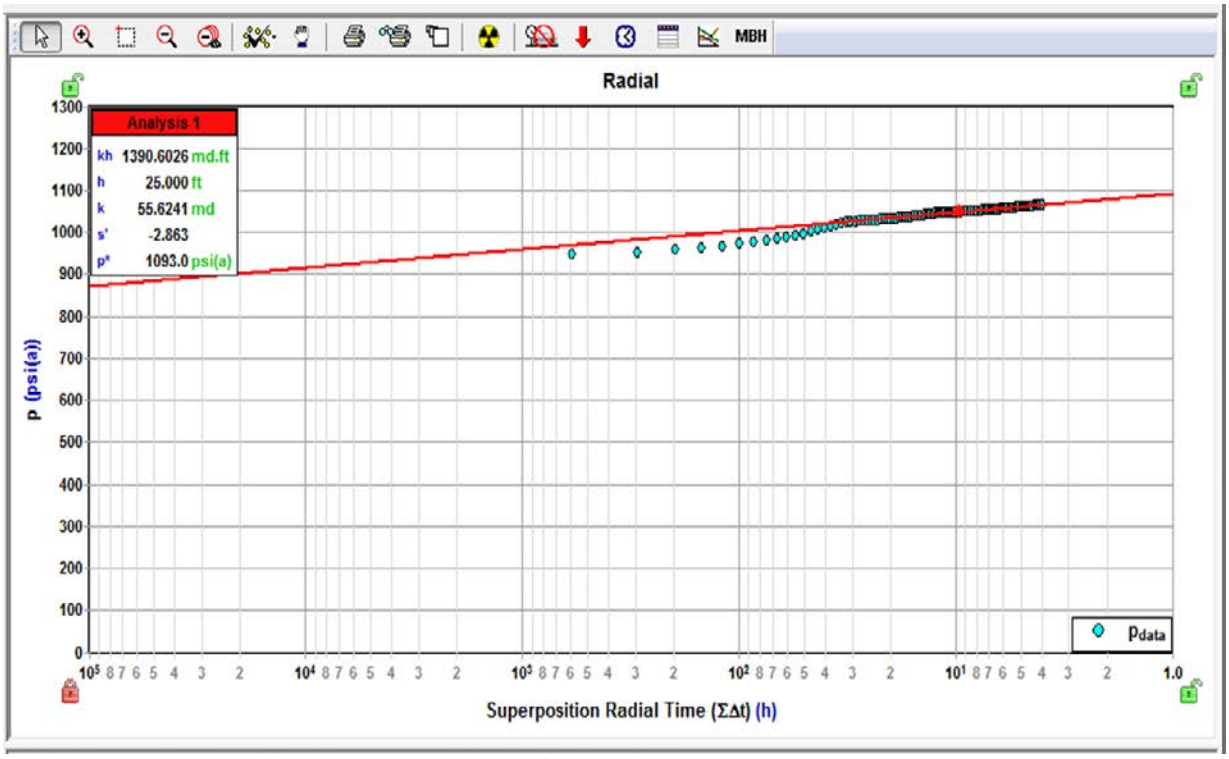

Figure 14. DST analysis in Vincent 1

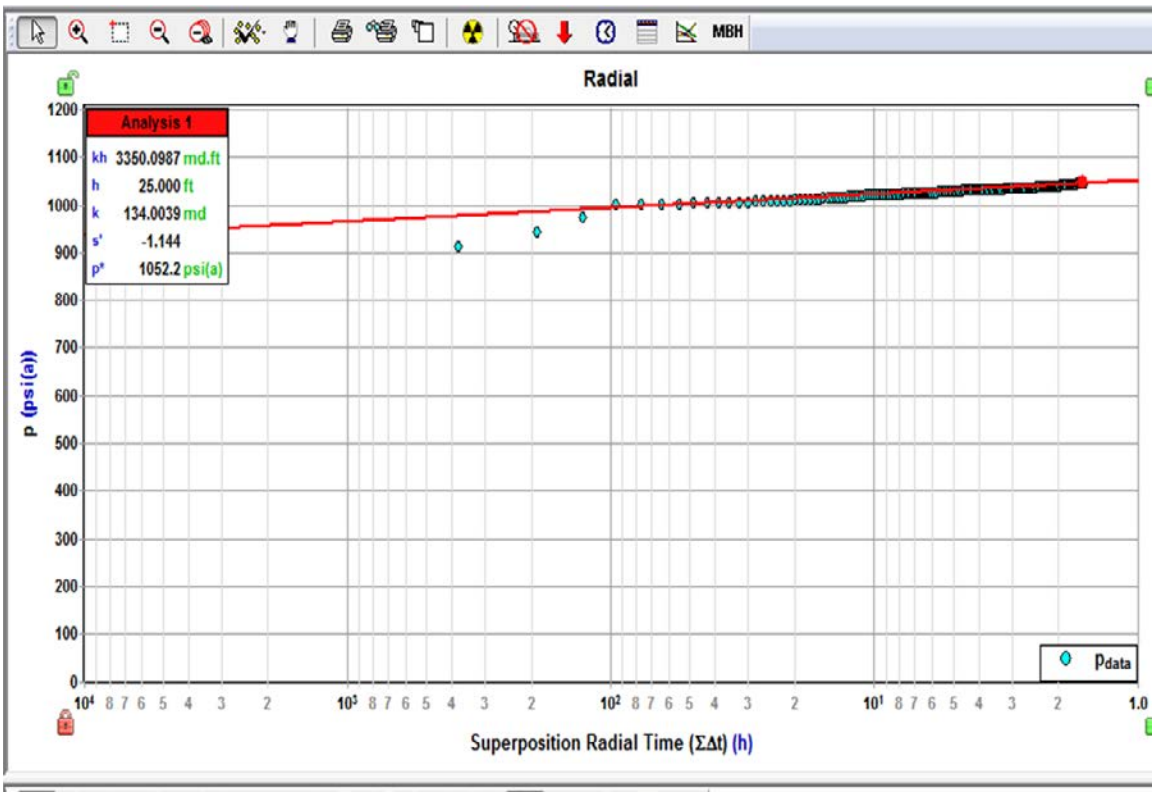

Figure 15. DST analysis in Eldridge 4

Arbuckle permeability

Permeability estimates for the Arbuckle were derived using two different approaches from the methods used for the Simpson, one based on local data (water injection in the Holoday 2 well), and the other using core analysis and NMR data from the Arbuckle in a distant well. There are no Arbuckle core data available in the region.

Arbuckle permeability by injectivity index

Permeability was determined for the Holoday 2, a saltwater disposal well in the Arbuckle where 1,600 barrels of brine are disposed of daily in 198 ft of open hole, on a vacuum. Having the injection rate, estimated bottom hole injection pressure and static pressure, an injectivity index was calculated. The injectivity index was then used in the Darcy equation of radial flow and permeability was calculated for 198 ft open hole in the Arbuckle. Three permeability estimates calculated by varying the skin factor are illustrated in Table 6.

Skin	Permeability, mD
-4	24.34
-5	18.08
-6	11.82

Table 6. Calculated average permeability for 198 ft of open hole in Holoday 2 by injectivity index.

Arbuckle permeability by correlations with distant core and NMR data

The second method for estimating permeability was using a neural network function trained on Arbuckle NMR-derived permeability data for the Berexco LLC #1-32 KGS Wellington well, a science well in the small-scale field demonstration project (DE-FE0006821) located approximately 120 miles southwest of this study area. Data from Wellington field were used for training and validation (blind test) where core data and NMR permeability were available. Well 1-32 was used for training and 1-28 was the validation well. The model and training dataset was limited to the Arbuckle. After a satisfactory result, the model was applied to Holoday 2 and the calculated average permeability for the 198 ft open interval is about 12.6 mD, Figure 16. This is a bit lower than the 18 mD average based on injectivity for the interval.

The Neural Network approach defined above was used on two other wells with modern log suites, the Davis 18 and Warren 1. Average permeability calculated in this manner for the Arbuckle interval in these two wells is 18 and 26 Md respectively. Well plots from TechLog are provided in Figures 17 and 18.

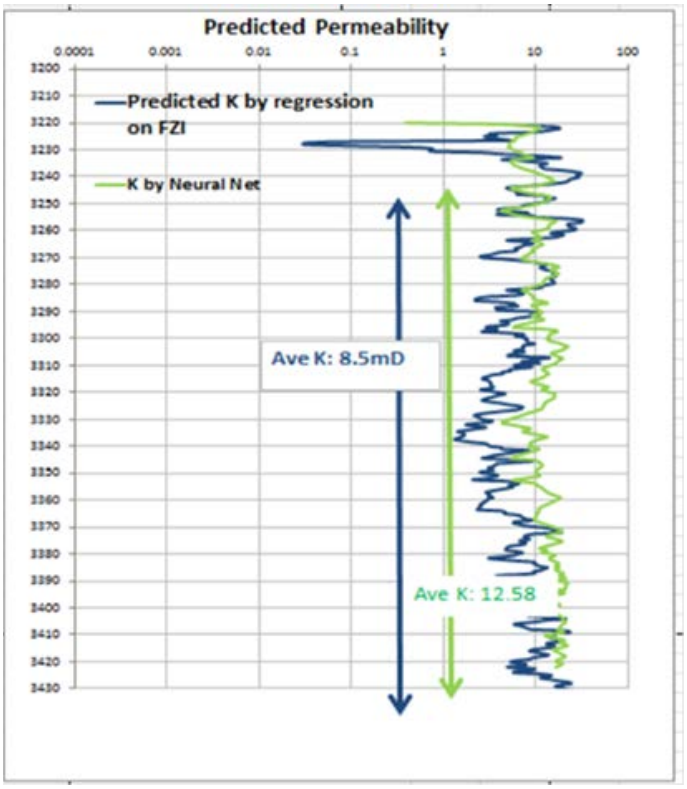

Figure 16. Permeability in Holoday 2 by Neural Network and regression

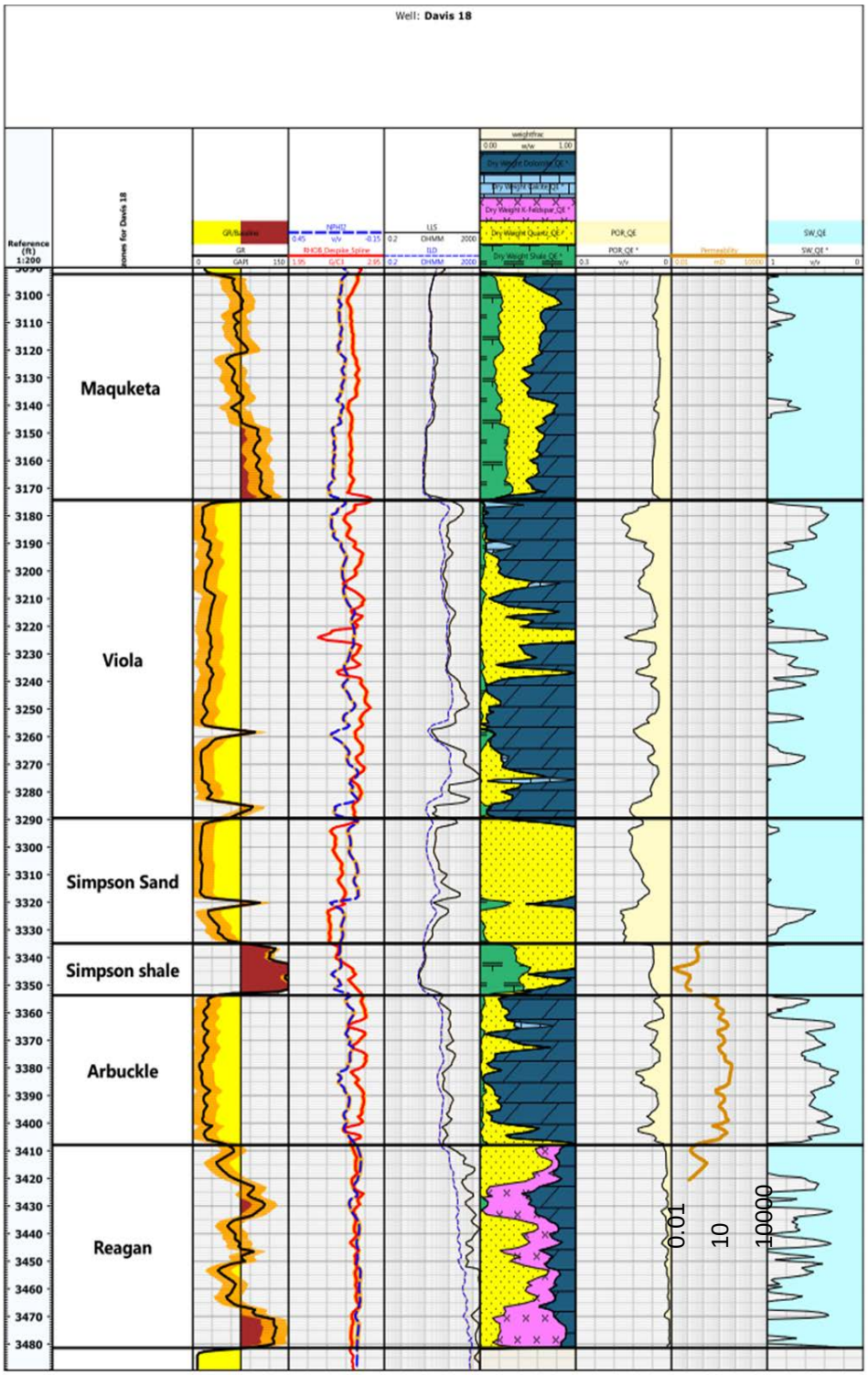

Figure 17. Log analysis and permeability by Neural Network in Davis 18. Permeability is in the second track from the right. Log scale ranges from 0.01 to 10,000 mD.

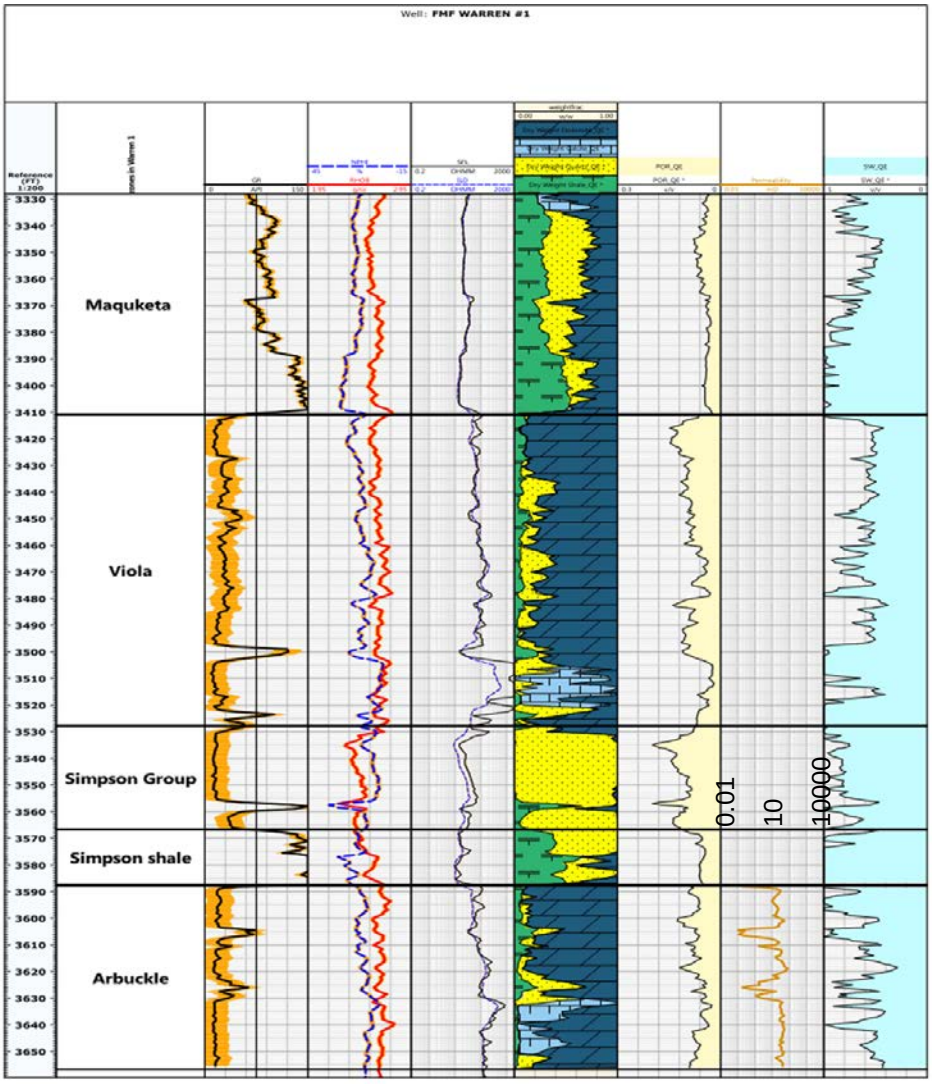

Figure 18. Log analysis and permeability by Neural Network in Warren 1. Permeability is in the second track from the right. Log scale ranges from 0.01 to 10,000 mD.

Arbuckle permeability by Flow Zone Indicator

In a third approach, permeability was calculated by regression using well 1-32 to predict the dependent variable Flow Zone Indicator (FZI) and therefore permeability from FZI. Given the independent variables of GR, porosity and conductivity, relationship between the dependent variable FZI and independent variables were estimated and the equation was used to predict FZI in Well Holoday 2. Permeability was calculated based on FZI and average estimated permeability is 8.5 mD, Figure 16. This is about the 18 mD average based on injectivity for the interval, and this approach was not considered further.

Estimating Arbuckle permeability in the study area wells

Despite the distance between the Wellington core and NMR data and the study area, the Arbuckle permeability estimates using the Neural Network approach were like that derived by the local injection data. Rather than applying the Neural Network methodology to the entire 25 well data set, a shortcut was taken. A porosity-permeability transform was developed by cross-plotting the porosity with the Neural Network predicted permeability for the Davis 18 and Warren 1 wells (Figure 12). Average permeability calculated using this transform is 14 mD for the Holoday 2 well, slightly higher than predicted by the neural network directly (13 mD), Davis. Permeability in the Arbuckle for the 22 other wells was estimated using the transform function.

DYNAMIC MODELING OF CO_2 INJECTION AT DAVIS RANCH AND JOHN CREEK SITES

The key objectives of the dynamic modeling were to determine the volume of CO_2 stored, resulting rise in pore pressure and the extent of CO_2 plume migration in the two fields in the Forest City Basin storage complex. An extensive set of computer simulations were conducted to estimate the potential impacts of CO_2 injection in the Arbuckle injection zone.

The reservoir simulations were conducted using the Computer Modeling Group (CMG) GEM simulator. GEM is a full equation of state compositional reservoir simulator with advanced features for modeling the flow of three-phase, multi-component fluids and has been used to conduct numerous CO_2 studies (Chang et al., 2009; Bui et al., 2010). It is considered by DOE to be an industry standard for oil/gas and CO_2 geologic storage applications. GEM is an essential engineering tool for modeling complex reservoirs with complicated phase behavior interactions that have the potential to impact CO_2 injection and transport. The code can account for the thermodynamic interactions between three phases: liquid, gas, and solid (for salt precipitates). Mutual solubilities and physical properties can be dynamic variables depending on the phase composition/system state and are subject to well-established constitutive relationships that are a function of the system state (pressures, saturation, concentrations, temperatures, etc.). The following assumptions govern the phase interactions:

- Gas solubility obeys Henry's Law (Li and Nghiem, June 1986)
- The fluid phase is calculated using Schmit-Wenzel or Peng-Robinson (SW-PR) equations of state (Soreide-Whitson, 1992)
- Changes in aqueous phase density with CO_2 solubility, mineral precipitations, etc., are accounted for with the standard or Rowe and Chou correlations.
- Aqueous phase viscosity is calculated based on Kestin, Khalifa, and Correia (1981).

Initial reservoir conditions and simulation constraints

The initial conditions specified in the reservoir model are specified in Table 7. The simulations were conducted assuming isothermal conditions. Although isothermal conditions were assumed, a thermal gradient of 0.008 °C/ft was considered for specifying petrophysical properties that vary with layer depth and temperature such as CO_2 relative permeability, CO_2 dissolution in formation water, etc. The original static pressure in the injection zone was set to reported field test pressures and the Arbuckle pressure gradient of 0.48 psi/ft was assumed for specifying petrophysical properties. Perforation zone was set at all permeable layers in Simpson and Arbuckle reservoirs. Injection rate was assigned according to maximum calculated based on well tests and reservoir properties.

	John Creek	Davis Ranch
Temperature	41 °C (106 °F)	38 °C (100 °F)
Temperature Gradient	0.008 °C/ft	0.008 °C/ft
Pressure	1,160 psi (7.99 MPa)	1,200 psi (8.27 MPa)
TDS	30 g/l	24 g/l
Perforation Zone	Simpson, Arbuckle	Simpson, Arbuckle
Injection Period	25 years	25 years
Injection Rate	2,100–3,000 MT/day	350–940 MT/day
Total CO_2 injected	21,000,000 MT	3,600,000 MT

Table 7. Model input specification and CO_2 injection rates

Physical processes modeled in the reservoir simulations included isothermal multi-phase flow and transport of brine and CO_2. Isothermal conditions were modeled because the total variation in subsurface temperature in the Arbuckle and Simpson intervals from the top to the base is only slightly more than 3°F (which should not significantly affect the various storage modes away from the injection well), and because it is assumed that the temperature of the injected CO_2 will equilibrate to formation temperatures close to the well. Uniform salinity concentration was assumed. Subsurface storage of CO_2 occurs via the following four main mechanisms: structural trapping, aqueous dissolution, and hydraulic trapping.

Models were optimized for maximum CO_2 storage capacity potential. Three wells completed at Simpson and Arbuckle intervals were introduced in high structural points for both modeled sites. No-flow boundary conditions were specified along the top of the Simpson Formation based on brine chemistry data and other evidence. The lateral boundary conditions were set as an infinite-acting Carter-Tracy aquifer (Dake, 1978; Carter and Tracy, 1960) with leakage. This is appropriate since the Simpson and Arbuckle are open hydrologic systems extending over the Forest City Basin.

The bottom hole injection pressure in the Arbuckle should not exceed 90% of the estimated fracture gradient of 0.75 psi/ft (measured from land surface) based on EPA and KDHE guidelines for UIC Class I & VI wells. Therefore, the maximum induced delta pressure at the top of Simpson and bottom of the Arbuckle Group should be less than 750 psi.

Relative permeability and capillary pressure curves (Figures 19 and 20) were calculated based on a recently patented formula (SMH reference No: 1002061-0002) that relates the end-points. This method and method validation is outlined in more details in Fazelalavi, 2017.

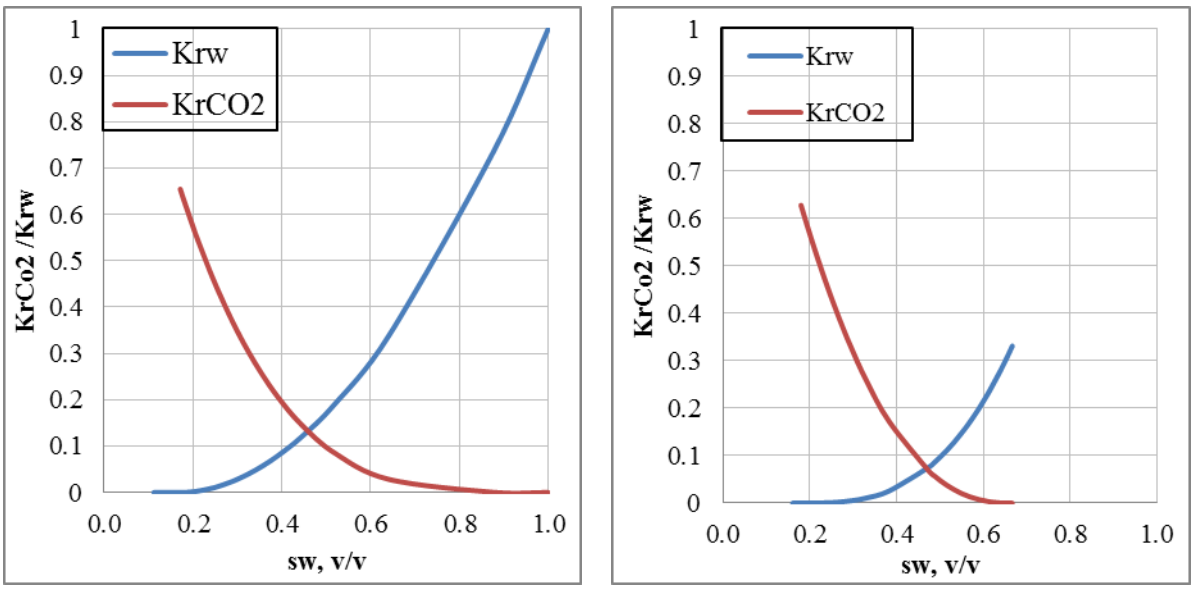

Figure 19. Calculated relative permeability for drainage (left) and imbibition (right).

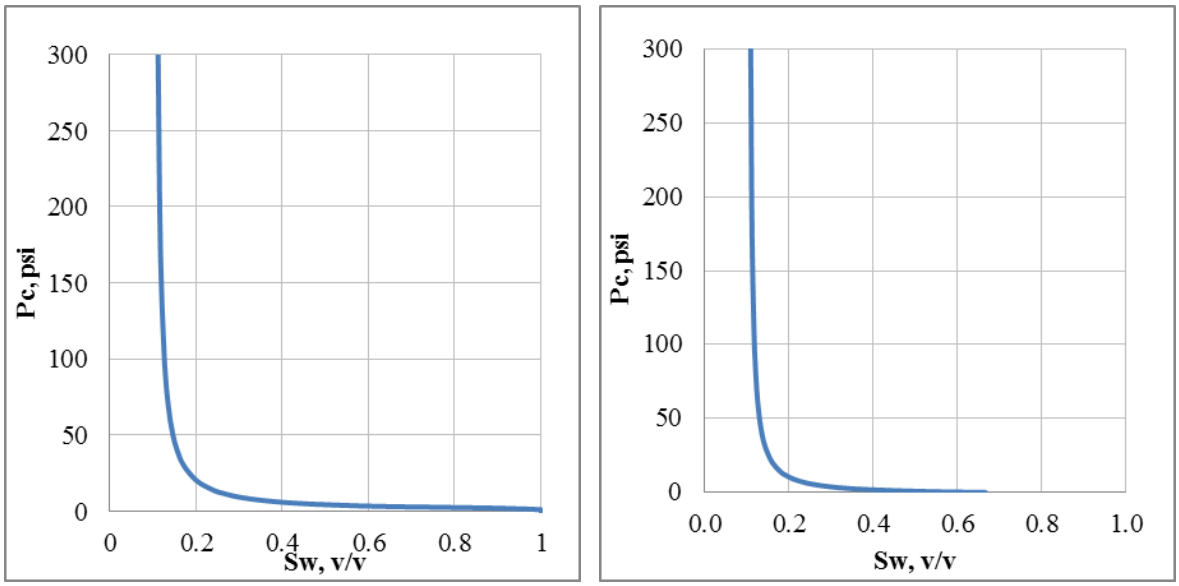

Figure 20. Capillary pressure curves for drainage (left) and imbibition (right).

Simulation results

Figure 21 shows the maximum lateral migration of the CO_2 plume approximately 25 and 15 years after cessation of CO_2 injection activities at John Creek and Davis Ranch sites respectively. The plume grows rapidly during the injection phase and is largely stabilized by the end of injection period. CO_2 travels throughout the reservoir for additional several years and enters stabilization phase after several years post injection commencement.

Figure 22 presents the distribution of reservoir pore-pressure at the maximum point of CO_2 injection. The pressure increases are estimated to be below 750 psi on commencement of injection and then pressure

gradually drops after the commencement of the injection as the capillary effects are overcome. The pressure decreases to almost pre-injection levels after approximately 50 years.

Figure 23 and 24 illustrate modeled maximum injection rates and cumulative injection volumes obtained via injection by three injection wells completed at Simpson and Arbuckle intervals. Maximum combined for three wells injection rate modeled for Davis Ranch Field was 940 metric tonnes/day. Maximum combined for three wells injection rate modeled for John Creek was significantly higher at 3,000 metric tonnes/day. Overall, John Creek Field proved to be better suited for accommodating a commercial CO_2 storage project. Although cumulative CO_2 injection was projected at 21MMT, it is possible to improve this projection via altering injection strategies and by expanding modeled areal extent.

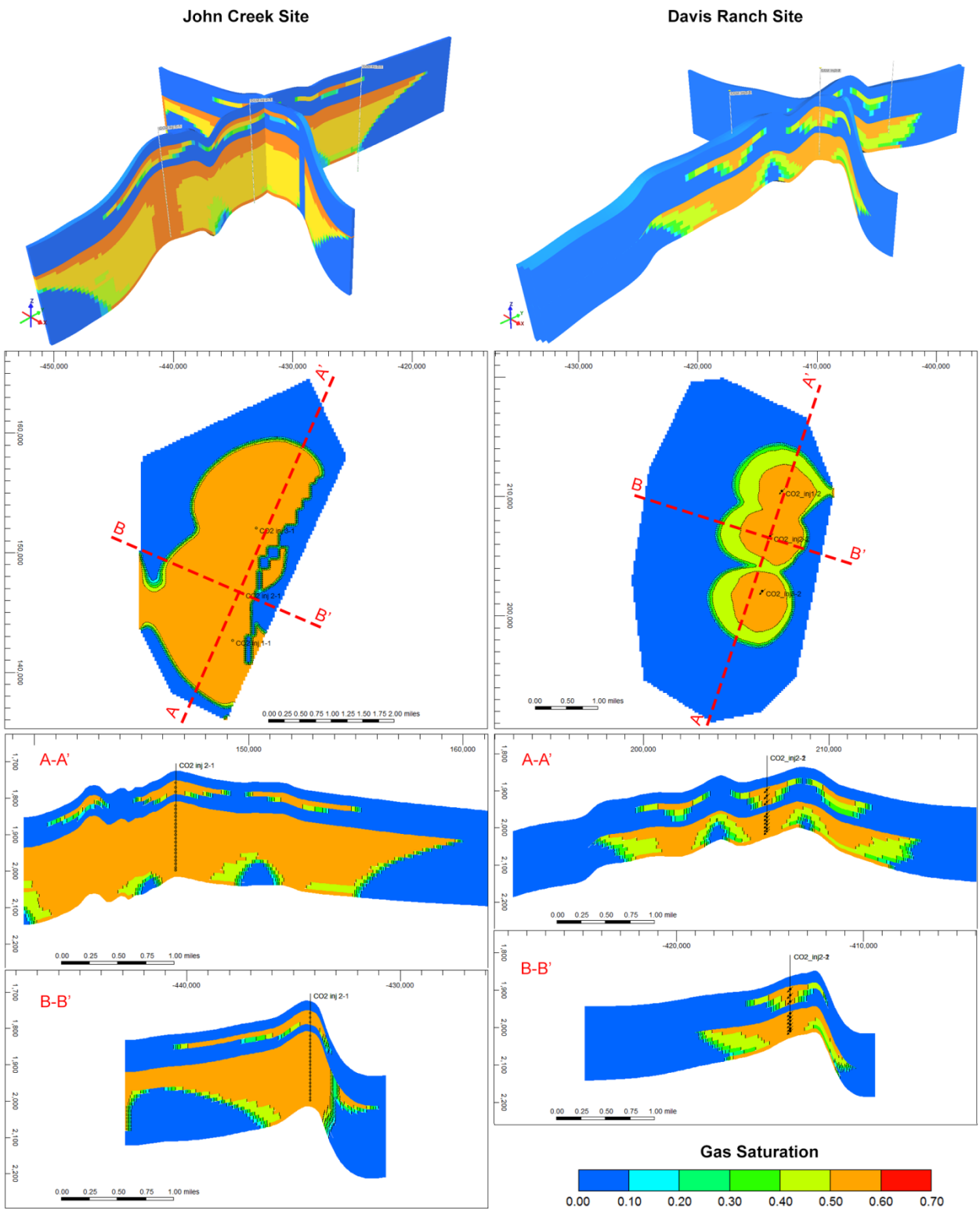

Figure 21. Maximum CO_2 plume distribution at John Creek (left) and Davis Ranch (right) sites

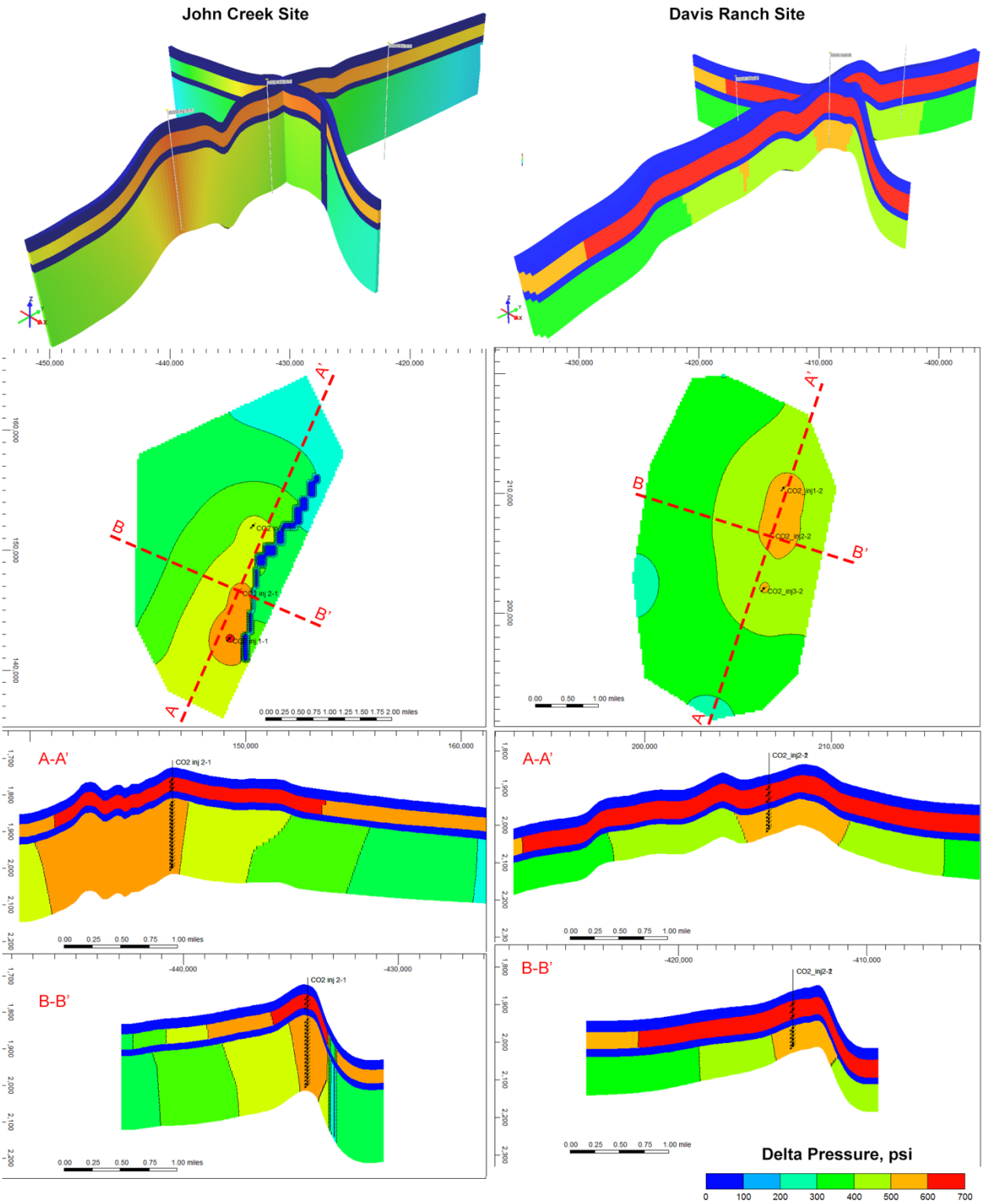

Figure 22. Maximum reservoir pressure increases because of CO_2 injection at John Creek (left) and Davis Ranch (right) sites

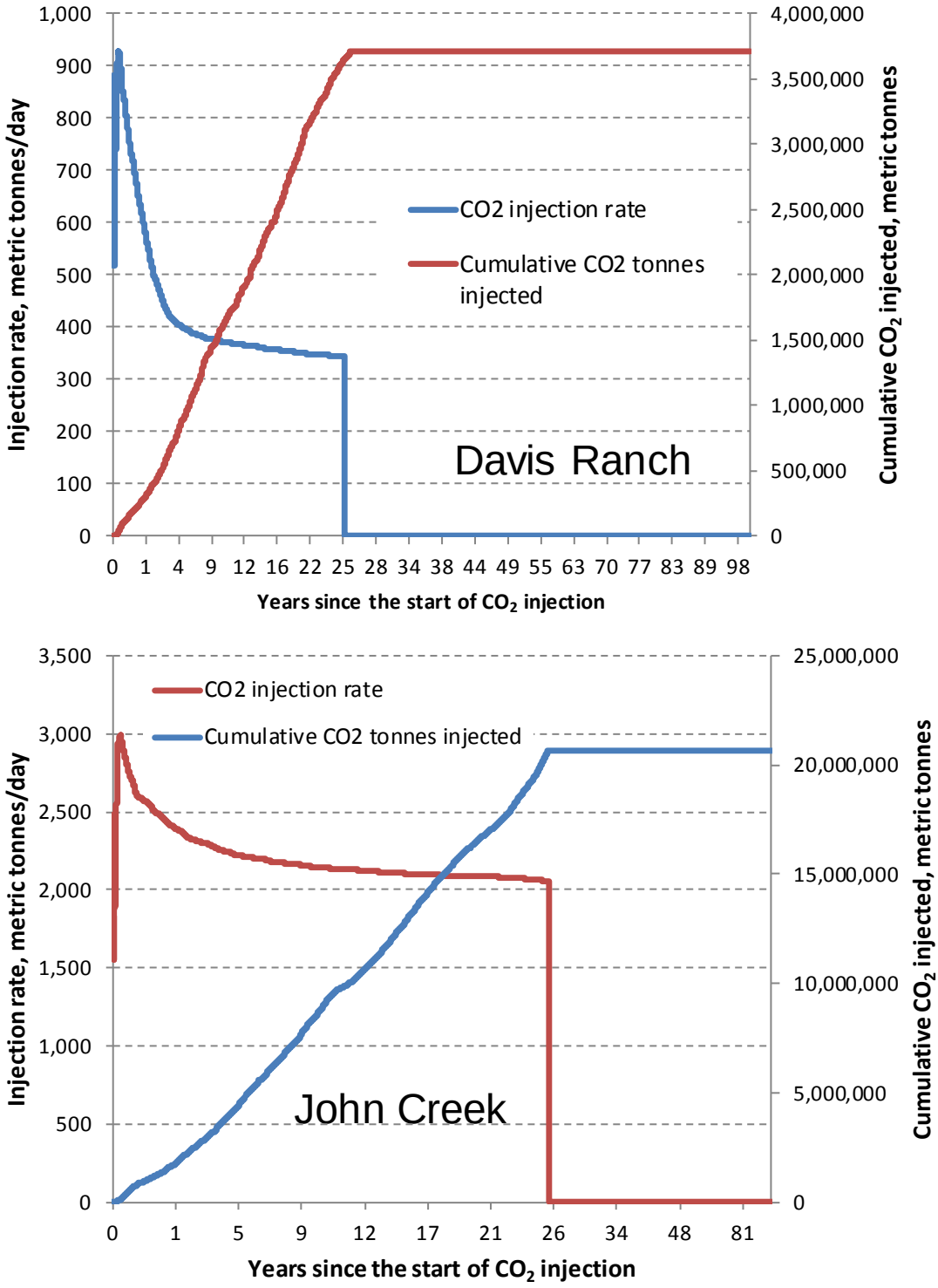

Figure 23. Cumulative CO_2 injected and CO_2 injection rate for Davis Ranch and John Creek sites. In both cases, the plots account for three wells completed at two intervals: Simpson and Arbuckle.

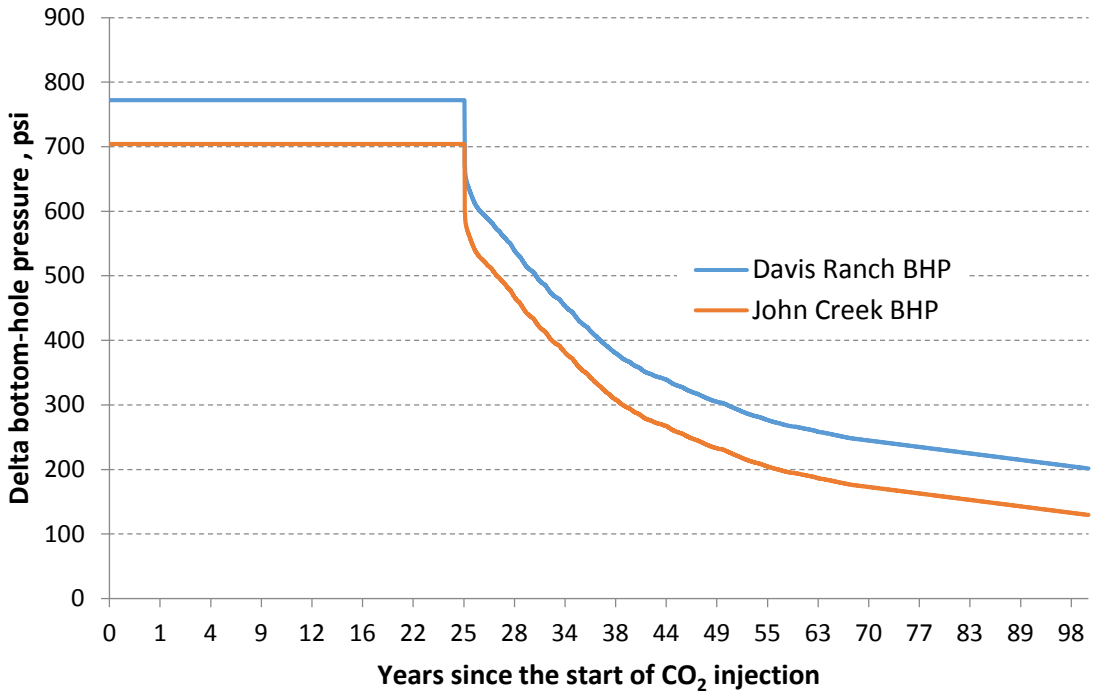

Figure 24. Bottom-hole pressure profiles for CO_2 injection

GEOCHEMISTRY

Geochemical analysis was deployed to verify the potential for seals above the target injections zones in the study area. The Forest City Basin is an oil producing region with traps contained by structures and vertical seals. Oil production in the two study fields is from the Kansas City Group, well above the Simpson, and the Viola, in close proximity above the Simpson (Figure 2). Although the Simpson Sandstone does not produce in either field, it does carry oil shows in the samples and is productive in nearby fields, indicating a vertical seal. The Arbuckle does not produce oil in the Forest City Basin.

Comparison of salinities in the reservoirs at John Creek and Davis Ranch Fields (Figure 25) has utility for inferring the potential for cross-stratigraphic flow, or *leakage*, between reservoirs. Gradually increasing salinity with depth regardless of apparently separate reservoir may indicate communication between reservoirs. Conversely, contrasts in the salinity of the waters in the principal reservoirs of the Davis Ranch Field and the nearby John Creek Field may indicate that the reservoirs are isolated from each other. Such salinity contrasts thus may assure that each reservoir will not leak when they are separately charged with CO_2. Salinity data were therefore examined for the Hunton, Viola, Simpson, and Arbuckle reservoirs.

Data availability and methodology

There are four basic sources of information on salinity: the Kansas Geological Survey on-line brine database, chemical analyses of produced water donated by oilfield operators, salinity analyses reported for water recovered in drill-stem tests, and salinity determined from geophysical well logs.

Very few analyses of produced water are available from the KGS on-line brine database. Similarly, drill-stem tests (DSTs) recovering sufficient amounts of water are not numerous near the Davis Ranch and

John Creek fields. Most chemical analyses donated by oil-field operators are limited to the producing intervals from each oil field (i.e., Hunton and Viola at Davis Ranch; Viola at John Creek). The well-log resistivity method thus had to be employed to generate most of the salinity data.

The well-log resistivity method uses a rearrangement of the Archie Equation to determine the resistivity of formation water (Rw). Rw is then converted to a salinity measurement (Doveton, 2004). Input into the formula includes porosity and resistivity measurements, usually averaged over a 2 ft vertical interval. The porosity used is an average of the neutron and density porosity measurements. The resistivity measurement is that of the deep induction log, to measure resistivity away from the vicinity of the well bore, which is subject to the effects of drilling mud and mud filtrate. Reservoir intervals with >50 API gamma ray units were not used in the analysis (so the effects of shaliness could be avoided), nor were tight zones measured where porosity is <8%. Oil-bearing zones were ignored, so that any resistivity measured in any given reservoir would be due principally to that of the formation water.

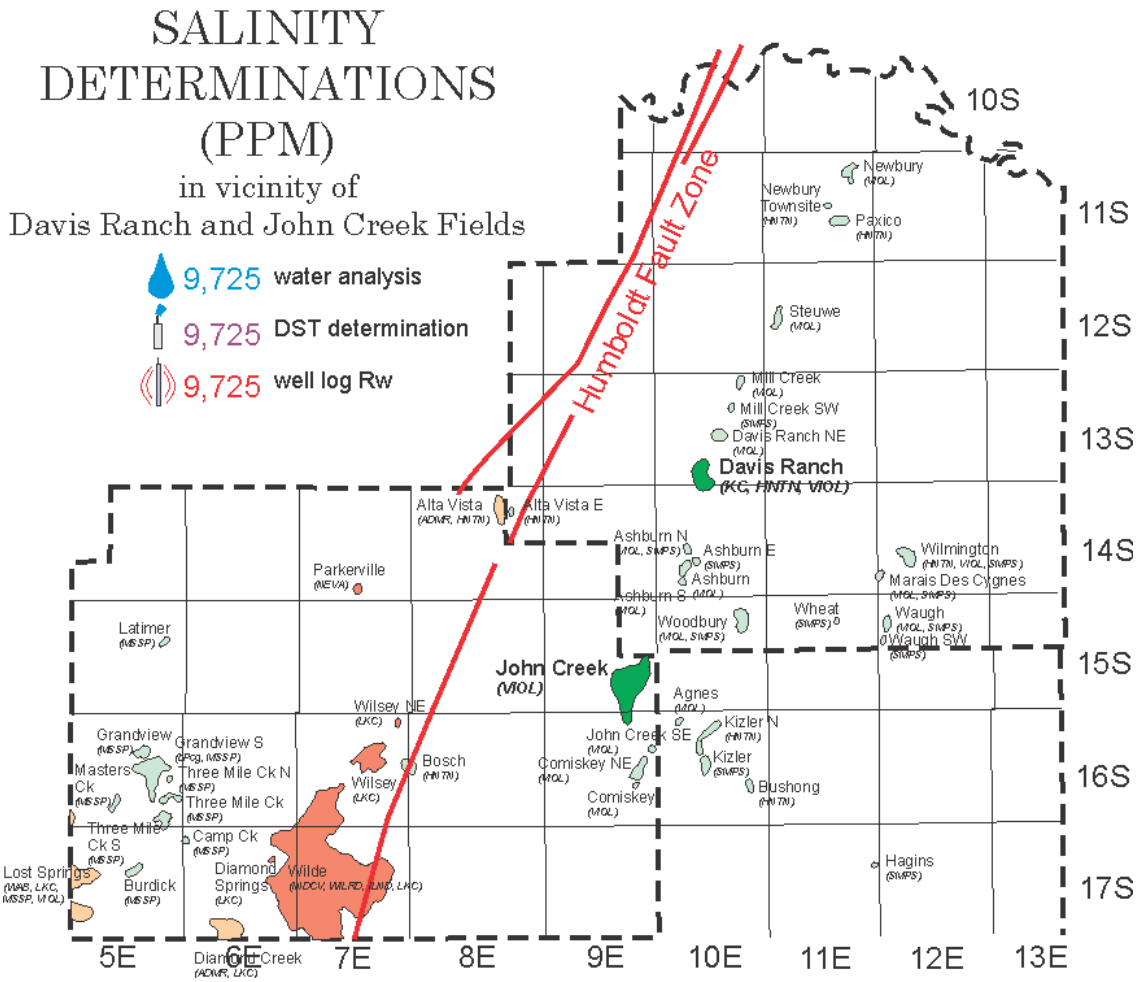

Figure 25. Map of a portion of the Forest City Basin, bounded by the Humboldt Fault Zone in northeast Kansas. The two study fields are color-filled green.

Analysis

Approximately two dozen wells were analyzed using the well-log resistivity method in the Davis Ranch-John Creek study area. Salinity was determined in the Hunton (Figure 26), Viola (Figure 27), Simpson

(Figure 29) and Arbuckle (Figure 29). If allowed by well-log coverage, as many as four reservoirs were examined in a well—Hunton, Viola, Simpson, and Arbuckle. In general, the Hunton—the shallowest of all the reservoirs examined—had the least saline water. Sandstone in the Simpson had the most saline water. Regionally, water in all four reservoirs increased in salinity eastward into the Forest City Basin. Diagrams of salinity vs. subsea depth at both Davis Ranch (Figure 30) and John Creek (Figure 31 show increased salinity downward, from Hunton, to Viola, and then in the Simpson. From Simpson to Arbuckle, however, this trend of increasing salinity reverses, and the Arbuckle is generally less saline than the overlying Simpson. This trend of increasing salinity with depth and age of reservoir, and then lesser salinity into the Arbuckle causes a dog-leg pattern in diagrams of depth vs. salinity for individual wells (Figures 30, 31).

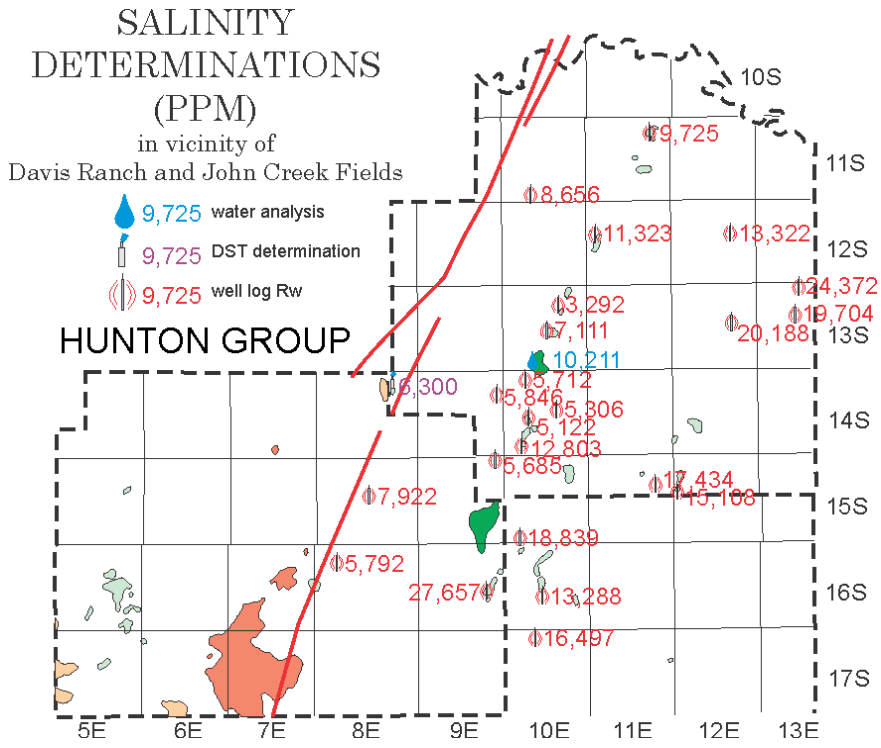

Figure 26. Salinity analysis for the Hunton Group.

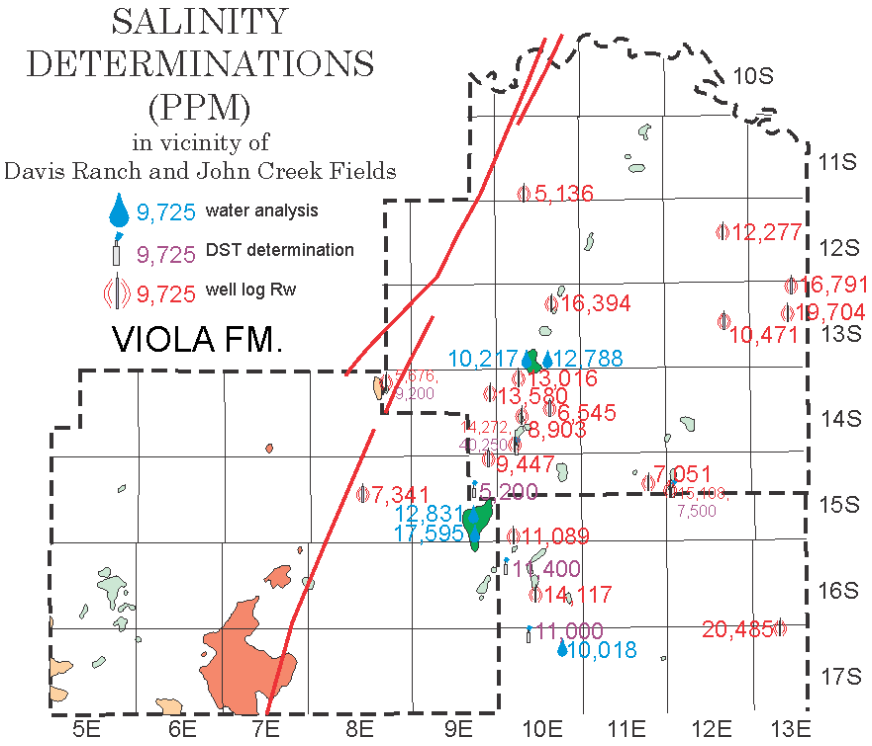

Figure 27. Salinity analysis for the Viola Formation.

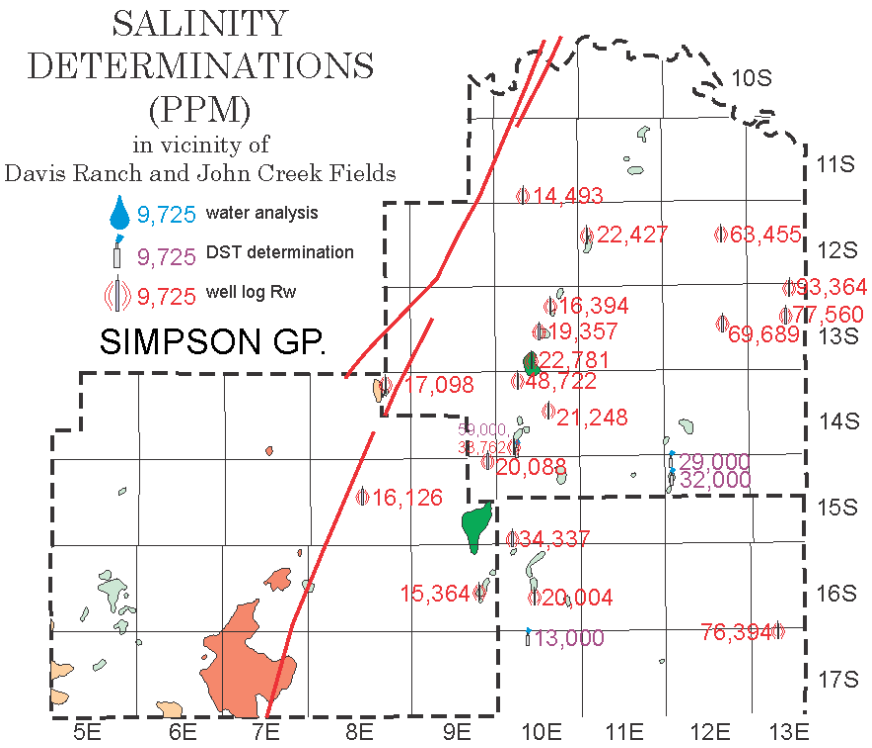

Figure 28. Salinity analysis for the Simpson Group.

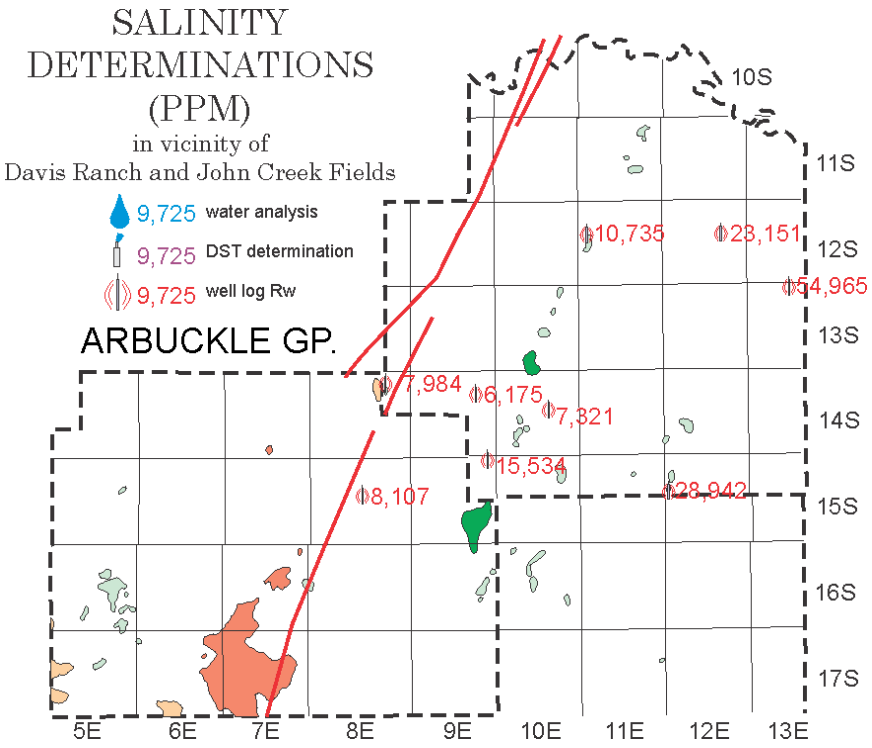

Figure 29. Salinity analysis for the Arbuckle Group.

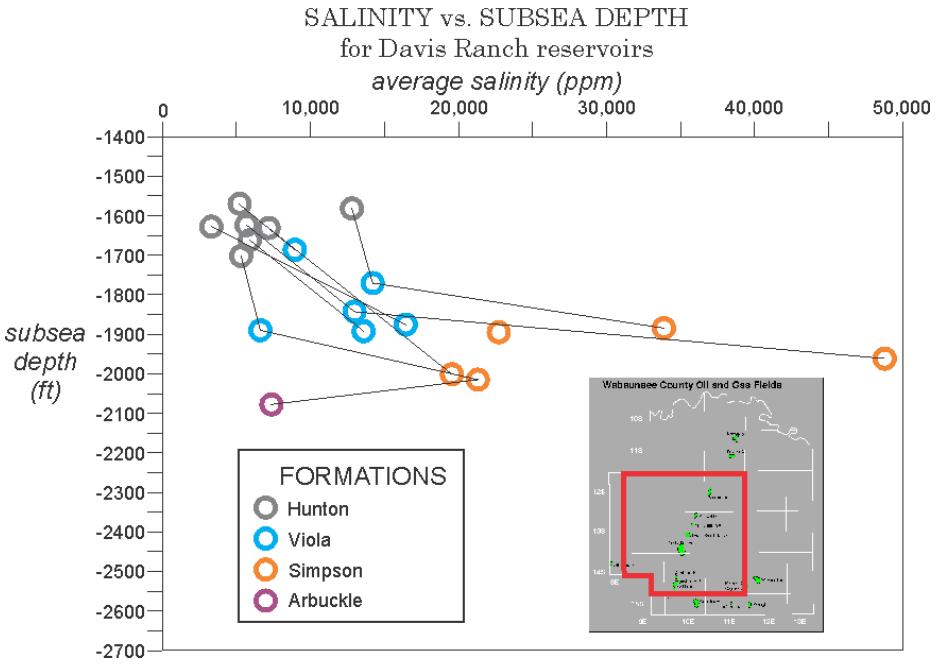

Figure 30. Salinity vs. depth plots for the Davis Ranch field. Lines connect dots from a common well.

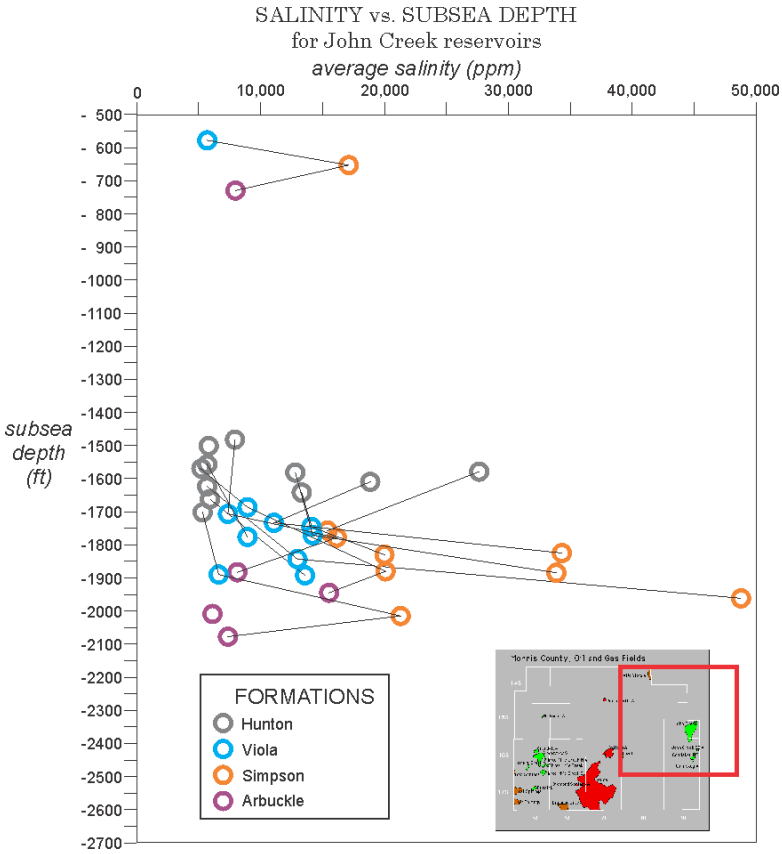

Figure 31. Salinity vs. depth plots for the John Creek field. Lines connect dots from a common well.

Discussion and Conclusions

Presumably, since several ionic species are being measured in set laboratory conditions, a chemical analysis of produced water will be the most accurate type of salinity measurement. In contrast, DSTs recover several hundred feet of water in pipe may be sampling unknown amounts of both formation water and drilling fluid, although the more water recovered in a DST would likely indicate that formation water represents a greater portion of any fluid recovered. Salinity analyses of water recovered in DSTs are also problematic in that the analysis may be performed at the well site under less-than-ideal conditions. Some inconsistencies are evident between some analyses and localities. For example, a Simpson DST in sec. 32-T.14S-R.10E. differs by more than 20,000 ppm from a well-log derived salinity in the same well (Figure 29). In this case the DST measurement is somewhat suspect, as it is more than all other measurements nearby. Some salinities also evidently change in short distances. For example, two chemical analyses from the Viola at the John Creek from samples taken less than two miles from each other registered 12,831 and 17,595 ppm (Figure 27).

Thick shale units, more than 50 ft thick, isolate the Hunton from other reservoirs (Figure 2). The Devonian-Mississippian Chattanooga Shale overlies the Hunton. The Upper Ordovician Maquoketa Shale underlies the Hunton, and separates the Hunton from the underlying Viola reservoir. The abruptly greater salinity of the Viola compared to the Hunton, and the presence of thick shales enveloping the Hunton indicates that the Hunton is isolated from the Viola, Simpson, and Arbuckle reservoirs.

Thin (10 to 20 ft thick) shales and non-porous limestone, 40 to 70 ft thick, separate the Simpson from the overlying Viola reservoir, whereas only thin shales separate the Simpson from the Arbuckle. The

drastically higher salinity in the Simpson compared to the Arbuckle at both Davis ranch and John Creek, however, strongly indicates that the Simpson is isolated from both the Viola above and the Arbuckle below. We thus conclude that there will be no natural leakage of sequestered CO_2 out of the four separate reservoirs at Davis Ranch and John Creek. None of the four reservoirs appears to be in communication with any of the other reservoirs.

References

Bui, L. H., Tsau, J. S., and Willhite, G. P., 2010, Laboratory investigations of CO_2 near-miscible application in Arbuckle Reservoir: SPE Improved Oil Recovery Symposium held in Tulsa, Oklahoma, 24–28 April 2010, SPE Publication 129710.

Carter, R. D., and Tracy, G. W., 1960, An improved method for calculating water influx: Petroleum Transactions, AIME, vol. 219, p. 415–417.

Chang, K. W., Minkoff, S. E., and Bryant, S. L., 2009, Simplified model for CO_2 leakage and its attenuation due to geological structures: Energy Procedia, v. 1, p. 3,453–3,460.

Dake, L. P., 1978, Fundamentals of Reservoir Engineering," Chapter 9, Elsevier Scientific Publishing Co., 1978.

Doveton, J. H., 2004, Applications of estimated formation water resistivities to brine stratigraphy in the Kansas subsurface: Kansas Geological Survey, Open-File Report 2004-22, 20 p.

Fazelalavi, M., 2017, Determination of relative permeability curves in the Arbuckle: Kansas Geological Survey Open File Report 2017-6, 12 p.

Kansas Geological Survey, 2003, MidCarb CO_2 online property calculator, http://www.kgs.ku.edu/Magellan/Midcarb/co2_prop.html. Accessed on July 12, 2017.

Kestin, J., Khalifa, H. E., and Correia, R. J., 1981, Tables of the dynamic and kinematic viscosity of aqueous NaCl solutions in the temperature range 20–150 °C and the pressure range 0.1–35 MPa: Journal of Physical and Chemical Reference Data, NIST, v. 10, p. 71–88.

Li, Y. K., and Nghiem, L. X., 1986, Phase equilibrium of oil, gas and water/brine mixtures from a cubic equation of state and Henry's Law: Canadian Journal of Chemical Engineering, June, p. 486–496.

Søreide, I., and Whitson, C. H., 1992, Peng-Robinson predictions for hydrocarbons, CO_2, N2, and H2S with pure water and NaCI brine: Fluid Phase Equilibria, v. 77, p. 217–240.

Watney, W. L., 2016, Integrated CCS for Kansas (ICKan) SF 424 R&R, Application for Federal Assistance, Phase I—Integrated CCS Pre-Feasibility Study activity under CarbonSAFE, DOE-NETL FOA 1584.

Watney, W. L., et al., 2015, Modeling CO_2 sequestration in saline aquifer and depleted oil reservoir to evaluate regional CO_2 sequestration potential of Ozark Plateau Aquifer System, South-Central Kansas, Final Report, Award Number: DE-FE0002056, submitted October 2, 2015, 4,867 p.

Appendix D: Development of the Cellular Static Model for the Lakin geologic site in the North Hugoton Storage Complex

Andrew Hollenbach, Kansas Geological Survey

Background

The Lakin oil field (field) of the North Hugoton Storage Complex is located in Kearny County, Kansas, approximately 6 miles south of the city of Lakin, Townships 25 and 26 South, Range 36 West (Figure 1). A technical evaluation of the saline aquifer beneath the field was conducted by building a sub-basin fine-grid static cellular 3-D model using Petrel™. The cells were then populated with porosity and permeability based well-scale wireline log data. The fine-grid model was then vertically upscaled and the field was exported for reservoir simulation in CMG™. This memorandum is meant to provide a record of the data, methodology, and results pertaining to the development of the field model in Petrel™.

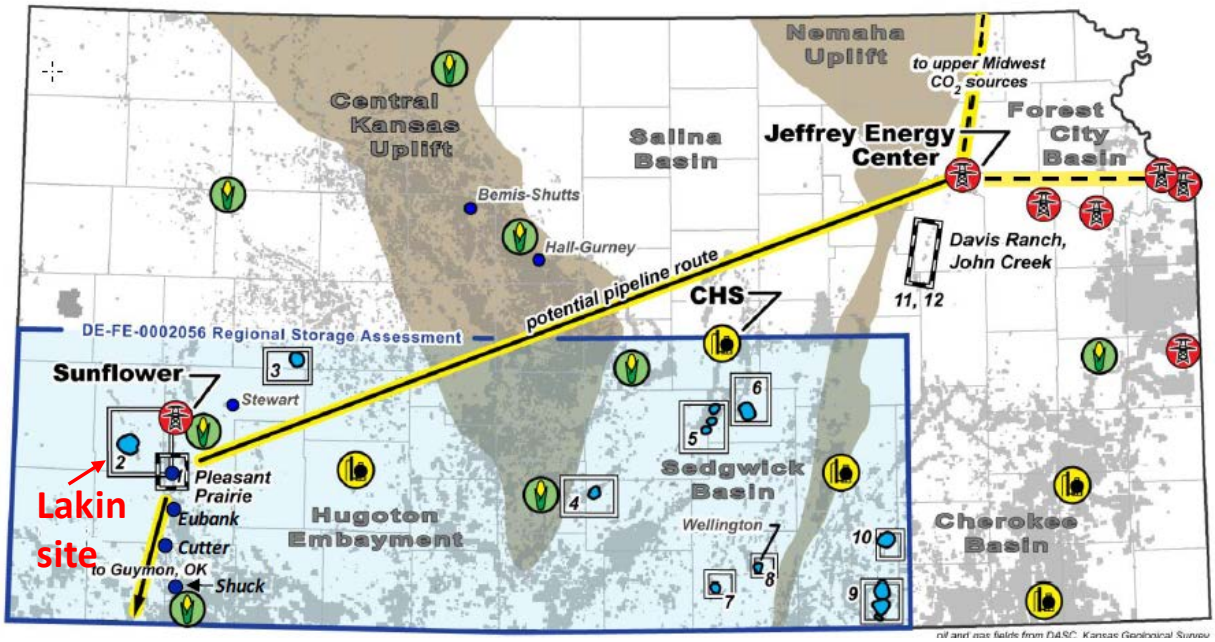

Figure 1. Map of Kansas showing location of Lakin field in southwest Kansas.

Modeling Workflow

The modeling work flow consisted of data collection and analysis, 2-D development of structural formation maps, 3-D structural development of a cellular 3-D model, upscale of digitized wireline logs, modeling of the upscaled petrophysical properties, vertical upscale of the model, and export for simulation in CMG™. Figure 2 presents a generalized workflow diagram.

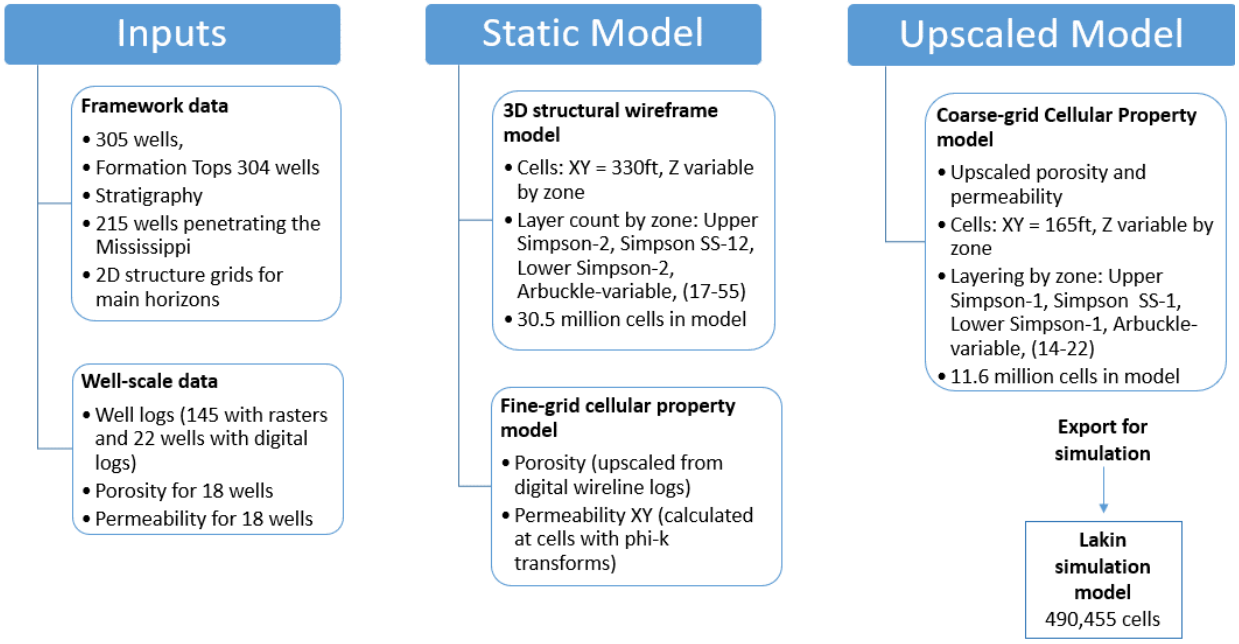

Figure 2. General workflow followed during the building of the Lakin 3-D geologic model.

For ease of review, this report has been formatted in a manner that parallels the modelling workflow; therefore, subsequent sections detail data collection and analysis and methods of model development.

Data

Collection

The data for the model were collected from the KGS and Robert F. Walters Digital Libraries. Model framework and well-scale data were gathered in the form of well header information (e.g., operator information or well name and number), locations, formation tops, and wireline logs in the form of image files. The data were then collected and analyzed in Petra™. A 26.5 mi. (42.65 km) x 21 mi. (33.8 km) rectangular area (1441.57 km^2) was selected for model development comprising the Lakin Northwest, Lakin, and Lakin South Oil Fields (Figure 3).

Analysis

There are 305 wells deeper than 4,500 ft in the model area (depth filtered to exclude shallow Hugoton gas wells). Of these, 304 wells contain formation top data including manually picked tops from the depth-calibrated wireline log images at 164 wells.

There are 211 wells with picked tops penetrating Mississippian strata, 60 wells penetrating the Salem Limestone, 26 wells penetrating the Warsaw, 13 wells penetrating the Viola, and 8 wells penetrating the Arbuckle. Figures 4a through 4f identify well penetrations per formation in the modeling area. Figure 5 identifies the distribution of raster and digital logs in the model area.

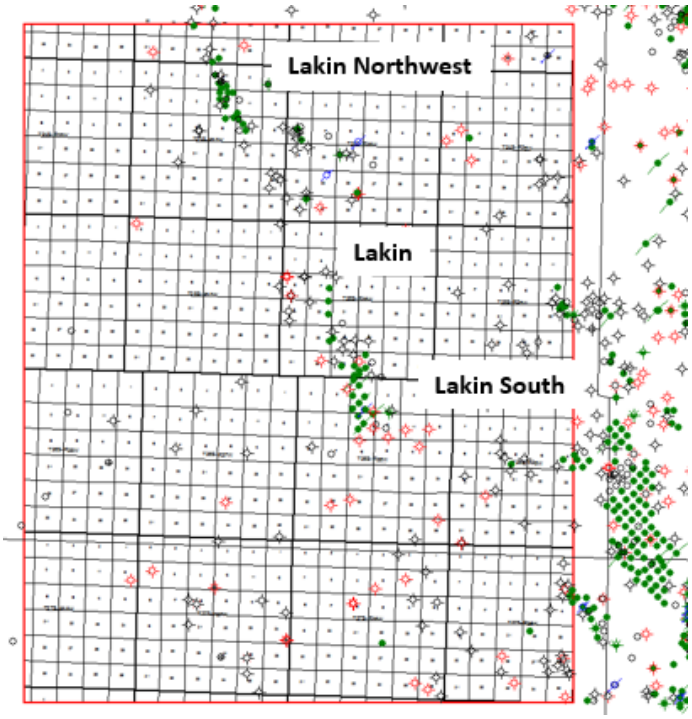

Figure 3. Plat showing field names and well locations in the Lakin model area, outlined in red. For scale, small grid blocks are one mile square and heavier grid lines outline townships (6 x 6 miles).

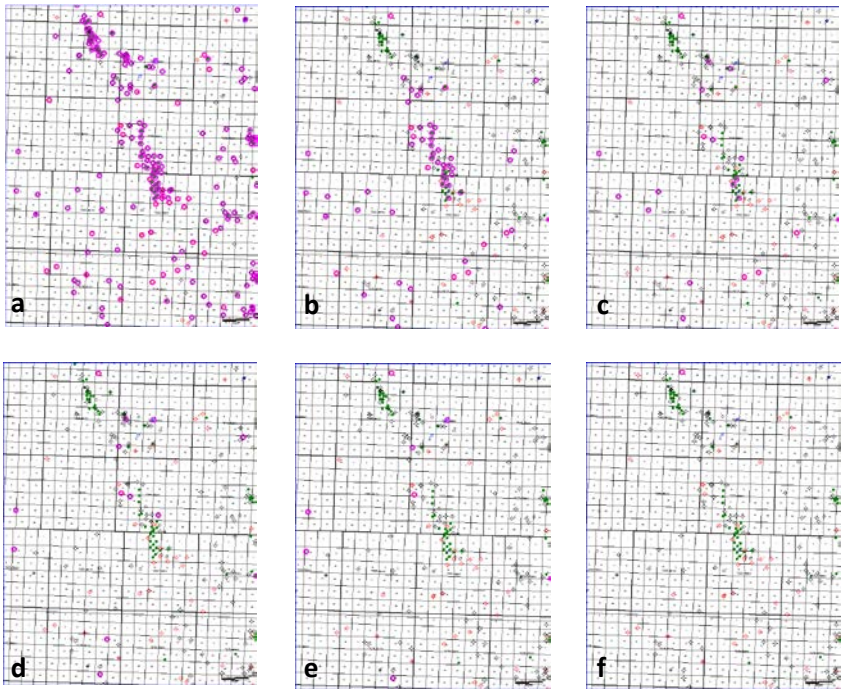

Figure 4. Plats showing well penetrations by formation (depth) inside the model area. a. 211 Mississippi Tops, b. 60 Salem Tops, c. 26 Warsaw Tops, d. 13 Viola tops, e. 8 Arbuckle tops, f. 1 base Arbuckle top. Grid scales are the same as in Figure 3.

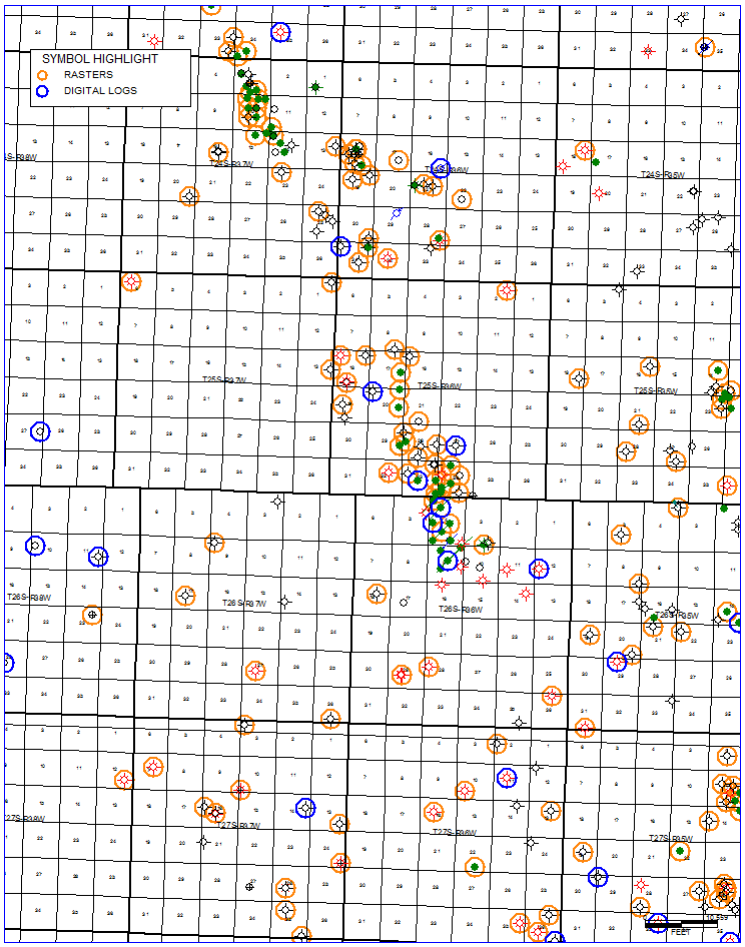

Figure 5. Map showing the well distribution in the model area. Red circled wells have static raster images of wireline logs and blue circles indicate wells with digital logs. Grid scales are the same as in Figure 3.

Methods of Model Development

2-D Structure Maps were generated in Petra™ and then exported to Petrel™ for 3-D modelling as described below.

2-D Formation Structure Maps

A formation structure map (grid) for the Meramec Formation (Mississippian) modeled from the tops data and manually input control points using a highly connected features (least squares) surface style with no faults. Formation isopachs were calculated and then subtracted from the Meramec grid downward in a sequential manner, grid-to-grid (i.e. grid – isopach = grid), until the structure of all target formations and seals were modelled, creating zones for the Osage, Viola, Arbuckle target reservoirs and respective seals.

The project grids, well header information, tops data, and digitized logs were checked for quality and then exported from Petra™ to Petrel™.

3-D High Resolution Cellular Structural Model

A 3-D skeletal grid was created in the model area by gridding 330 ft northerly increments by 330 ft easterly increments to form a 3-D skeletal grid. This skeletal grid is used in both a high-resolution (fine grid) model and a low resolution (coarse grid) model. The formation zones were layered as described below, to form cell z-values along the pillars of this skeletal grid.

Fine Grid Layering

The layering is proportional to zone thickness and consists of the Upper Osage (13 layers), Osage (36 layers), the Kinderhook (10 layers), the Viola (45 layers), the Simpson (3 layers), and the Arbuckle (64 layers).

Petrophysical Model

Calculated porosity was upscaled using an arithmetic average from the 18 digitized wireline logs, treated as lines, to neighbor cells.

The Schlumberger sequential Gaussian function simulation method was used to model zone porosity. The simulation used a default spherical variogram model with a sill of 0.99 and range of 500 ft.

Permeability was then calculated by layer at each cell from porosity-to-permeability transform functions resulting from petrophysical analysis.

Permeability of the Osage was calculated using the exponential function:

$$(0.1897)e^{(\text{Porosity}*30.47)}.$$

Permeability of the Viola formation was calculated using the exponential function:

$$(0.0186)e^{(\text{Porosity}*52.19)}.$$

Permeability of the Viola formation was calculated using the power function:

$$(4667.7)(\text{Porosity})^{(2.9242)}.$$

Permeability of the seals (upper and lower Simpson Group) were assigned .000001 mD for simplicity during simulation.

Low Resolution Cellular Structural Model for Simulation

The 330 ft by 330 ft skeletal grid described above is used for both the high-resolution (fine grid) model and the low resolution (coarse grid) model.

Coarse Grid Layering

The course grid layering is also proportional to zone thickness and consists of the Upper Osage (6 layers), Osage (12 layers), the Kinderhook (5 layers), the Viola (15 layers), the Simpson (3 layers), and the Arbuckle (20 layers). Vertical slices show the fine and coarse grids for comparison at the intersection of a key well in Figure 7.

Petrophysical property upscale to low resolution structural model

Porosity was upscaled to the low resolution model using volume-weighted arithmetic averaging algorithm. Permeability was upscaled using volume-weighted geometric averaging. Histograms of porosity and permeability in the Arbuckle for the course and fine grid models are presented as Figure 7. A comparison of porosity histograms porosity in the Arbuckle at the well, upscaled, and at the model is presented as Figure 8.

Field Export

A small portion of the larger model was extracted from the larger area model, including porosity and permeability properties (Figure 9). The model was then exported under Rescue format.

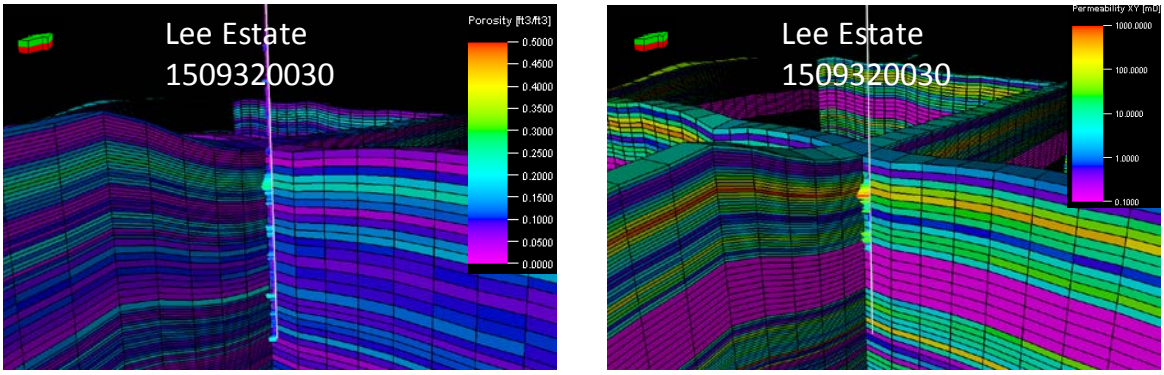

Figure 6. Porosity (left) and permeability (right) fence diagrams of the illustrating fine and coarse grids at the Lee Estate well. Vertical exaggeration =10

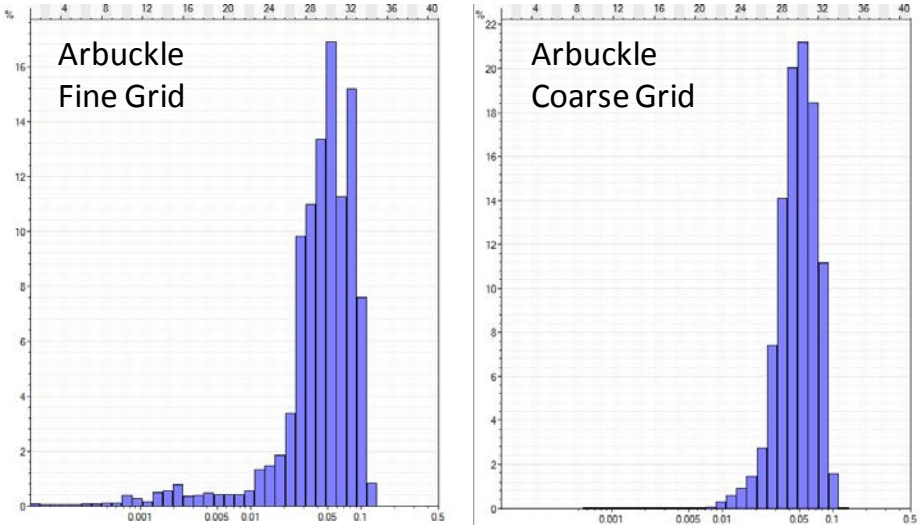

Figure 7. Histograms illustrating the distribution of permeability in the Arbuckle for the fine and coarse grid models

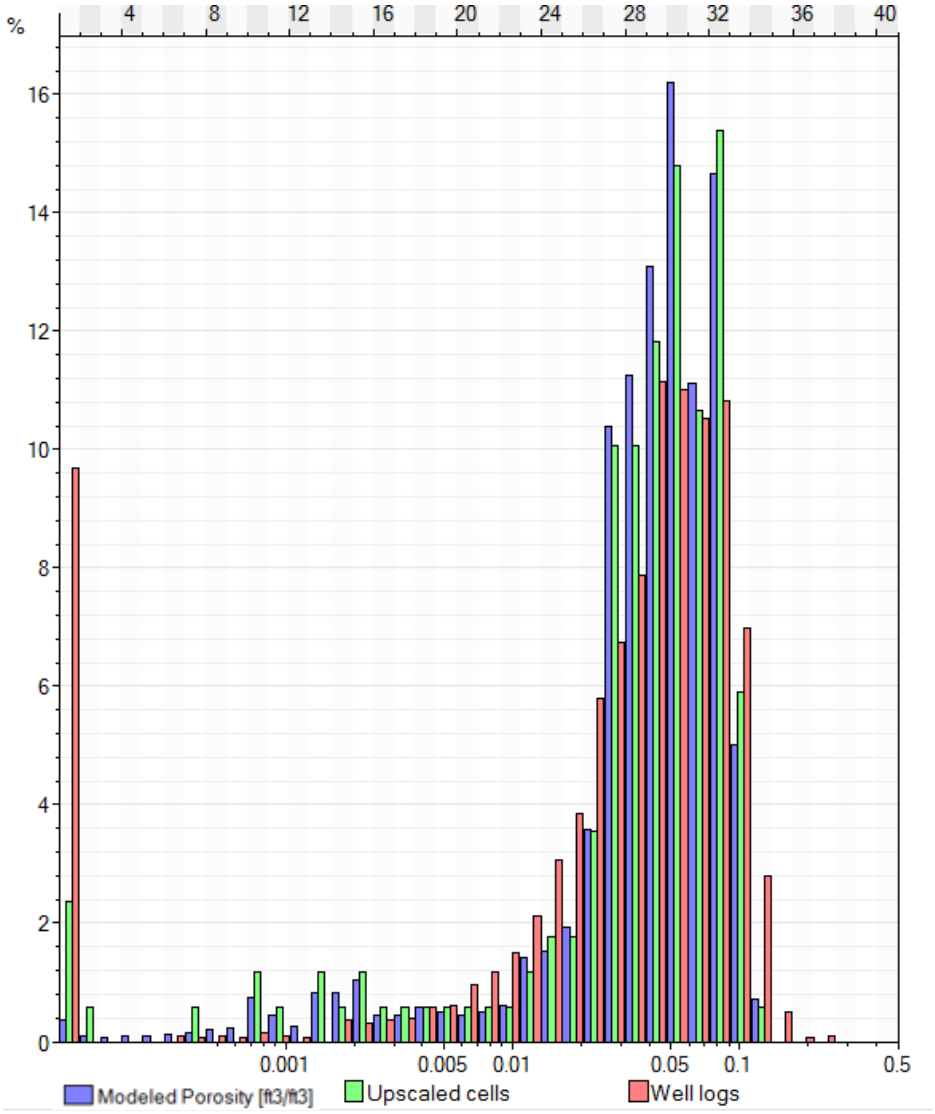

Figure 8. Histograms of porosity in the Arbuckle at the well (half-foot scale), red; upscaled at the layer height scale, green; and at the fine-grid model scale, blue.

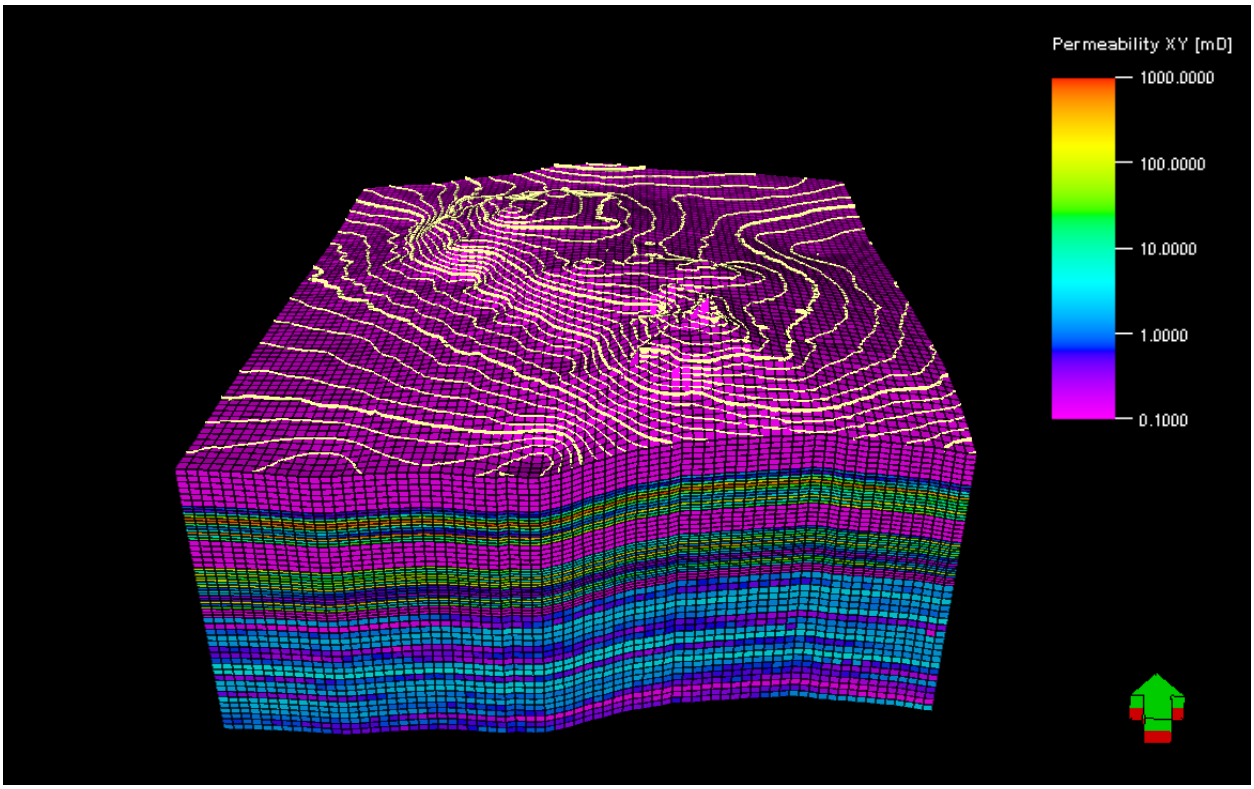

Figure 9. Lakin Field simulation model upscaled and extracted for simulation. Property is permeability.

Appendix E: Petrophysical analysis in the North Hugoton Storage Complex

Mina Fazelalavi, Kansas Geological Survey

Log Interpretation

Total porosity of eight wells, three in the Pleasant Prairie and the rest near Pleasant Prairie, was calculated from Osage formation down to the Arbuckle. GR, porosity and resistivity logs were used to analyze the wells by a Schlumberger application, Techlog multi-mineral analysis module. Well logs from the Berexco Cutter-KGS 1 well, 30 miles south of the Pleasant Prairie field, was a key well because of it having an extensive set of data and wireline logs including conventional and nuclear magnetic resonance (NMR) logs, and core data. This well was selected as the key well for estimating permeability in wells without core.

Permeability in Cutter-KGS 1

Permeability in Cutter-KGS 1 was calculated using three methods:

1) Coates
2) R35 Winland
3) FZI-SWPHI (IPTC-17429-MS)

Permeability by all three methods are in agreement with minor differences, Figure 1. Permeability by R35 Winland, FZI-SWPHI and core are compared in the fourth track from the right. Permeability by FZI-SWPHI, Coates and core are compared in third track from the right, and finally permeability by Coates, R35 Winland and core are compared in the second track from the right.

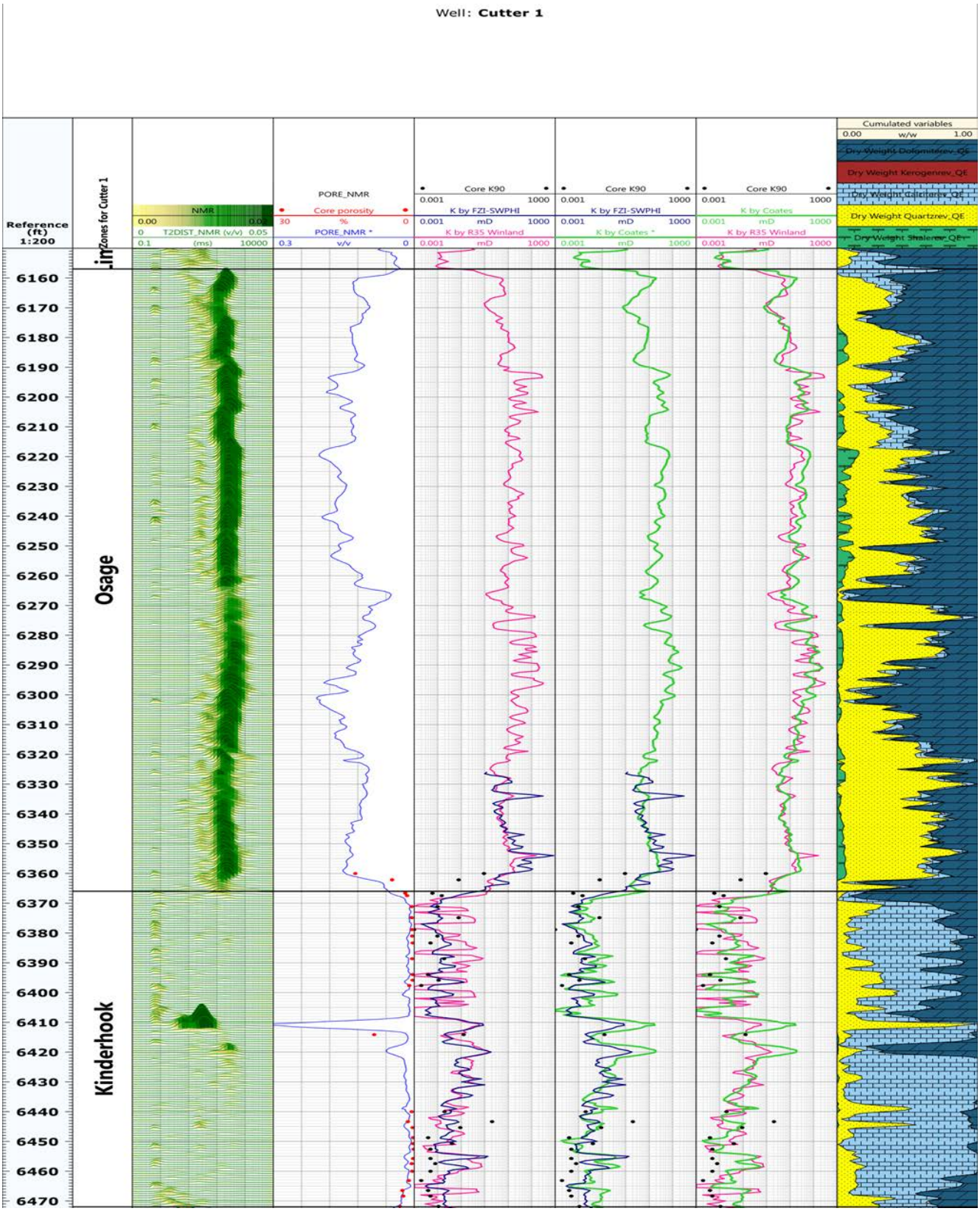

FIGURE 1: Calculated permeability by three methods compared to core in the Cutter-KGS *1 well. Figure 1 extends to the following three pages.

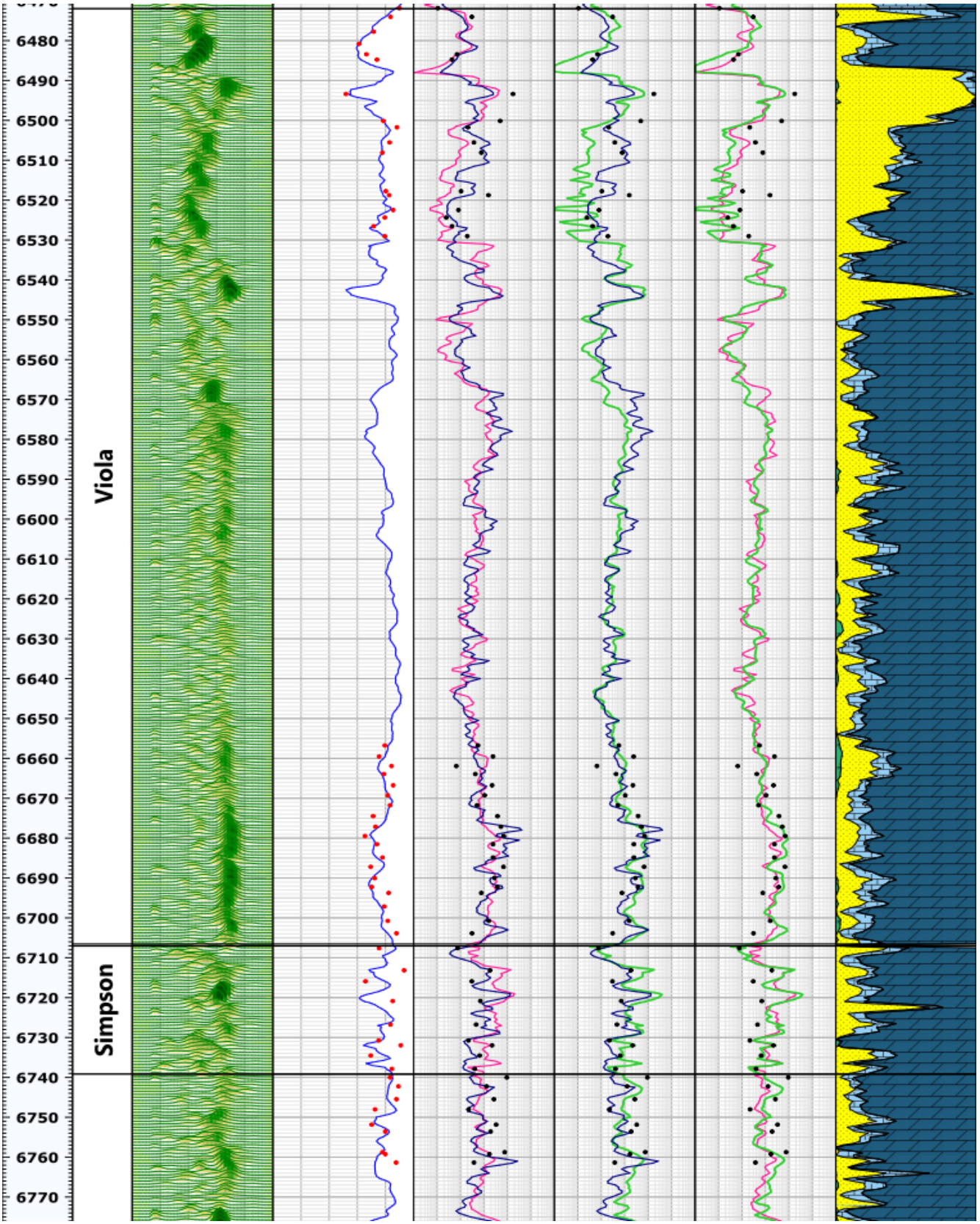

FIGURE 1, CONTINUED

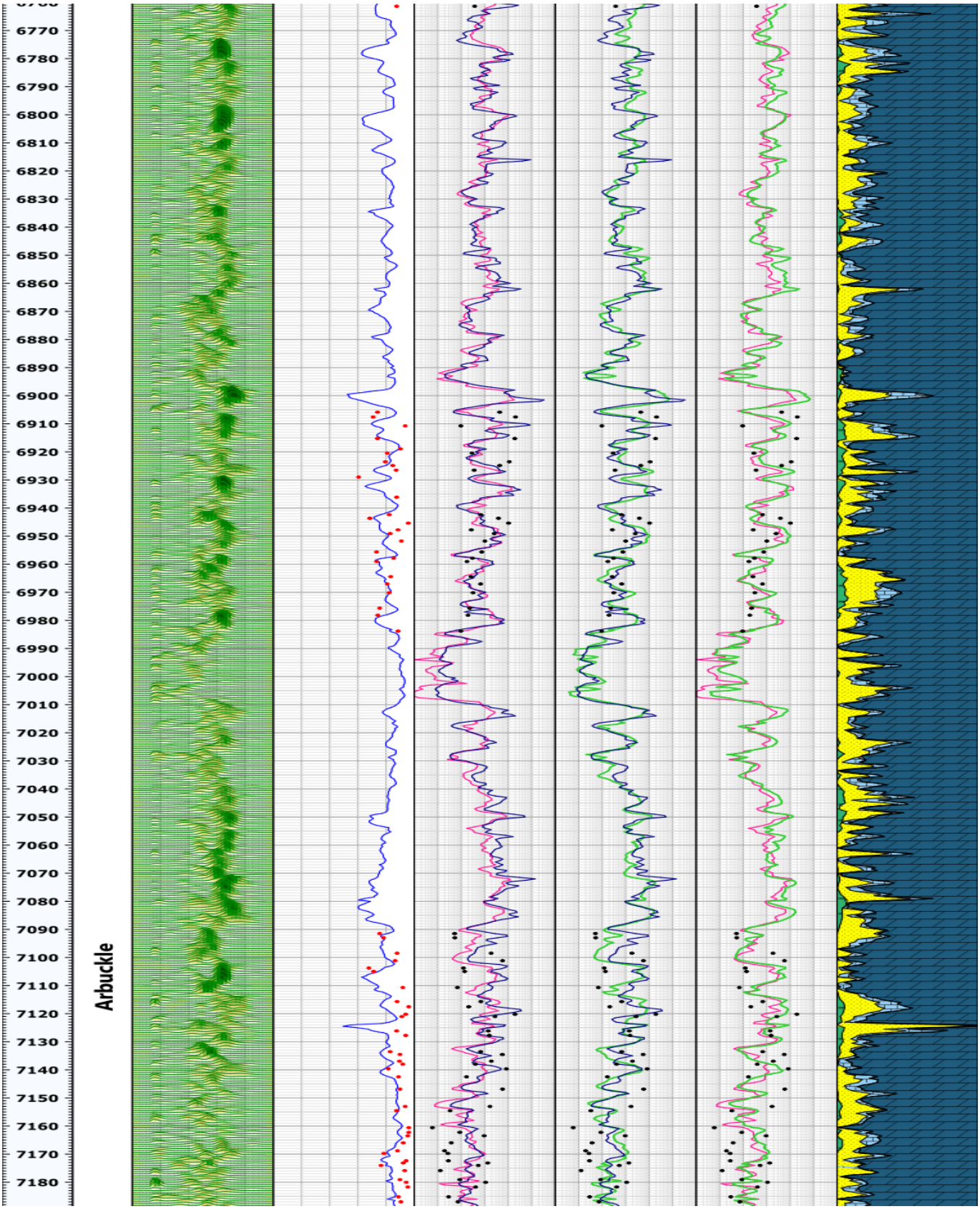

Figure 1, continued

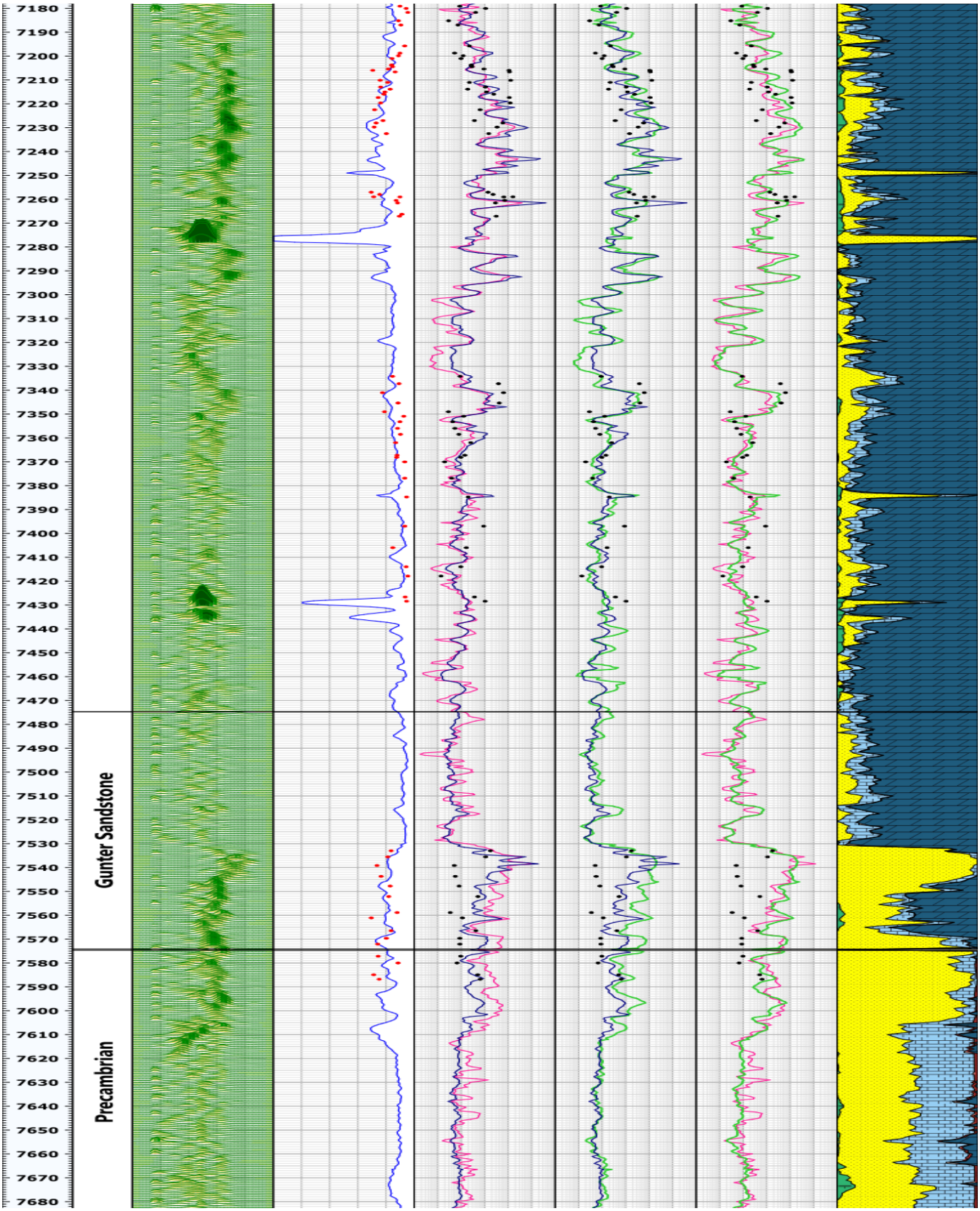

Figure 1, continued

Permeability Solution in Wells without Core

A. Permeability Transforms in Osage and Viola

Because the estimated permeability from all methods are in agreement and Coates permeability is the most widely used permeability method, permeability by Coates was chosen to derive permeability transforms for wells without core data in Viola, Osage and the Arbuckle.

To derive the permeability-porosity transforms, Coates permeability was plotted against effective porosity from NMR for each formation. A single K-PHI relationship was derived for the Osage and Viola. Predicted permeability by a single relationship resulted in a reasonable prediction compared to Coates with small deviations in some intervals. However, two K-PHI relationships in each formation result in a better match between predicted permeability from the K_PHI transforms and Coates.

A single K-PHI relationship for Osage and Viola are in Figure 2 and 3 and two K_PHI relationships are shown in Figures 4, 5, 6, 7. Predicted permeability by K-PHI transforms are plotted against Coates permeability in Figure 8.

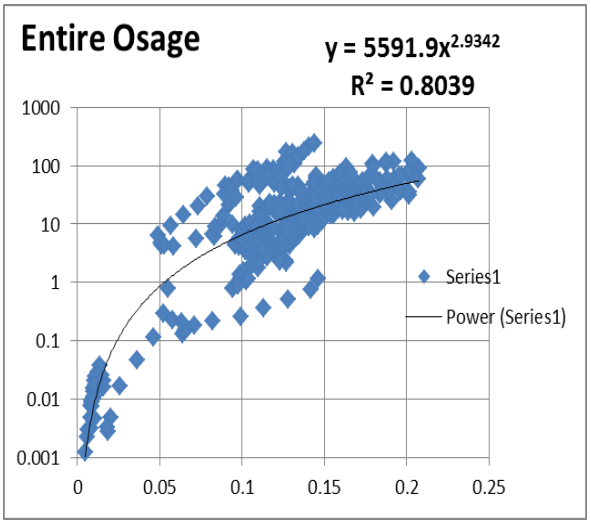

Figure 2: A single K-PHI relationship for entire Osage

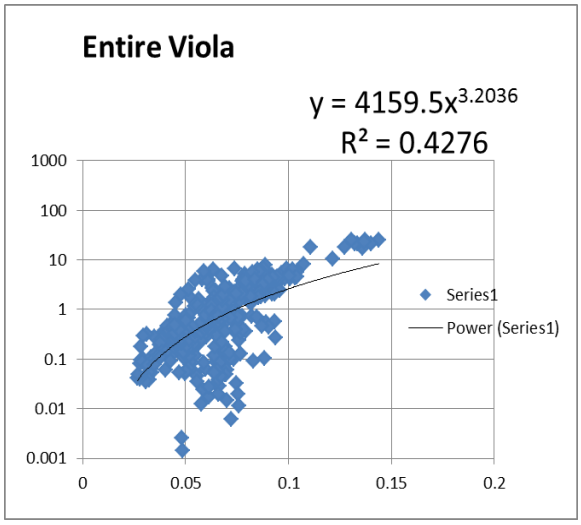

Figure 3: A single K-PHI relationship for the entire Viola

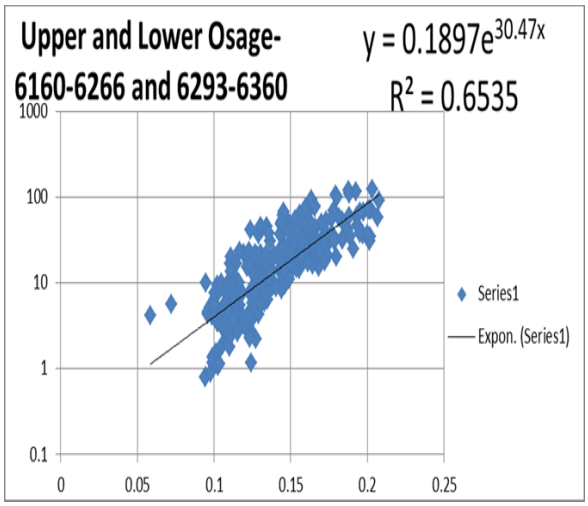

Figure 4: K-PHI relationship for upper and lower Osage 6293):

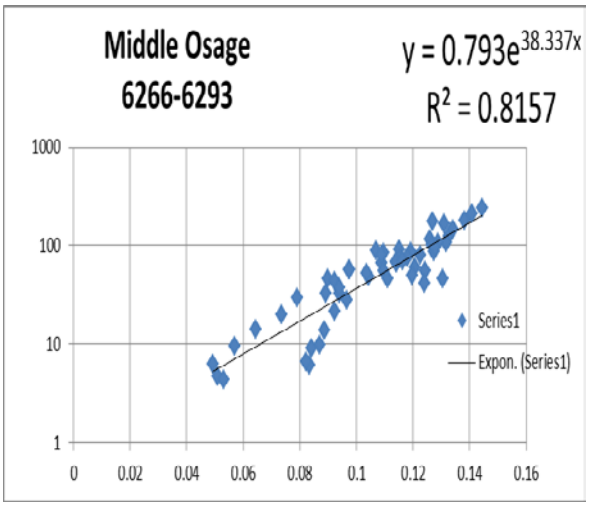

Figure 5: K-PHI relationship for middle Osage (6266-

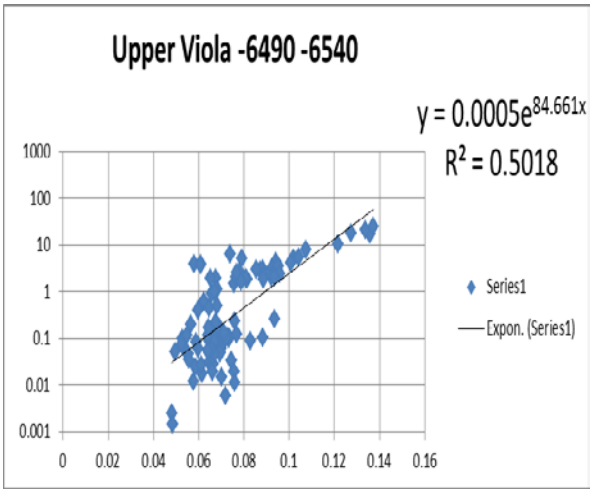

Figure 6: K-PHI relationship for lower Osage

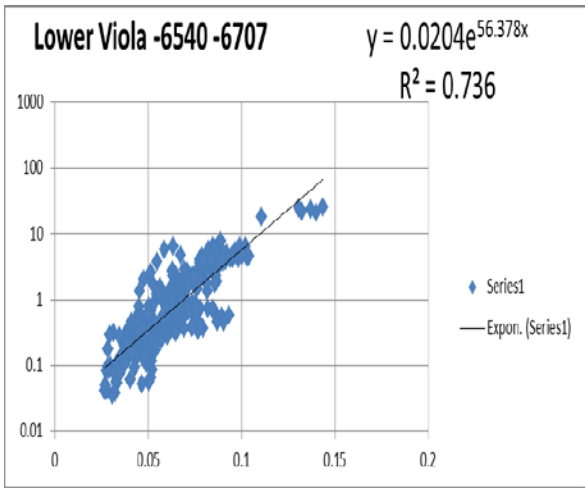

Figure 7: K-PHI relationship for upper viola

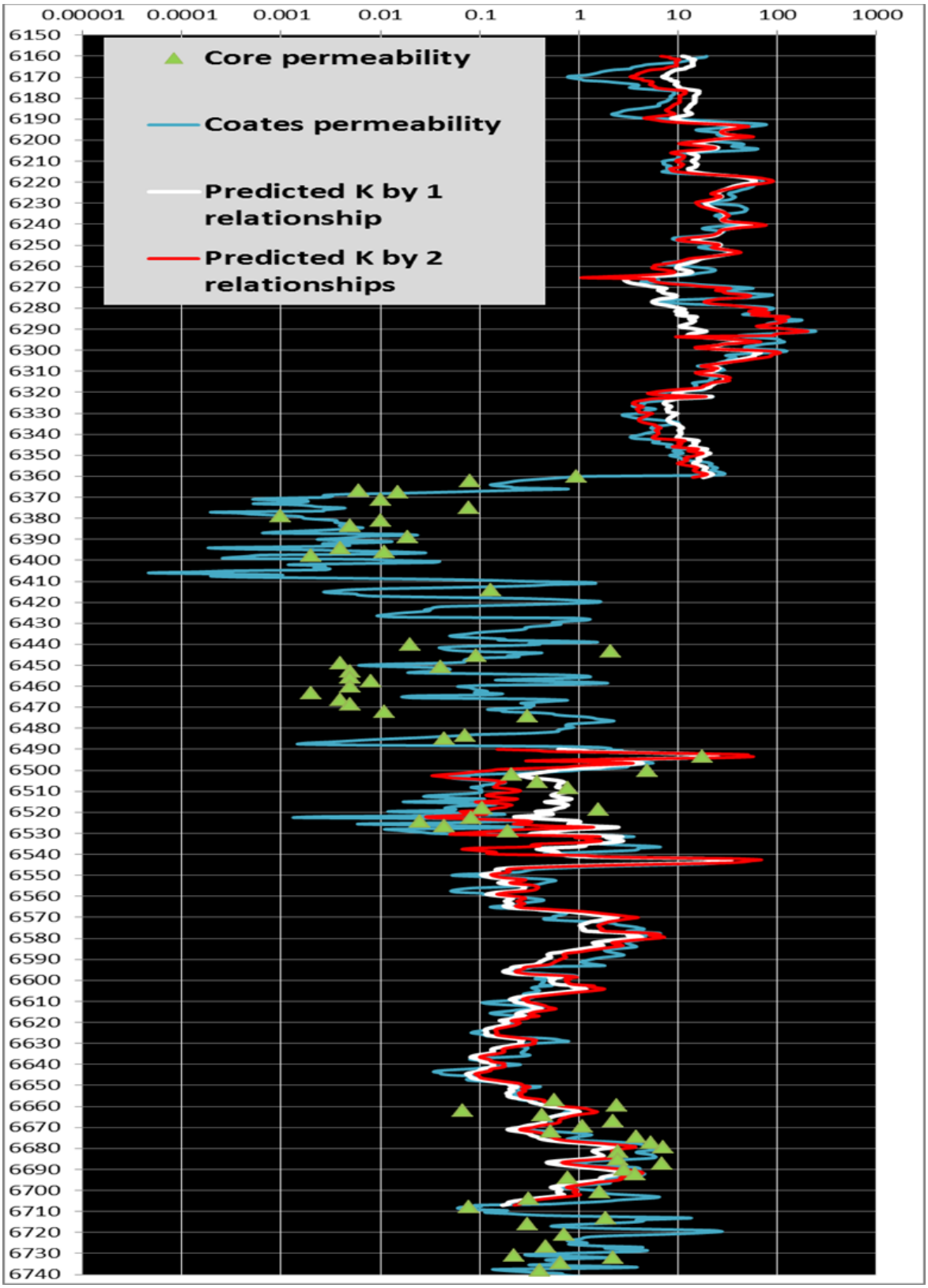

Figure 8: Predicted permeability by K-PHI relationship

B. Permeability in Simpson

Coates permeability was plotted against effective permeability from NMR for Simpson and a single K-PHI relationship was derived for Simpson, Figure 9. Calculated permeability using the K-PHI relationship resulted in reasonable prediction against the original Coates permeability, Figure 10.

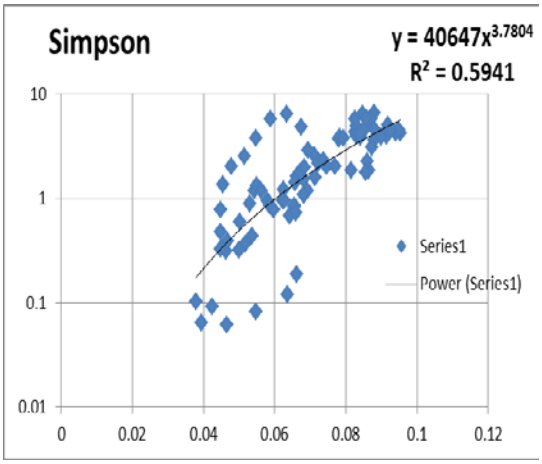

Figure 9: K-PHI relationship for Simpson

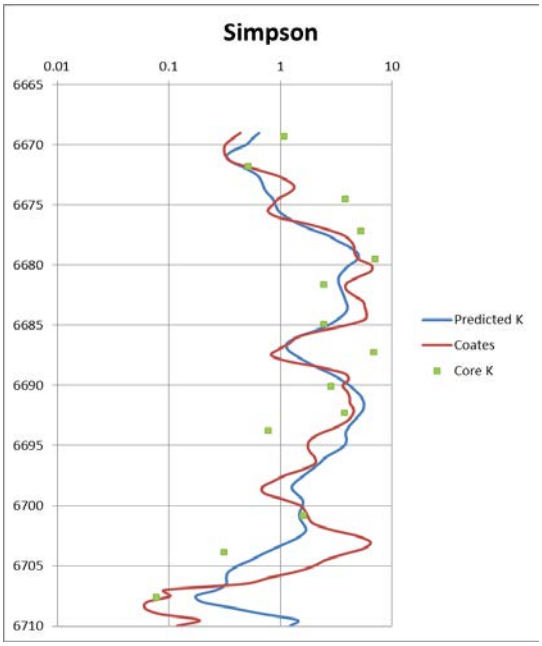

Figure 10: Comparison of K from core, Coates and transform in Fig. 9.

C. Permeability Transforms in the Arbuckle

The Arbuckle is vertically heterogeneous with pore size varying with depth over short intervals, Therefore, permeability varies with depth. A single K_PHI relationship is not effective over the entire Arbuckle interval, making permeability prediction a challenge. Acceptable permeability-phi relationships were achieved by evaluating K_PHI over discrete GR ranges. Four K-PHI relationships for four GR ranges (GR<13, GR 13–19, GR 19–30 and GR 30–70) were derived and illustrated in Figures 11, 12, 13 and 14. Predicted permeability by K-PHI relationships is plotted in Figure 15 and compared to K from Coates and core.

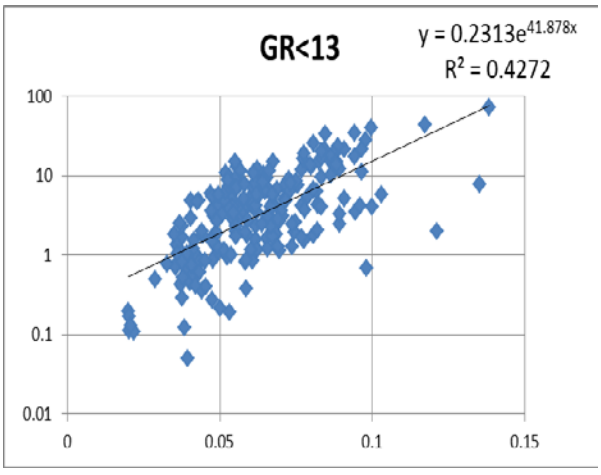

Figure 11: K-PHI relationship for GR<13 for the Arbuckle

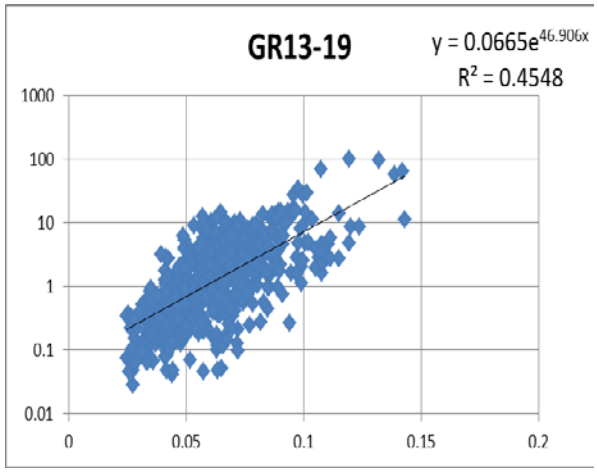

Figure 12: K-PHI relationship for GR 13 through 19

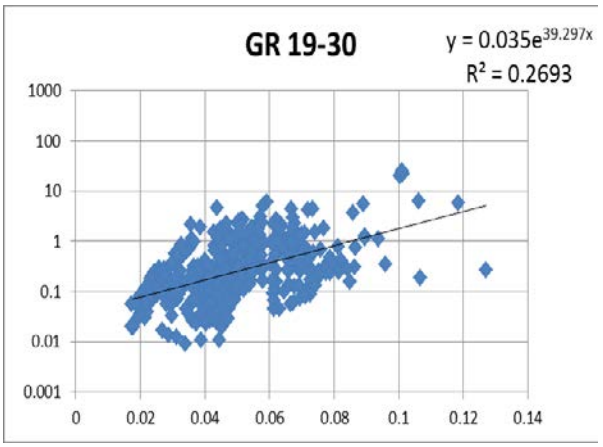

Figure 13: K-PHI relationship for GR 19 through 30

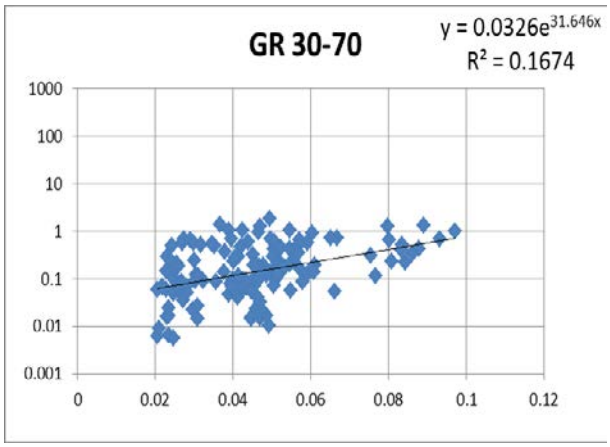

Figure 14: K-PHI relationship for GR 30 through 70

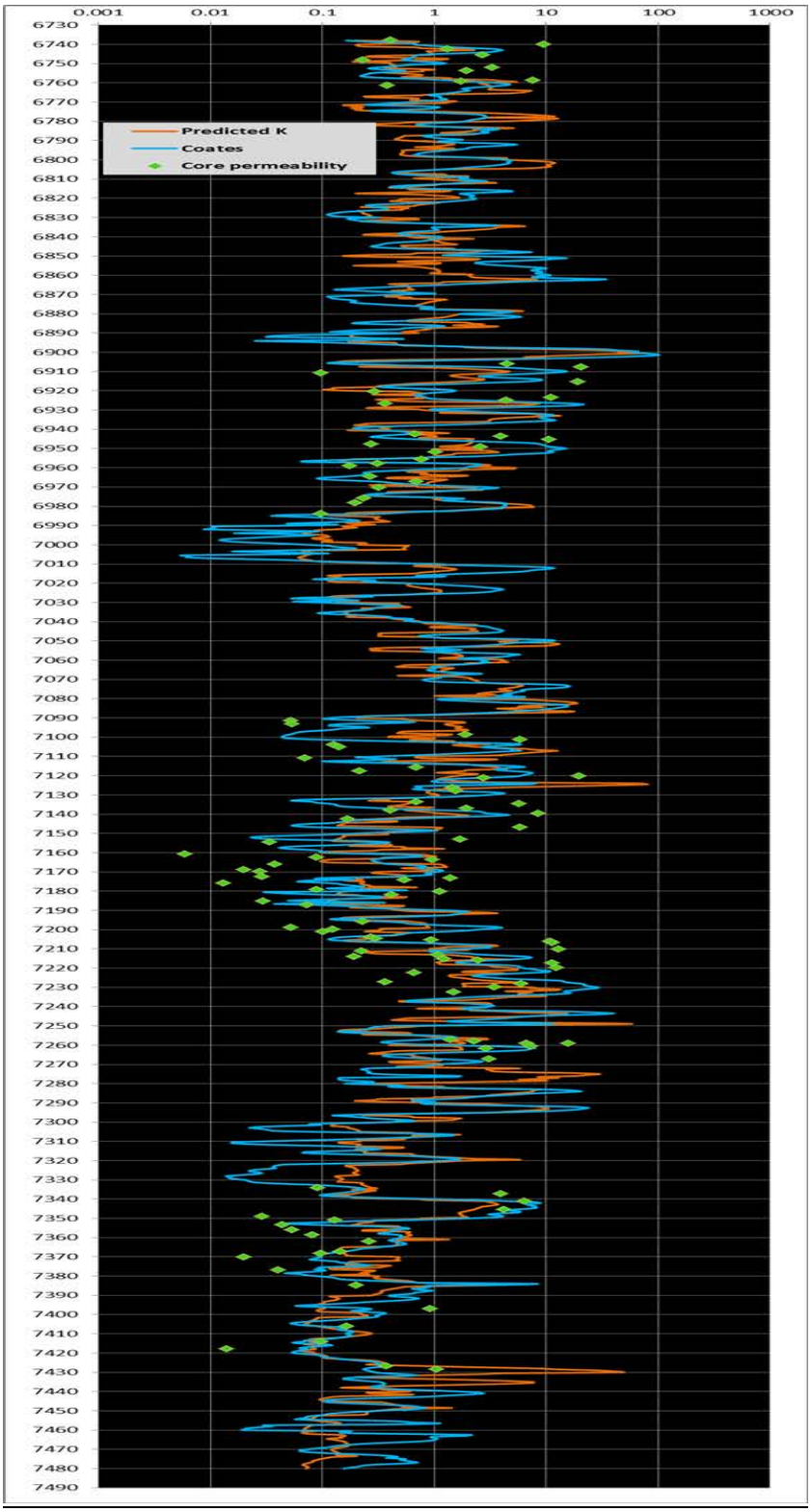

Figure 15: Predicted permeability by K-Phi relationship based on GR subdivision compared to Coates and core.

Alternative K-Phi relationships for the Arbuckle

Reducing four K-Phi relationships to two

Dealing with four GR ranges is a bit cumbersome. K-Phi transforms over two GR ranges. An alternative was to create two equations for K versus porosity based on GR subdivisions, one equation for GR>25 and the other for GR<25 (Figure 16).

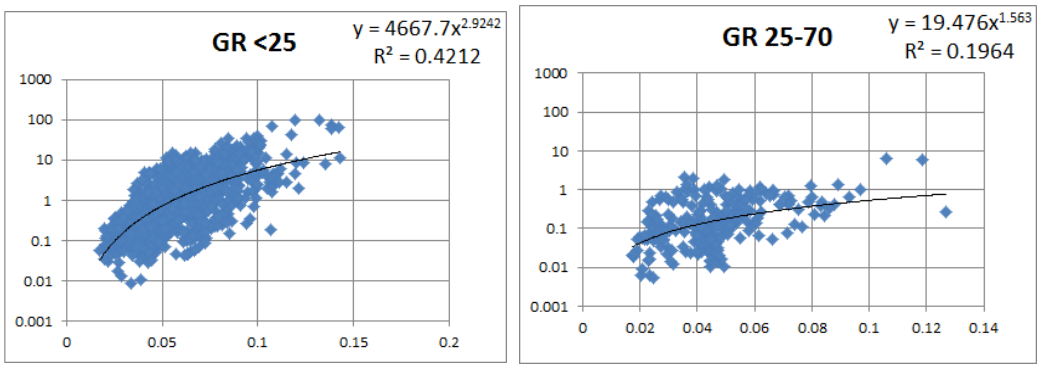

Figure 16: K-PHI relationship for GR<25 and for GR 25-70.

A single, two variable permeability transform

A single equation was derived for the Arbuckle based on Coates permeability, effective porosity from NMR and GR log. This equation is a power equation as a function of porosity and GR:

$$K=1E+09 * GR^{-4.84} * \varphi^{(9.37 \times GR^{-0.49})}$$

This equation is effective for wells with insufficient logs and datasets. Permeability in the Arbuckle was calculated by the equation above and it resulted in a good agreement with Coates permeability, Figure 17.

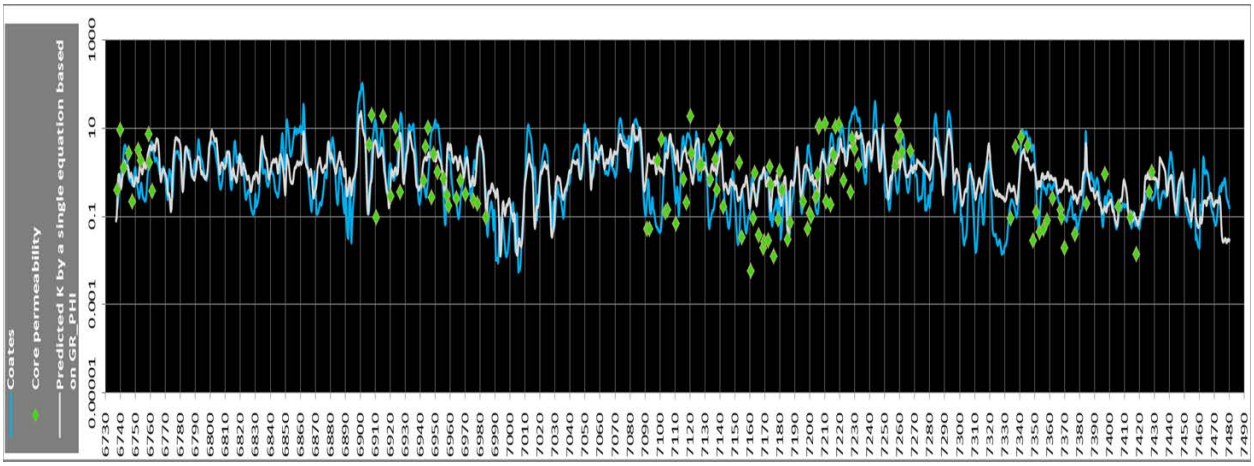

Figure 17. Comparison of permeability from core (green dots), Coates, and two variable transform – GR and porosity (white)

A single relationship between K-PHI as stated above did not work as well for the Arbuckle because of the heterogeneity of the Arbuckle over short intervals; however, the single equation based on GR and porosity is more effective for the Arbuckle and it can result in a reasonable prediction as shown below.

The coefficients in the equation above may change for different regions, depending on the heterogeneity of the Arbuckle formation over a wide range such as different counties.

Sealing Integrity of Cap-rock

In order for CO_2 to enter shale (cap-rock), the differential pressure between the CO_2 column and the water zone below must exceed the minimum capillary entry pressure of cap-rock (threshold pressure). In other terms, the capillary entry pressure (P_e) or threshold is the minimum pressure difference between gas and the water below that is required for the gas to enter the cap-rock.

Capillary entry pressure can be calculated by correlations and NMR module of Techlog. Capillary entry pressure was calculated by 1) a correlation that relates pore throat radius (r_{neck}) to R35 Winland (SPE-181305-MS) 2) NMR capillary pressure module where pore size (T2 distribution) is converted to pore throat radius as a function of capillary pressure using a proportionally constant Kappa (K) according to the following relationship proposed by Volokin and others (2001):

$$K = \frac{P_c}{T_2^{-1}} = \frac{2\sigma \cos\theta R_{pore}}{\rho r_{neck}}$$

Where,

K=Kappa

ρ=NMR surface relaxivity

σ = Interfacial tension

θ = Contact angle

r_{neck}= pore throat radius

R_{pore} = pore body radius

Capillary entry pressures by both methods are in an excellent match in many intervals below the Mississippian. There is a small discrepancy between the calculated P_e by NMR and calculated P_e by correlation in the Mississippian and above the Mississippian formation. This discrepancy could be related to Coates permeability, which was used to calculate R35 Winland and hence to calculate P_e. Capillary entry pressure from both methods represent where seals and tight formations are located, Figure 17. Intervals with high entry capillary pressure and low vertical permeability are potentials for seals and they are circled in blue in Figure 17.

The minimum capillary entry pressure of cap-rock can be used to estimate the height of CO_2 column that can be trapped by shale cap-rock, also called sealed capacity. Therefore, the column of CO_2 determines whether CO_2 enters the cap-rock or not. The equation to estimate the height of CO_2 is:

$$h = P_e/(\rho_w - \rho_{CO2})g$$

Where,

H=Height of CO_2 column that can be trapped by cap-rock

P_e= Capillary entry pressure

ρ_w= Density of brine at formation P-T

ρ_{CO2}=Density of CO_2 at formation P-T

g= Gravity

Formation	mid-depth	Pressure	Temperature	CO2 Density	CO2 Density
	ft	psig	F	kg/m3	g/cc
Viola	6580	2044.447	160.56	457.25	0.46
Osage	6250	1892.317	156.39	420.02	0.42

The table above shows density of CO_2 for formation pressure—temperature at mid-depth of Viola and Osage in Stevens County. Temperature and pressure were obtained from DSTs and CO_2 densities were calculated for pressure-temperature mid-depths.

To determine the height of the CO_2 column for P_e=100 psi:

Average ρ_w=1.09 g/cc

Average ρ_{CO2}=0.46 g/cc

P_e=100 psi

H=366.58 ft

For 100 psi entry pressure, the CO_2 column must be more than 366.58ft for the CO_2 to enter the cap-rock. Figure 14 shows entry pressure about 100 psi in some intervals above Viola (6,513–6,530 ft), which could be a good seal for Viola. In addition, the Kinderhook above Viola has intervals with high entry pressure about 100 psi and more. Salem limestone has a few discrete intervals with high entry pressure and the Mississippian reservoir has also a few discrete high entry pressure intervals that are seals for Osage. In addition to the seals in the Mississippian, there is a thicker seal above the Mississippian (5,000–5,080 ft) that prevent any bypassed CO_2 from migrating up.

Sealing integrity was only assessed in Cutter KGS1 and well-to-well correlation technique can give lateral continuity and thickness of the cap rock formation across the field.

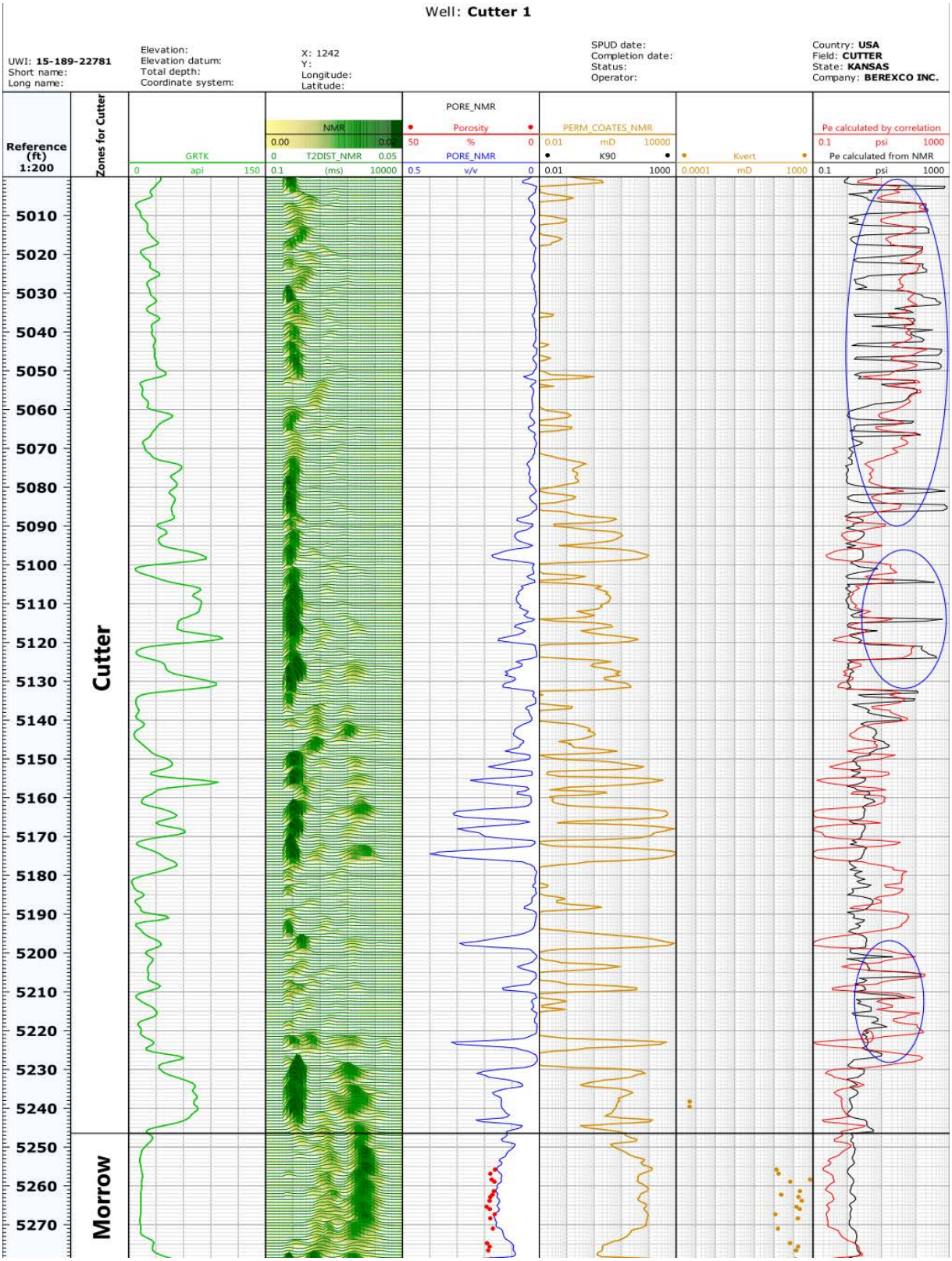

Figure 17: Layout of calculated entry capillary pressures by two methods, pore size distribution vertical and horizontal permeability. Figure 14 continues onto the next five pages.

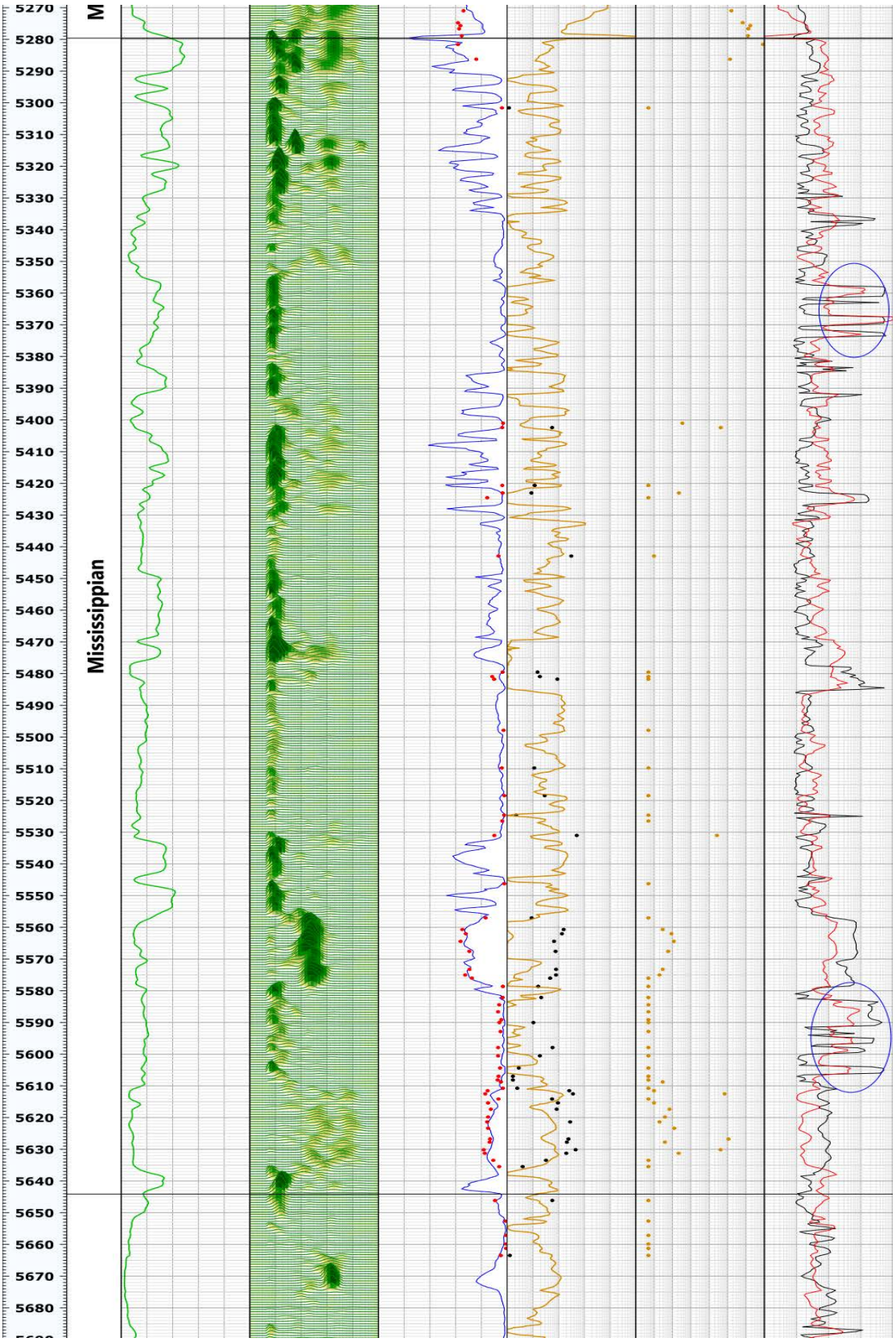

Figure 17, continued

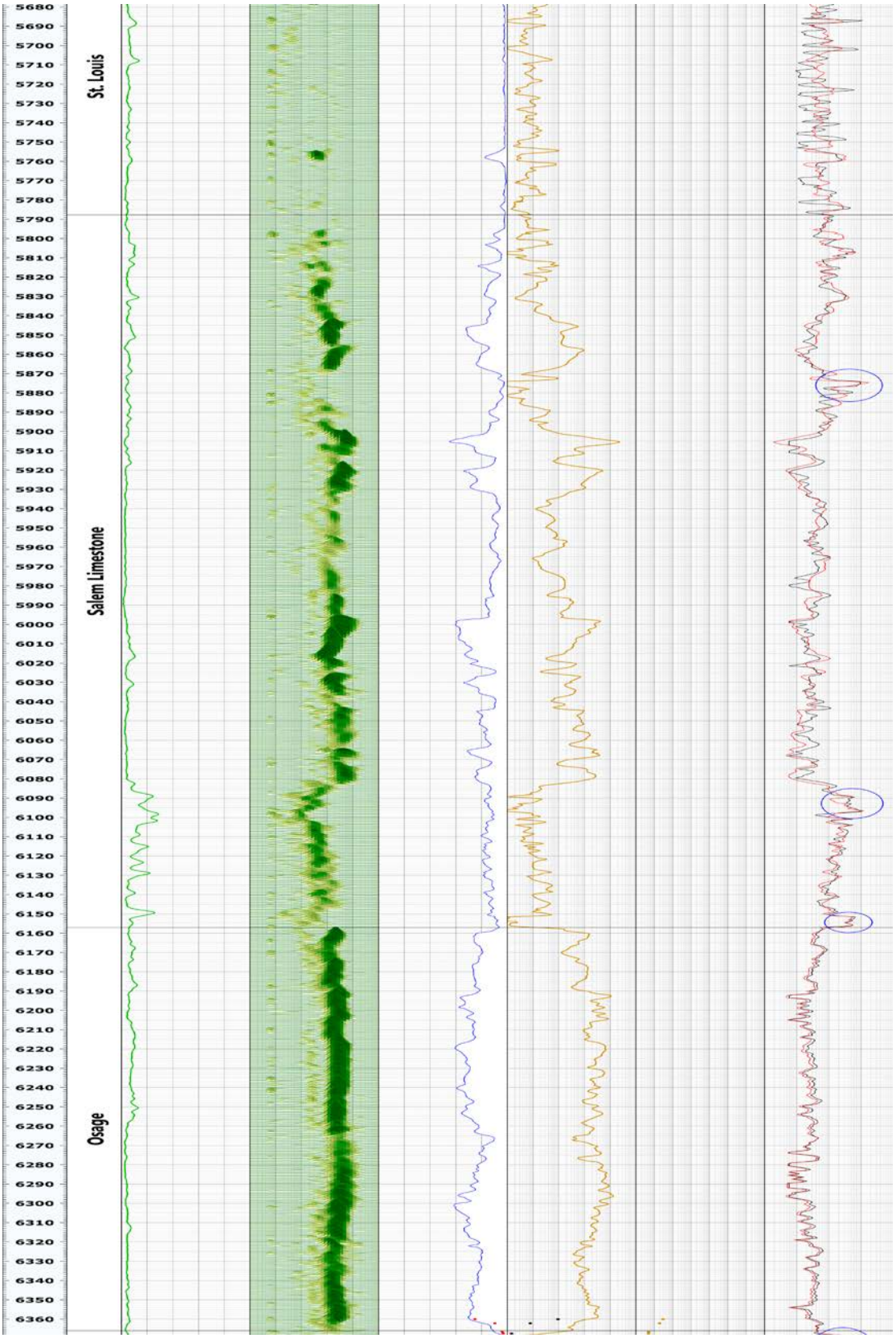

Figure 17, continued

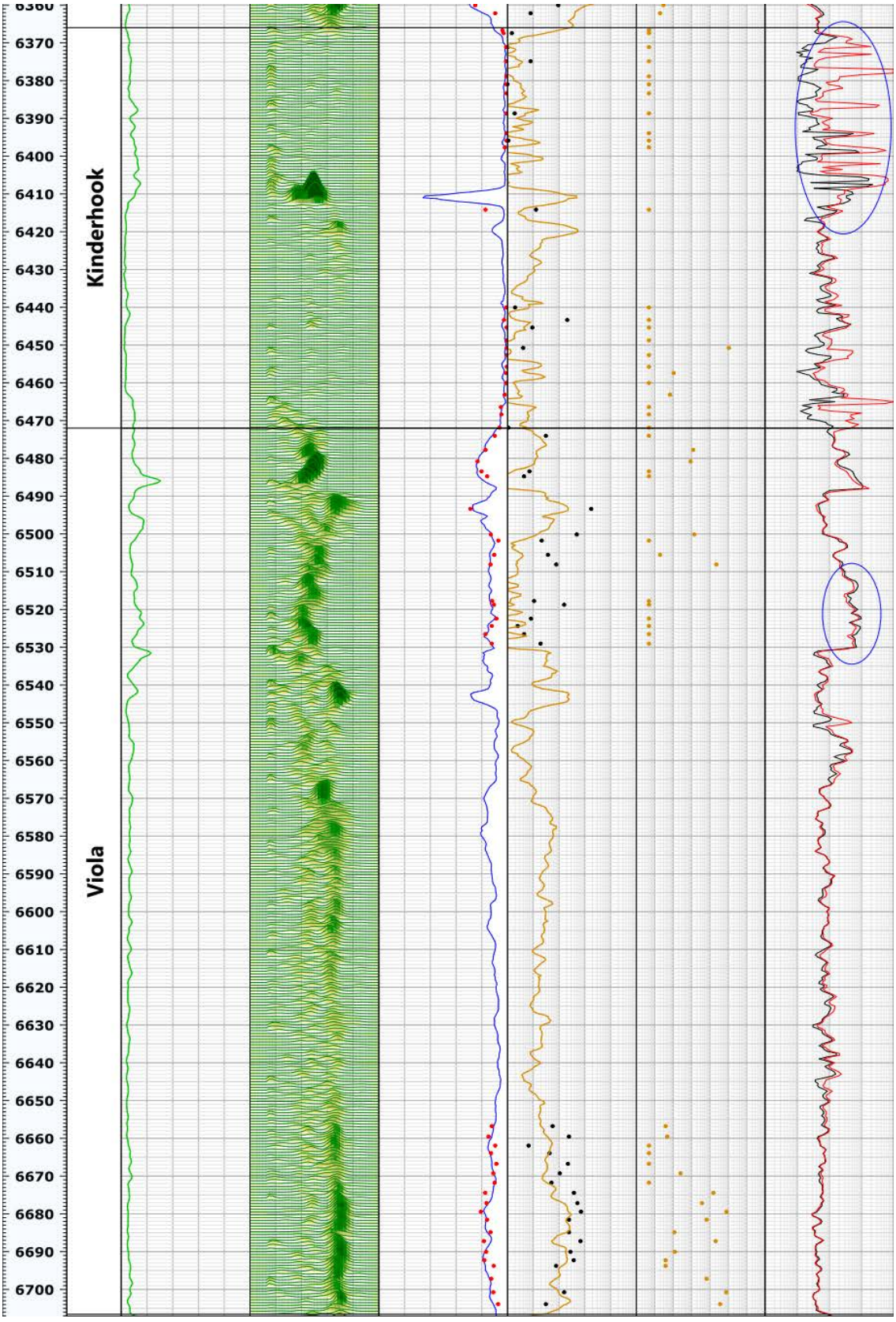

Figure 17, continued

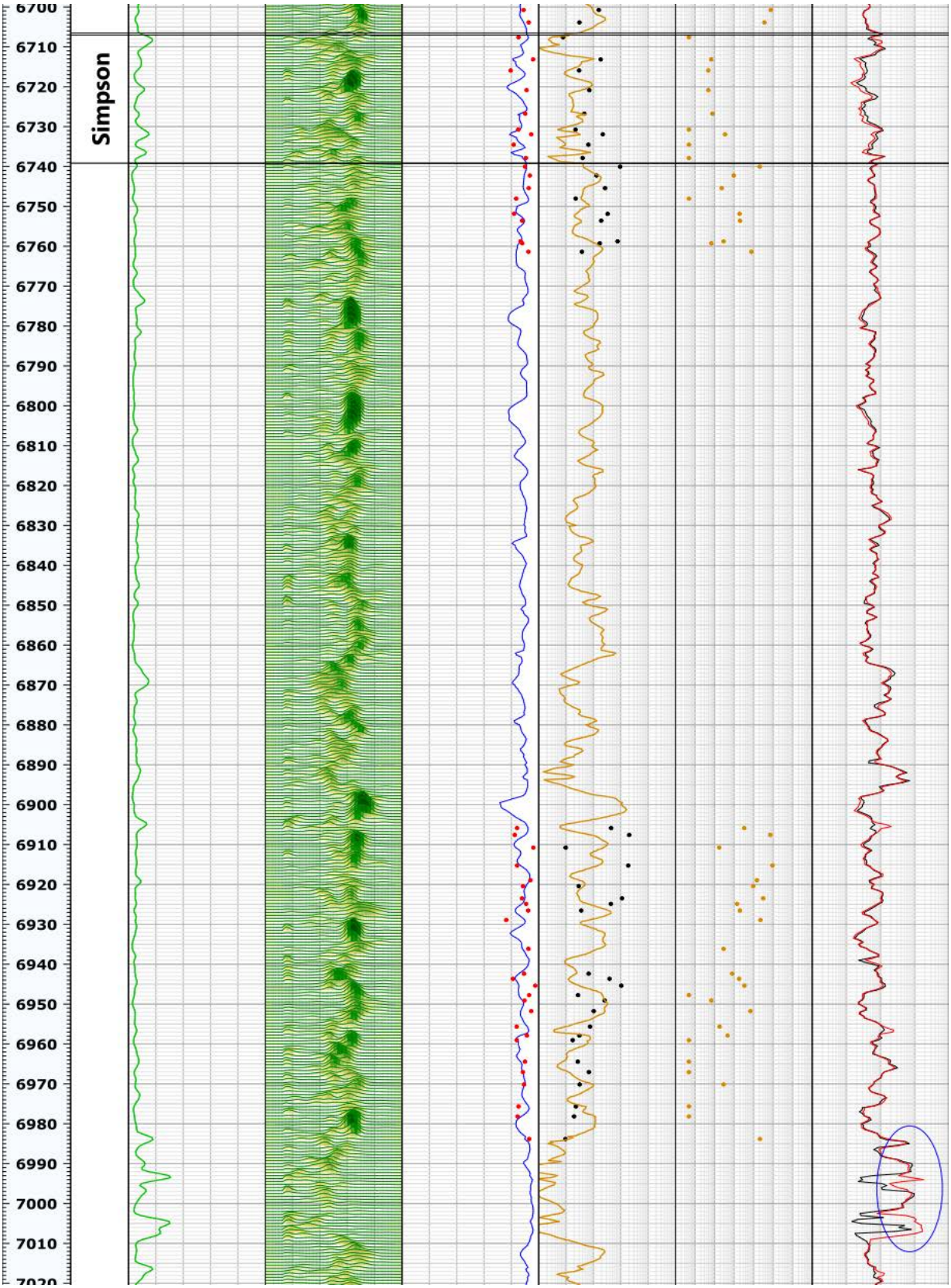

Figure 17, continued

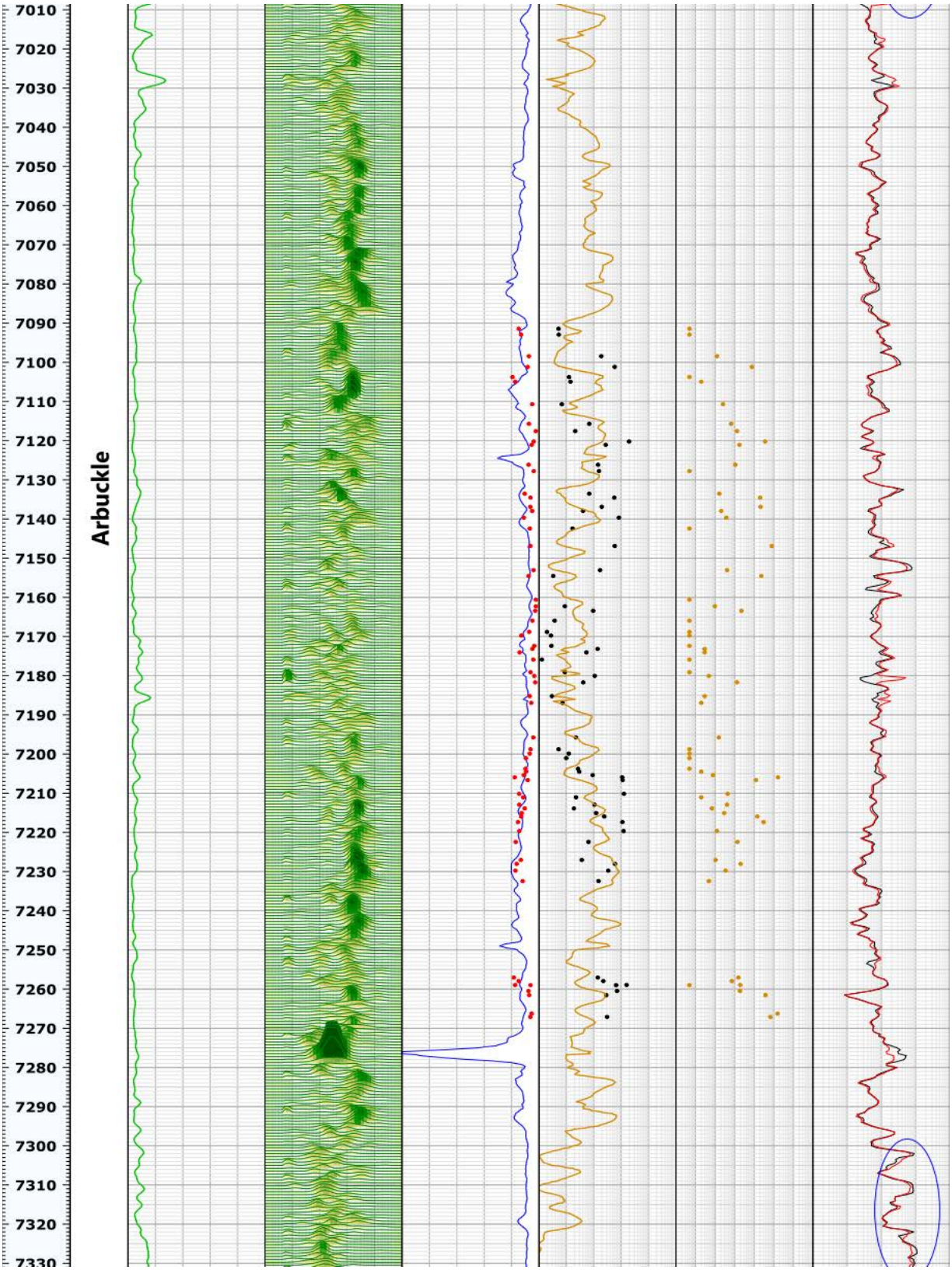

Figure 17, continued

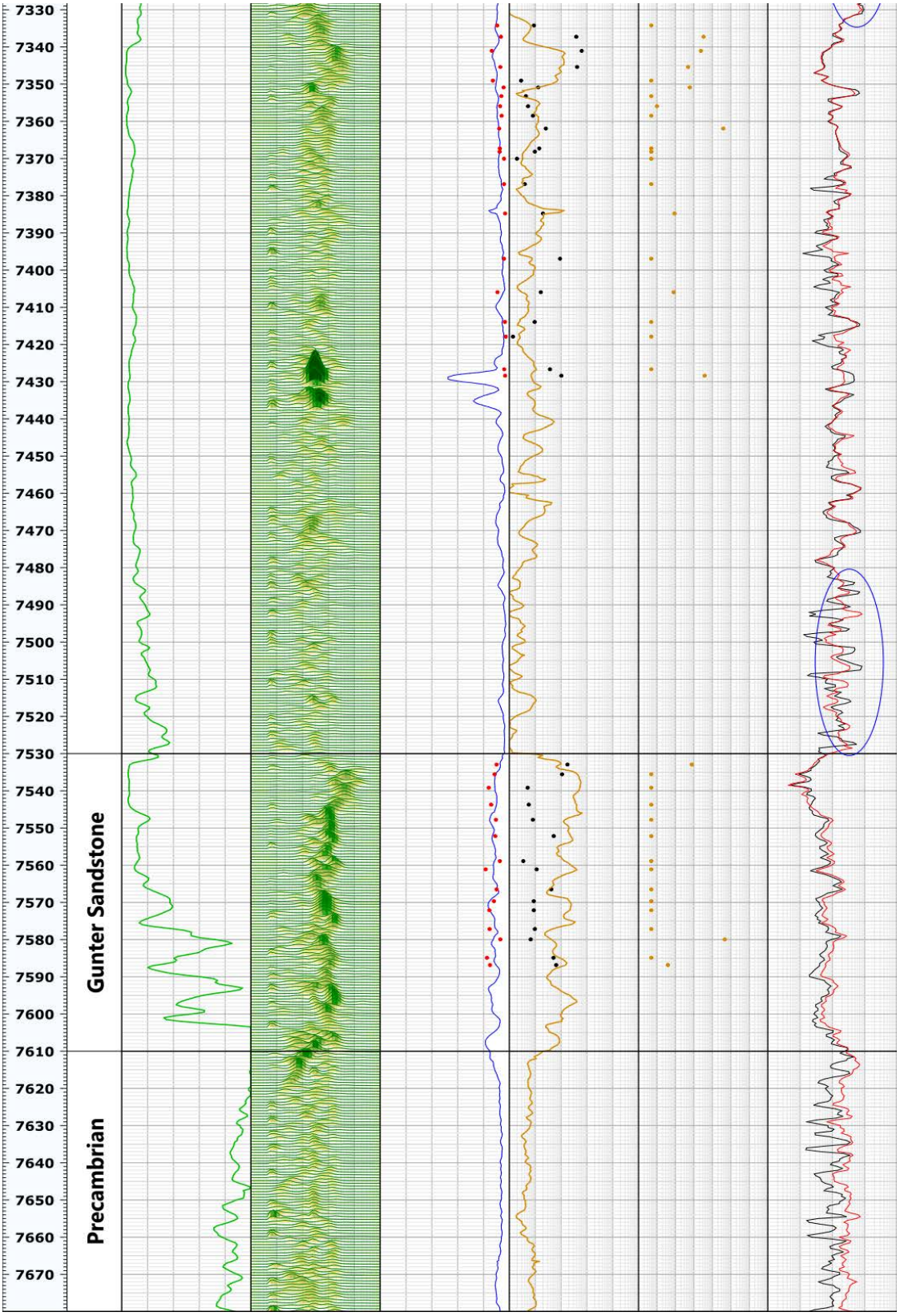

Figure 17, continued

Appendix F: Brine geochemistry and implications for seal efficiency in the North Hugoton Storage Complex

David Newell, Kansas Geological Survey

The following is a compilation of two water geochemistry reports covering three geological sites in the North Hugoton Storage Complex: Pleasant Prairie, Lakin, and Patterson.

Pleasant Prairie and Lakin geological sites

Comparison of salinities in the reservoirs at the Pleasant Prairie and Lakin fields (Fig. 1) has utility for inferring the potential for cross-stratigraphic flow, or *leakage*, between reservoirs. Gradually increasing or similar salinity with depth regardless of apparently separate reservoir may indicate communication between reservoirs. Conversely, contrasts in the salinity of the waters in the principal reservoirs of the fields may indicate that the reservoirs are isolated from each other, in that drastic salinity contrasts would not be expected for reservoirs in close hydraulic communication. Salinity contrasts thus may assure that each reservoir will not readily leak when they are separately charged with CO_2. Salinity data were therefore examined for the Chester Mississippian, underlying Mississippian carbonates, Viola, Simpson, and Arbuckle reservoirs.

There are four basic sources of information on salinity: the Kansas Geological Survey on-line brine database, chemical analyses of produced water donated by oilfield operators, salinity analyses reported for water recovered in drill-stem tests, and salinity determined from geophysical well logs. For the Pleasant Prairie area, no operator-donated analyses were available.

Sixteen (16) analyses (A though P in Fig. 1) were from DST chlorinity and salinity field measurements. Scans of DST tests are available on-line at the Kansas Geological Survey website. Two (2) analyses (Q and R in Fig. 1) were available from the KGS on-line brine database. Salinity measurements from DSTs or swab tests from the KGS Cutter well, 22 miles to the south of Pleasant Prairie Field, were available from DOE quarterly reports, via personal communication from Kansas Geological Survey Scientist Mina Fazelalavi. The Cutter #1 well represents the nearest locality where there is a spread of salinity measurements over several geologic formations. The well-log resistivity method (Doveton, 2004) was employed to generate most of the salinity data.

The well-log resistivity method uses a rearrangement of the Archie Equation to determine the resistivity of formation water (Rw). Rw is then converted to a salinity measurement (Doveton, 2004). Input into the formula includes porosity and resistivity measurements, usually averaged over a 2 ft vertical interval. The porosity used is an average of the neutron and density porosity measurements. The resistivity measurement is that of the deep induction log, so as to measure resistivity away from the vicinity of the well bore, which is subject to the effects of drilling mud and mud filtrate. Reservoir intervals with >50 API gamma ray units were not used in the analysis (so the effects of shaliness could be avoided), nor were tight zones measured where porosity is <8%. Oil-bearing zones were ignored, so that any resistivity measured in any given reservoir would be due principally to that of the formation water.

The well-log salinity measurements at Pleasant Prairie were from the H&P #16 USA 'A' well. Porous carbonates in the Mississippian in this well show drastically varying salinity—from dense basinal brines approaching 200,000 ppm, to dilute brines with ~20,000 ppm salinity—over narrow depth ranges (< 100 ft). Although Upper Ordovician Viola water in the H&P #16 USA 'A' well is generally more saline than Mississippian water (Fig. 1), water from the deeper Middle Ordovician Simpson sandstones is less saline than the Viola. The deepest geologic formation examined—the Cambrian-Ordovician Arbuckle—has varying salinity with depth. Several measurements in the Cutter well in the Arbuckle also show varying

salinity.

The varying salinity with depth, both sharply within the Mississippian carbonates and salinity varying between different formations at depth, indicates that there is likely no natural communication between waters in the various porous zones at Pleasant Prairie and Lakin. No susceptibility of natural leakage of sequestered CO_2 out of the Mississippian and deeper reservoirs is thus indicated, although impermeable beds between the porous units can be thin.

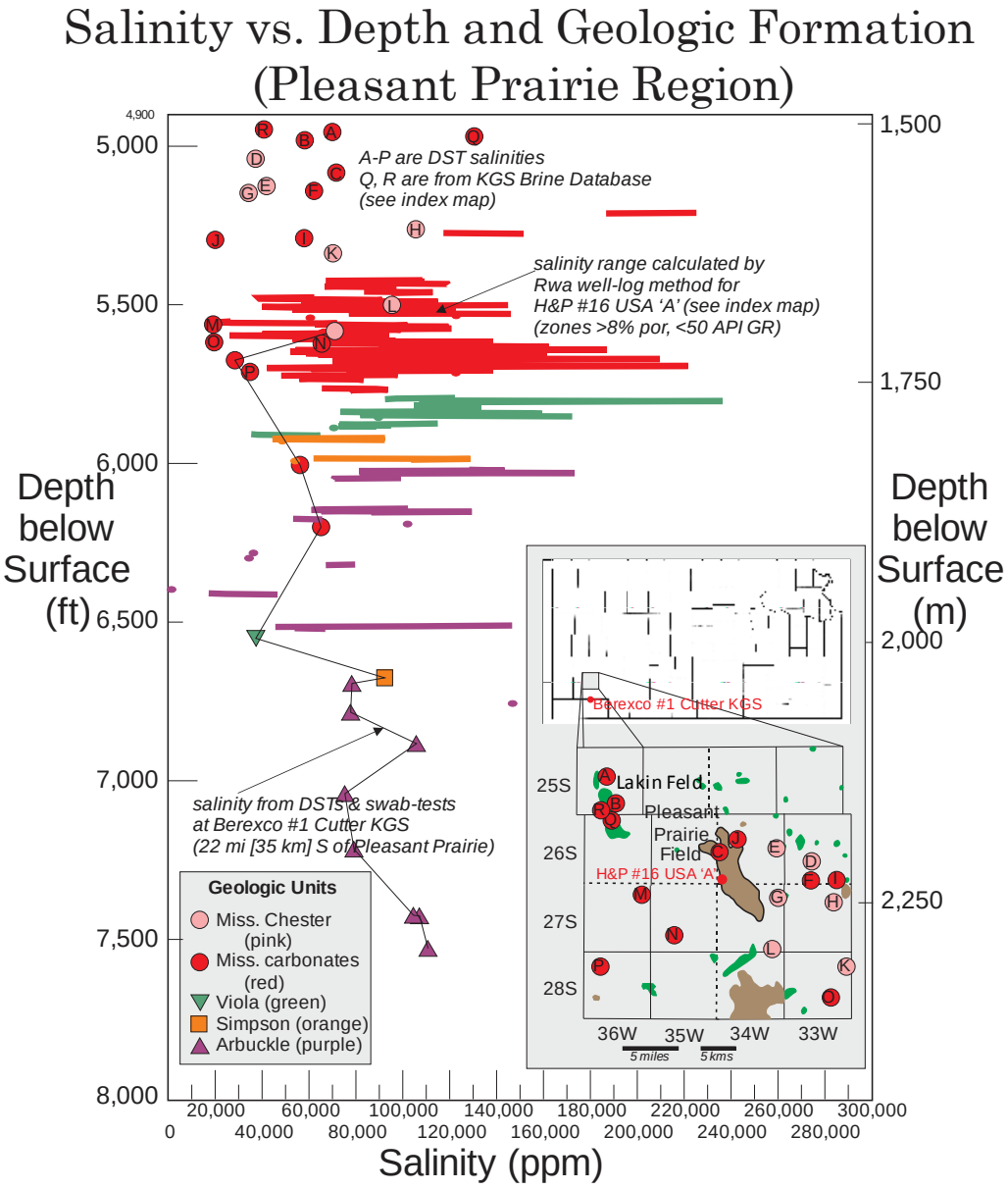

Figure 1. Salinity vs. depth of porous zones in the vicinity of Pleasant Prairie Field, southwestern Kansas. Measurements from swab tests and DSTs and production water are designated by geometric figures (circle, square, triangle) whereas calculated salinities from geophysical well logs are smaller dots and lines. Geologic formations are also color-coded.

Patterson geological site

There are only isolated salinity and total dissolved solids (TDS) analyses in the Patterson geologic site region (Patterson, Heinitz, and Hartland oil pools). Most of these are isolated drill-stem tests with limited recovery of formation water. Lacking these direct salinity measurements, well-log techniques can be employed to determine salinities. These techniques are outlined in Doveton (2004) and in this particular region around the Patterson site, the deep induction resistivity log and neutron-density porosity measurements are used. In order that the apparent resistivity (Rwa) of the water can be determined by well-log analysis, no hydrocarbons can be present in the porous zones analyzed. Off-structure wells are thus better for this type of analysis. In addition, the zone being analyzed cannot be too shaly, thus all depth intervals with 50 or greater API gamma-ray units were ignored. The minimum porosity (average of the neutron and density measurements) considered for analysis is 8%, and the minimum thickness of the porous zone has to be 2 feet or greater, otherwise the induction log focal area will also read higher than normal resistivity due to the effects of the induction device also reading any non-porous strata adjacent to the porous zones of interest.

Salinity by depth is plotted for three deep wells analyzed in Figure 2. If the porous zones in each well were in vertical communication by either fluid-transmitting faults or stratigraphic contact, then a steady increase in salinity with depth would be expected, because highly saline water, being denser would sink, or seek out, the lowest level to which it could settle. Concomitantly less-saline (and less dense) water would be displaced upward. However, water within the Viola and Arbuckle in all three wells decreases in salinity with depth within each unit. Physical separation, or impermeability of the nonporous units between porous zones in each unit is thus indicated. Porous zones in the Mississippian (Meramec, Spergen, Warsaw, Osage) of each well are more vertically isolated than in the sub-Mississippian units. The varying salinity of each of these porous zones in the Mississippian implies that they are also isolated from each other. The Osage appears to have the most laterally contiguous porous zones of the Mississippian sub-units.

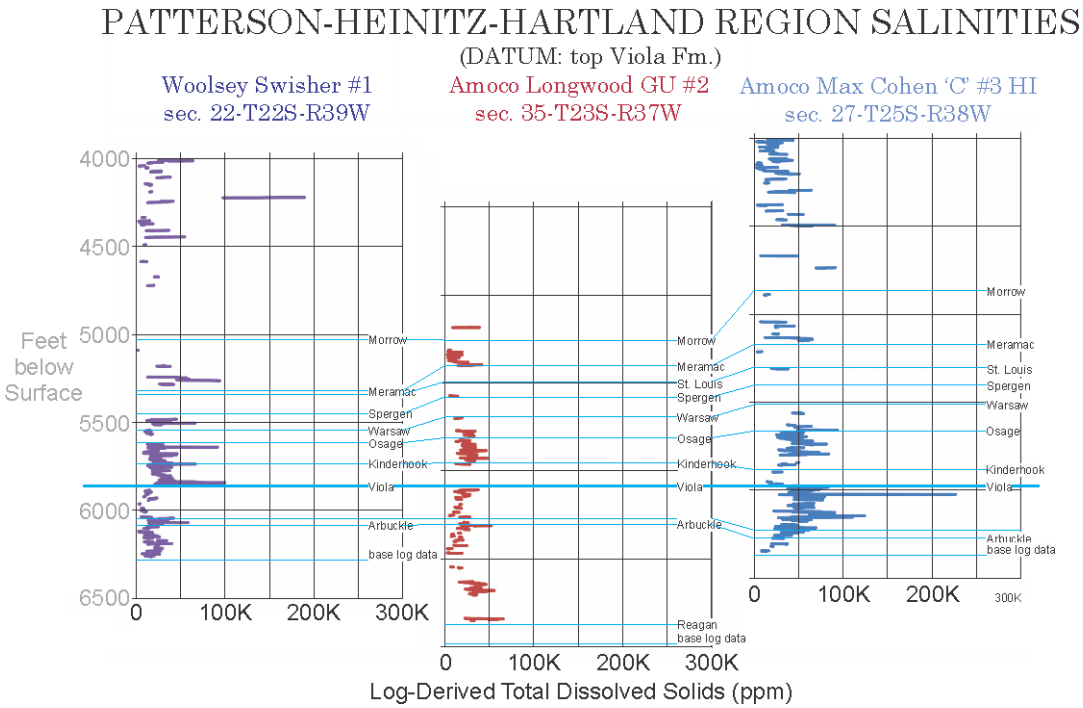

Figure 2. Salinity vs. depth plots for three wells in the Patterson site area. Cross section datum is the top of the Viola.

In general, salinity increases regionally southward toward the Cohen well. The Longwood well generally has the least porosity. Some zones in the Pennsylvanian above the Morrow in all three wells can have relatively fresh water (5,000–10,000 ppm TDS). The reason for this is unclear, but perhaps these porous zones are physically isolated from ion-contributing shales, or perhaps are subject to being washed by relatively fresh water coming in from near the surface. Like the salinity that characterizes the Mississippian, salinity in the Arbuckle is relatively low (~25,000 ppm TDS). This salinity level exceeds that of the maximum for potable water (i.e., 10,000 ppm TDS), but is less than that of sea water (i.e., 34,000 ppm TDS).

Reference

Doveton, J. H., 2004, Applications of estimated formation water resistivities to brine stratigraphy in the Kansas subsurface: Kansas Geological Survey, Open-File Report 2004-22, 20 p.

Appendix G: Assessing CO_2 injection risks using NRAP (National Risk Assessment Partnership) Tools

Esmail Ansari[1] and Martin K. Dubois[2]
[1] Kansas Geological Survey, [2] Improved Hydrocarbon Recovery, LLC

Reservoir Evaluation (REV) tool: REV tool from NRAP (King, 2016a) is used to assess CO_2 injection into the Osage, Viola and Arbuckle formations at the Patterson Field. The REV tool uses the results from other simulators and visualizes several important metrics for studying the response of the formation to carbon storage. These metrics include CO_2 plume size and pressure plume size. Obtaining these metrics are useful for determining the post injection fate of the carbon dioxide such as the post shut-in decay rate of pressure, plume growth rate in a long-term period, and maximum pressure increase at the shut-in time.

The inputs of the REV tool are the pressure and saturations for all grid-blocks as time-series obtained from reservoir simulation models. The tool has a defined threshold for pressure and saturation and calculates the differential pressure and CO_2 plume size in all grid blocks, and then maps it into a 2-D horizontal surface to visualize the area of plume and its evolution through time. The saturation threshold defines the extent of the CO_2 plume and is set to 0.2 in the current study while the pressure threshold defines the extent of overpressure front, depends on factors such as wellbore pressure and is set to 400 psi as deemed appropriate for the study. Other parameters in the tool, such as depth of the storage reservoir or brine density, are the same as values used in the reservoir simulation model.

The REV tool was not able to process the corner point grids. We created an equivalent regular-rectangular Cartesian grid for our corner point gridding of the Patterson area (Figure 1). The REV metrics for assessing CO_2 injection into the Arbuckle and Osage formations are shown in Figures 2–5. The REV tool version 2018 is used in this study.

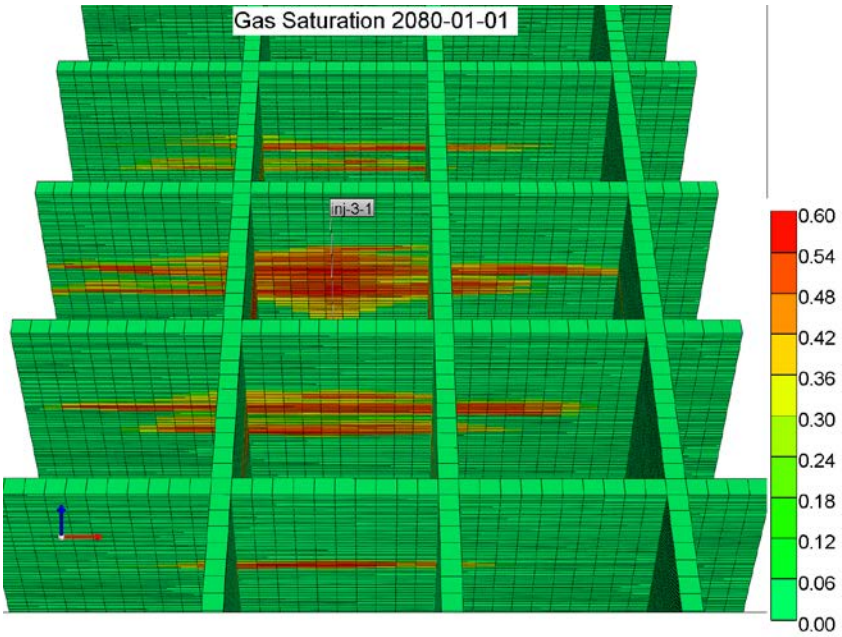

Figure 1: Projected grid blocks from corner point to the Cartesian grid. The figure shows the CO_2 plume in the Osage formation after 60 years (30 years of injection).

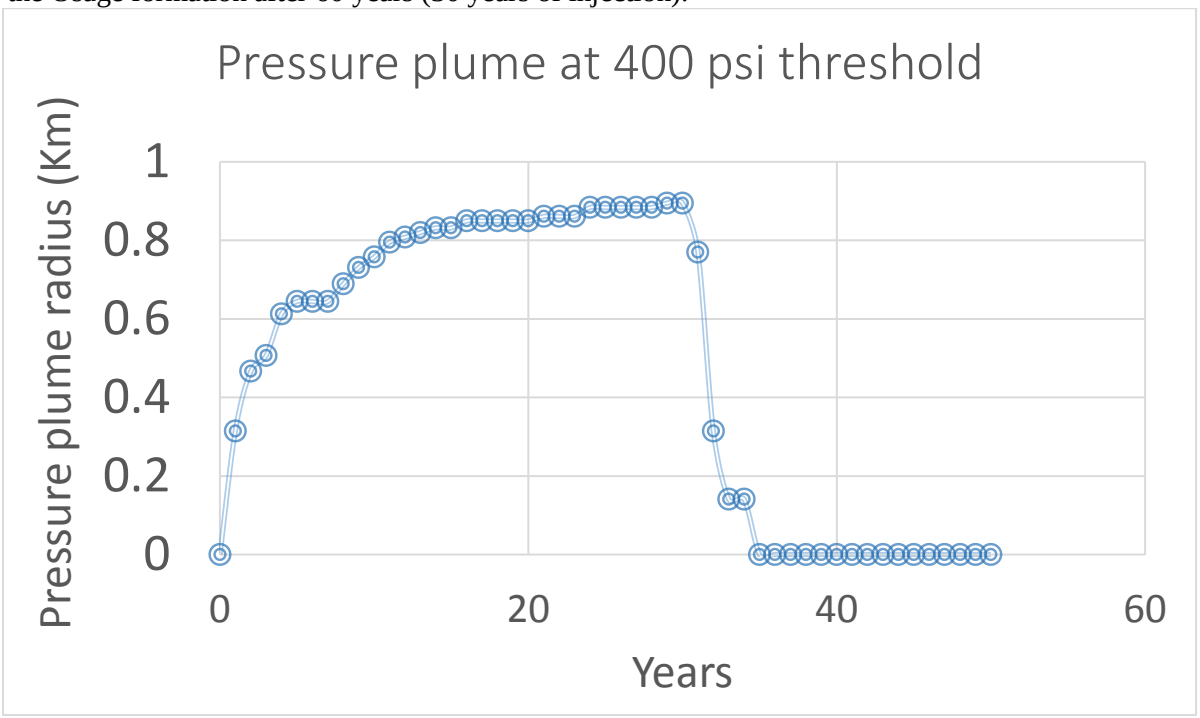

Figure 2: Pressure plume evolution in the Arbuckle. Injection stops after 30 years, and within ~5 years the overpressure plume dissipates in the Arbuckle formation.

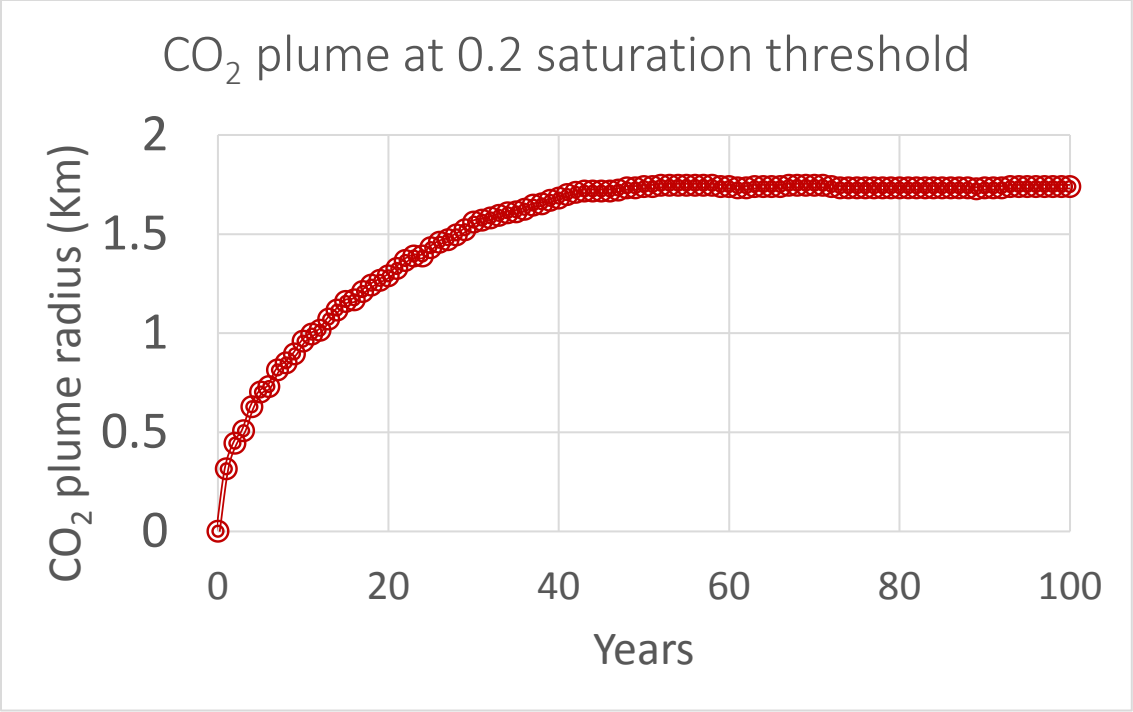

Figure 3: CO_2 plume evolution at 0.2 saturation threshold in the Arbuckle formation. The plume growth decreases after the injection period (30 years), and its growth stops after another ~15 years at ~1.75 km distance from the well.

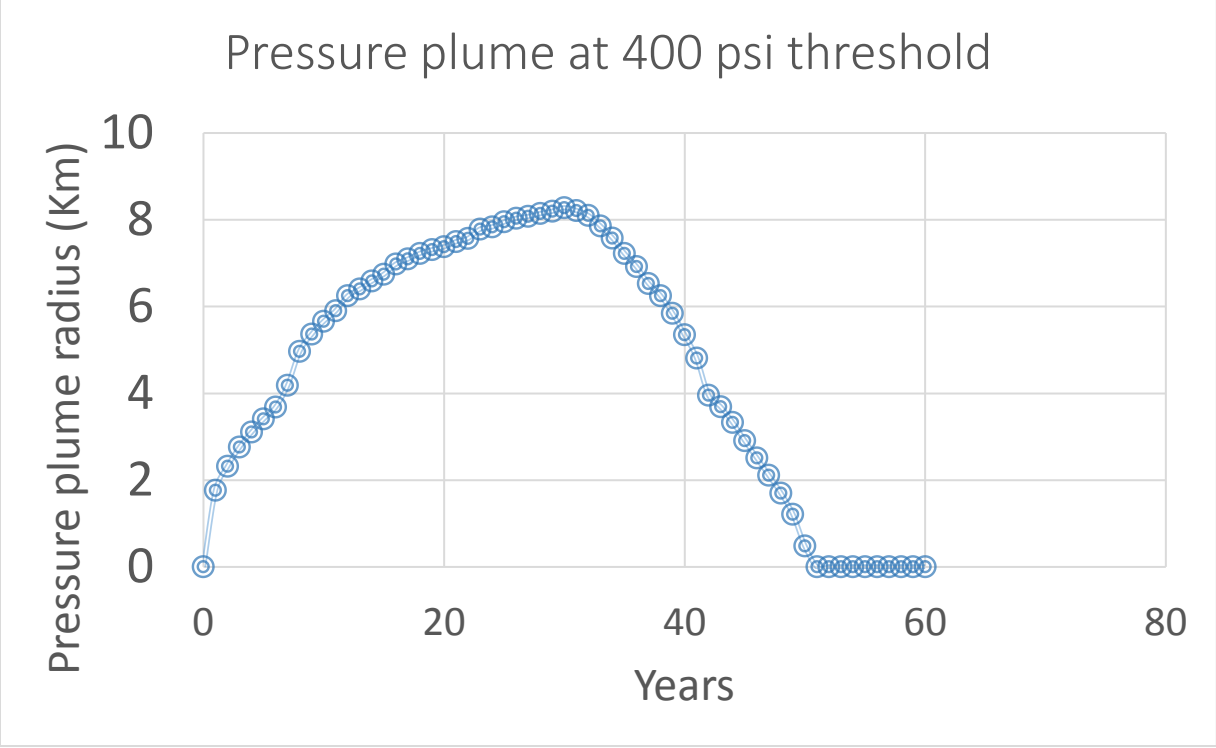

Figure 4: Pressure plume evolution at 400 psi threshold in the Osage formation. The overpressure plume dissipates in the formation and disappears 20 years after shut-in (30 years).

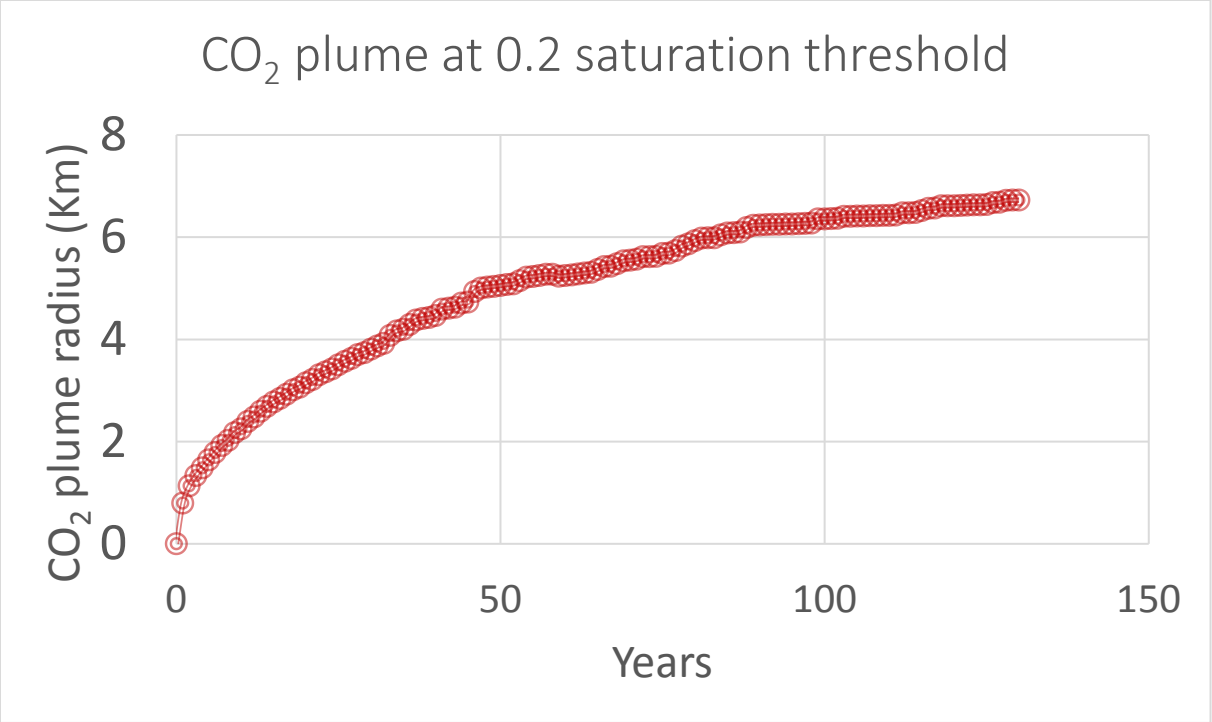

Figure 5: CO_2 plume evolution at 0.2 saturation threshold in the Osage formation. The CO_2 plume reaches a distance of ~4 km; after the injection stops (30 years), its slower rate growth reaches 6 km after ~90 years.

NSealR (NRAP Seal Barrier Reduced-Order Model) tool: NSealR offers a one-dimensional model for analyzing two-phase flow of supercritical CO_2 through brine-saturated rock (Lindner, 2016). This toolkit uses a 1-D Darcy equation to describe the flow and leakage of CO_2 through the seal (i.e., low permeability rock) and uses two-phase (CO_2-brine) relative permeability models.

We use NSealR to quantify and assess the leakage risk of injected CO_2 into the Arbuckle, Osage and Viola groups in the Patterson Field. Simpson shale, Kinderhook and Spergen-Meramec are the caprock barriers for the Arbuckle, Viola and Osage, respectively. The main barrier is the thick, non-permeable limestone, Meramec-Spergen, overlying the Osage. Additionally, the Morrow shale, the seal of Kansas petroleum reservoirs, acts as the ultimate barrier. Tables 1 and 2 summarize the properties of the seals used in the NSealR tool. Morrow shale properties are based on the S1537 and S1461 samples presented by Krushin (1997).

Table 1: Range of properties of the caprock seals.

Caprock seal $Min - Max$	Formation top (ft)	Elevation Depth (ft)	Thickness (ft)	Porosity	Horizontal Permeability (md)
Morrow-Chester shale	4,750	1,300–1,968	44.6–282.5	0.0141–0.18	0.0117–3.926
Morrow shale	4,750	1,300–1,968	40–70	1e-10–0.03	5.13e-11–0.001
Meramec limestone	4,900	1,435–2,028	0–225.4	1e-10–0.1	1e-10–0.6832
Lower Meramec	4,965	1,500–2,111	28.6–126.8	1e-10–0.12	1e-10–0.9315
Spergen limestone	5,100	1,578–2,235	82.63–124.8	1e-10–0.16	1e-10–76.061
Kinderhook limestone	5,475	1,900–2,646	102.5–168.8	1e-10–0.2	0.0021–5.45
Simpson shale	5,775	2,170–2,853	19.9–35.57	0.0334–0.14	0.1–69.11

Table 2: μ_x and σ_x for the properties of the caprock seals.

Caprock seal	Porosity μ_x, σ_x	Horizontal Permeability (md) μ_x, σ_x
Morrow-Chester shale	0.0458, 0.0231	0.269, 0.4357
Morrow shale	0.022, 0.010	5.1e-6, 0.001
Meramec limestone	0.0249, 0.0201	0.0677, 0.122
Lower Meramec	0.0260, 0.0182	0.0739, 0.1321
Spergen limestone	0.0265, 0.0180	0.7696, 4.3102
Kinderhook limestone	0.0587, 0.0319	0.5784, 0.7846
Simpson shale	0.0682, 0.0201	2.0850, 2.4329

The vertical permeability is assumed to be 0.1 of the horizontal permeability. The maximum and minimum values for the vertical permeability are assumed to come from a log-normal distribution. We use NSealR's default relative permeability and capillary pressure model for caprock. At a reference depth of 5,260 ft, the reference brine pressure is 1,650 psi and the reference temperature is 140 ºF. The salinity

is assumed to be 100 g/l. The affected seal area (i.e., maximum plume area) is calculated using CMG GEM to have an average diameter of 2.9 mile (4.6 km), when approximately 8 Mt CO_2 is injected per well into the Osage (storage zone below Meramec). We sampled 50 realizations using the Monte Carlo method. Figures 6–9 show the seal assessment results for the Morrow shale and Meramec limestone, the topmost seal barriers.

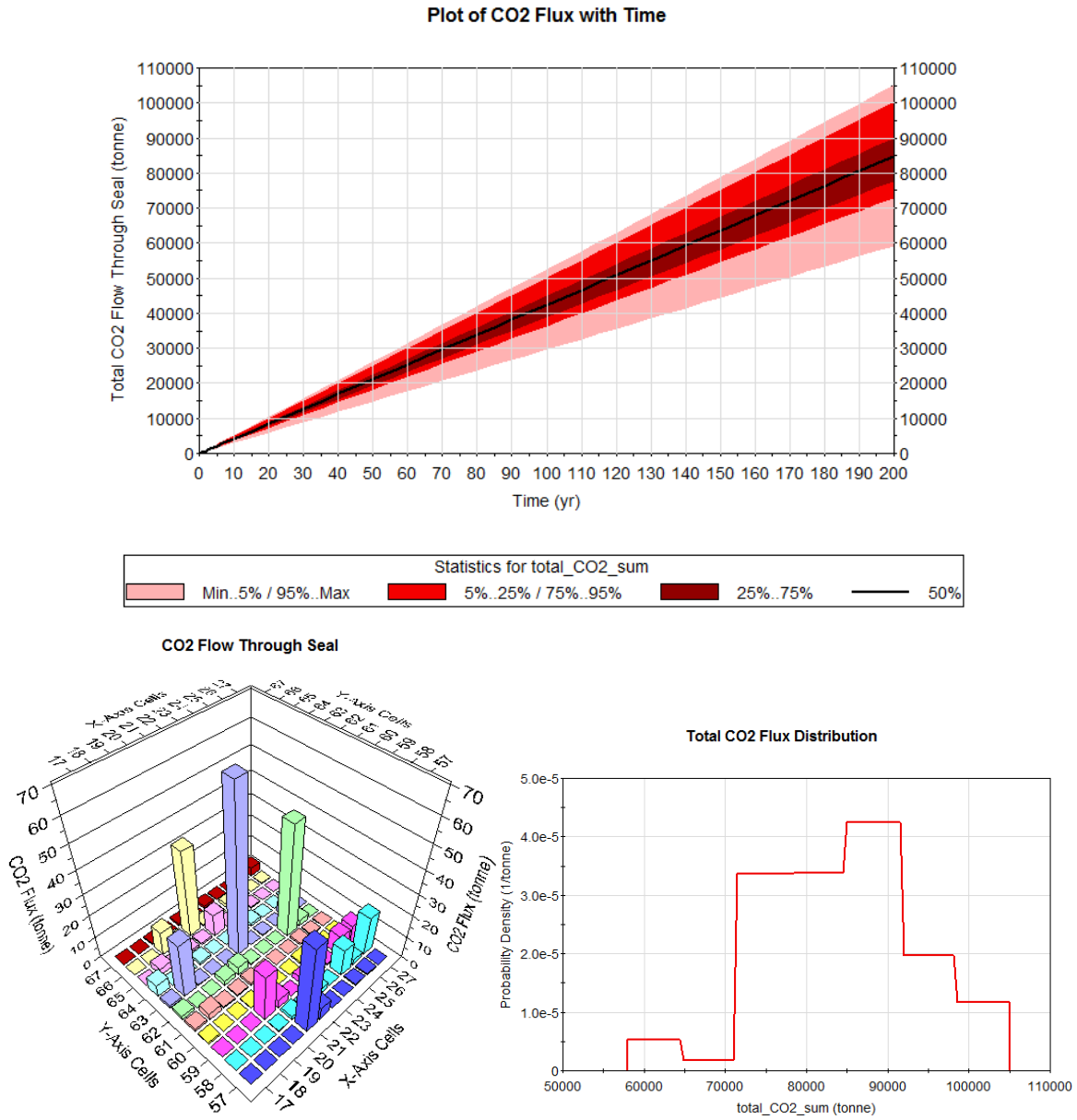

Figure 6: CO_2 flux through the Morrow shale. The top figure shows total CO_2 leakage and its corresponding probability versus time. The bottom left figure shows one realization for the CO_2 leakage rate assuming the entire seal is divided into 100 × 100 grid blocks. The bottom right figure shows the probability distribution for total CO_2 leakage.

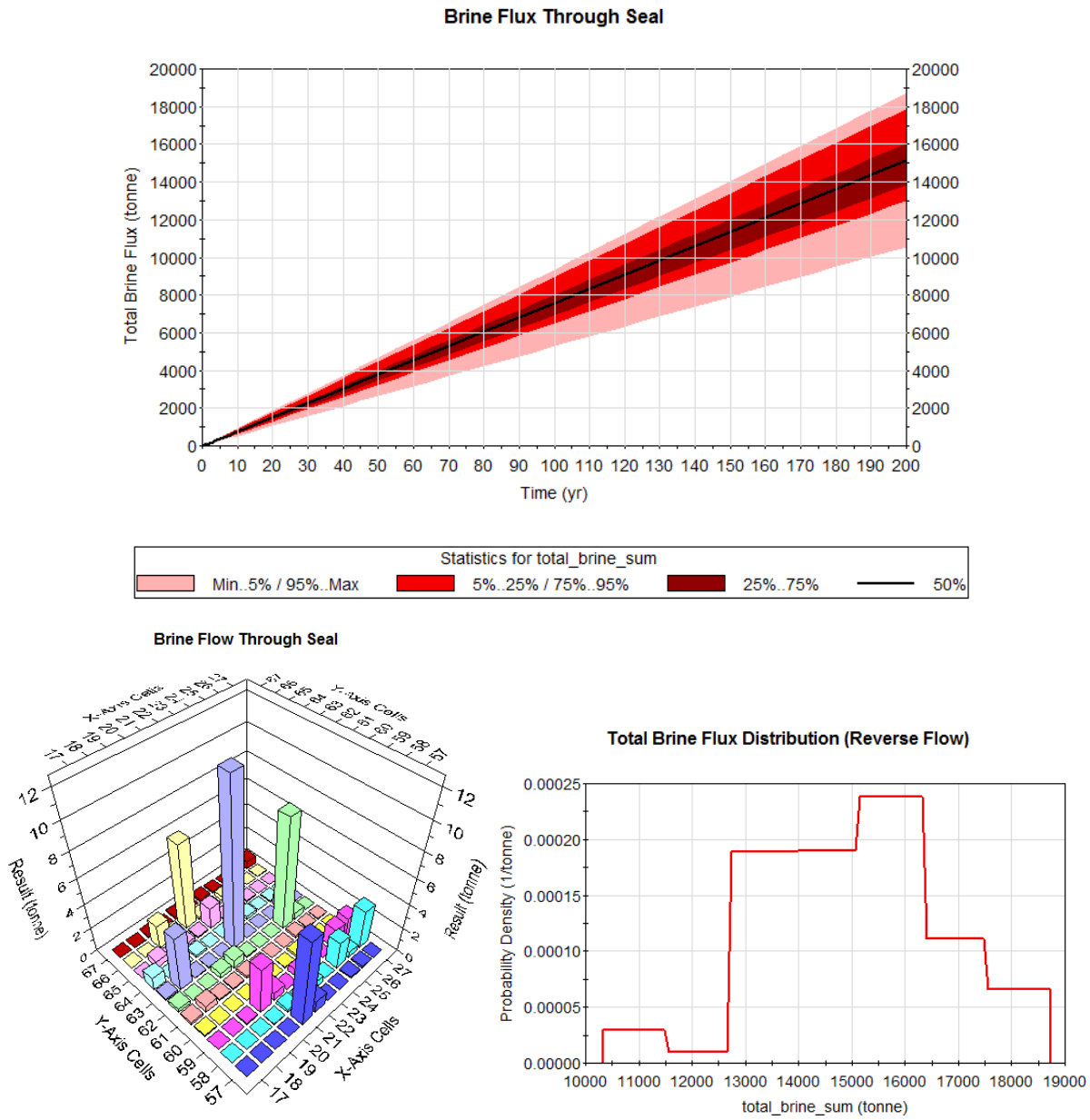

Figure 7: Brine flux through the Morrow shale. The top figure shows total brine leakage and its corresponding probability versus time. The bottom left figure shows one realization for the brine leakage rate assuming the entire seal is divided into 100 × 100 grid blocks. The bottom right figure shows the probability distribution for total brine leakage.

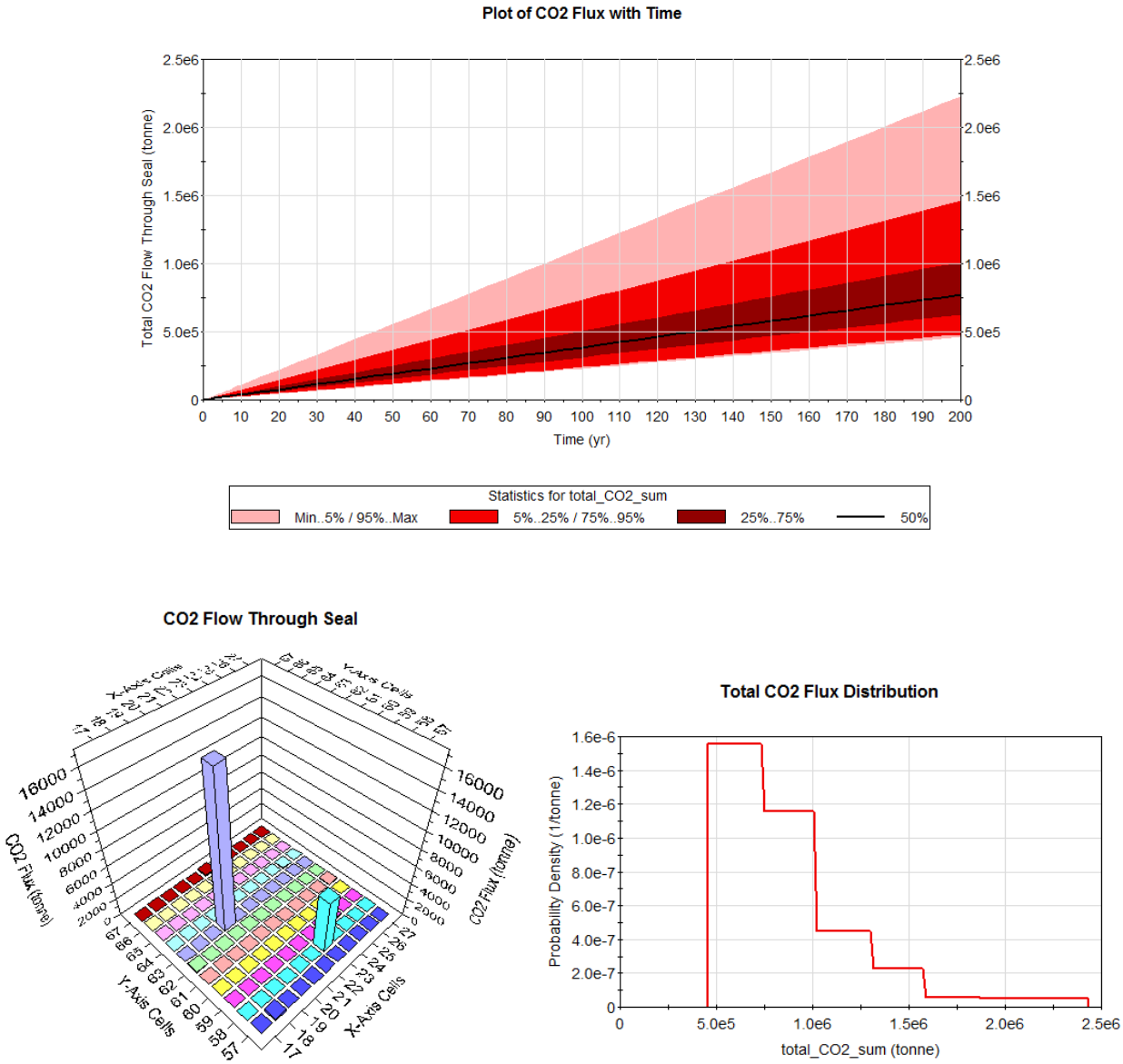

Figure 8: CO_2 flux through the Meramec limestone. The top figure shows total CO_2 leakage and its corresponding probability versus time. The bottom left figure shows one realization for the leakage rate assuming the entire seal is divided into 100×100 grid blocks. The bottom right figure shows the probability distribution for total CO_2 leakage.

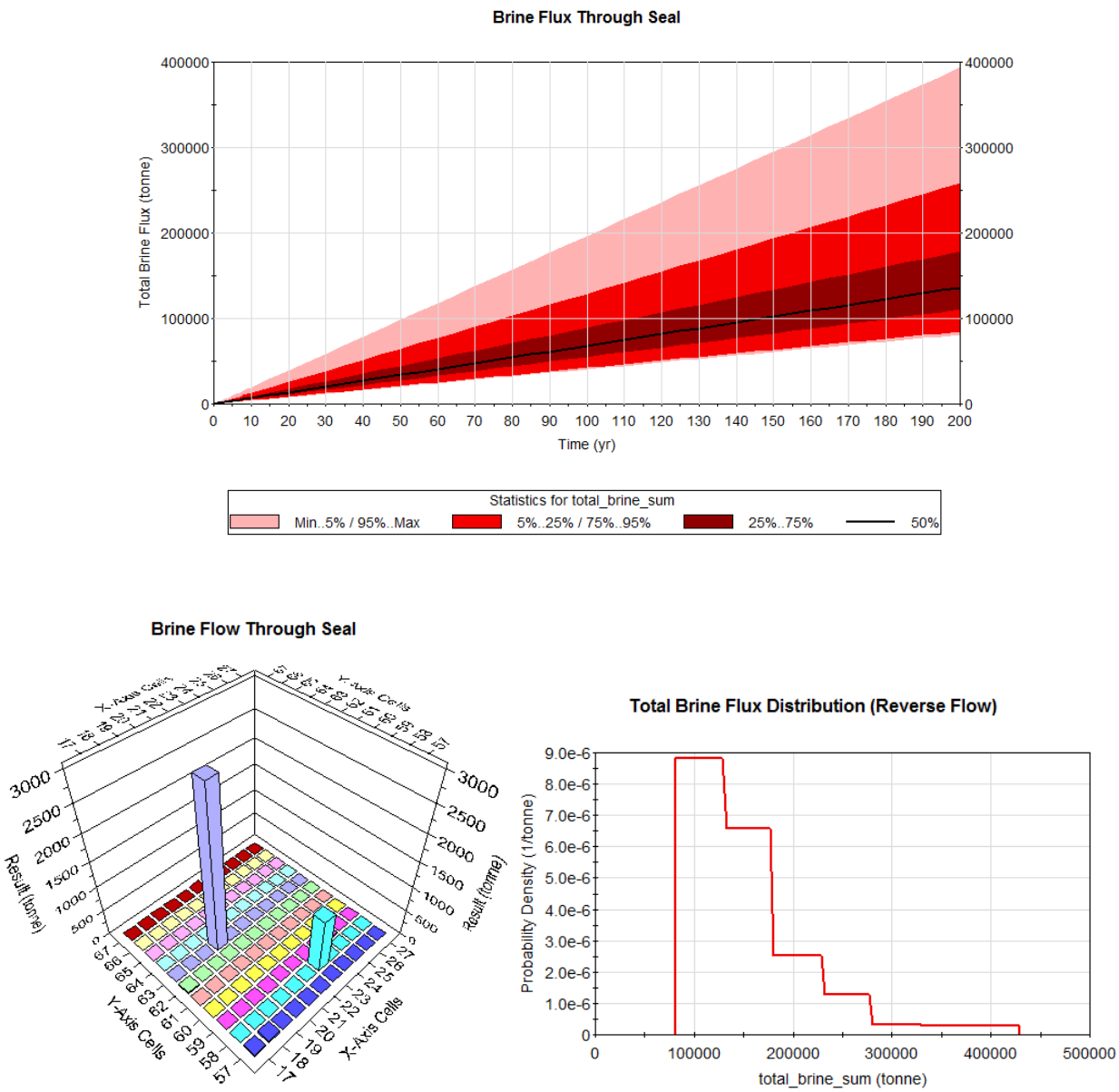

Figure 9: Brine flux through the Meramec limestone. The top figure shows total brine leakage and its corresponding probability versus time. The bottom left figure shows one realization for the leakage rate assuming the entire seal is divided into 100 × 100 grid blocks. The bottom right figure shows the probability distribution for total brine leakage.

NETL CO_2 –SCREEN: The US-DOE methodology known as NETL CO_2-SCREEN (Goodman, Sanguinito, & Levine, 2016) is used for estimating CO_2 storage potential in the Patterson area. The methodology is general and could be applied globally; however, we refined the required data using the currently available information for the Patterson area. The Patterson area is an open system (no impermeable boundary) with closures to vertically constrain and trap the injected CO_2 within the injected area. Thus the percentage of pore space that can be filled with CO_2 primarily depends on storage efficiencies and is independent of bottom hole pressure. The Patterson field has an approximated area of 50 mile^2 (129.5 km^2) with three potential injection formations: Osage (limestone), Viola (dolomite), and Arbuckle (dolomite). Table 3 summarizes the geological properties of each formation as needed by CO_2-SCREEN.

Table 3: Properties of the Patterson area.

Grid #	Area* (km^2)	Gross Thickness* (m)		Total Porosity* (%)		Pressure† (MPa)		Temperature† (°C)	
	Mean	Mean	Std Dev	Mean	Std Dev	Mean	Std Dev	Mean	Std Dev
1	129.5	45.72	0	12.3	6.4	11.38	0	53.89	0
2	129.5	54.86	0	7.5	2.5	11.51	0	55.56	0
3	129.5	173.7	0	5.4	3.7	11.72	0	58.33	0

The storage efficiency of the saline formations (G_{CO2}) is calculated by:

$$G_{CO2} = A_t h_{gross} \phi_{tot} \rho_{CO_2} E_{saline}$$

in which pore space ($A_t h_{gross} \phi_{tot}$) obtained using Table 3 parameters is multiplied by ρ_{CO_2} to convert to CO_2 mass in the reservoir and then multiplied by the storage efficiency factor for saline formations (E_{saline}), defined as:

$$E_{saline} = E_A E_h E_\phi E_v E_d$$

In which E_A is the net-to-total area, E_h is the fraction of total thickness that meets minimum permeability and porosity requirements, E_ϕ is the fraction of interconnected porosity, E_v is the volumetric displacement efficiency defining the volume that can be contacted by the CO_2 plume, and E_d is the microscopic displacement efficiency describing the fraction of water in water-filled pore volume that can be displaced by contacting CO_2. Table 4 summarizes the efficiency values based on Goodman et al., 2011. The E_A *and* E_h values are chosen higher than the global recommended values considering that the Osage, Viola and Arbuckle formations in the Patterson area have good net-to-total area and net-to-gross thickness. These values can be refined as more data become available.

Table 4: Storage efficiencies for the Patterson area.

Grid #	Lithology and Depositional Environment	E_A		E_h		E_ϕ		E_v		E_d	
		P_{10}	P_{90}	P_{10}	P_{90}	P_{10}	P_{90}	P_{10}	P_{90}	P_{10}	P_{90}
1	Limestone: Unspecified	0.6	0.9	0.85	0.95	0.64	0.75	0.27	0.42	0.33	0.57
2	Dolomite: Unspecified	0.6	0.9	0.75	0.85	0.53	0.71	0.57	0.64	0.26	0.43
3	Dolomite: Unspecified	0.6	0.9	0.35	0.65	0.53	0.71	0.57	0.64	0.26	0.43

Table 5 summarizes the injection capacity of each formation and the probability results the calculated storage efficiency factors (i.e. $p(E_{saline})$) assuming one grid block for each formation. The injection capacity of the Arbuckle and Osage are high because the former has high thickness and the latter has higher porosity and is limestone. Table 6 shows the total CO_2 capacity for the Patterson area. Results of Tables 5–6 are summarized in Figures 10–11.

Table 5: Calculated storage efficiency factors for each formation.

Grid	P_{10} (Mt)	P_{50} (Mt)	P_{90} (Mt)	Lithology and Depositional Environment	Saline Efficiency (%)		
					P_{10}	P_{50}	P_{90}
1	9.940	21.244	44.767	User Specified	4.54	7.21	10.57
2	9.887	17.570	30.728	User Specified	5.18	7.73	10.87
3	7.892	20.415	50.436	User Specified	2.79	4.72	7.32

Table 6: Calculated storage for the Patterson area.

	P_{10}	P_{50}	P_{90}	
Summed CO_2 Total	27.72	59.23	125.93	Mt
Average CO_2 per Grid	9.24	19.74	41.98	Mt

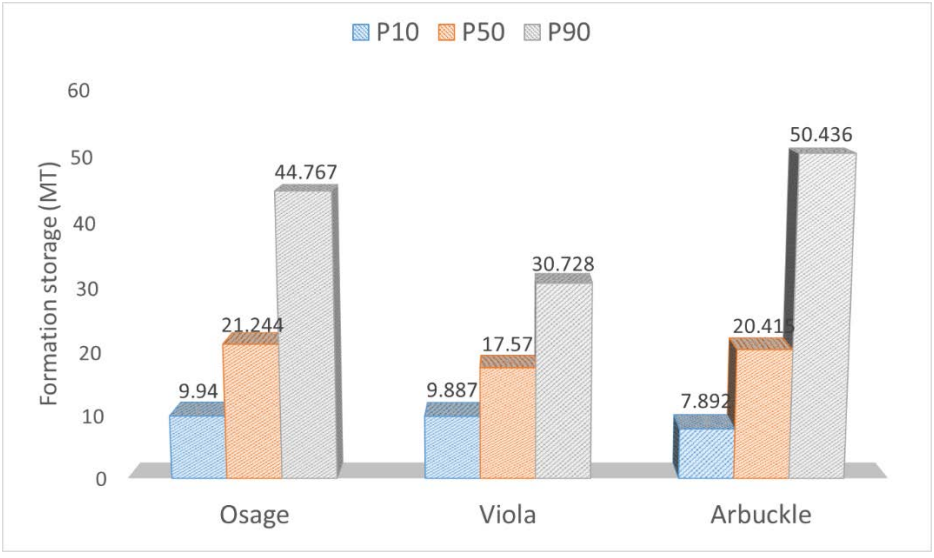

Figure 10: Formation capacity for the formations in the Patterson area.

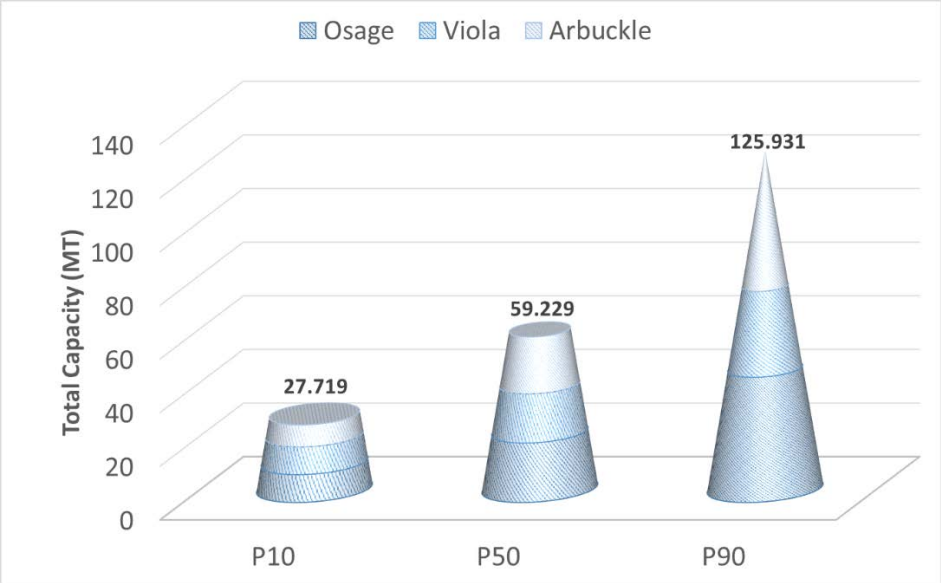

Figure 11: Maximum storage for the Patterson area.

RROM-GEN tool (Reservoir Reduced Order Model Generator): The RROM-GEN (King, 2016b) uses interpolation to reduce the simulation model dimension into a 100 × 100 grid blocks representation in the horizontal direction and outputs the file in a format readable by the Integrated Assessment Model (IAM) tool. The RROM-GEN also extracts a single layer for representing the reservoir-seal boundary. Figure 12 shows the reduced order model generated for the Patterson area. RROM-GEN version 2018 was obtained from the author for this study.

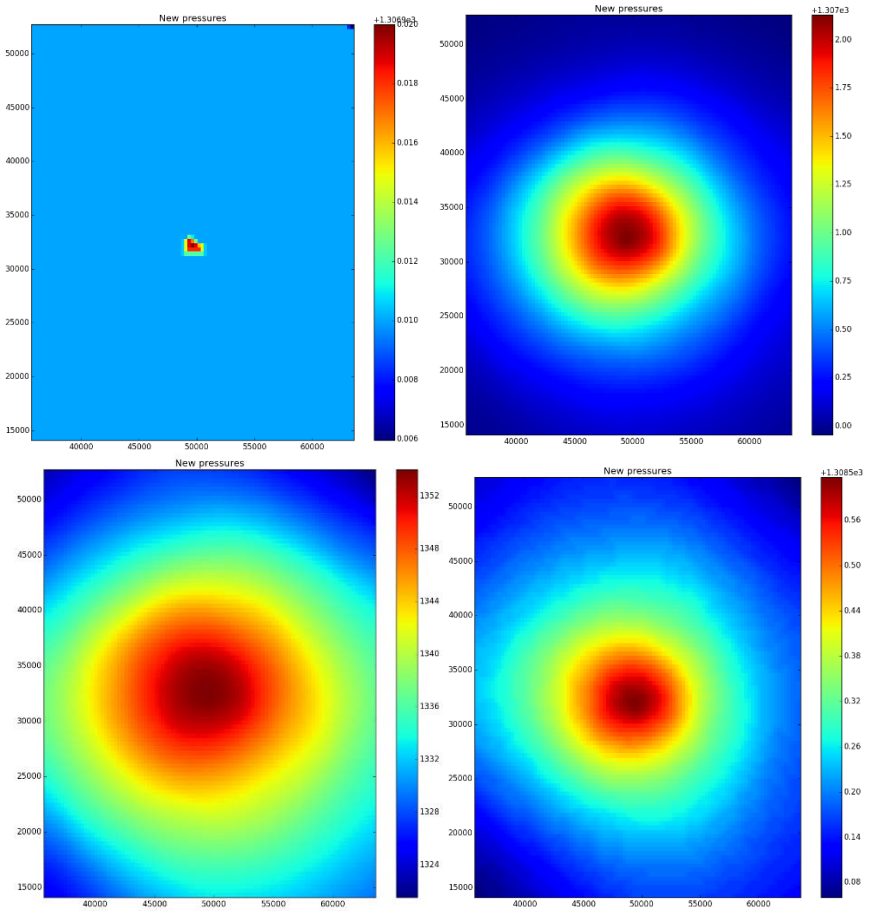

Figure 12: Pressure plume after 31 days, 1 year, 30 years, and 100 years. RROM-GEN is used to reduce the CMG-GEM model to 100 × 100 grid blocks. The Integrated Assessment Model (IAM) tool requires the reduced order model generated by RROM-GEM as input.

NRAP-IAM-CS: The NRAP Integrated Assessment Model (IAM) for Carbon Storage (CS) tool (Stauffer, Chu, and Tauxe, 2016) accounts for key geological parameters to model long-term leakage behavior to the groundwater aquifer or atmosphere through the legacy wellbores and caprock. The tool quantifies the uncertainty and probability of leakage using the Monte Carlo approach. The tool is used to model leakage from the Osage formation in the Patterson Field given the range of properties in Tables 7–8.

Table 7: Osage formation properties.

Storage zone $Min - Max$	Formation top (ft)	Elevation depth (ft)	Thickness (ft)	Porosity	Horizontal Permeability (md)
Osage	5,310	1,767–2,520	129.3–155.98	0.0229–0.3118	0.0876–184.3813

Table 8: Osage formation properties.

Storage zone μ_x, σ_x	Porosity	Horizontal Permeability (md)
Osage	0.1124, 0.0645	18.4587, 29.535

The Patterson Field is assumed to be a rectangle having an area of 50 square miles (129.5 km^2) with a 3/1 aspect ratio and the injection well located in the middle of the reservoir. The legacy wells are cemented and their density in the Patterson area is ~2.5 to 3 wells/km^2. The cement permeability is assumed to FutureGen low rate wells distribution in the tool among three other options available (based on Alberta wells, based on Gulf of Mexico wells, high rate FutureGen wells) because Kansas wells are not overpressured and their flow rates are low (Carey, 2017). The groundwater aquifer and atmosphere properties are set to the tool's default here and will be refined as more data become available. The default properties of the groundwater aquifer and atmosphere are summarized in Tables 9–10. Figures 13–14 show the CO_2 and brine leakage, respectively, through all legacy wells to the groundwater aquifer, and Figure 15 shows CO_2 leakage to the atmosphere. Figure 16 shows the importance of various factors contributing to the leakage indicating that the Legacy wellbores and their cement permeability pose the highest leakage risk among other factors such as reservoir permeability, reservoir porosity or caprock permeability.

Table 9: Shallow aquifer properties.

Depth	100 m (below mean sea-level)
Pressure	1 MPA
Temperature	20.25 °C
Permeability	$1.148 \times 10^{-12}\ m^2$
Porosity	0.2

Table 10: Atmosphere properties.

Wind speed at 10 m above land surface	1 m/s
Ambient temperature	20 °C
Ambient pressure	1 atm
Leaked gas temperature	20 °C
Threshold concentration	0.002
Number of checking points	7

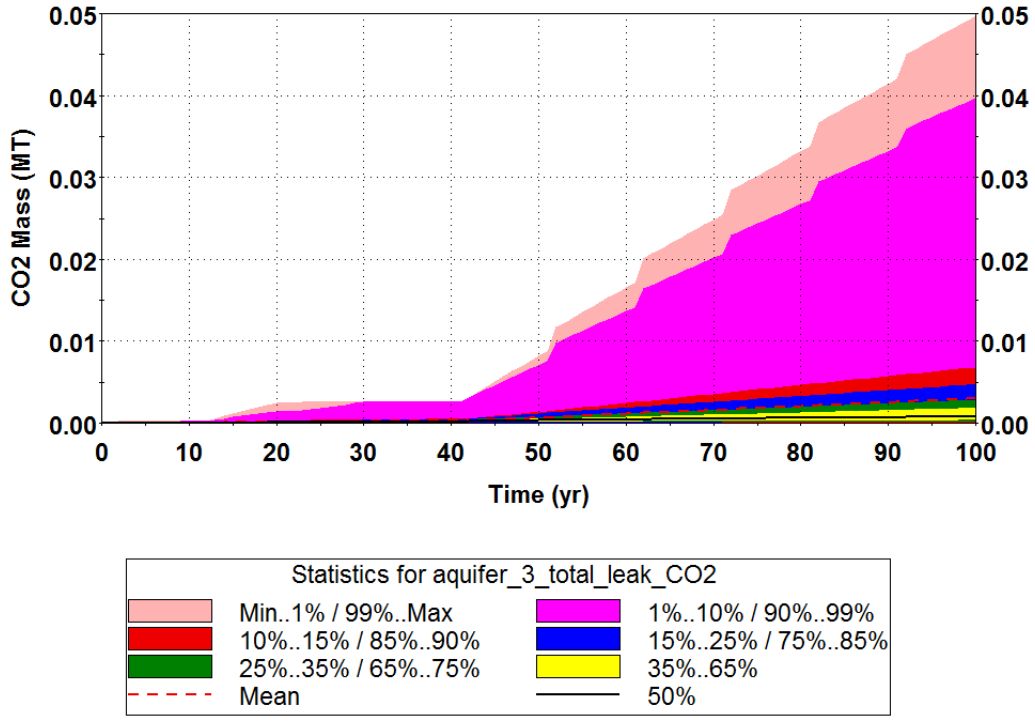

Figure 13: The probability of total CO_2 leakage to the groundwater aquifer through legacy wellbores.

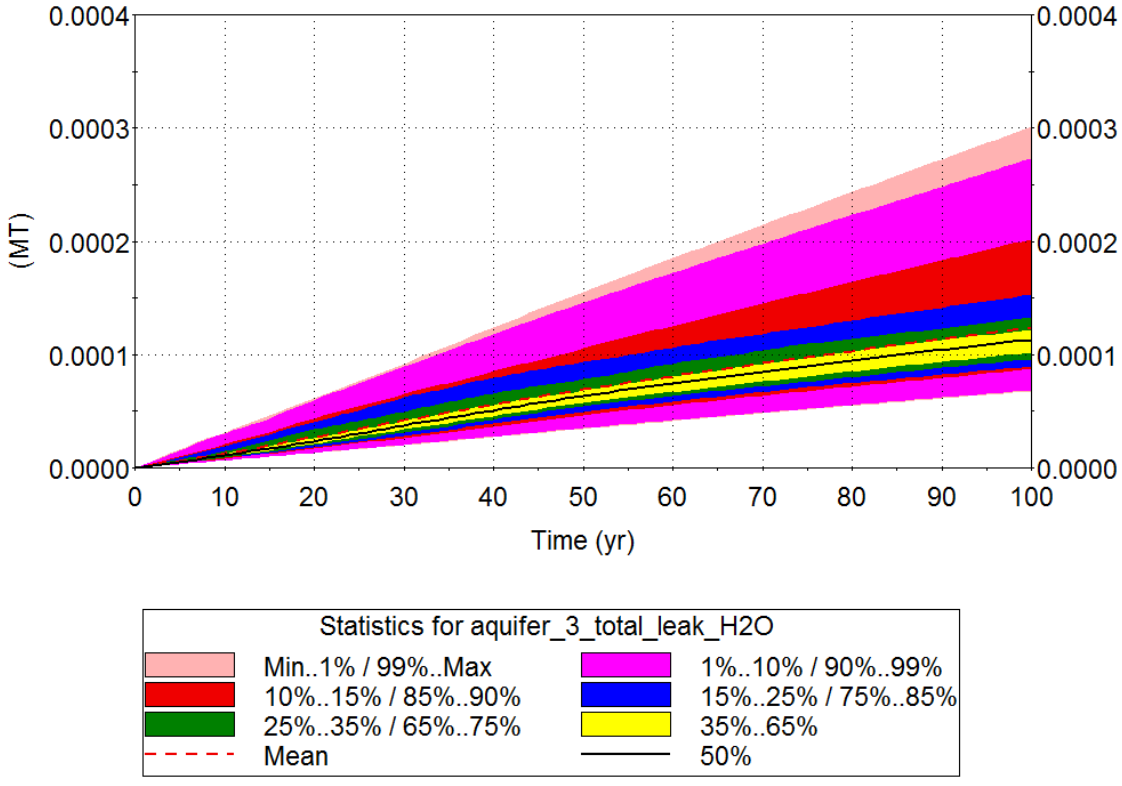

Figure 14: The probability of total brine leakage to groundwater aquifers through legacy wellbores.

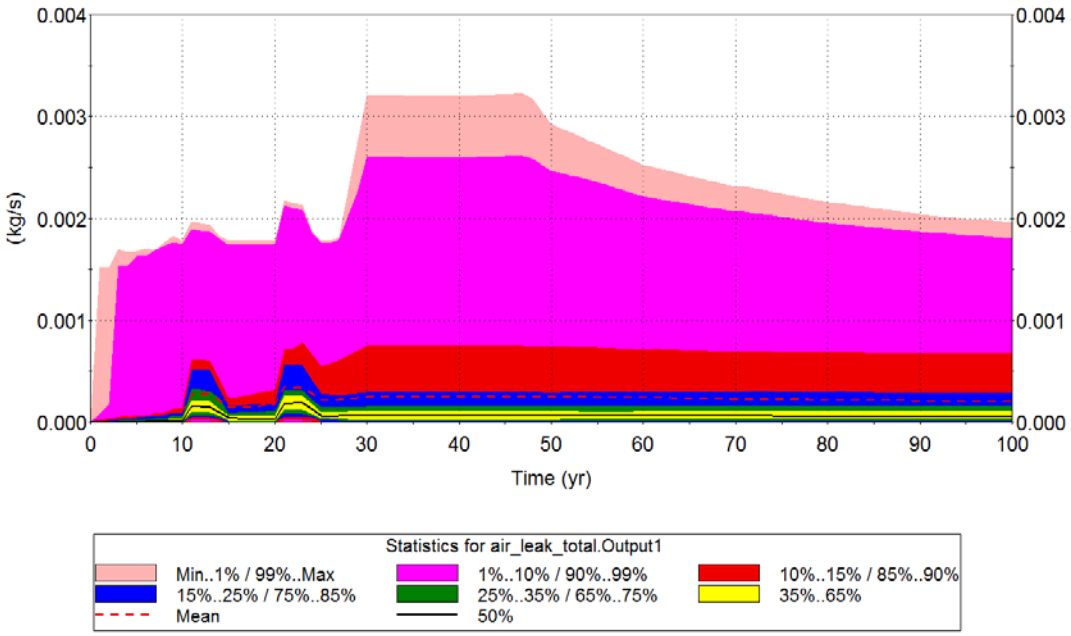

Figure 15: The probability of CO_2 leakage to the atmosphere (in kg/s) through legacy wellbores.

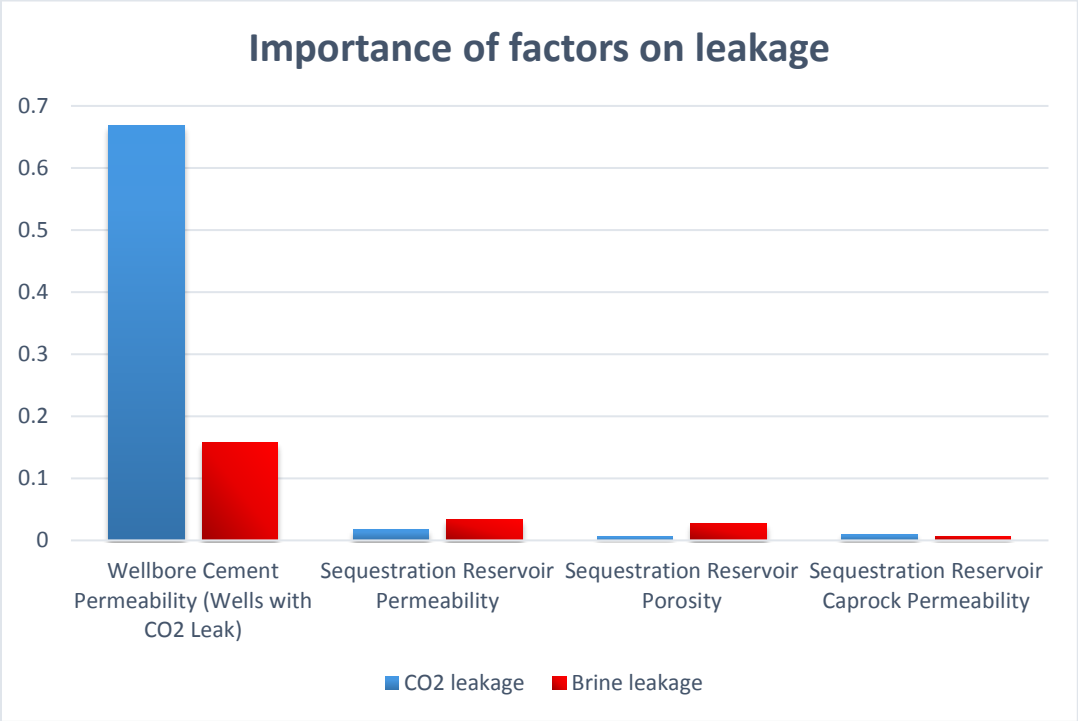

Figure 16: Importance of different factors on CO_2 and brine leakage. Legacy wellbores and their cement permeability pose the highest leakage risk.

WLAT (Well Leakage Analysis Tool): WLAT tool is useful for evaluating the leakage through the injection well or legacy wells (Huerta and Vasylkivska, 2016). The tool has options for a thief zone and a shallow aquifer to calculate the leakage to each of these zones and to the atmosphere. The critical data for the tool are the wellbore diameter, cement permeability, thief zone and shallow aquifer properties (i.e., permeability and depth). The tool also requires pressure and saturation at the leak point (i.e., wellbore) over time inferred from the numerical simulation in the format of separate time series. The well can be cemented, multi-segmented, or open (in case of legacy wells). An effective wellbore permeability (k_{eff}) of 1e-4 md, Osage depth of 5,310 ft, and pressure and saturation profile at the bottom of the CO_2 injector well (Figure 17) and the tool's default properties for the shallow aquifer and atmosphere are used for calculating the leakage rates (Figure 18). NOTE: IAM-CS results are more reasonable for cemented wellbores. Currently, the cemented wellbore model in WLAT is giving an error, so an open wellbore model with very small permeability (1e-4 md) is used here.

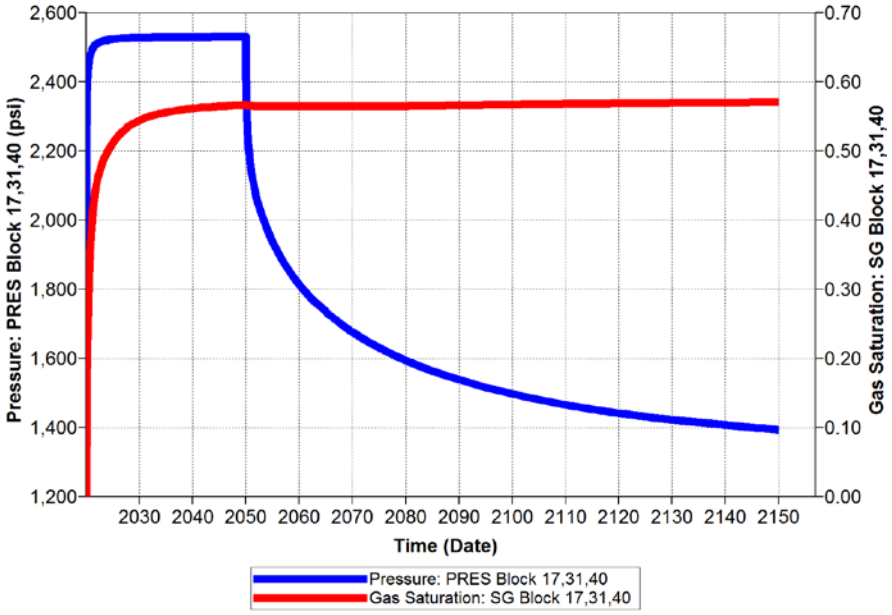

Figure 17: Pressure and saturation profile at the CO_2 injection well.

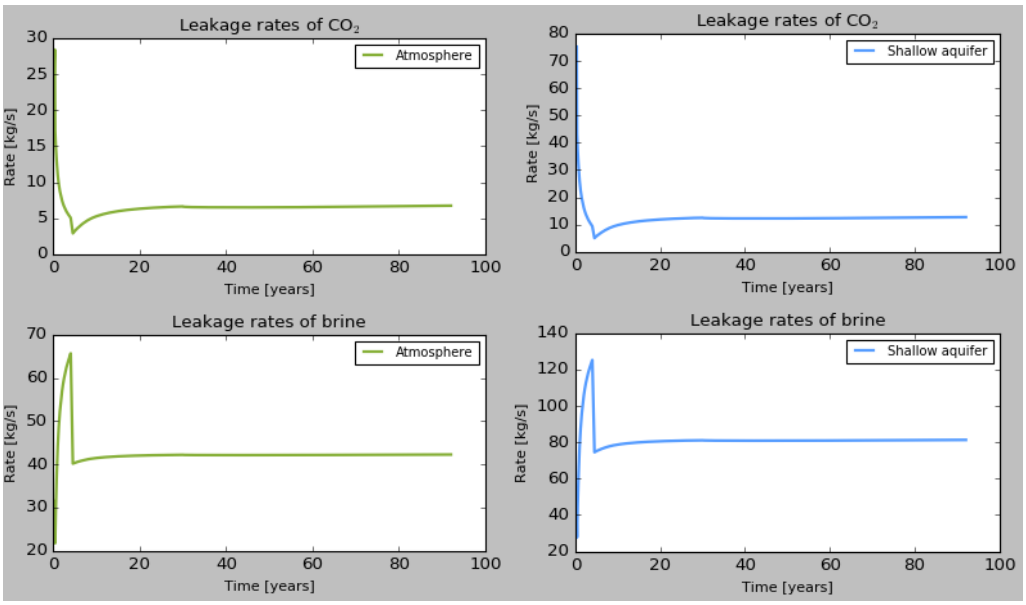

Figure 18: CO_2 leakage rate to the shallow aquifer and atmosphere.

References

Carey, W. (2017). Probability Distributions for Effective Permeability of Potentially Leaking Wells at CO 2 Sequestration Sites, (April). Retrieved from http://www.netl.doe.gov/research/on-site-research/publications/featured-technical-

Goodman, A., Hakala, A., Bromhal, G., Deel, D., Rodosta, T., Frailey, S., … Guthrie, G. (2011). U.S. DOE methodology for the development of geologic storage potential for carbon dioxide at the national and regional scale. *International Journal of Greenhouse Gas Control*, *5*(4), 952–965. https://doi.org/10.1016/j.ijggc.2011.03.010

Goodman, A., Sanguinito, S., & Levine, J. S. (2016). Prospective CO 2 saline resource estimation methodology: Refinement of existing US-DOE-NETL methods based on data availability. *International Journal of Greenhouse Gas Control*, *54*, 242–249. https://doi.org/10.1016/j.ijggc.2016.09.009

Huerta, N. J.; Vasylkivska, V. S. (2016). Well Leakage Analysis Tool (WLAT) User's Manual, (November).

King, S. (2016a). Reservoir Evaluation and Visualization (REV) Tool User's Manual, Version: 2016.

King, S. (2016b). Reservoir Reduced-Order Model – Generator (RROM-Gen) Tool User's Manual, Version: 2016.11-1.2, (November).

Krushin, J. T. (1997). Seal Capacity of Nonsmectite Shale. *Seals, Traps, and the Petroleum System*, (67), 31–47. Retrieved from http://search.datapages.com/data/specpubs/mem67/ch03/ch03.htm.

Lindner, E. N. (2016). NRAP Seal Barrier Reduced-Order Model (NSealR) Tool User's Manual, Version: 2016.11-14.1, (November).

Philip Stauffer, Shaoping Chu, Cameron Tauxe, R. P. L. (2016). NRAP Integrated Assessment Model-Carbon Storage (NRAP-IAM-CS) Tool User's Manual, Version : 2016 . 04-1 . 1.

Appendix H: Faults and seismicity risks associated with commercial-scale CO_2 injection and storage in southwestern Kansas

Tandis S. Bidgoli[1] and Jeffrey C. Jennings[2]
[1] Kansas Geological Survey (now University of Missouri), [2] Kansas Geological Survey

The following is a report on seismicity risk in southern Kansas, including the North Hugoton Storage Complex, that provides supplemental details to the summary provided in the final report Subtask 4.2.

Faults and seismicity risks in the North Hugoton Storage Complex and the greater southern Kansas

1. Overview

The rapid rise in seismicity in Kansas and other parts of the central and eastern United States (CEUS) is without precedent and has quickly changed the hazard landscape for injection activities in the state, including for commercial-scale injection of CO_2. A major challenge for stakeholders in Kansas is that subsurface faults and stresses are not well known, making it difficult to properly site new injection wells or make decisions regarding operations of existing wells (e.g., Class I and II wastewater injection wells). Industry 2-D or 3-D seismic datasets that could aid in identifying subsurface faults are generally not available storage site assessments, and well-log and test data that could provide constraints on *in situ* stresses have not been evaluated in a rigorous way.

In response to this new and evolving seismic hazard, we focus on mapping subsurface faults and lineaments, present-day stresses, and brine disposal data across southern Kansas to identify sites that may be at risk for injection-induced seismicity. We cover more than 40 counties (29 complete; 14 partial) in the southern part of the state, where oil and gas production is most active and where available data are concentrated (Figure 1). The area of analysis also corresponds to area covered by prior Department of Energy-sponsored projects, in particular the regional storage assessment area covered by award DE-FE0002056. New structure contour maps of 18 major stratigraphic boundaries were used to map potential faults. The maps were constructed from a dense sampling of stratigraphic tops, established from the KGS's well database. To identify potential faults, we used a range of surface analysis methods (e.g., slope, aspect, curvature, etc.). To identify faults that have the highest risk for failure, we mapped *in situ* stress orientations and magnitudes using well log (e.g., image, caliper, dipmeter) and test data (e.g., leak off, interference, step rate test data) and performed slip and dilation tendency analysis. The resulting fault maps and stress data were used to assess the reactivation potential of faults, that when evaluated in conjunction with brine disposal data can be used to flag areas at risk for injection-induced earthquakes.

2. Data and Methods

The mapped area (regional storage assessment area covered by award DE-FE0002056) and region of interest for CO^2 storage (Patterson injection site in the North Hugoton Storage Complex) are shown in Figure 1. The mapped area covers more than 60,000 km^2 of Kansas and includes more than 40 counties (29 complete; 14 partial) in the southern part of the state, where oil and gas production is most active and where available data are concentrated. The workplan focused on four major tasks: (1) subsurface fault and lineament mapping from tops-based structure contour maps, (2) analysis of *in situ* stress indicators and magnitudes from well log and test data, (3) fault slip and dilation tendency analysis, and (4) integration with other datasets (e.g., 3-D seismic data and saltwater disposal data). Individual methods are described in detail below.

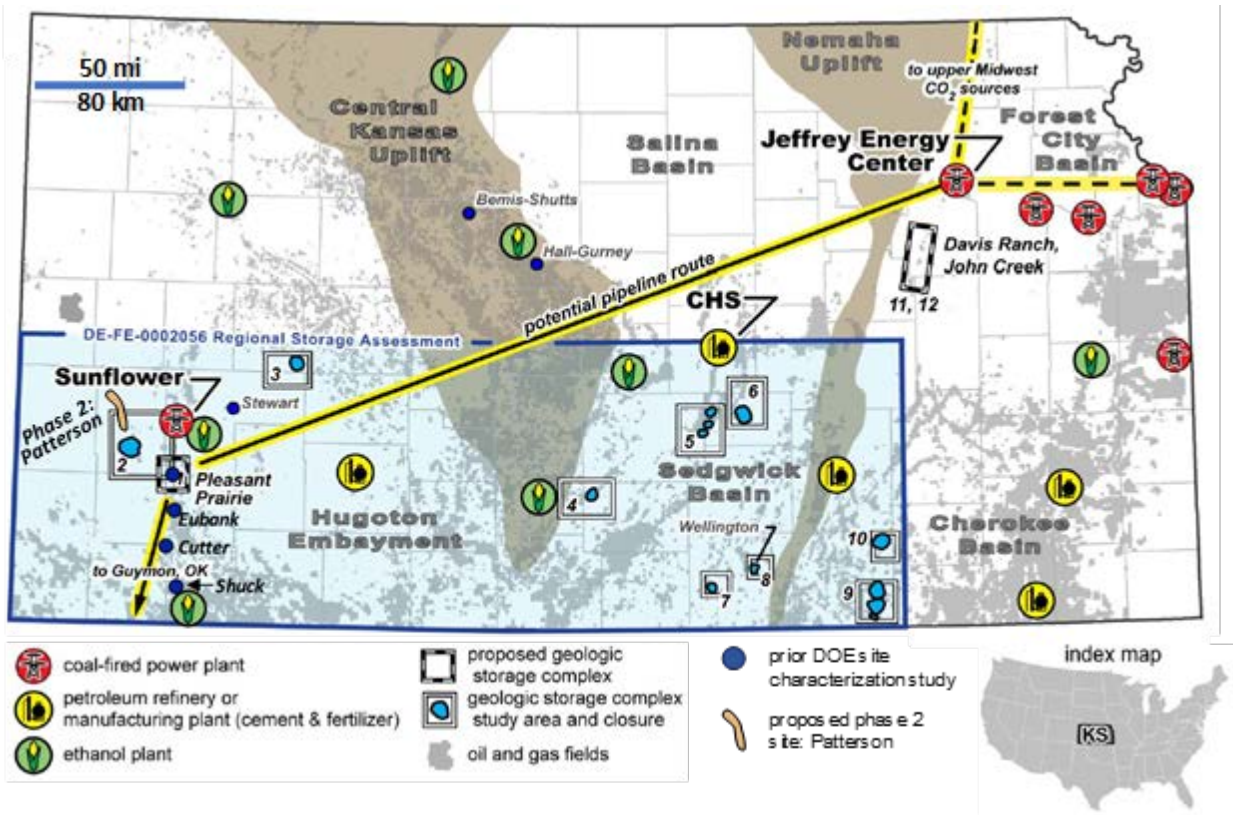

Figure 1. Kansas map showing location of the Patterson site, a variety of CO_2 sources, possible CO_2 pipeline routes, other possible CO_2 injections sites (numbered 1–12) identified in Watney et al. (2015) located inside the DE-FE0002056 study areas (blue), and oil fields (gray). The primary sources in this study are labeled. The figure is modified from ICKan proposal SF 424 R&R, 2016 (Watney et al., 2016).

2.1 Subsurface fault and lineament mapping

2.1.1 Well tops-based structure-contour maps

The study incorporates a catalog of more than 500,000 stratigraphic tops or picks for stratigraphic surfaces across the study area. The well tops data are derived from the Kansas Geological Survey's well database and include picks for 18 primary stratigraphic boundaries between the present-day surface and Precambrian basement (Figure 2). Most of these boundaries have more than 10,000 tops or well picks associated with them; however, the density of the picks is variable from east to west. In a few cases, the boundaries or surfaces have more than 30,000 picks constraining them (e.g., Top High Plains, Top and Base Dakota Formation, Heebner Shale, and Top Mississippian; Figure 3). The well-tops data were evaluated for consistency through visual inspection and gridded using appropriate algorithms given the final density and distribution of the data.

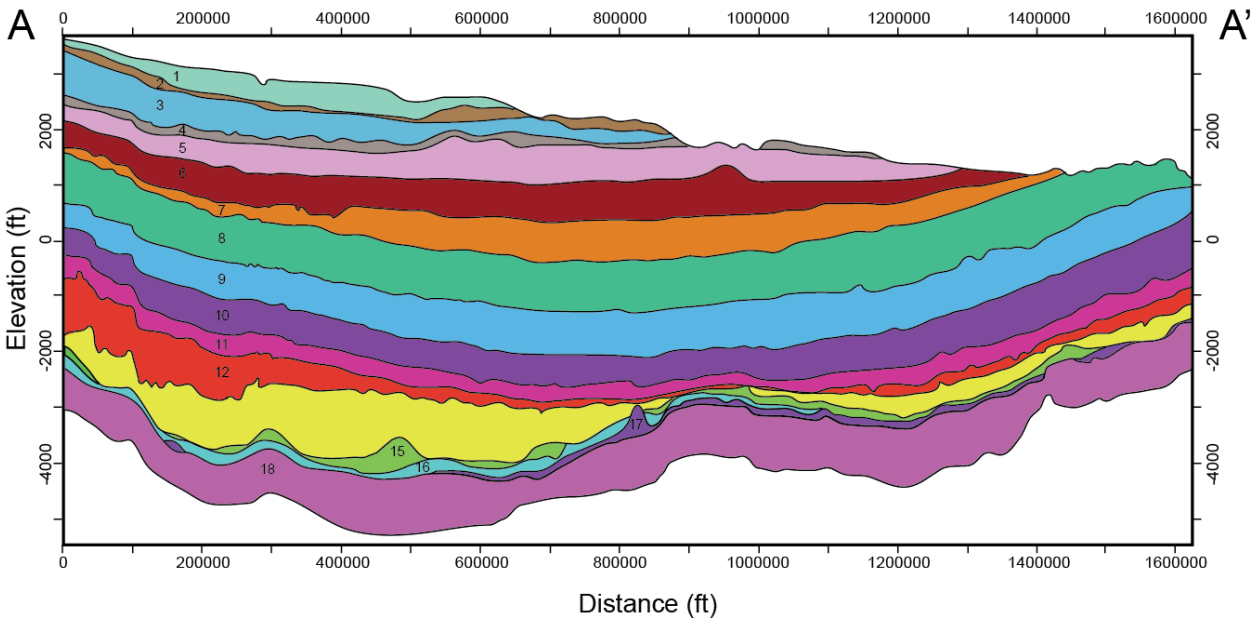

1. Present-day surface
2. High Plains base (Neogene)
3. Top Dakota (Cretaceous)
4. Base Dakota (Cretaceous)
5. Blaine Formation (Permian)
6. Cedar Hills Formations (Permian)
7. Top Stone Corral Formation (Permian)
8. Hutchinson Salt (Permian)
9. Top Chase Group (Permian)
10. Root Shale (Upper Pennsylvanian)
11. Heebner Shale (Upper Pennsylvanian)
12. Stark Shale (Upper Pennsylvanian)
13. Top Cherokee Group (Mid. Pennsylvanian)
14. Top Mississippian (Upper Mississippian)
15. Top Pierson Formation (Mid. Mississippian)
16. Top Viola Limestone (Middle Ordovician)
17. Top Simpson Group (Middle Ordovician)
18. Top Arbuckle (Lower Ordovician)

Figure 1. Stratigraphic surfaces analyzed between present-day surface and Precambrian basement. Cross section location shown in Figure 1.

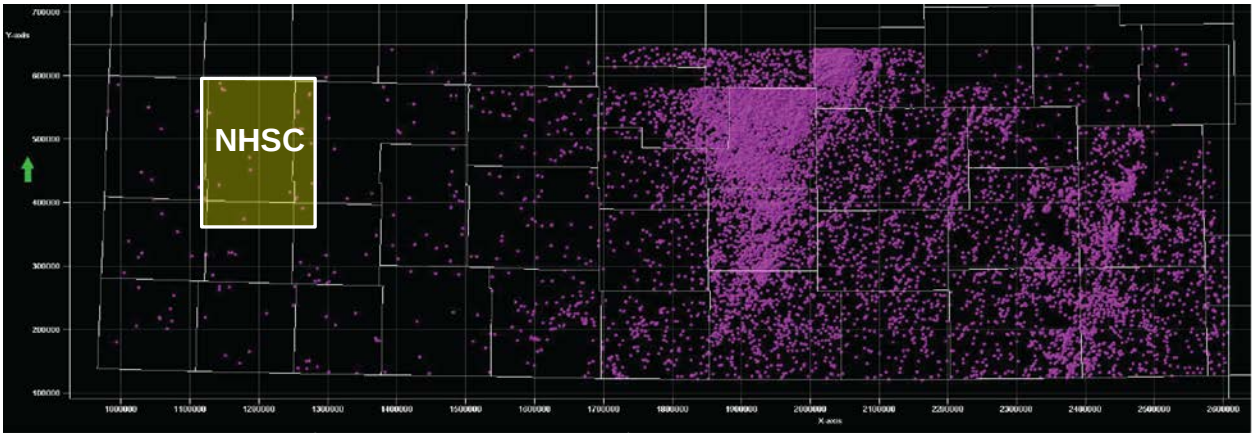

Figure 2. Well tops for the Arbuckle Group showing spatial variability in pick density across the analysis area. White polygons are county boundaries shown in Figure 1. White outline shows the area of the North Hugoton Storage Complex (NHSC).

2.1.2 Spatial analysis techniques

To identify discontinuities within the subsurface that may be faults, we applied a range of GIS-based spatial analysis techniques to the depth structure maps. Such spatial analysis techniques have proved effective in the identification of faults from elevation data (e.g., DeLong et al., 2011) and seismic data (e.g., Manzi et al., 2012). Spatial analysis tools employed in this study included hillshade, slope, aspect, slope curvature, edge detection, and trend surface or residual analysis. A brief description of each of the

surface analysis techniques is provided below.

Hillshade maps: Shaded relief or hillshade maps were generated from structure-contour maps by applying lighting at specific illumination angles (azimuth and altitude of the light source). The maps were used much in the same way as low-sun-angle photography for identification of faults and other features.

Slope analysis: The slope of each surface was calculated as the maximum rate of change in a 3 x 3 cell neighborhood. Slope maps can be useful in identifying faults across low-relief topography and in distinguishing specific types of landforms.

Aspect: The aspect is defined as the direction of the maximum slope, reported in azimuth, and was calculated using a 3 x 3 weighted neighborhood. Aspect maps can do an excellent job of illuminating discontinuities like faults, particularly where there is an abrupt change in the slope direction.

Slope curvature analysis: We used slope curvature analysis to delineate areas of rapid change in slope, which can be associated with linear discontinuities like faults. The slope curvature was determined by applying a fourth-order polynomial to 3 x 3 cell neighborhood and calculating the second derivative of that surface (i.e., slope of the slope). The sign of the curvature corresponds to the convexity (positive) or concavity (negative) of the curvature, while the magnitude of the curvature describes the rate of change in slope.

Edge detection analysis: Edge detection can be accomplished using a number of spatial filters, including high-pass, directional, Laplace, and Sobel filters. Each of these techniques involves GIS-based calculations accomplished using cell neighborhoods and map algebra. The various filters are effective at identifying rapid rates of change in surface elevation data, which may correspond to faults and other linear structural features.

Trend surface or residual analysis: Trend surface analysis (TSA) is an effective tool for mapping faults, fault-related structures, and structural trends (e.g., Evenick et al., 2005) that is widely used in the oil and gas industry. The technique separates observed data (i.e., depth structure map) into a modeled surface and a residual surface. The modeled surface or trend surface is calculated through regression analysis and represents the regional dip, while the residual surface is calculated by subtracting the trend surface from the original data. The residual surface often contains subtle features that may have been masked in the original dataset.

2.2 Stress field mapping

To predict whether mapped lineaments or faults are prone to reactivation, it is necessary to understand what present-day stresses are. For Kansas, relatively little is known about the state of stress. For example, the World Stress Map (Heidbach et al., 2010), a global compilation of crustal stress data, only incorporates a single stress constraint for the entire state of Kansas. The same can be said for much of the upper midcontinent, which has few published in situ stress constraints or measurements.

2.2.1 Methods for determining stress orientations

To determine the orientation of present-day stresses, we analyzed 14 image and 7 caliper logs for borehole breakouts and drilling induced fractures using standard criteria (e.g., Heidebach, 2010). Individual techniques are described below.

Borehole breakouts: Borehole breakouts are zones of wellbore elongation or enlargement that are triggered by stress concentrations around a well bore (Bell and Gough, 1979). In an open hole, stresses concentrate around the wellbore walls (called the circumferential or hoop stress) and are variable with azimuth. The circumferential stress is lowest at the azimuth of the maximum horizontal stress (S_{Hmax}) and

highest at the azimuth of the minimum horizontal stress (S_{hmin}). For a breakout to occur, the circumferential stress must exceed the strength of the wellbore rocks (Zoback et al., 1985; Bell, 1990). In vertical wells, breakouts or elongations form in an orientation that is parallel with S_{hmin} and perpendicular to S_{Hmax}. The breakout orientation is usually consistent within a well and across oil or gas fields (e.g., Bell and Babcock, 1986; Plumb and Cox, 1987). Borehole breakouts and their orientations can be determined from caliper logs (e.g., 4- or 6-arm caliper logs) and resistivity and acoustic image logs (e.g., Formation Micro Imager or Borehole Televiewer) and must be distinguished from other types of borehole enlargements (e.g., key sets or washouts).

Drilling induced fractures: In contrast to borehole breakouts, drilling-induced fractures occur when the wellbore wall goes into tension (Aadnoy, 1990). This is often the case when there is a large difference between S_{hmin} and S_{Hmax} (Aadnoy, 1990; Moos and Zoback, 1990). These tensile wall fractures form parallel to S_{Hmax} and are easily recognized in image logs. Drilling-induced fractures can be a very reliable stress indicator (e.g., Wiprut and Zoback, 2000).

Quality rankings: Stress indicators incorporated into this study were ranked by quality according to internationally established criteria (e.g., Heidebach et al., 2010). The rankings range from A to E, with high-quality orientation data, those determined to be accurate to within +/-15°, assigned an A-quality rank, whereas low-quality measurements that are deemed unreliable will be assigned an E-quality rank. The evaluation and assignment of quality ranking for stress indicators ensures that study results can be compared to or later incorporated into other published datasets (e.g., World Stress Map; Heidebach et al., 2010).

2.2.2 Methods for determining stress magnitudes

Vertical stress: The vertical stress (Sv) was estimated using density logs in the study area. The magnitude of the vertical stress is equal to the weight of the overlying column of rock. Where accurate density log data are available, the vertical stress can be calculated by integrating the data from the surface to a target depth, as follows:

$$Sv = \int_0^z \rho(z) g \, dz \approx \bar{\rho} g z$$

where S_v = vertical stress, MPa; $\rho(z)$ = density as a function of depth, g/cm^3; g = gravitational acceleration constant, and $\bar{\rho}$ = average density. Overburden estimates at depths greater than the measured data were calculated by assuming a density of 2.75 g/cm^3, an accepted average density for basement rocks that agrees with shallow basement measurements taken from density logs in south-central Kansas (Smithson, 1971).

Minimum and maximum horizontal stresses: Although there are a number of methods available for estimation of the horizontal stress magnitudes (summary in Zoback et al., 2003), earthquake hypocenters in the region suggest the relevant stress state is at depths of 3–7 km, far below the sedimentary column. Therefore, stress magnitudes at basement depths of 5 km were calculated using a stress polygon (e.g., Moos and Zoback, 1990; Zoback et al., 2003), assuming a coefficient of friction (μ) of 0.6 (Byerlee, 1978). The boundaries of the stress polygon represent the failure limits for different stress states (NS, SS, or RS) and defined by F(μ) (equation 1) and SHmax (equation 2) (Moos and Zoback, 1990; Zoback et al., 2003). SHmin was calculated using equation 3, with values for Sv and P_p taken from the pressure gradients, described in Section 3.3.

1) $F(\mu) = \text{sqrt}(\mu^2 + 1) + \mu^2$
2) $SHmax = F(\mu)(Sv - Pp) + Pp$
3) $SHmin = (Sv - Pp)/F(\mu) + Pp$

2.3 Slip tendency analysis

To predict whether mapped faults are prone to reactivation, we performed slip and dilation tendency analysis using 3DStress® (e.g., Morris et al., 1996; Moeck et al., 2009). The analysis is based on Amonton's law for fault reactivation, in which the shear stress (τ) is equal to the product of the effective normal stress (σ_{neff}) and the coefficient of sliding friction (μ_s; Byerlee, 1978).

$$\tau = \mu_s \times \sigma$$

For slip to occur on a cohesionless fault surface (i.e., reactivation of a preexisting structure), the resolved shear stress must be equal to or greater than the frictional resistance to sliding (i.e., effective normal stress, σ_{neff}). Thus, slip tendency (T_s) is governed by the ratio of resolved shear to resolved normal stress on a fault surface (Morris et al., 1996).

$$T_s = \tau / \sigma_{neff}$$

Values for the shear and normal stress acting on a fault plane and thus, the slip tendency are dependent on both the stress field (stress tensor) and the orientation of the fault (Morris et al., 1996). The stress field is defined by the orientations and magnitudes of the effective stresses, such that $\sigma_{1eff} = (\sigma_1 - P_f) > \sigma_{2eff} = (\sigma_2 - P_f) > \sigma_{3eff} = (\sigma_1 - P_f)$, where P_f is the pore fluid pressure (Jaeger et al., 2007). Thus, the shear and normal stress acting on a fault plane can be calculated using:

$$\sigma_{neff} = \sigma_{1eff} \times a^2 + \sigma_{2eff} \times b^2 + \sigma_{3eff} \times c^2$$
$$\tau = [(\sigma_1 - \sigma_2)^2 a^2 b^2 + (\sigma_2 - \sigma_3)^2 b^2 c^2 + (\sigma_3 - \sigma_1)^2 a^2 c^2]^{1/2}$$

where a, b, and c are the cosine of the angle between the principal stress axes and the normal to the fault plane. The equations describe the normal and shear stress for compressional stress states but can be easily modified for extensional and strike-slip stress states.

2.4 Brine data analysis

In addition to mapping subsurface faults and stresses, we evaluated available saltwater disposal (SWD) data for a five-year window, from 2010 to 2014. The data were provided by the Kansas Corporation Commission, the regulatory body in charge of permitting and management of UIC Class II wells. The primary objectives of this portion of the study were to compile and summarize the brine disposal data across the state, including overall volumes and volume injected by geologic zone, focusing on temporal and spatial trends in SWD by county.

To accomplish these tasks, we created a database of UIC Class II SWD wells in the study area using ArcGIS. The database incorporates yearly injection data from the KCC. Individual well records were evaluated against well completion records and other public data for individual SWD wells. The resulting database was queried and analyzed for well counts, injection volumes, well-head pressures, and injection depths. The results were compared to fault and stress maps to identify specific faults and regions that may be at higher risk for injection-induced seismicity.

3. Results

3.1 Data interpolation and new structure-contour maps

To create the structure-contour maps used in this study, it was necessary to interpolate the well tops data. The large volume and variability in data density across the different stratigraphic horizons posed challenges for gridding in ArcGIS; therefore, data interpolation was accomplished using Petrel™ 2015. Maps were constructed for the Arbuckle Group, Simpson Group, Viola Limestone, Pierson Formation, Mississippian Group, Cherokee Group, Stark Shale, Heebner Shale, Root Shale, Chase Group, Hutchinson Salt, Stone Corral, Cedar Hills, Blaine Formation, Dakota Formation, and the High Plains aquifer (Ogallala Formation).

Moving Average

Moving average interpolation technique uses an average Z value over a search radius, weighted by inverse distance, to interpolate between points. The closer the points, the more accurate the surface is; however, in areas of low point density, accuracy of the surface falls off quickly (Figure 4). These low data density areas appear as flats and bullseyes. In areas of very low data density, the search radius limits the interpolation, creating null value areas (Figure 4).

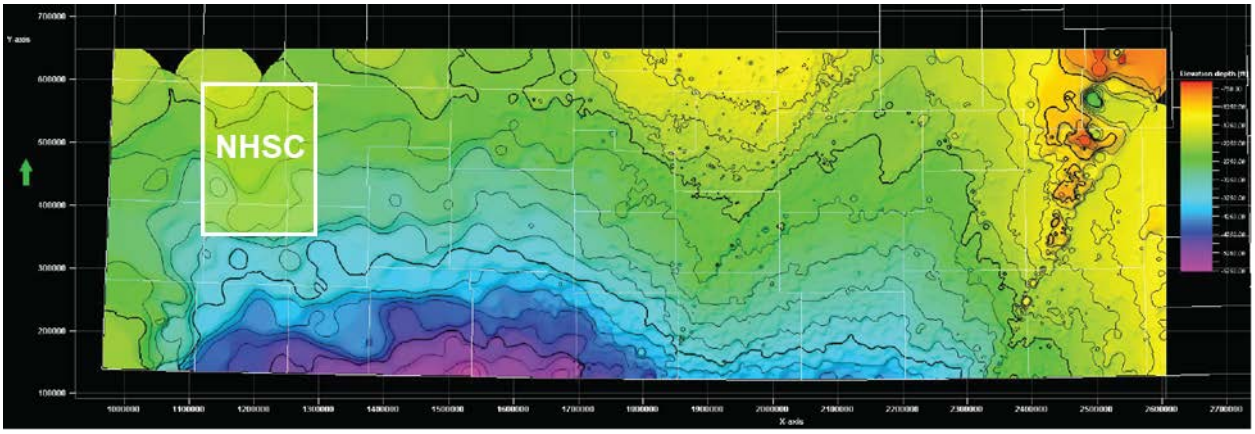

Figure 3. An example of the moving average interpolation technique for the top Arbuckle surface. Being limited by a search radius, this technique creates areas gaps and bullseyes in areas of low data density. White outline shows the area of the North Hugoton Storage Complex (NHSC).

Kriging

Kriging, although initially a favored method for its accuracy and cross-validation of data, also produced bullseyes in certain surfaces. Large pockets of missing data were a particular problem for some maps (Figure 5). Variogram and general setting adjustments were able to reduce the size of data holes but never completely removed them. The lack of surface continuity also posed a challenge for surface analysis for some stratigraphic boundaries.

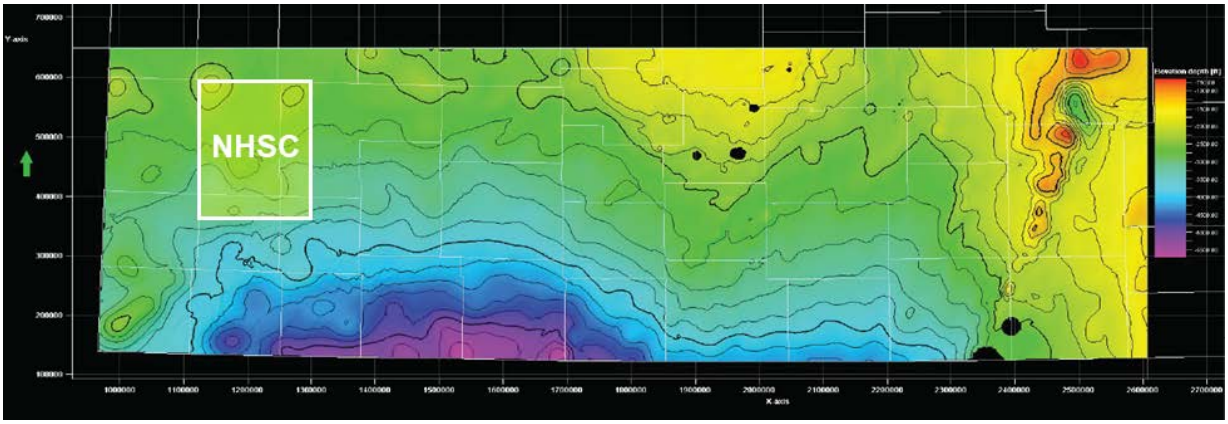

Figure 4. Kriging produced maps with two visible errors in interpolating a surface. First, some of the mapped surfaces had holes, as shown above. Second, bullseyes are created in areas of low data density as seen in the upper left of the figure. White outline shows the area of the North Hugoton Storage Complex (NHSC).

Minimum Curvature

Minimum curvature surfaces passed initial quality checks of being continuous across the study region and having somewhat geologically reasonable outputs (Figure 6). Upon further examination of the interpolated surfaces, geological inaccuracies were discovered. In particular, where data points are lacking or low in density, minimum curvature continues the closest trend, resulting in a structure with abnormal highs and lows, particularly along grid margins (Figure 6).

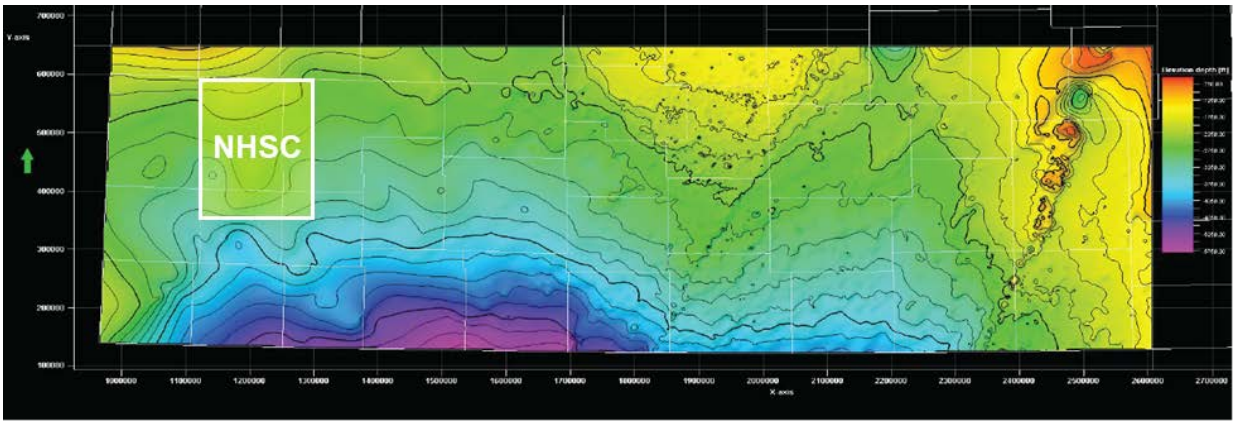

Figure 5. An example of the top Arbuckle structure-contour map using minimum curvature interpolation. White outline shows the area of the North Hugoton Storage Complex (NHSC).

Convergent Interpolation

Convergent interpolation combines a Taylor series with a minimum curvature smoothing approach. The interpolated surfaces were continuous across the study area and made sense geologically (Figure 7). Comparisons with maps generated using the other data interpolation techniques showed that the largest differences occur at grid margins and in low data density areas (Figure 8).

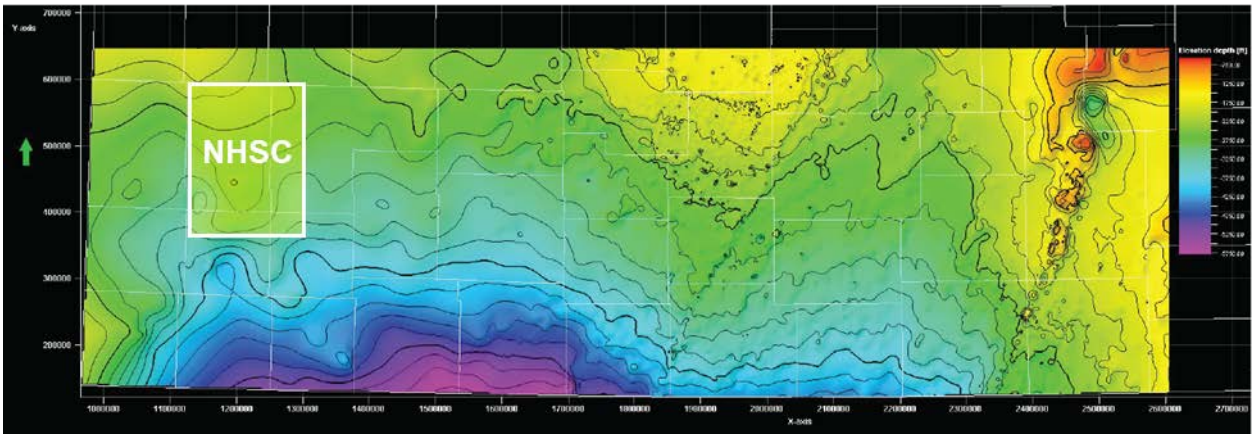

Figure 6. Convergent interpolation proved to be the most robust interpolation technique, with a consistent surfaces and more geologically accurate outputs throughout. White outline shows the area of the North Hugoton Storage Complex (NHSC).

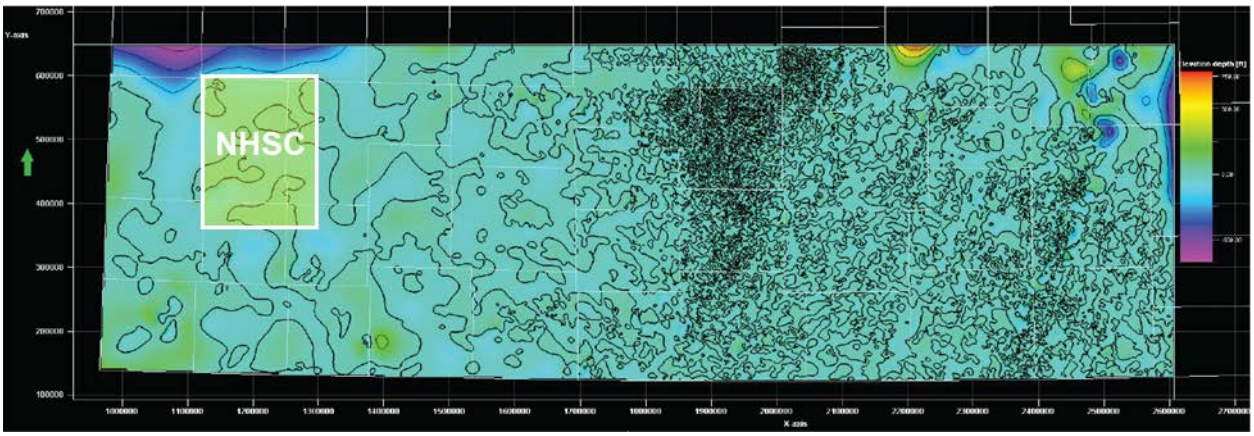

Figure 7. Difference map of minimum curvature and convergent interpolation shows the consistency in areas of high data density and good agreement in areas of lower data density. The largest differences can be seen near the edges where there is low data density. White outline shows the area of the North Hugoton Storage Complex (NHSC).

3.2 Surface analysis and lineament/fault maps

The final interpolated surfaces were imported into ArcGIS for surface analysis. Although we explored several methods (see section 2.1.2), slope and curvature maps provided the most definitive lineaments in both high and low data density areas (Figures 9 and 10). Hill shade and aspect were also used for surface analysis, but did not provide clear results or strong delineation of lineaments (Figure 11). Trend surface analysis was also considered as it removes the global slope of the regional study area, making local structures more evident. The resulting TSA surfaces provided a more visually defined surface, where lineaments and subtle changes in elevation (depth) were clearer and better defined (Figure 12). The TSA surfaces were also processed using other surface analysis techniques to check improvement of results; however, little change was observed in lineament definition.

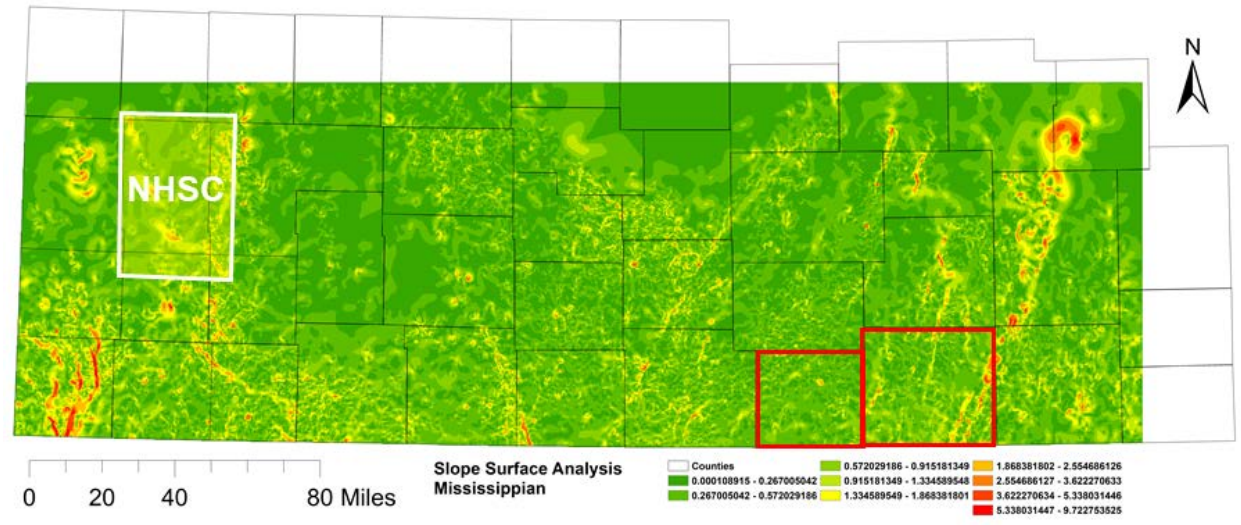

Figure 8. Slope of top Mississippian depth structure map. Red outlines are Harper (west) and Sumner (east) counties, where recent seismicity is concentrated. White outline defines the North Hugoton Storage Complex (NHSC).

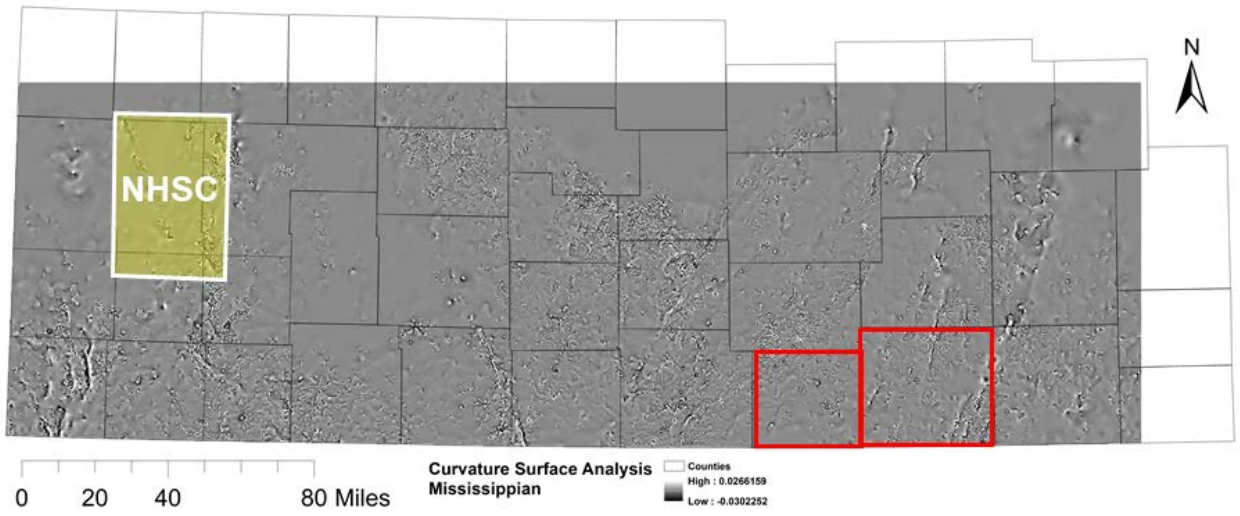

Figure 9. Curvature of the top Mississippian depth structure map. White outline defines the North Hugoton Storage Complex (NHSC). Red outlines are Harper (west) and Sumner (east) counties.

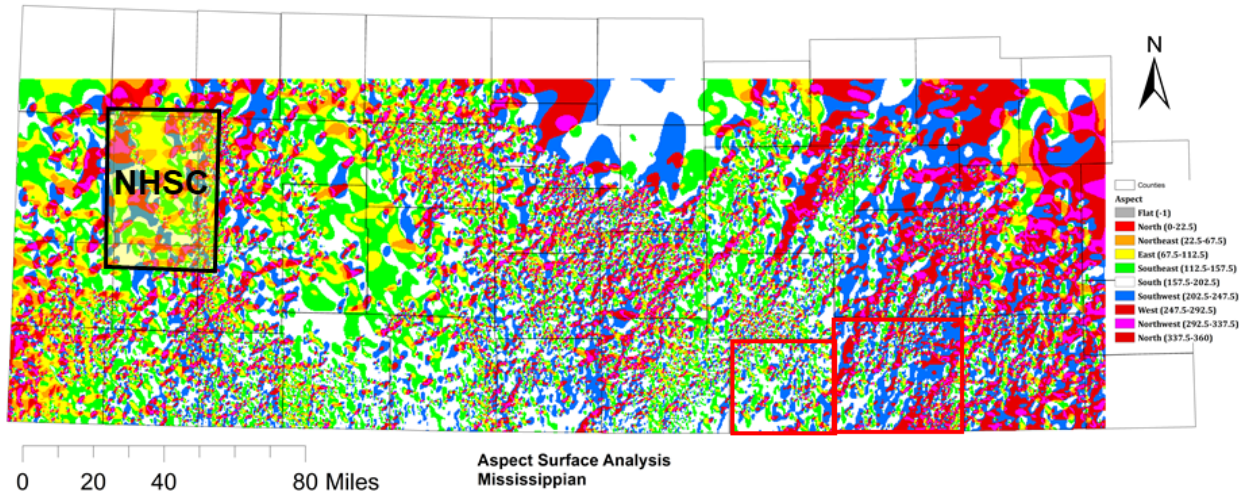

Figure 10. Aspect of the top Mississippian depth structure map. Black outline defines the North Hugoton Storage Complex (NHSC). Red outlines are Harper (west) and Sumner (east) counties.

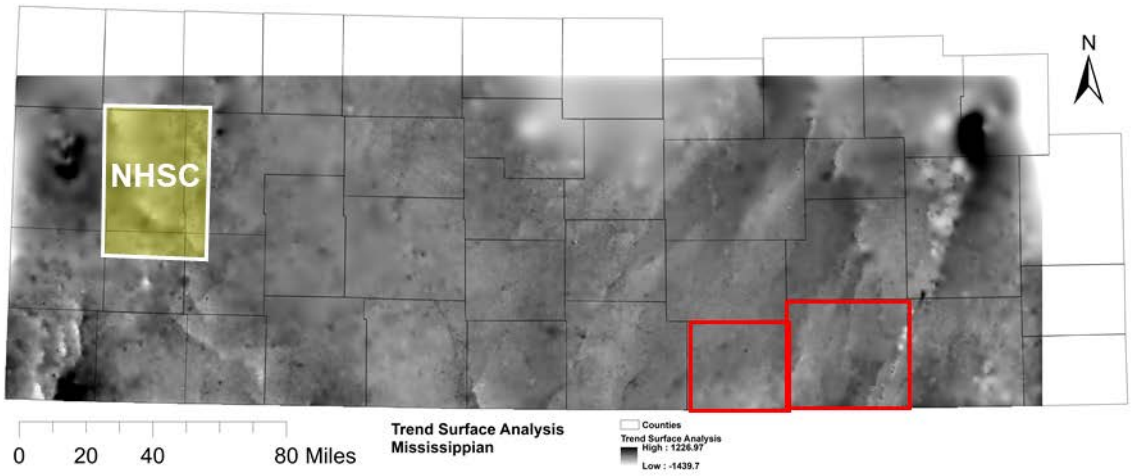

Figure 11. Residual map after subtraction of regional trend surface from top Mississippian depth structure map. White outline defines the North Hugoton Storage Complex (NHSC). Red outlines are Harper (west) and Sumner (east) counties.

The resulting mapped lineaments are shown in Figures 13, 14, and 15 and range in length from 2 to 30 miles (3 to 50 km), with two prevailing trends revealed: (1) NNE-trending lineaments are dominant in the eastern half of the study area. These structures are aligned with the known structures within the state, including the Midcontinent Rift System and Nemaha Ridge-Humboldt fault zone (NRHF). The Midcontinent Rift System is recognized across the region by a pronounced positive gravity anomaly along much of its length, which may be related to thick successions of mafic igneous rocks that were intruded during the rifting event (Ocola and Meyer, 1973; Somanas et al., 1989). The Nemaha Ridge-Humboldt fault zone (NRHF) is a 50 km wide NNE-trending structure that extends through Nebraska, Kansas, and Oklahoma (Lugn, 1935; Lee, 1954; Steeples et al., 1979; Stander and Grant, 1989; Figure 1). The NRHF is one of several major structures within the U.S. midcontinent that have been identified from analysis of subsurface data, including potential field anomalies (e.g., Kruger, 1997), limited seismic reflection data (e.g., Steeples, 1989; Stander and Grant, 1989), and well log data (e.g., McBee, 2003). The NRHF likely formed during Precambrian rifting, but was later reactivated in the Pennsylvanian and possibly Permian (Jewett, 1951; Berendsen and Blair, 1986; Dolton and Finn, 1989). (2) NW trending lineaments are well-aligned with the Central Kansas Uplift, one of the largest structural features in the state. Like the NRHF, it experienced a major episode of Pennsylvanian deformation (Merriam, 1963; Figure 1).

Several lineaments were documented in the North Hugoton Storage Complex (Figure 15). The lineaments predominantly trend NNW and bound structural closures that make the oil and gas fields in the area. A few WNW- and NE-trending lineaments were also documented across the storage complex area. The lineaments, overall, are poorly identified in the Arbuckle through Mississippian stratigraphic surfaces (Figure 13) and well documented in the surfaces from Cherokee Group through Blaine Formation (Figure 14), which likely relates to quality of the structure contour maps for those horizons. Deeper stratigraphic boundaries have few tops constraining them and may cause grids to be oversmoothed, increasing the potential for missed faults/lineaments.

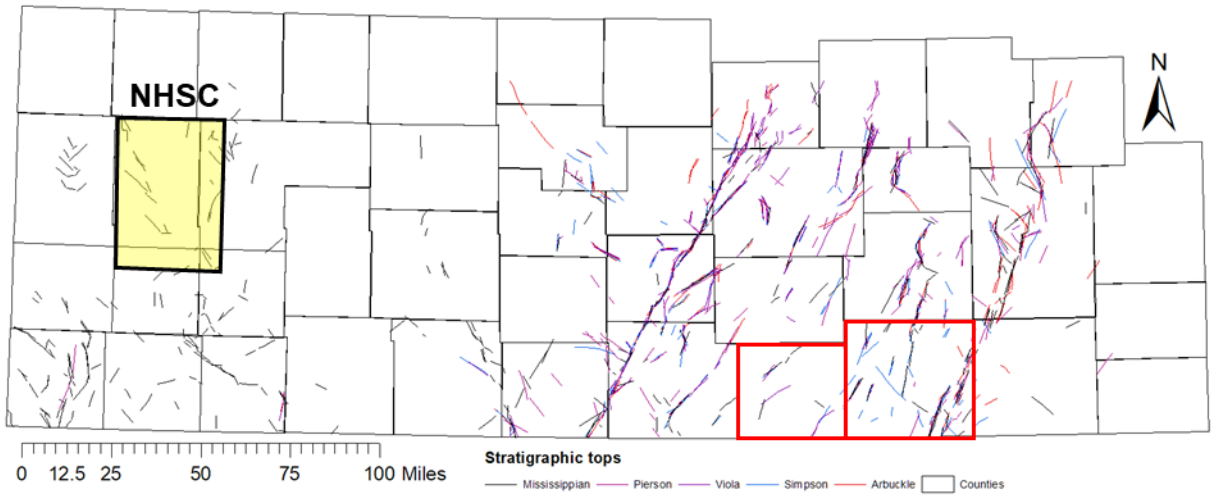

Figure 12. Mapped lineaments from Arbuckle through Mississippian. Black outline defines the North Hugoton Storage Complex (NHSC). Red outlines are Harper (west) and Sumner (east) counties.

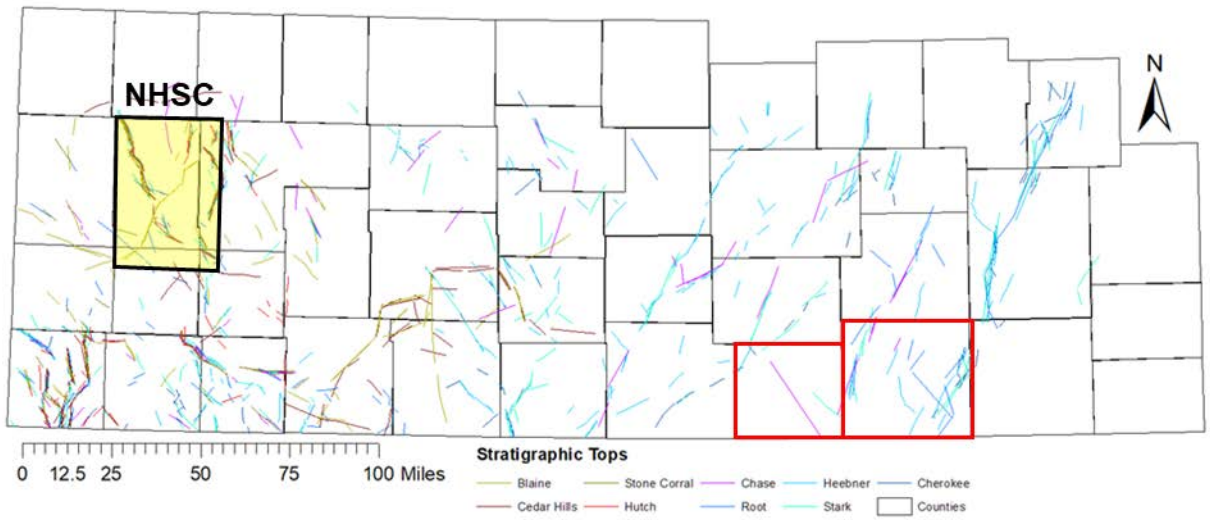

Figure 13. Mapped lineaments from Cherokee Group through Blaine Formation. The lineament density increases westward through the stratigraphic column and tracks with data density. Lineaments visible in the top Arbuckle surface remain present into the Heebner Shale and partially into the Root Shale. Black outline defines the North Hugoton Storage Complex (NHSC). Red outlines are Harper (west) and Sumner (east) counties.

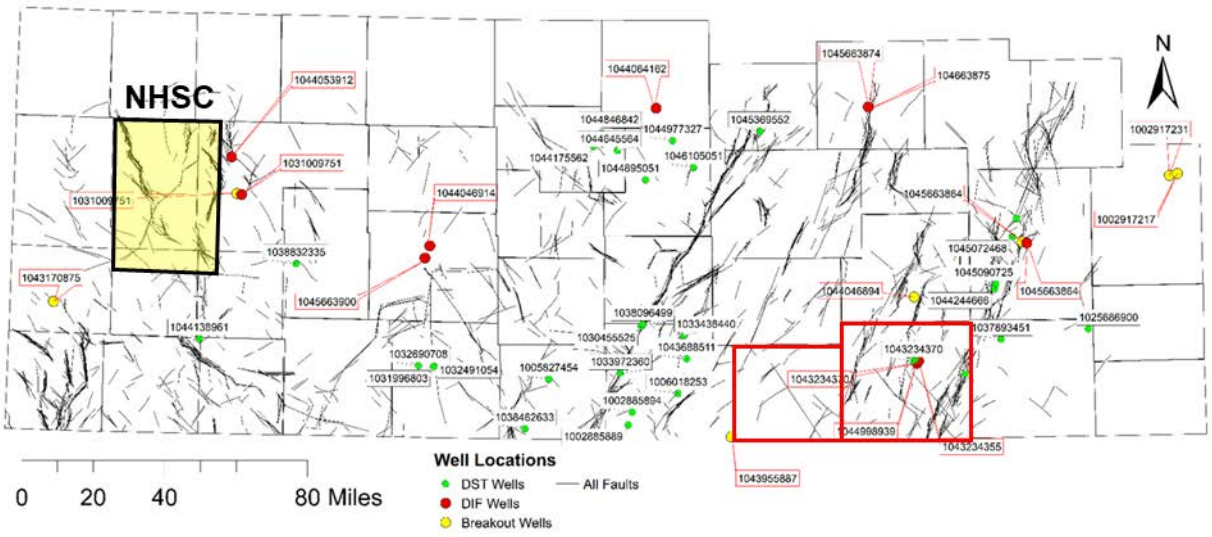

Figure 14. Composite map of lineaments documented from surface to the Cambrian-Ordovician. Note the dominant NNE and NNW structural trends. Locations and API of wells used for analysis of in situ stresses are shown as colored circles. Black outline defines the North Hugoton Storage Complex (NHSC). Red outlines are Harper (west) and Sumner (east) counties.

3.3 Stress orientations and magnitudes

The orientation of the maximum horizontal stress was estimated from 469 drilling-induced fractures in 14 wells across the study region (Table 1; Figure 16). Most of the drilling-induced fractures occur at depths of 2,000 ft or greater. The length of fractures ranged from 0.15 to 10.2 m (0.5 to 33.5 ft), with an average of 3.2 m (10.6 ft) across all the documented fractures. The measured fractures are a mixture of centerline and petal fracture, although centerline fractures were more common. Using the stress-indicator grading scale established by Heidbach et al. (2010), the wells were ranked A–D. Although most of the wells used fell into the B–C grade, three of the wells fell into the D category due to low fracture counts (Table 1). The maximum stress orientation follows a trend of ENE-WSW (Figure 16). The total range was 060–090°, with an average of 075–080°.

The minimum horizontal stress orientation was determined from 9 wells containing 35 borehole breakouts. The borehole breakouts analyzed fell into C–D rankings, as many of the wells had low feature counts. The minimum stress orientation follows a trend of NNW (Figure 16) and, as expected, is roughly orthogonal to the maximum stress direction. Overall, stress orientations determined by this study agree well with stress orientations from other studies in this part of the U.S. midcontinent (e.g., Dart, 1990; Holland, 2013; Alt and Zoback, 2015).

Stress magnitudes were estimated using well log and test data across the region. Pore fluid pressures were determined from shut-in or stabilization pressures obtained from drill stem tests (DSTs; Figure 17). Vertical stress gradients were estimated using the average calculated density, which ranged from 2.4 to 2.5 g/cm^3 across much of the study area. However, an average density of as high as 2.65 g/cm^3 was documented in the southwestern part of the study area. A density of 2.45 g/cm^3 was used to a depth of 1.5 km, which is average depth to Precambrian basement in the region. At depths greater than 1.5 km, a density of 2.75 g/cm^3 was used. A stress magnitude versus depth graph was created with these values and used to calculate Sv at 5 km depth, a typical hypocentral depth for induced earthquakes in the state of Kansas (Figure 17). SHmin and SHmax gradient values for normal faulting regimes were estimated at 15.4 MPa/km and 26 MPa/km, respectively. Strike-slip faulting regimes had SHmin and SHmax gradient values of roughly 26 and 60 MPa/km respectively.

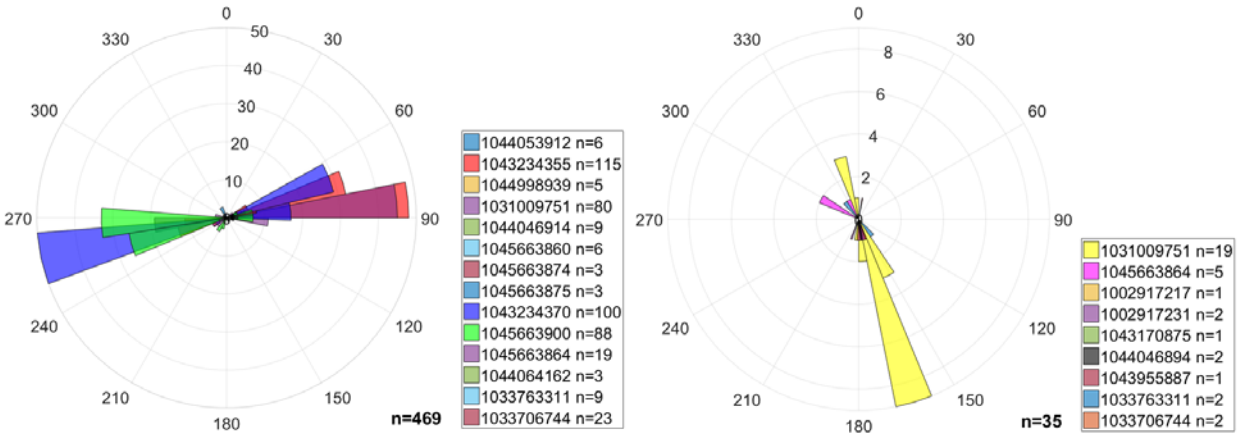

Figure 15. (Left) Drilling induced fracture orientations from 14 wells within the study area, identified by their Kansas unique well identification number or KID. (Right) Borehole breakout orientations from 9 wells in the study area, labeled by KID.

Table 1. Summary of stress indicator data.

Well KID	Stress Indicator	Count	Ranking
1044053912	DIF	6	C
1043234355	DIF	115	B
1044998939	DIF	5	C
1031009751	DIF	80	B
	BO	19	B
1043234370	DIF	100	B
1044064162	DIF	3	D
1044046914	DIF	9	C
1045663860	DIF	6	D
1045663874	DIF	3	D
1045663875	DIF	3	D
1045663900	DIF	88	B
1045663864	DIF	19	B
	BO	5	C
103376331	DIF	9	B
	BO	2	D
1033706744	DIF	23	B
	BO	2	D
1002917217	BO	1	D
1002917231	BO	2	D
1043170875	BO	1	D
1044046894	BO	2	D
1043955887	BO	1	D

Abbreviations: BO=Break out; DIF=drilling-induced fracture

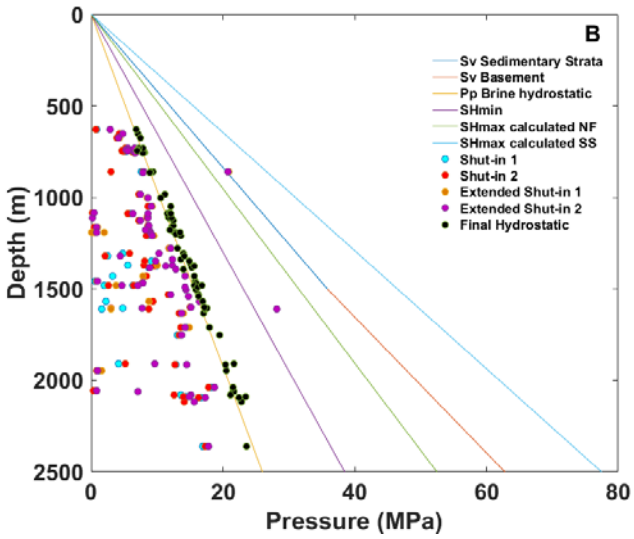

Figure 16. Stress gradients based on well-log-based average densities, drill-stem test data, and estimations from the stress polygon (Zoback et al., 2003).

3.5 Fault slip and dilation tendency analysis

To analyze slip tendency, we imported the mapped lineaments into 3DStress. Magnitudes for Sv (130 MPa), Shmin (77 MPa), and SHmax (295 MPa) at 5 km depth were derived from stress gradients, described in Section 2.2.2. Our analysis presumed a strike-slip stress state (SHmax>Sv>Shmin) and the largest value for SHmax, so that lineaments with any potential for reactivation were aggressively identified. Results from the slip tendency analysis are shown in Figure 18 for SHmax oriented 075°. Slip tendency values ranged from 0 to 0.72, with lineaments at or above 0.6 at a critical state. The analysis revealed at this basement depth, two lineament orientation ranges were already at or near failure, 040–060° and 090–120°. As expected, lineaments better aligned with the maximum horizontal stress direction showed a greater likely for being at or near failure conditions, whereas lineaments oriented orthogonal to the maximum stress appear stable and can likely accommodate large increases in pore fluid pressures (>20 MPa) in their vicinity.

For the North Hugoton Storage Complex, the slip tendency analysis suggests that most of the documented lineaments are stable under current stress states and reservoir conditions. The majority of the lineaments are green and blue, corresponding to a slip tendency of <0.5. Such faults can accommodate increases in pore pressure without failing.

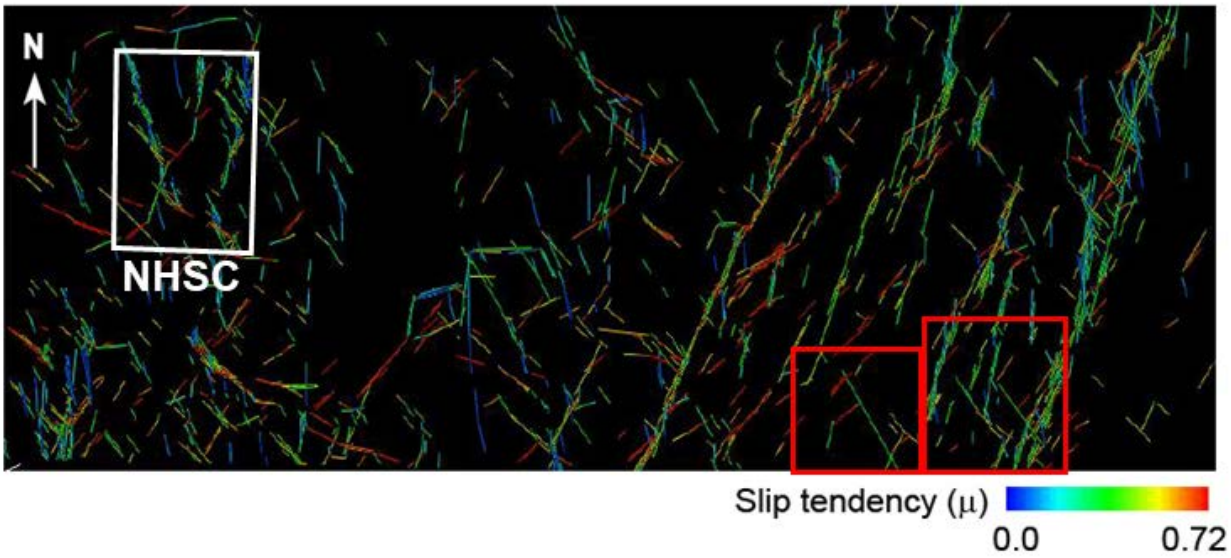

Figure 17. Slip tendency of mapped lineaments (as shown in Figure 15). Lineaments with NE and NW strikes (red) are critically stressed under the presumed stress state and are most likely to reactivate with small changes in pore fluid pressure with injection. N-striking faults (blue) are stable and may accommodate large pore fluid pressure increases. White outline defines the North Hugoton Storage Complex (NHSC). Red outlines are Harper (west) and Sumner (east) counties.

3.6 Validation of results

Comparison of our results with 3-D seismic reflection data volumes are encouraging. The mapped features correspond with similarly oriented faults recognized in higher resolution datasets in the Pleasant Prairie, Cutter, and Wellington fields, suggesting that the method may be a useful approach for high-level, first-order mapping of regional structures and trends. For example, analysis by Schwab et al. (2017) recognized dominantly north-northeast-striking faults in 3-D seismic data in Wellington Field in north-central Sumner county. The faults cut from the Precambrian basement but are overlapped by the top Mississippian horizon, suggesting motion predates that surface. The documented lineaments in the same area of Sumner County, although crude, are oriented similarly. They are also poorly documented in surface analysis of structure contour maps of post-Mississippian (mid-Pennsylvanian through Permian) stratigraphic surfaces (e.g., Cherokee Group through Blain Formation), suggesting mostly pre-Pennsylvanian motion (Figures 13 and 14). Similar agreement was recognized for the southern part of the North Hugoton Storage Complex, where 3-D seismic data are available over the Pleasant Prairie field and (Figure 19).

Although the results of our analysis are promising for fault mapping in areas without seismic data, we also find limitations to the analysis. The analysis cannot distinguish between faults and other types of linear surface deflections. For example, incised valleys in southwestern Kansas appear as north-trending lineaments. Without prior knowledge of such features and their locations, one might assume that these lineaments are faults. Low density of formation tops in an area can also contribute to over smoothing of grids used in surface analysis. Faults that may be present could be missed in such maps. Such issues may be minimized through rigorous validation of the results using other datasets. Clear assignment or designation of the quality or confidence of the documented features is also important. Nonetheless, the analysis could serve as an important tool for further data gathering at potential storage sites.

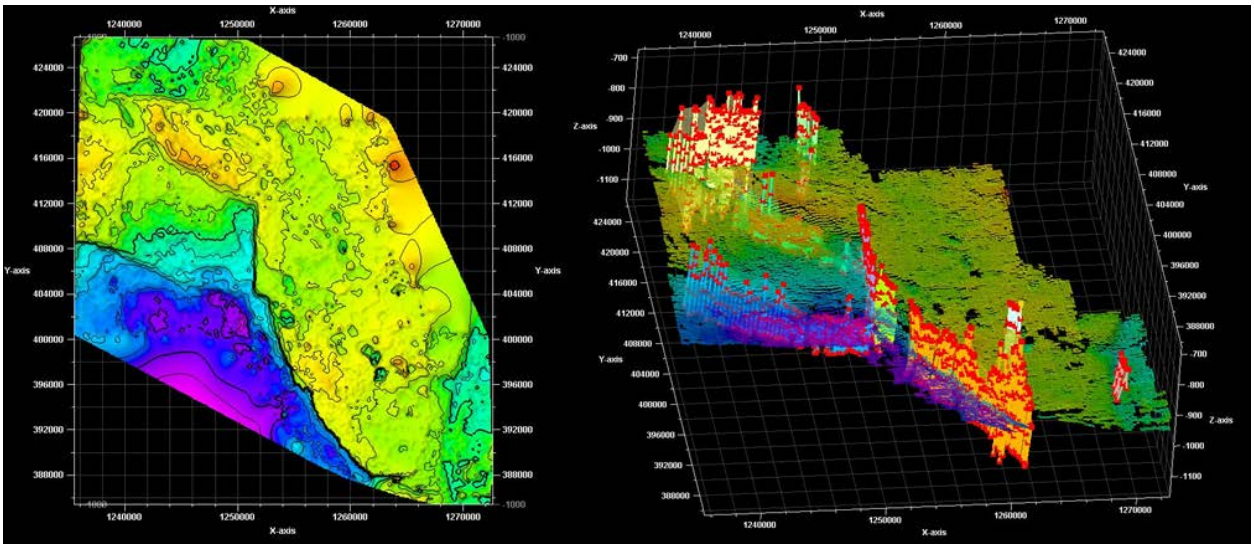

Figure 18. Faults documented in 3-D seismic reflection data over the Pleasant Prairie field in the southern part of the North Hugoton Storage Complex. Left figure is a grid of the time structure map on the Top Arbuckle horizon. Right shows line interpretation of surface and documented faults, shown as fault sticks that define the 3-D fault planes.

4. Integration of results

Brine injection data were obtained from the Kansas Corporation Commission for 2010–2014. SWD wells were separated from EOR wells, and geologic intervals of completion (disposal formations) were identified via well completion reports and other well documents from the Kansas Geological Survey database and the Kansas Geological Society Walters Digital Geological Library. Well completion intervals were grouped into 13 geologic disposal zones, based on formation or group age: Cretaceous, Permian, Virgilian, Missourian, Desmoinesian, Atokan-Morrowan, Mississippian, M. Ordovician-Devonian, U. Cambrian-L. Ordovician (Arbuckle Group), Precambrian-Cambrian, Undifferentiated Arbuckle-Basement, Undifferentiated, and Unknown (Figure 20). The majority (~75% by volume) of brine disposal in Kansas occurs in the Arbuckle Group, a thick Cambrian-Ordovician carbonate unit that rests unconformably atop the basement rock in many parts of the state (Figure 20). The remaining ~25% of brine disposal occurs in Middle Ordovician to Cretaceous rocks (Figure 20).

Spatial analysis of injection volumes in the state of Kansas show that in 2014, when injection induced earthquakes initiated, several counties across central and south-central Kansas saw substantial volumes of saltwater disposed of in Class II wells (Figure 21). Harper county Class II wells, in particular, accommodated more than 100 million barrels of saltwater into the Cambrian-Ordovician Arbuckle Group. Additionally, in Figure 22 it can be seen that, while many counties were seeing reductions in disposal volumes between 2013 and 2014, central and south-central Kansas counties, and in particular Harper and Reno counties, saw large increases in disposal volumes.

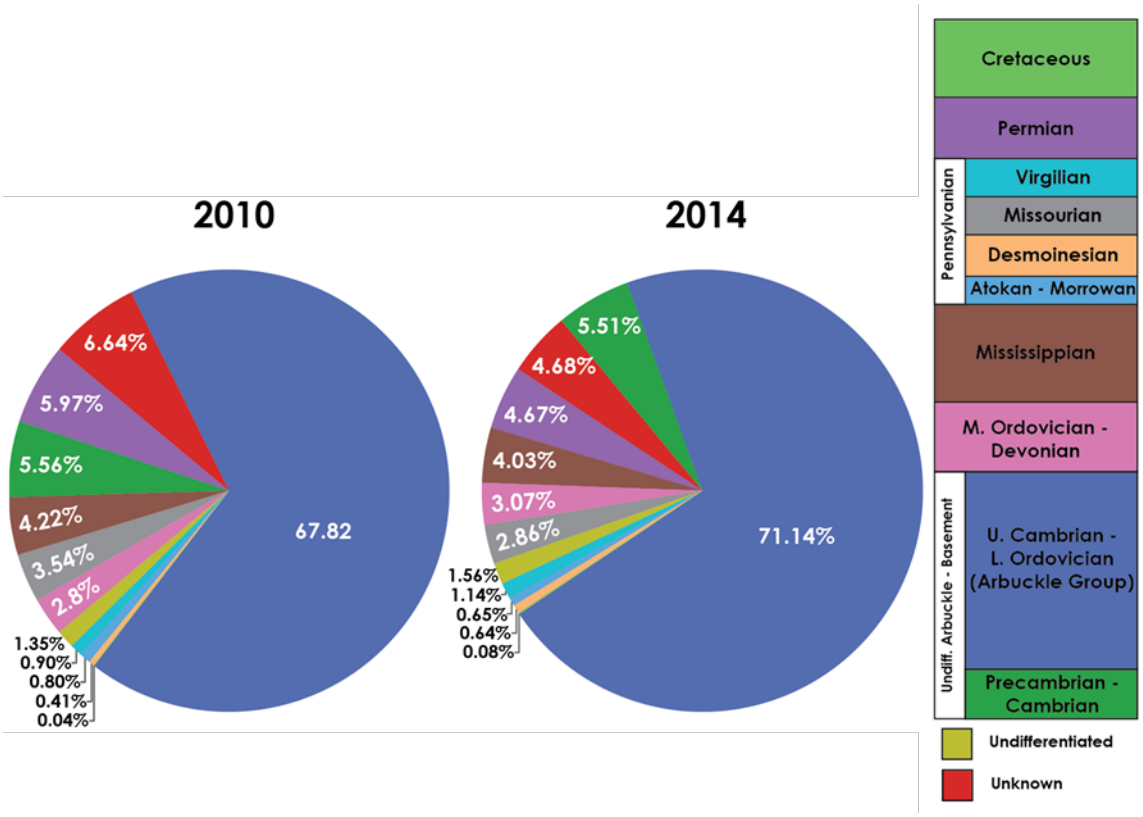

Figure 20. Pie charts show relative distribution of volume of Class II saltwater injection by disposal zone. Injection into the Cambrian-Ordovician and older zones accounts for >75% of the total disposal activity in the state.

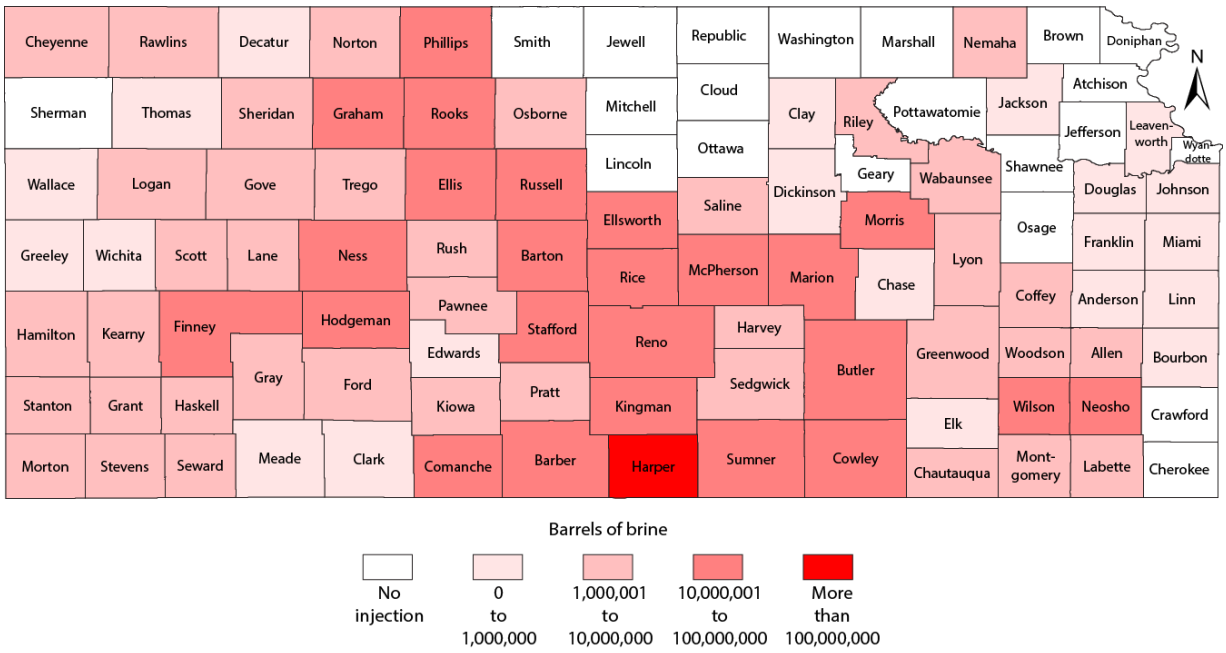

Figure 21. Map of Class II saltwater disposal volumes (barrels) for each county in 2014.

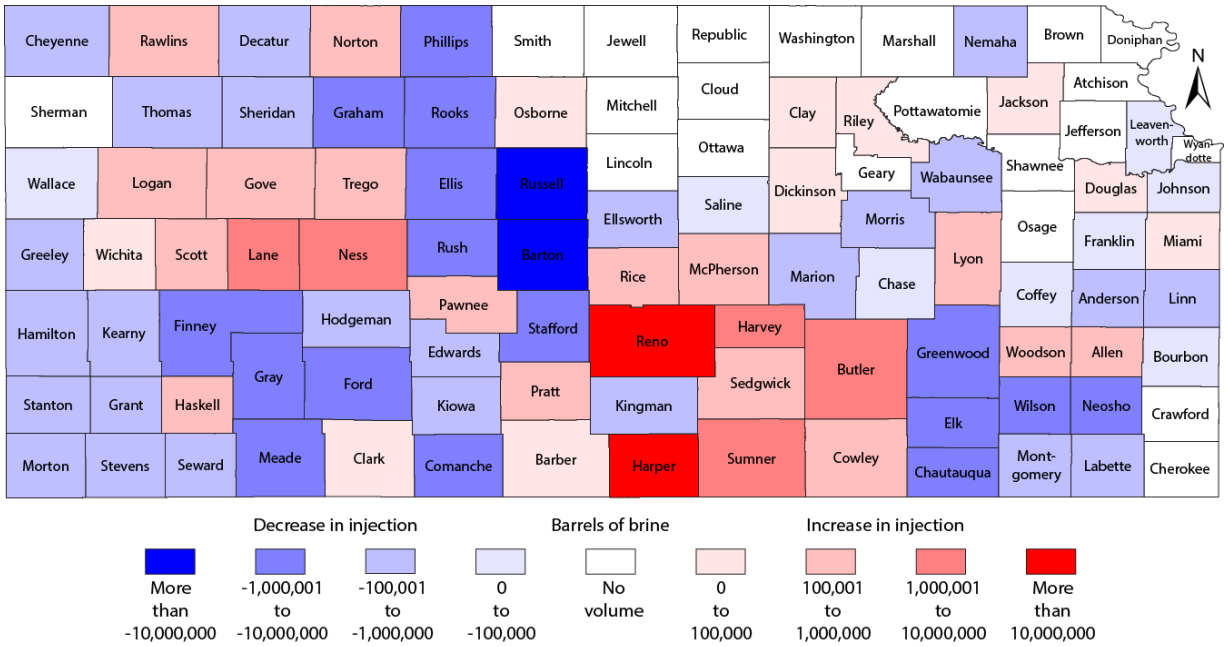

Figure 22. Change in saltwater disposal volumes between 2013 and 2014. Harper and Reno counties saw increases in disposal volumes, while many other counties in the state saw overall reductions in disposal activities.

The slip tendency analysis, when paired with the disposal trends for Kansas counties, demonstrates that the combination of optimally oriented lineaments (faults) with high rates of injection explains the recent increase in seismicity observed in the south-central part of the state, particularly in Harper County. The analysis also suggests that continued injection into Reno County and nearby counties (e.g., Rice, McPherson, Harvey, and Pratt counties) is concerning, as a number of suitably oriented structural features are recognized in these counties. Recent earthquakes in Reno County may be confirming this prediction.

By comparison, the analysis suggests that, although there may be some well-oriented structural features in the North Hugoton Storage Complex, overall reductions in disposal volumes in most of these counties contributes to a lower chance of such structures reactivating in the near future. This observation paired with below hydrostatic conditions for reservoirs such as the Arbuckle Group mean that large pore pressure increases, like those observed in the southern and central part of the state, are less likely to occur. However, continued monitoring of statewide disposal activity and refinement of structural maps and dynamic data (e.g., injection volumes, injection pressures, etc.) are critical to characterizing this evolving seismic hazard.

References

Aadnoy, B.S., 1990, In situ stress direction from borehole fracture traces.: Journal of Petroleum Science and Engineering, v. 4, p. 143–53.

Alt, R. C., and Zoback, M. D., 2015, A Detailed Oklahoma Stress Map for Induced Seismicity Mitigation: In AAPG Annual Convention and Exhibition.

Bell, J.S., 1990, Investigating stress regimes in sedimentary basins using information from oil industry wireline logs and drilling records, in Hurst, A., Lovell, M.A., and Morton, A.C., eds., Geological Applications of Wireline Logs: Geological Society Special Publication 48, p. 305-325.

Bell, J.S. and Babcock, E.A., 1986, The stress regime of the Western Canadian Basin and implications for hydrocarbon production: Bulletin of the Canadian Petroluem Geology, v. 34, p. 364-378.

Bell, J.S. and Gough, D.I., 1979, Northeast-southwest compressive stress in Alberta: evidence from oil

wells: Earth and Planetary Science Letters, v. 45, p. 475–82.
Berendsen, P. and Blair, K.P., 1986, Subsurface structural maps over the Central North American rift system (CNARS), central Kansas, with discussion: Kansas Geological Survey Subsurface Geology Series 8, 16p.
Byerlee, J., 1978, Friction of rocks: Pure Applied Geophysics, v. 116, p. 615–626.
Dart, R. L., 1990, In situ stress analysis of wellbore breakouts from Oklahoma and the Texas Panhandle, No. 1866, Department of the Interior, US Geological Survey.
Dolton, G.L., and Finn, T.F., 1989, Petroleum geology of the Nemaha Uplift, central mid-continent: USGS Open-File Report 88-450D, 39 p.
Evenick, J.C., Jacobi, R.D., Baker, G.S., and Mitchell, C.E., 2005, Subsurface evidence for faults in the Appalachian basin, western New York State: Northeastern Geology and Environmental Sciences, v. 27, p. 1-17.
Heidbach, O., Tingay, M. Barth, A., Reinecker, J., Kurfeb, D., and Muller, B., 2010, Global crustal stress pattern based on the World Stress Map database release 2008: Tectonophysics, v. 482, p. 2-15.
Holland, A. A., 2013, Optimal fault orientations within Oklahoma. Seismological Research Letters, 84(5), 876-890.
Jaeger, J.C., Cook, N.G.W., and Zimmermann, R.W., 2007, Fundamentals of Rock Mechanics, 4th edition: Blackwell, Oxford
Jewett, J.M, 1951, Geologic structure in Kansas: Kansas Geological Survey, Bulletin 90, p. 105–172.
Kruger, J. M., 1997, On-line gravity and magnetic maps of Kansas: Kansas Geological Survey Open-File Report 96-51, http://www.kgs.ku.edu/PRS/PotenFld/potential.html.
Lee, W., and Merriam, D. F. (1954). Preliminary study of the structure of western Kansas: Kansas Geological Survey, Oil and Gas Inv. 11, p. 1-23.
Lugn, A. L. (1935) The Pleistocene Geology of Nebraska: Nebraska Geol. Survey, Bull. 10, pp. 223 p.
Manzi, M.S.D., Durrheim, R.J., Hein, K.A.A., and King, N., 2012, 3D edge detection seismic attributes used to map potential conduits for water and methane in deep gold mines in the Witwatersrand basin, South Africa: Geophysics, v. 77, p. WC133-WC147.
McBee Jr, W. (2003). Nemaha strike-slip fault zone. Paper presented at the AAPG Mid-Continent Section Meeting, Tulsa, Oklahoma.
Merriam, D.F., 1963, The geologic history of Kansas: Kansas Geological Survey Bulletin 162, 317p.
Moeck, I., Kwiatek, G., and Zimmermann, G., 2009, Slip tendency analysis, fault reactivation potential and induced seismicity in a deep geothermal reservoir: Journal of Structural Geology, v. 31, p. 1174-1182.
Moeck, I., Kwiatek, G., and Zimmermann, G., 2009, Slip tendency analysis, fault reactivation potential and induced seismicity in a deep geothermal reservoir: Journal of Structural Geology, v. 31, p. 1174-1182.
Moos, D. and Zoback, M.D., 1990, Utilization of observations of well bore failure to constrain the orientation and magnitude of crustal stresses: application to continental deep sea drilling project and ocean drilling program boreholes: Journal of Geophysical Research, v. 95, p. 9305–9325.
Morris, A. and Ferrill, D.A., Henderson, D.B., 1996, Slip-tendency analysis and fault reactivation: Geology v. 24, p. 275–278.
Ocola, L.C. and Meyer, R.P., 1973, Central North American rift system: 1. Structure of the axial zone from seismic and gravimetric data: Journal of Geophysical Research, v. 78, p. 5173-5194.
Plumb, R.A. and Cox, J.W., 1987, Stress directions in eastern North America determined to 4.5km from borehole elongation measurements: Journal of Geophysical Research, v. 92, p. 4805-4816.
Schwab, D.R., Bidgoli, T.S., and Taylor, M.H., 2017, Characterizing the potential for injection-induced fault reactivation through subsurface structural mapping and stress field analysis, Wellington Field, Sumner County, Kansas: Journal of Geophysical Research: Solid Earth, v. 122, p. 10,132–10,154, https://doi.org/10.1002/2017 JB014071.
Smithson, S. B. (1971). Densities of metamorphic rocks: Geophysics, 36(4), 690-694.

Stander, T. W., and Grant, J. L. (1989). A case history of petroleum exploration in the southern Forest City basin using gravity and magnetic surveys: In Geophysics in Kansas: Kansas Geological Survey Bulletin 226, edited by D.W. Steeples, p. 245-256, Univ. of Kansas, Lawrence, Kansas.

Somanas, C., Knapp, R.W., Yarger, H.L., and Steeples, D.W., 1989, Geophysical model of the midcontinent geophysical anomaly in northeastern Kansas, in Steeples, D.W., ed., Geophysics in Kansas: Kansas Geological Survey Bulletin, v. 226, p. 215-228.

Watney, W. L. et al., 2015, Modeling CO_2 sequestration in saline aquifer and depleted oil reservoir to evaluate regional CO_2 sequestration potential of Ozark Plateau aquifer system, south-central Kansas, final report, Award Number: DE-FE0002056, submitted October 2, 2015, 4,867 p.

Watney, W. L. et al., 2016, Integrated CCS for Kansas (ICKan) SF 424 R&R, application for federal assistance, Phase I—Integrated CCS pre-feasibility study activity under CarbonSAFE, DOE-NETL FOA 1584.

Wiprut, D. and Zoback, M.D., 2000, Fault reactivation and fluid flow along a previously dormant normal fault in the northern North Sea: Geology, v. 28, p. 595–598.

Zoback, M.D., Moos, D., Mastin, L., and Anderson, R.N., 1985, Wellbore breakouts and in situ stress: Journal of Geophysical Research, v. 90, p. 5523-5530.

Zoback, M.D., C.A. Barton, M. Brudy, D.A. Castillo, T. Finkbeiner, B.R. Grollimund, D. B. Moos, P. Peska, C.D. Ward, D.J. Wiprut, 2003, Determination of stress orientation and magnitude in deep wells, International Journal of Rock Mechanics and Mining Sciences, v. 40, p. 1049-1076.

Appendix I: Modifications to FE/NETL CO_2 Transport Cost Model and preliminary CO_2 pipeline cost estimates

Martin k. Dubois[1] and Dane Mcfarlane[2]
[1] Improved Hydrocarbon Recovery, LLC, [2] Great Plains Institute

Overview

Understanding the economics of and exploring options and strategies to transport CO_2 from large-scale anthropogenic sources, particularly coal-fired power plants, in the most optimal manner is a key component of the Integrated CCS for Kansas project (ICKan). Estimating cost for variety of pipeline scenarios is the first step in the process. Because large-scale coal-fired power plants (e.g.: Jeffrey Energy Center) are distant to potential storage sites, pipelines are the only option for transporting large volumes of CO_2. However, pipelines have extremely high capital costs that negatively impact the overall costs and feasibility for CCS projects. The ICKan project considers the option of reducing the net costs for CO_2 transported for CCS by combining CO_2 captured from power plants and/or a refinery with CO_2 destined for EOR operations. One case would include a very large-scale system where CO_2 is captured from 32 ethanol plants in the Upper Midwest and joined with CO_2 captured from a power plant (Westar's Jeffrey Energy Center). CO_2 would then be transported to a saline aquifer storage site as well as to EOR markets. Both sides would benefit by the economies of scale for the pipeline system. Another case considered (without the ethanol CO_2 component) is for the capture be scaled large enough to sell CO_2 for EOR, again gaining the benefits from scale and possibly from revenues generated by the sale of CO_2 for EOR. In this high-level study we used a modified Transport Cost Model developed by the National Energy Technology Laboratory (NETL) to estimate costs (Grant, et al., 2013; Grant and Morgan, 2014). In the very large-scale scenario described above, the modeled pipeline system could transport 13.4 million tonnes of CO_2/year at an approximate cost of $16/tonne, excluding interest and business margin.

FE/NETL CO_2 Transport Cost Model and modifications

The Great Plains Institute (GPI) and Improved Hydrocarbon Recovery, LLC (IHR), collaborators on the ICKan project, identified the National Energy Technology Laboratory's (NETL) CO_2 Transport Cost Model as a resource for estimating the technical requirements and costs of CO_2 transport through pipelines. The NETL model takes a wide variety of inputs—including pipeline route length, CO_2 capacity, pressure, project financing, and other areas—and calculates multiple components of capital and operating and maintenance costs, as well as technical specifications such as minimum pipeline diameter. Calculations are done through both spreadsheet formulas and more complex Excel Visual Basic for Applications (Excel VBA) functions.

The ICKan project requires the assessment of pipeline networks comprising multiple trunk segments and many feeder lines connected to individual CO_2 sources; however, the original NETL model calculates specifications and costs for only one pipeline at a time. To streamline the process of calculating many pipeline network segment costs, GPI created additional Excel VBA macro functionality to interact with the NETL cost model. Without changing or modifying the NETL spreadsheets or VBA code in anyway, GPI created a VBA macro that collects inputs from a list of pipeline segments, inputs the parameters for each segment, and records the model outputs for each segment individually. The inputs and outputs are summarized in Table 1. Model costs are in 2011 dollars, the model default.

Table 1: Model inputs and outputs. Abbreviations: MT/yr—million tonnes/year, psig—pounds per square inch gauge, ID—inside diameter, ROW—right of way, O&M—operations and maintenance.

Inputs (by segment)	**Outputs (by segment)**
length (miles)	minimum pipeline ID (inches)
number of booster pumps	pipeline nominal diameter (inches)
annual CO2 transport capacity (MT/yr)	materials costs
capacity factor	labor costs
input pressure (psig)	ROW-damage costs
output pressure (psig)	miscellaneous costs
change in elevation (feet)	CO2 surge tanks costs
	pipeline control system costs
	pump costs
	Total capital cost
	pipeline O&M
	other equipment and pumps O&M
	electricity costs for pumps
	Total annual operating expenses

CO_2 Sources: Midwestern ethanol and Kansas energy facilities

Ethanol plants from the upper Midwest and energy facilities in Kansas are the CO_2 sources in this study. Four Kansas energy facilities are industry partners in the ICKan project: Westar Jeffrey Energy Center, Kansas City Board of Public Utilities' Dearman Creek, CHS McPherson refinery, and the Sunflower Holcomb Station power plant. All except CHS are coal-fired power plants. CO_2 emitted annually and the estimated volume that could reasonably be available from each facility is provided in Table 2.

Table 2. Industry partner CO_2 source data. Abbreviations: Mwe—megawatt electric, MT/yr—million tonnes/year.

	Mwe	**Approx. CO2 Emitted (MT/yr)**	**Est. Vol. Available (MT/yr)**
Jeffrey Energy Center	2400	12.5	2.5
Dearman Creek	261	1.2	?
Holcomb Station	350	1.8	?
CHS refinery	NA	1.4	0.76

The location and production capacity of U.S. ethanol plants is sourced from the U.S. Department of Energy (U.S. DOE, 2017). Table 3 shows 32 ethanol plants within the region that could supply CO_2 to a modeled pipeline network. These plants represent a total of approximately 3.6 billion gallons of ethanol production per year and 10.9 million metric tons of CO_2. The volume of CO_2 was calculated at a rate of 6.624 lbs. CO_2/gallon ethanol (Dubois et al., 2002).

Table 3. Thirty-two ethanol plants considered in a large-scale CO_2 gathering system. The abbreviation MGPY is million gallons per year.

Company	Ethanol Plant	State	Ethanol Capacity (MGPY)	CO2 output (Tonne/year)
ABSOLUTE ENERGY LLC	ST ANSGAR	IA	110	330,449
ADM CEDAR RAPIDS IA DRY MILL	CEDAR RAPIDS DRY MILL	IA	300	901,224
ADM CLINTON IA	CLINTON	IA	237	711,967
BIG RIVER UNITED ENERGY LLC	DYERSVILLE	IA	100	300,408
CARGILL INC	FORT DODGE	IA	113	339,461
FLINT HILLS RESOURCES FAIRBANK LLC	FAIRBANK	IA	100	300,408
FLINT HILLS RESOURCES LLC	ARTHUR	IA	100	300,408
FLINT HILLS RESRCS MENLO LLC	MENLO	IA	100	300,408
FLINT HILLS RESRCS SHELL ROCK	SHELL ROCK	IA	100	300,408
FRONTIER ETHANOL LLC	GOWRIE	IA	60	180,244
GOLDEN GRAIN ENERGY LLC	MASON CITY	IA	107	321,436
HOMELAND ENERGY SOLUTIONS LLC	LAWLER	IA	100	300,408
LITTLE SIOUX CORN PROCESSORS LP	MARCUS	IA	92	276,375
LOUIS DREYFUS COMMODITIES	GRAND JUNCTION	IA	100	300,408
PENFORD PRODUCTS CO	CEDAR RAPIDS	IA	45	135,183
VALERO RENEWABLE FUELS LLC	ALBERT CITY	IA	110	330,449
VALERO RENEWABLE FUELS LLC	CHARLES CITY	IA	110	330,449
VALERO RENEWABLE FUELS LLC	FORT DODGE	IA	110	330,449
VALERO RENEWABLE FUELS LLC	HARTLEY	IA	110	330,449
PRAIRIE HORIZON AGRI-ENERGY LLC	PHILLIPSBURG	KS	40	120,163
US ENERGY PARTNERS	RUSSELL	KS	55	165,224
ABENGOA BIOENERGY OF NEBRASKA LLC	RAVENNA	NE	88	264,359
ADM COLUMBUS NE DRY MILL	COLUMBUS DRY MILL	NE	313	940,277
ADM COLUMBUS NE WET MILL	COLUMBUS WET MILL	NE	100	300,408
AVENTINE - AURORA WEST LLC	AURORA WEST	NE	108	324,440
CARGILL INC	BLAIR	NE	210	630,857
CHIEF ETHANOL FUELS INC	HASTINGS	NE	70	210,285
FLINT HILLS RESOURCES	FAIRMONT	NE	100	300,408
GREEN PLAINS CENTRAL CITY LLC	CENTRAL CITY	NE	100	300,408
GREEN PLAINS WOOD RIVER LLC	WOOD RIVER	NE	110	330,449
NEBRASKA ENERGY LLC	AURORA	NE	45	135,183
VALERO RENEWABLE FUELS LLC	ALBION	NE	100	300,408

Cost projections for four cases

In an initial analysis, equipment requirements and estimated capital and operating costs for four separate pipeline scenarios were determined using the modified Transport Cost Model. In the largest scenario a pipeline network was designed to gather CO_2 from 32 ethanol plants and Jeffrey Energy Center, Kansas' largest CO_2 source, and transport the CO_2 through Kansas to a saline aquifer storage site (Pleasant Prairie). From there it would continue to the Permian Basin, an area with an active enhanced oil recovery (EOR) industry (Figure 1). ESRI ArcGIS geographic information system mapping program and the North

American Datum 1983 (2011 national adjustment) geographic projection, were used to build the system and estimate the length of straight-line pipeline segments. Because actual pipeline siting is not a straight line, involving rights-of-way deliberations and physical obstacles, each segment was multiplied by a factor of 1.2 to approximate additional routing requirements.

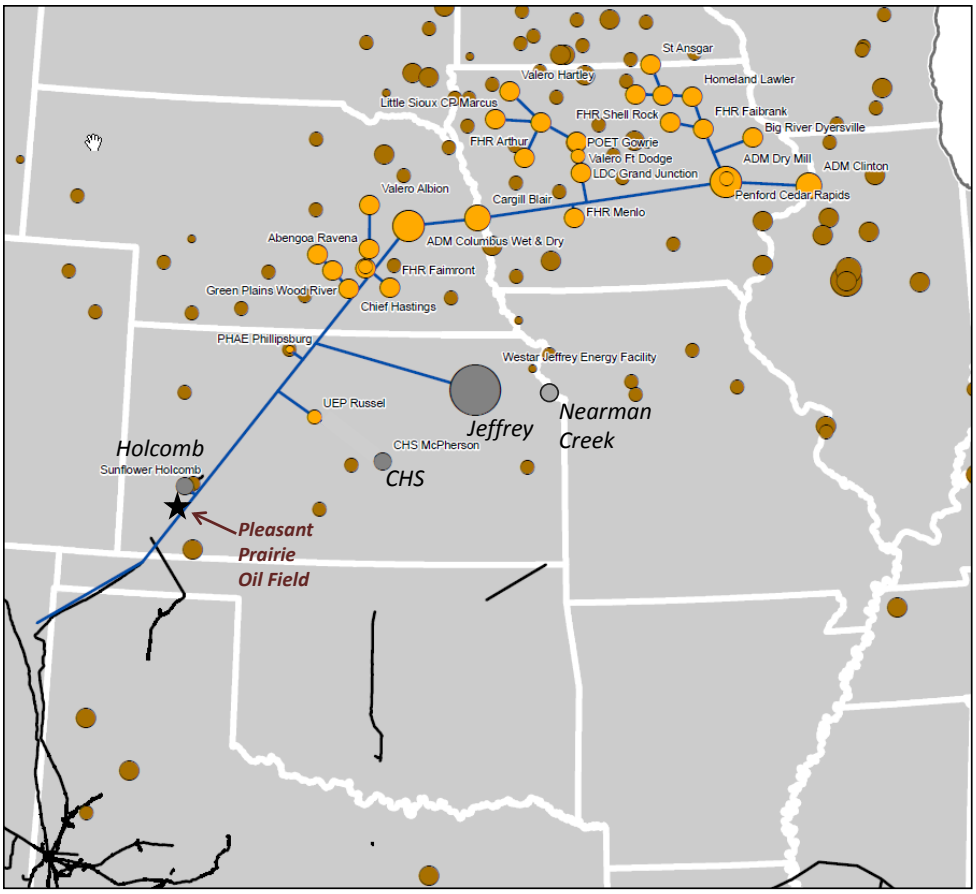

Figure 1. Pipeline Scenario 1, connecting 32 ethanol plants and delivering CO_2 to Kansas, Oklahoma and Texas. Bubbles are sized according to CO_2 volume. Ethanol plants are yellow (in the evaluated scenario) and brown (not in the scenario). Gray circles are ICKan industry partners, one of which is shown to be connected under this scenario. Pleasant Prairie is one of the storage sites considered in the project. Black line segments are existing CO_2 pipeline infrastructure.

Table 4 is an input/output table that represents the modified portion of the model for the large-scale project described above. Inputs are provided by the user and the balance of the table is calculated output based on the input data. The cost model assumes that CO_2 is delivered into the pipeline system at a set pressure, 2,200 psig in this case. For this analysis, the pressure was allowed to drop to 1,600 psig before it was pumped back to 2,200 psig by booster pumping stations along the route. A minimum of one pump per segment is required by the model. Costs are most sensitive to pipeline diameter and the diameter required is a function of pressure and volume to be transported. Because booster pump stations in this model are relatively inexpensive in comparison to the pipeline, one can optimize for cost by varying the number of pump stations to reduce pipeline diameter, as was done in this analysis. The number of pump stations ranges from one to fifteen and pipe diameter is from 4 to 24 inches in diameter.

Inputs								Pipeline Diameter		Capital Cost								Annual O&M Cost			
Segment ID	Length (X1.2)	# of Pumps	Annual CO2	Capacity factor	Input Pressure	Outlet Pressure	Change in Elev.	Minimum Pipeline Inner Diameter	Pipeline Nominal Diameter	Materials	Labor	ROW-Damages	Miscellaneous	CO2 Surge Tanks	Pipeline Control system	Pumps	Total Capital	Pipeline O&M	Pipeline related equipment and pumps	Electricity costs for pumps	Total annual operating expenses
#	mi	#	MT/yr	dec.	psig	psig	ft	in	in	$K	$K	$K	$K	$K	$K	$K	$K	$K	$K	$K	$K
20	44.6	2	1.24	0.8	2200	1600	0	6.97	8.00	$4,880	$19,083	$2,020	$5,346	$1,245	$112	$931	$33,617	$378	$92	$413	$883
13	47.8	2	0.30	0.8	2200	1600	0	4.11	6.00	$4,199	$19,083	$2,088	$4,458	$1,245	$112	$353	$31,538	$405	$68	$100	$573
16	43.0	2	0.30	0.8	2200	1600	0	4.03	6.00	$3,786	$17,215	$1,885	$4,028	$1,245	$112	$353	$28,623	$364	$68	$100	$533
26	0.7	1	0.14	0.8	2200	1600	0	1.47	4.00	$122	$644	$82	$195	$1,245	$112	$125	$2,525	$6	$59	$23	$88
11	8.6	1	1.06	0.8	2200	1600	0	5.17	6.00	$812	$3,732	$417	$922	$1,245	$112	$411	$7,650	$73	$71	$177	$320
27	3.5	1	0.14	0.8	2200	1600	0	1.98	4.00	$318	$1,670	$196	$373	$1,245	$112	$125	$4,038	$30	$59	$23	$112
12	21.5	1	0.60	0.8	2200	1600	0	4.96	6.00	$1,926	$8,781	$967	$2,085	$1,245	$112	$269	$15,384	$182	$65	$100	$347
23	31.9	2	0.98	0.8	2200	1600	0	5.98	6.00	$2,827	$12,868	$1,412	$3,027	$1,245	$112	$773	$22,264	$270	$85	$328	$683
30	46.1	2	0.30	0.8	2200	1600	0	4.08	6.00	$4,056	$18,434	$2,018	$4,309	$1,245	$112	$353	$30,526	$391	$68	$100	$559
29	63.0	2	2.18	0.8	2200	1600	0	9.27	12.00	$10,564	$31,333	$3,019	$10,802	$1,245	$112	$1,515	$58,589	$534	$115	$729	$1,378
3	25.6	1	0.30	0.8	2200	1600	0	3.94	4.00	$1,872	$9,832	$1,105	$1,786	$1,245	$112	$176	$16,127	$217	$61	$50	$328
31	0.6	1	0.34	0.8	2200	1600	0	1.98	4.00	$110	$580	$75	$184	$1,245	$112	$188	$2,494	$5	$62	$57	$123
15	15.5	1	1.91	0.8	2200	1600	0	7.26	8.00	$1,747	$6,895	$738	$1,960	$1,245	$112	$672	$13,368	$132	$81	$318	$531
14	18.7	1	2.09	0.8	2200	1600	0	7.79	8.00	$2,084	$8,206	$876	$2,324	$1,245	$112	$728	$15,574	$158	$83	$348	$590
5	32.6	2	2.39	0.8	2200	1600	0	8.44	12.00	$5,507	$16,413	$1,589	$5,668	$1,245	$112	$1,641	$32,175	$277	$120	$797	$1,194
7	48.0	2	0.33	0.8	2200	1600	0	4.27	6.00	$4,217	$19,166	$2,097	$4,477	$1,245	$112	$371	$31,686	$407	$69	$110	$586
8	8.8	1	0.81	0.8	2200	1600	0	4.67	6.00	$830	$3,816	$426	$942	$1,245	$112	$332	$7,703	$75	$68	$134	$276
22	37.1	2	1.25	0.8	2200	1600	0	6.76	8.00	$4,069	$15,928	$1,688	$4,469	$1,245	$112	$940	$28,451	$314	$92	$418	$824
6	49.8	2	0.28	0.8	2200	1600	0	4.01	6.00	$4,372	$19,868	$2,174	$4,639	$1,245	$112	$338	$32,747	$422	$68	$92	$582
24	29.5	1	0.32	0.8	2200	1600	0	4.15	6.00	$2,618	$11,919	$1,308	$2,808	$1,245	$112	$183	$20,193	$250	$62	$54	$365
4	14.7	1	0.30	0.8	2200	1600	0	3.54	4.00	$1,102	$5,790	$655	$1,086	$1,245	$112	$176	$10,165	$124	$61	$50	$236
1	17.9	1	0.12	0.8	2200	1600	0	2.59	4.00	$1,333	$7,004	$790	$1,296	$1,245	$112	$121	$11,900	$152	$59	$20	$231
10	24.0	1	0.26	0.8	2200	1600	0	3.70	4.00	$1,757	$9,232	$1,038	$1,682	$1,245	$112	$165	$15,230	$203	$61	$44	$308
2	48.9	2	0.17	0.8	2200	1600	0	3.29	4.00	$3,510	$18,439	$2,064	$3,275	$1,245	$112	$269	$28,914	$414	$65	$55	$534
21	36.4	2	0.30	0.8	2200	1600	0	3.90	4.00	$2,635	$13,844	$1,552	$2,480	$1,245	$112	$353	$22,220	$309	$68	$100	$478
25	35.6	2	0.33	0.8	2200	1600	0	4.03	6.00	$3,152	$14,340	$1,572	$3,366	$1,245	$112	$371	$24,157	$302	$69	$110	$482
17	466.9	15	13.44	0.8	2200	1600	0	19.85	24.00	$274,554	$490,382	$26,188	$152,694	$1,245	$112	$63,475	$1,008,650	$3,958	$2,593	$33,657	$40,208
18	75.4	3	7.25	0.8	2200	1600	0	14.39	16.00	$20,893	$49,838	$3,825	$16,857	$1,245	$112	$6,963	$99,734	$639	$333	$3,631	$4,603
19	272.4	9	6.62	0.8	2200	1600	0	14.92	16.00	$75,296	$179,012	$13,689	$60,527	$1,245	$112	$19,138	$349,019	$2,309	$820	$9,945	$13,074
28	91.0	3	0.71	0.8	2200	1600	0	6.12	8.00	$9,878	$38,529	$4,066	$10,748	$1,245	$112	$910	$65,487	$771	$91	$356	$1,218
0	180.7	5	2.50	0.8	2200	1600	0	10.46	12.00	$30,167	$89,173	$8,563	$30,705	$1,245	$112	$4,275	$164,239	$1,532	$225	$2,086	$3,843
9	26.6	1	0.59	0.8	2200	1600	0	5.15	6.00	$2,370	$10,794	$1,186	$2,549	$1,245	$112	$267	$18,523	$225	$65	$99	$390
	1867									**$487,563**	**$1,171,841**	**$91,365**	**$352,069**	**$39,832**	**$3,581**	**$107,259**	**$2,253,510**	**$15,827**	**$6,027**	**$54,628**	**$76,482**
	Total Length																**Total Capital Costs**				**Total Operating Costs**

Table 4. Data by pipeline segment for scenario 1, connecting 32 ethanol plants and Jeffrey Energy Center in a large scale pipeline system. Abbreviations: mi—mile, MT/yr—million tonnes/year, dec—decimal, psig—pounds per square inch gauge, ft—feet, in—inch. Costs are in thousands of dollars.

The four scenarios summarized below are illustrated in Figures 1–3. Statistics and costs for all cases are tabulated in Tables 5 and 6.

1. Jeffrey + Ethanol to storage and EOR market: CO_2 from 32 ethanol plants, most having been contacted by EBR, plus CO_2 from Westar's Jeffrey Energy Center transported to Pleasant Prairie saline aquifer storage site and the majority to EOR markets. Approximately 1,867 miles of pipeline would gather and transport 13.44 million tonnes of CO_2 per year (MT/yr), 10.94 from 32 ethanol sources and 2.5 from Jeffrey.
2. Jeffrey to nearby storage: 2.5 MT/yr CO_2 from Westar's Jeffrey Energy Center transported in 51 miles of pipeline to the Davis Ranch and John Creek oil fields for saline aquifer storage.
3. Jeffrey + CHS to distant storage: 2.5 MT/yr CO_2 from Westar's Jeffrey Energy Center and 0.75 MT/yr CO_2 from CHS refinery transported in pipelines covering 353 miles to the Pleasant Prairie field for saline aquifer storage.
4. Jeffrey to distant storage: 2.5 MT/yr CO_2 from Westar's Jeffrey Energy Center transported in 353 miles of pipeline to the Pleasant Prairie oil field for saline aquifer storage.

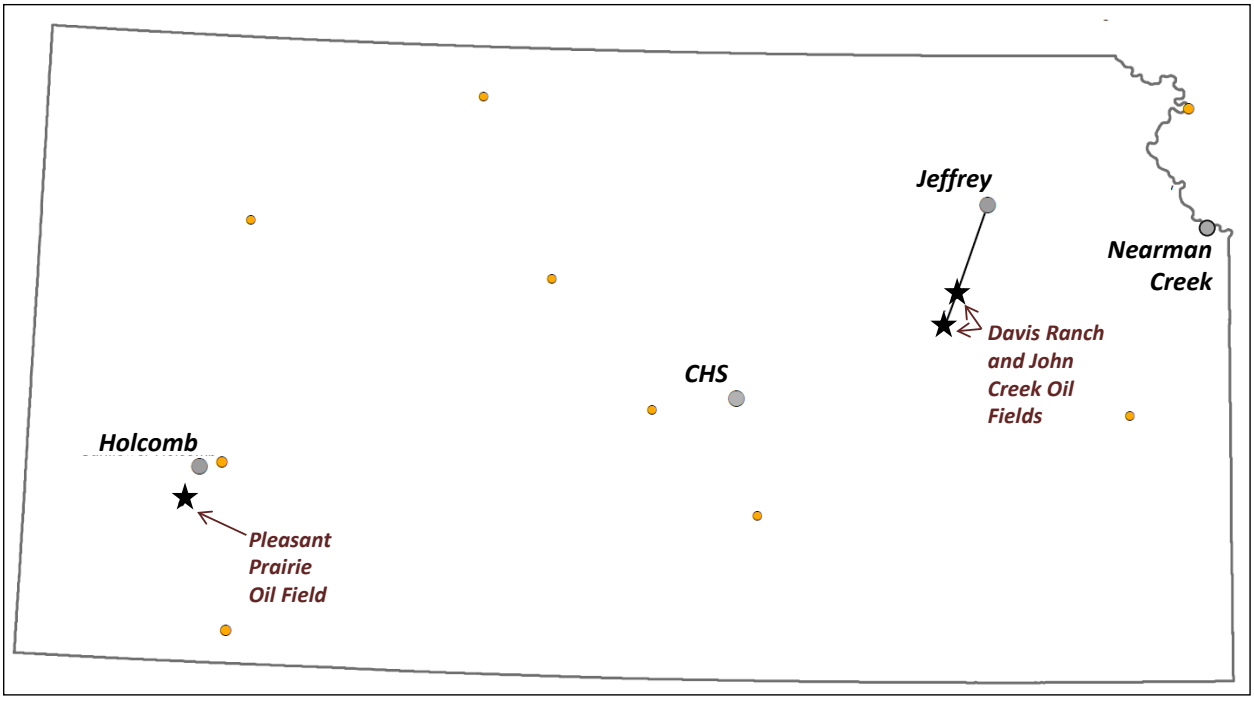

Figure 2. Pipeline Scenario 2, connecting Westar's Jeffrey Energy Center to Davis Ranch and John Creek oil fields. Potential CO_2 sources include ICKan industry partners (gray circles) and ethanol plants (yellow circles). Possible saline aquifer storage sites are beneath oil fields.

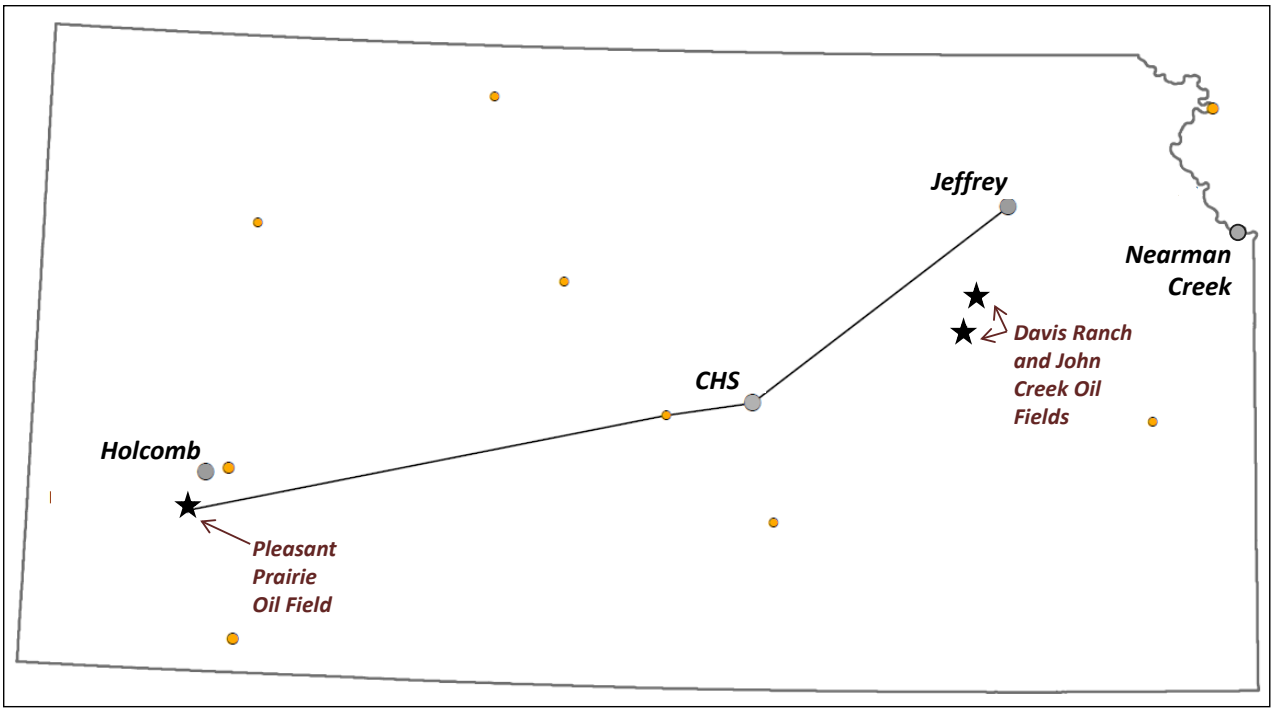

Figure 3. Pipeline Scenarios 3 and 4. Scenario 3 connects Westar's Jeffrey Energy Center the CHS Refinery and then to the Pleasant Prairie oil field. Potential CO_2 sources include ICKan industry partners (gray circles) and ethanol plants (yellow circles). Possible saline aquifer storage sites are beneath oil fields.

Table 5. Scenario 1 gathering and transportation system summary statistics, and capital and operating costs.

Number of Segments	32
Distance X 1.2 (mi)	1,867
CO2 Volume (Mtonnes/yr)	13.44
Pipeline sizes (in)	4" to 24"
Booster Station Count	75
NETL Model CapX ($M)	$2,254
NETL Model OpX/yr ($M)	$76.5
*Additional Pump Station Count	32
*Additional Pump CapX ($M)	$46
*Additional Pump OpX ($M/yr)	$23.3
Total Capital Costs ($M)	$2,300
Total Operating Costs ($M/yr)	$99.8

* NETL cost model does not account for additional pump stations where segments join. Costs are estimated.

Table 6. Scenarios 2, 3, and 4 gathering and transportation system summary statistics, and capital and operating costs. Jeffrey to main trunk line segment is also included.

	Scenario No.	Distance (mi)	Distance (mi) X 1.2	Volume (MT/yr	Size (inches)	CapX ($Million)	Annual OpX ($Million)
Jeffrey EC to MidCon Trunk	**part of 1**	151	181	2.5	12"	$164	$3.8
Jeffrey EC to Davis Ranch and John Creek	**2**	42	51	2.5*	12" & 8"	$47	$1.3
Jeffrey EC to CHS and Pleasant Prairie	**3**	294	353	3.25**	12"	$323	$8.0
Jeffrey EC to Pleasant Prairie	**4**	294	353	2.5	12"	$322	$7.2

Discussion

The purpose of this investigation was to determine whether the FE/NETL CO_2 Transport Cost Model could be modified to enable it to be a useful tool to efficiently calculate detailed cost estimates for complicated pipeline scenarios. The work presented here demonstrates that the tool is stable with the modifications made and provides ICKan with a means to quickly evaluate a variety of complex pipeline scenarios.

Although economic analysis was not part of the of this investigation, capital and operating costs, excluding interest and business margin, are easily calculated relative to the volume of CO_2 delivered. For Scenario 1, the large-scale example: assuming a 20-year operating life, the model projects capital costs of $8.56/tonne ($0.45/mcf), operating costs of $7.43/tonne ($0.39/mcf), and total costs of ($15.98/tonne ($0.84/mcf).

References

Dubois, M. K., S. W. White, and T. R. Carr, Co-generation, 2002, Ethanol Production and CO_2 Enhanced Oil Recovery: a Model for Environmentally and Economically Sound Linked Energy Systems: Proceedings 2002 AAPG Annual Meeting, Houston, Texas, p. A46. Kansas Geological Survey Open-File Report 2002-6. http://www.kgs.ku.edu/PRS/Poster/2002/2002-6/index.html Accessed 7/1/2017.

Grant, T., D. Morgan, and K. Gerdes, 2013, Carbon Dioxide Transport and Storage Costs in NETL Studies: Quality Guidelines for Energy Systems Studies: DOE/NETL-2013/1614, 22 p.

Grant, T. and D. Morgan, 2014, FE/NETL CO_2 Transport Cost Model. National Energy Technology Laboratory. DOE/NETL-2014/1667. https://www.netl.doe.gov/research/energy-analysis/analytical-tools-and-data/co2-transport. Accessed 6/28/2017.

U.S. Department of Energy, Energy Information Administration, 2017, Ethanol Plans (EIA-819M Monthly Oxygenate Report, March 27, 2017. https://www.eia.gov/maps/layer_info-m.php Accessed June 1, 2017.